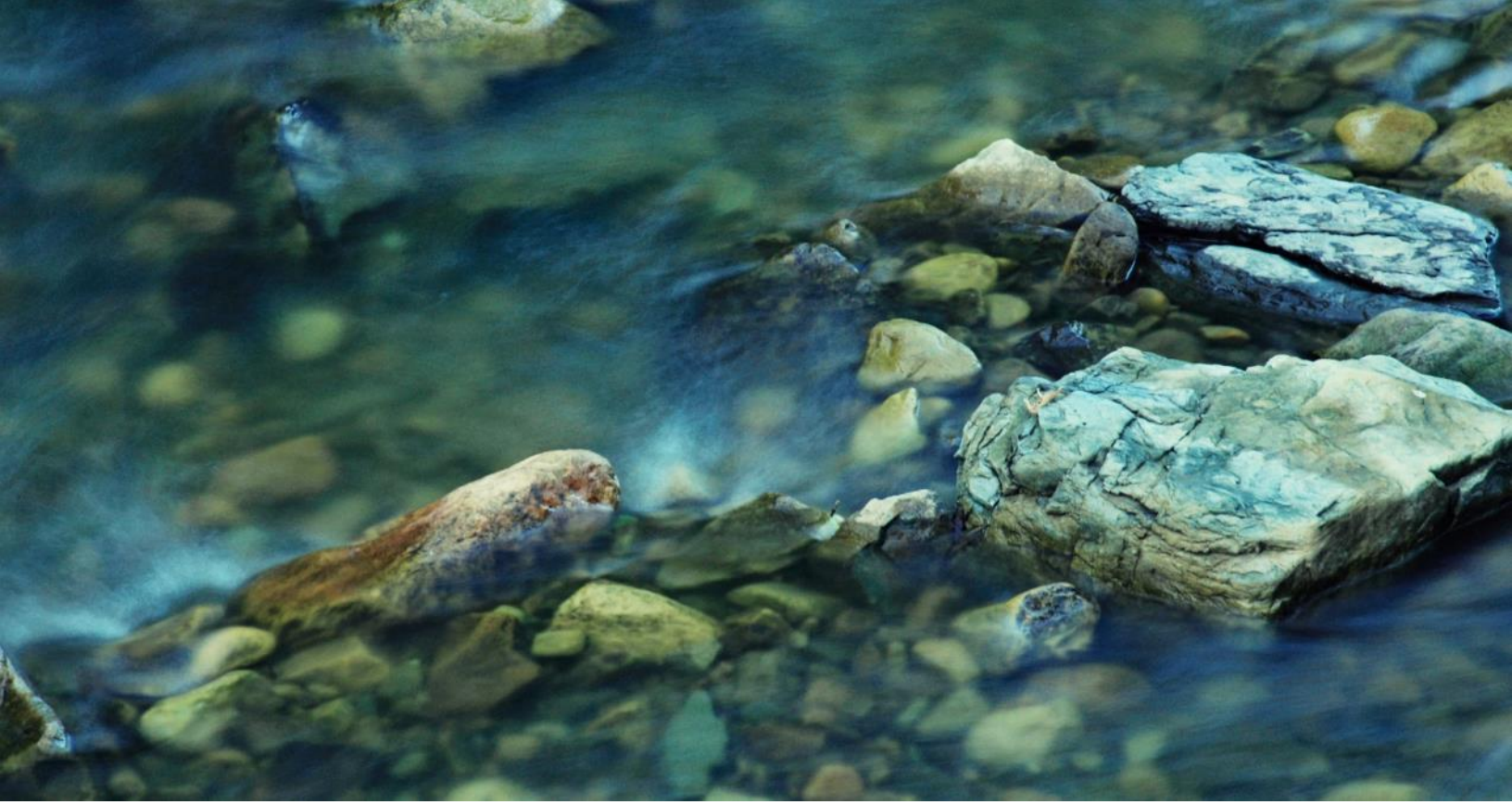

July 2019
Lower Passaic River Study Area Remedial Investigation/Feasibility Study

Remedial Investigation Report

Prepared for Lower Passaic River Cooperating Parties Group

July 2019
Lower Passaic River Study Area Remedial Investigation/Feasibility Study

Remedial Investigation Report

Prepared for
Lower Passaic River Cooperating Parties Group

Prepared by
Anchor QEA, LLC
(Woodcliff Lake, New Jersey;
Boston, Massachusetts)

With contributions from
AECOM (Chelmsford, Massachusetts)
de maximis, inc. (Clinton, New Jersey)
Integral Consulting (Louisville, Colorado)
mab environmental, LLC (Hilton Head Island, South Carolina)
Moffatt & Nichol (New York, New York)
Windward Environmental LLC (Seattle, Washington)

Project Number: 120980-02.09
\\Boston1\jobs\Passaic_CPG\DOCUMENTS\RI_Master\Final_Submittal_For_Submittal\Final_PDF_Upload_8-6-2019\LPR_RI_Main_Text.docx

TABLE OF CONTENTS

* The bioaccumulation modeling summary (Appendix P) referenced in these sections will be developed and finalized at a later date in coordination with USEPA.

TABLES

FIGURES

APPENDICES

ABBREVIATIONS

µg/dL	microgram per deciliter
µg/kg	microgram per kilogram
µm	micrometer
2,3,7,8-TCDD	2,3,7,8-tetrachlorodibenzo-p-dioxin
ANOVA	analysis of variance
AOC	administrative order on consent
BERA	Baseline Ecological Risk Assessment
BHHRA	Baseline Human Health Risk Assessment
CARP	Contaminant Assessment and Reduction Project
CAS	creel/angler survey
CERCLA	Comprehensive Environmental Response, Compensation, and Liability Act
cfs	cubic feet per second
CFT	contaminant fate and transport
CLH	Chemical Land Holdings
cm	centimeter
COC	chemical of concern
COI	chemical of interest
COPC	chemical of potential concern
COPEC	chemical of potential ecological concern
CPG	Cooperating Parties Group
Cs-137	cesium-137
CSM	conceptual site model
CSO	combined sewer overflow
CTE	central tendency exposure
CWA	Clean Water Act
CWCM	Chemical Water Column Monitoring
cy	cubic yard
CYP450	Cytochrome P450
DDD	dichlorodiphenyldichloroethane
DDE	dichlorodiphenyldichloroethylene
DDT	dichlorodiphenyltrichloroethane
DDx	dichlorodiphenyltrichloroethane and its breakdown products
DLC	dioxin-like congener
DO	dissolved oxygen
DOC	dissolved organic carbon
ECOM	Estuarine Coastal Ocean Model

EMBM	Empirical Mass Balance Model
EPC	exposure point concentration
ERA	ecological risk assessment
ETM	estuarine turbidity maximum
FFS	Focused Feasibility Study
f_E	fraction equilibrium
FS	feasibility study
ft/day	feet per day
ft^2	square feet
g/cm^3	grams per cubic centimeter
GIS	geographic information system
HD	hydrodynamic
HFI	hydrodynamic field investigation
HHRA	human health risk assessment
HI	hazard index
HMW	high molecular weight
HOT	head-of-tide
HQ	hazard quotient
HQI	HDR|HydroQual
HSD	Honest Significant Difference
HV	high-volume
IQR	interquartile range
JDG	Joint Defense Group
K_{ow}	
LMW	low molecular weight
LOAEL	lowest-observed-adverse-effect level
LOE	line of evidence
LPR	Lower Passaic River
LPRRP	Lower Passaic River Restoration Project
LPRSA	Lower Passaic River Study Area
LRC	Low Resolution Coring
m	meter
mg/kg	milligrams per kilograms
mg/L	milligrams per liter
MLW	mean low water
mm	millimeter
MPA	mass-per-area

MPI	Malcolm Pirnie, Inc.
MT	metric tons
NBSA	Newark Bay Study Area
NCP	National Contingency Plan
ng/kg	nanograms per kilogram
NGVD 29	National Geodetic Vertical Datum of 1929
NJ	New Jersey
NJDEP	New Jersey Department of Environmental Protection
NJTRWP	New Jersey Toxics Reduction Work Plan
NOAEL	no-observed-adverse-effect level
NPL	National Priorities List
NY	New York
OC	organic carbon
OCC	Occidental Chemical Corporation
OU	Operable Unit
PAH	polycyclic aromatic hydrocarbon
Pb-210	Lead-210
PCB	polychlorinated biphenyl
PCDD	polychlorinated dibenzo-p-dioxin
PCDF	polychlorinated dibenzofuran
PFD	Problem Formulation Document
pg/L	picogram per liter
POC	particulate organic carbon
ppth	parts per thousand
PREmis	Passaic River Estuary Management Information System
PRG	preliminary remediation goal
PWCM	Physical Water Column Monitoring
QAPP	Quality Assurance Project Plan
RARC	Revised Risk Analysis and Risk Characterization
RI	remedial investigation
RM	river mile
RME	reasonable maximum exposure
RPD	redox potential discontinuity
SAV	submerged aquatic vegetation
SLERA	screening-level ecological risk assessment
SOD	sediment oxygen demand
SPI	sediment profile imaging

SQT	sediment quality triad
SSC	suspended sediment concentration
SSD	species sensitivity distribution
SSP	Supplemental Sampling Program
SSP2	Second Supplemental Sampling Program
SSS	side scan sonar
ST	sediment transport
SUF	Site Use Factor
sv	small-volume
SVOC	semivolatile organic compound
SWO	stormwater outfall
TBT	tributyltin
TEF	toxic equivalency factors
TEQ	toxic equivalency quotient
tetra-CB	tetrachlorobiphenyl
TIN	triangulated irregular network
TMDL	Total Maximum Daily Load
TOC	total organic carbon
TPH	total petroleum hydrocarbon
TRV	toxicity reference value
TSI	Tierra Solutions, Inc.
TSS	total suspended solids
UCL	upper confidence limit
UPR	Upper Passaic River
USACE	U.S. Army Corps of Engineers
USEPA	U.S. Environmental Protection Agency
USGS	U.S. Geological Survey
VOC	volatile organic compound
ww	wet weight
WY	water year

Executive Summary

Since 2004, the Cooperating Parties Group (CPG) has been participating in the Remedial Investigation (RI) and Feasibility Study (FS) for the Lower Passaic River Study Area (LPRSA), the 17.4-mile stretch of the Lower Passaic River (LPR) between Dundee Dam and Newark Bay. The CPG provided funding for the U.S. Environmental Protection Agency (USEPA)-performed RI/FS from 2004 to 2006, and then in 2007 entered into an Administrative Order on Consent to take over the performance of the LPRSA RI/FS from USEPA (2007). The goals and objectives of the RI, as outlined in the Settlement Agreement and Order on Consent and Statement of Work (USEPA 2007) are as follows:

1. Identify and quantify the hazardous contaminants present in sediment, water, and biota
2. Understand the vertical and horizontal distribution of hazardous contaminants in the LPRSA
3. To the extent practicable, identify sources of historical hazardous contamination
4. Quantify any significant continuing sources of hazardous contaminants
5. Understand the geomorphological setting and processes (e.g., resuspension, transport, deposition, and weathering) affecting the stability of sediment
6. Understand the key chemical and biological processes affecting the fate, transport, and bioavailability of hazardous contaminants
7. Identify the complete or potentially complete human and ecological exposure pathways for the hazardous contaminants
8. Identify current and potential future human and ecological risks posed by the hazardous contaminants
9. Collect data necessary to evaluate the potential effectiveness of natural recovery, in situ capping, sediment removal, and promising innovative technologies
10. Provide a baseline of data that can be used to monitor remedy effectiveness in all appropriate media (generally sediment, water, and biota)

To that end, the RI has generated an extensive dataset of physical, chemical, and biological measurements, including more than 12,000 samples and 2.5 million contaminant measurements, bathymetry data, and side scan sonar data. These data and their interpretation show that contamination in the sediment, water column, and biological tissue generally follows spatial and temporal patterns that reflect the evolution of the river's sediment deposits, the nature of the sediments, the location of the contaminant sources, the flow regime, sediment erosion and deposition, other contaminant fate and transport processes, and food web dynamics. Gaps in understanding remain, but the knowledge gained provides the understanding needed to craft remediation strategies aimed at mitigating contaminant impacts and ultimately achieving Comprehensive Environmental Response, Compensation and Liability Act- (CERCLA-) compliant risk-based remedial goals protective of human health and ecological receptors.

ES.1 System Characteristics

The LPR begins at Dundee Dam and ends at Newark Bay (Figure ES-1). Freshwater and solids loading to the LPR from the watershed are dominated by the inflow from the Upper Passaic River (UPR) at Dundee Dam, with several tributaries contributing to a lesser degree. The LPR also receives brackish water and solids from Newark Bay via tidal exchange and density-driven currents, which, together with the freshwater flow, dictate the movement of sediments within the estuary. A 15.4-mile-long federal navigation channel was created in the late nineteenth century to facilitate industrial activity along the river. The channel between U.S. Army Corps of Engineers (USACE) river mile (RM) 1.9[1] and USACE RM 8.3 was last maintained in or before 1950. The last maintenance dredging in the lower 1.9 miles of the channel was conducted in 1983. Most of the channel upstream of USACE RM 8.3 was last dredged in the 1970s.[2] Infilling and trapping of sediment-bound contaminants within the navigation channel has occurred to varying degrees since the cessation of maintenance dredging. Infilling was initially rapid (approximately 4 inches per year [LBG 2014]) and has since slowed. Extensive infilling occurred downstream of RM 8 where sections of the river have accumulated 10 feet or more of sediment (Figure ES-2). The coincidence of lower velocities in the expanded cross section produced by navigational dredging and the period of peak contaminant discharges facilitated sediment and contaminant accumulation and subsequent burial. The rates at which sediments accumulated relate to geomorphology. For example, sedimentation rates were lower on the outer bends and in higher-velocity reaches of the river than within the main channel.

Urbanization and industrial development starting in the late eighteenth century degraded habitat quality, eliminating wetland areas and most shoreline vegetation, and transformed the LPR into a highly channelized river. Currently, the majority of the riverbank in the lower 8 miles consists of bulkhead and/or riprap and supports a limited amount of vegetation. Farther upstream, the riverbank is dominated by mixed vegetation, generally over steep banks. Wetland habitats are limited to small patches or isolated areas due to development. While development and urbanization have affected ecological habitat, mudflat and bank-to-bank water habitats that are present in the LPR are important to the aquatic species and wildlife that use them. Intertidal mudflat areas provide key foraging habitat for shorebirds, and the associated nearshore subtidal shallow areas provide key foraging areas for small forage fish and other prey species.

The benthic invertebrate community, which forms the base of the ecological food web, is dominated by deposit feeders, filter feeders, and detritivores (Appendix D, Section 2.2.1.3). Fish surveys

[1] The USACE and USEPA RI RMs on the site differ by approximately 0.3 mile due to the specification of the zero RM location. The USACE RM can be seen in Figures 1a and 1b of USACE (2010). In this document, USACE RMs are designated by the prefix USACE, while the RI RMs have no prefix. An approximate conversion to RI/FS RMs is to subtract 0.3 from the USACE RMs; the exact conversion varies along the river.

[2] The stretches of the navigation channel from USACE RM 8.5 to USACE RM 9.6, USACE RM 10 to USACE RM 10.6, USACE RM 11 to USACE RM 12.1, USACE RM 12.4 to USACE RM 12.8, USACE RM 13.9 to USACE RM 14, and USACE RM 14.3 to USACE RM 15 were last maintained before 1950.

conducted in 2009 and 2010 indicate that the LPR fish community is primarily benthic-feeding species (Appendix D, Section 2.3.6). The LPR provides a limited and fragmented habitat for avian and mammalian species. Several bird species are observed in the LPR year-round and may breed in nearby areas with suitable breeding and nesting habitat. Gulls, geese, and ducks were the most commonly observed bird species during the four seasonal surveys conducted in the LPR during 2010 and 2011 (Appendix D, Section 2.4.6). No surveys of water-associated mammals were conducted in the LPR, though few mammalian species were noted during the surveys for habitat, avian species, and aquatic biota. It is likely that muskrats and raccoons are present in some areas along the river banks (Appendix D, Section 2.5).

The LPR is a classic partially mixed coastal plain estuary[3] with an expanding cross section from Dundee Dam to Newark Bay, containing meanders reflective of its ancestral river channel. The transport of sediment in the LPR is governed by the freshwater discharge, estuarine circulation, and tidal asymmetry (Section 3.4). While freshwater discharge transports water and solids from upstream to downstream, tidal transport also moves downstream water and solids to upstream regions. The salt front (i.e., the interface between the fresh and brackish waters) typically coincides with the estuarine turbidity maximum (ETM), i.e., the region of an estuary with maximum turbidity that is associated with solids trapping. During low to moderate flows, net suspended solids fluxes tend to be directed upstream within the salt front and directed downstream in the tidal river upstream of the salt front. During high-flow conditions, net suspended solids fluxes are generally directed downstream throughout the river.

Overall, the sediment characteristics of the LPR are typical of a large estuary, with along-river trends that reflect sediment transport patterns influenced by the expanding cross section, tides, river inflow, and geomorphologic changes (Figure ES-3). The coarsest sediments are in the upper reaches, and finer sediments become more common as the river widens and deepens. Along bends, the lower water velocities along the inner portion and the lateral circulation moving bottom water toward the inner portion result in the accumulation of finer sediments. Conversely, the higher water velocities along the outer portion prevent the accumulation of finer sediments and result in coarser sediments being present. Moving from the inner bend across the channel toward the outer bend, there is typically a gradual transition from finer to coarser sediments. The fine sediments along the inner bend tend to form point bars, most notably the RM 10.9 point bar, which was partially dredged and capped in 2013 and 2014 (excluding the utility corridor) to address elevated 2,3,7,8-tetrachlorodibenzo-p-dioxin (2,3,7,8-TCDD), polychlorinated biphenyl (PCB), polycyclic aromatic hydrocarbon (PAH), and mercury levels (2,3,7,8-TCDD levels, in some instances, exceeded 50,000

[3] Coastal plain estuaries are estuaries formed due to the rising sea levels associated with melting ice after the last ice age. The melted waters entered low-lying coastal river valleys, and these estuaries are characterized by shallow river valleys with gently sloping bottoms, with increasing depth toward the mouth of the river (in the case of the LPR, the depth increases toward Newark Bay but is enhanced by navigational deepening).

nanograms per kilogram [ng/kg]). Sediments tend to be coarse or absent (i.e., the bottom is rock and gravel) near structures such as bridge abutments and at tributary confluences due to associated turbulence, particularly under higher flows, that prevents long-term accumulation of fine sediments or, in particularly high-energy areas, any sediment.

Net deposition since the period of highest contamination in the 1950s and 1960s has occurred in much of the lower 8 miles of the river and in portions of the river between RM 8 and RM 15. The evidence for this includes buried Cesium-137 (Cs-137) peaks[4] and buried peak contaminant concentrations. Notable exceptions to this pattern are found in the upstream portions of a number of mudflat point bars at and upstream of RM 7, which appear to have not accumulated sediment since the 1960s, perhaps as a result of having evolved to a stable configuration by the 1960s. Even where net deposition has occurred on the scale of decades, dynamic erosion and deposition likely occurred and continues to occur on short timescales. Evidence for cyclical erosion and deposition comes from changes in bathymetry documented in the series of multibeam bathymetry surveys conducted between 2007 and 2012.

Tidal resuspension is a major driver of water column concentrations of suspended sediment and contaminants, and during low-flow conditions, it reflects mainly the mobilization of a thin layer of unconsolidated sediments, termed a fluff layer. Erosion of the underlying consolidated sediment bed occurs mainly during significant storm events, during which the eroded sediments may re-deposit elsewhere or migrate out of the river. Erosion appears to be most significant on edges of the channel, downstream of bridge abutments, in areas of constricted cross sections, and in the more sinuous portions of the lower 5 miles.

Details on system characteristics are provided in Sections 3, 4, and 5.

ES.2 Nature and Extent of Contamination

Many of the contaminants tend to be found at their highest concentrations in fine sediments (example distribution for 2,3,7,8-TCDD is shown in Figure ES-4). This association reflects the higher amount of organic matter in fine sediments and the importance of organic carbon in sorbing many of the contaminants in the river. The increasing occurrence of fine sediments moving downstream contributes to the large-scale longitudinal trend in contaminant concentrations. That trend also

[4] Cs-137 is a man-made radionucleotide that is produced during the nuclear fission of Uranium-235. Most of the Cs-137 present on the earth's surface was produced during atmospheric nuclear testing that took place between 1954 and 1963. The lowest Cs-137 activities are found in areas that have not experienced sediment accumulation since the 1950s. Regions that have been net depositional with similar sediments since at least the 1950s contain well-defined buried peak Cs-137 activities. Regions that accumulated different types of sediment at different times or experienced some sediment removal (erosion or dredging) after the 1960s do not contain a well-defined peak. Regions that attained geomorphic equilibrium in the early 1960s often contain the maximum Cs-137 activity at the surface. Most of the LPR contains maximum Cs-137 concentrations that are buried at depth. Cs-137 data are analyzed in detail in Section 4.

reflects the estuarine transport patterns that facilitate upstream as well as downstream movement of water, solids, and associated contaminants.

Examining the data at a finer spatial scale, as is done in Section 4, reveals patterns in 2,3,7,8-TCDD, total PCBs, total DDx[5], and mercury concentrations that are largely driven by variations in sediment type and depositional/erosional history. Concentrations of these contaminants generally correlate (to varying degrees) with sediment type, as discussed above, although the range of concentrations is large, particularly within fine sediments. That range seems to reflect geomorphic evolution and susceptibility to episodic erosion and cyclic erosion/deposition. The higher surface (0- to 6-inch) concentrations tend to be in fine sediments in areas that have not been net depositional in the last few decades. Surface concentrations in fine sediments in depositional areas are reflective of contaminant concentrations in particulate matter in the water column. PAH concentrations do not tend to vary with sediment type; comparable levels of high-molecular-weight polycyclic aromatic hydrocarbons (HMW PAHs) and low-molecular-weight polycyclic aromatic hydrocarbons (LMW PAHs) are found in fine and coarse sediments.

These patterns are illustrated in the following section using surface sediment 2,3,7,8-TCDD concentrations.

Surface Sediment Contaminant Concentration Patterns

Surface sediment 2,3,7,8-TCDD concentrations greater than 500 ng/kg have rarely been observed upstream of RM 12 and are confined mainly to fine sediment regions that have been influenced by upstream transport from the lower river, which extends to beyond RM 14. Outside the fine sediment deposits, 2,3,7,8-TCDD concentrations above RM 12 are mostly less than 100 ng/kg and above RM 14.6 are less than 1 ng/kg, reflecting the low concentrations at the upstream boundary at Dundee Dam and the coarse nature of the sediments.

Moving downstream, fine sediments and 2,3,7,8-TCDD concentrations greater than 500 ng/kg become more numerous. Point bars such as those that formed at RM 10.9, RM 10.1, and RM 7.3 generally have higher 2,3,7,8-TCDD concentrations in the central area of the point bar and lower concentrations in nearshore and offshore portions. In the RM 10.9 point bar (shown in Figure ES-5 as an example), concentrations greater than 1,000 ng/kg occur where 1960s-era sediments are at the surface. Sharp transitions to lower concentrations are typically observed moving toward the edge of the channel. The channel in the vicinity of this point bar is characterized by concentrations generally in the range of 10 to 100 ng/kg, consistent with the coarse nature of the sediments. Concentrations are typically less than 500 ng/kg in the southerly portion of the RM 10.9 point bar, which is

[5] Total DDx refers to the sum of the 2,4'- and 4,4'- isomers of dichlorodiphenyltrichloroethane (DDT), dichlorodiphenyldichloroethylene (DDE), and dichlorodiphenyldichloroethane (DDD).

consistent with ongoing evolution characteristic of the downstream portion of a point bar. Similar patterns are also observed 0.5 to 1.5 feet below the surface.

Downstream of RM 7.8, the river bed is composed mostly of fine sediments. The pattern of higher concentrations in the shoals continues in this region, although concentrations greater than 500 ng/kg and occasionally greater than 1,000 ng/kg occur in the channel. These values appear to reflect local conditions. For example, a concentration of 28,000 ng/kg was found on the steep western slope at RM 7.3, reflecting erosion of the channel side wall into earlier deposited material. Similarly, concentrations of 10,800 and 21,900 ng/kg were found on the slope of the channel along the outside of the bend at RM 4.6. A sample in the center of the channel at RM 3.6 yielded a concentration of 11,700 ng/kg. It was collected after Hurricane Irene in a region that experienced more than 3 feet of scour due to the event, thus exposing older sediment.

In the lowermost portion of the river (i.e., downstream of RM 3.5), 2,3,7,8-TCDD concentrations in the shoals are typically higher than in the channel. Surface concentrations in the channel are generally representative of recent deposition.

The concentration patterns for total PCBs, total DDx, and mercury tend to mirror those of 2,3,7,8-TCDD in the region downstream of RM 14. As noted previously, patterns of HMW PAHs and LMW PAHs vary from those of the other contaminants, with no clear difference between concentrations in fine and coarse sediments. Upstream of RM 14, none of these contaminants show the dramatically lower concentrations evident for 2,3,7,8-TCDD because of the greater influence of sources from above Dundee Dam. Differences from 2,3,7,8-TCDD also exist near the mouth of the river due to influences from sources in Newark Bay and beyond.

A detailed examination of sediment contamination patterns can be found in Section 4.

Biota Contaminant Concentration Patterns

While there is variability in contaminant levels in biota tissue, spatially, as well as within and between species, some general trends were observed based on the benthic invertebrate and fish tissue data collected from the LPR. Organic contaminants, including 2,3,7,8-TCDD, total PCBs, and total DDx, are generally highest in large benthic omnivorous fish, with the highest concentrations found in carp. Concentrations of 2,3,7,8-TCDD, total PCBs, and total DDx tend to be highest in fish from the middle reaches of the LPR (e.g., Reaches 3 to 5) and lowest in fish tissue samples from above Dundee Dam. However, this is not true for all species. The close association of carp and other large benthic omnivorous fish with surface sediments influences their accumulation of organic contaminants. HMW PAHs and LMW PAHs are also generally higher in the benthic omnivores. Mercury concentrations in LPR fish tissue generally increase with increasing trophic level and are similar or even lower than those measured in fish collected above Dundee Dam.

A detailed examination of contamination patterns in biota is provided in Section 5.

Contaminant Transport and Mass Inventory Patterns

The surface sediment patterns above reflect a complex exchange of contaminants between the sediment bed and the water column, which occurs primarily through erosion and deposition. Erosion during low flows is generally limited to a millimeter-scale surficial fluff layer of unconsolidated sediments and extends into the underlying bedded sediments during higher flows. Resuspended contaminants are transported along the river via the riverine and estuarine processes noted previously, mixing with contaminants originating from other portions of the LPR and from external sources (e.g., Dundee Dam and tributaries) while redistributing in a contaminant of potential concern (COPC)-specific manner to the dissolved phase and other suspended solids. The sorbed fraction may settle to the sediment bed, thus creating a mechanism for areas of high concentration to influence areas of lower concentration (and vice versa). Water column measurements indicate that 2,3,7,8-TCDD concentrations are low at Dundee Dam, highest within the LPR in the vicinity of the ETM, and decreasing through the lower miles of the LPR into Newark Bay in a manner analogous to the surface sediments. Modeling indicates that the LPR is a net exporter of 2,3,7,8-TCDD to Newark Bay, with the export being strongest during high-flow events when some areas of the river bottom experience scour.

Integrated over time, these transport processes have led to the accumulation of contaminant mass within the LPR sediments. Contaminant mass inventory patterns in the sediments differ from the surface concentration patterns that influence human and ecological exposure because they reflect long-term infilling patterns more so than recent erosion and deposition patterns. The mass inventory patterns are useful because they provide insights about contaminant source locations and along-river transport. Mass inventory was estimated by interpolating core data and summarized by 2-mile reaches in order to see the distribution of mass throughout the LPR and Newark Bay.

The mass of 2,3,7,8-TCDD is centered in the vicinity of the Lister Avenue site (located at RM 3.1); 74% of the total mass of 2,3,7,8-TCDD is located in the lower 6 miles of the LPR and only 18% is in Newark Bay, with the remaining 8% residing above RM 6 (Figure ES-6). The overall pattern demonstrates net upstream transport to approximately RM 14 (declining with distance upstream, particularly above RM 12) and downstream transport across Newark Bay. In contrast, the mass distribution of total PCBs, HMW PAHs, and mercury are shifted toward Newark Bay (containing 67%, 67%, and 80% of the total mass, respectively) and lack the dramatic drop-off in mass-per-area above RM 12 that is seen in the 2,3,7,8-TCDD distribution (Section 6.3.2; Figures 6.14a, 6-14b and 6-14e). The patterns indicate a greater importance of upstream and downstream sources for the other contaminants. Total 4,4′-DDx mass (i.e., the sum of the 4,4′ isomers only, used here instead of total DDx because much of the historical core data lack the 2,4′ isomers) has elements of both 2,3,7,8-TCDD and the other COPCs (Section 6.3.2; Figures 6-14d and 6-15); while the mass distribution is

strongly centered near the Lister Avenue site (DDT was produced and discharged there), outside of the RM 2 to RM 4 reach the mass is more distributed than for 2,3,7,8-TCDD and suggestive of upstream and downstream sources (though much weaker than the Lister Avenue source). Likewise, LMW PAH mass is centered in the RM 4 to RM 6 reach, presumably due to a local source, but with mass that is otherwise more distributed across Newark Bay and above RM 14 than 2,3,7,8-TCDD—again suggesting upstream and downstream influences (Section 6.3.2; Figure 6-14c). Loading history relative to dredging history likely also plays a role in the mass distributions (e.g., maintenance dredging occurred downstream of RM 2 and in pockets above RM 8 after the cessation of 2,3,7,8-TCDD discharges at Lister Avenue).

Further discussion of the mass distributions of contaminants in the LPR can be found in Section 6, and detailed evaluations of contaminant fate and transport can be found in Sections 6 and 7.

Natural Recovery

Sedimentation has reduced average contaminant concentrations in LPR surface sediments since the 1950s and 1960s, when the most substantial releases of contamination occurred. Areas with high sedimentation rates have exhibited the greatest recovery since the 1960s as evidenced by lower surface sediment concentrations relative to concentrations at-depth (Figure ES-7).

Changes in surface sediment 2,3,7,8-TCDD concentrations from the mid-1990s (i.e., 1995 to 1999 data) to the late 2000s (i.e., 2005 to before Hurricane Irene in 2011) can be examined in the reach between RM 1 and RM 7. These changes (Figure ES-8) suggest that recovery occurred in areas that experienced 6 inches or more of net deposition and perhaps in shallow areas outside the extent of the bathymetry surveys. In the net depositional areas, mean, median, and variability of 2,3,7,8-TCDD concentrations are lower in the late 2000s dataset than in the mid-1990s dataset. The data in the shallow areas outside the extent of the bathymetric surveys exhibit qualitatively similar changes but to a lesser extent. There is no evidence of recovery in areas that experienced 6 inches or more of net erosion. The eroded sediments coming from these areas likely inhibit recovery of the river. Areas that have experienced 6 inches or less of change (i.e., changes within the uncertainty of the bathymetric survey differencing) exhibit no clear temporal trend. Similar recovery patterns are noted for total PCBs, total 4,4'-DDx, and mercury. HMW PAHs and LMW PAHs show no evidence of recovery, likely due to ongoing sources.

The 2010 surface sediment concentrations in depositional areas match the levels on recently deposited sediment, implying a connection to the water column (which may also exist for the fine sediment fraction in coarse sediments). Such a connection suggests these areas should respond to downward trends in water column concentrations. In other words, they have the potential for recovery. The extent to which recovery occurs is likely controlled by the areas subject to net erosion

and the areas where cyclical erosion-deposition brings higher subsurface concentrations into the surface layer.

It appears that erosion during the 1-in-90-year high flow that resulted from Hurricane Irene caused an uptick in concentrations that impacted recovery. Average surface sediment concentrations in the post-Hurricane Irene dataset exceed those pre-Irene for most of the chemicals examined.

Recovery of biota tissue 2,3,7,8-TCDD, total PCBs, total 4,4′ DDx, mercury, LMW PAHs, and HMW PAHs concentrations was assessed by comparing concentrations from historical (1995 to 2004) and more recent (2009 to 2010) datasets. Generally, total PCB concentrations were found to have declined, but patterns for other chemicals are not clear. Variability in concentration trends may be due to the number of samples, timing of the sampling, species sampled, metabolization of PAHs, and other factors. The large degree in variability in tissue data collected from the LPR inhibits definitive conclusions regarding trends.

Additional details on Natural Recovery are provided in Sections 4 and 10.

Impact of Ongoing Sources

Contaminant sources outside the LPR influence recovery and can limit the benefits of active remediation by recontaminating remediated areas. Such sources exist for all the contaminants (total PCBs, PAHs, mercury, and total DDx) except 2,3,7,8-TCDD. As observed in Figure ES-9, concentrations of total PCBs, PAHs, mercury, and DDx are comparable in the LPR to those in the UPR and/or Newark Bay. Thus, remediation of the LPR sediments in the absence of source control has the potential to significantly reduce the levels of 2,3,7,8-TCDD but may not achieve similar long-term reductions of the other contaminants (i.e., total PCBs, PAHs, mercury, and total DDx) due to recontamination from the UPR and Newark Bay. Source control efforts in the UPR and Newark Bay that address the other contaminants or reductions occurring via natural recovery would reduce the effects of recontamination.

Point sources (e.g., combined sewer overflows [CSOs], stormwater outfalls [SWOs], industrial, and municipal discharges) also have the potential to be ongoing sources. Targeted sampling of LPRSA CSO/SWO point sources, performed as part of the Contaminant Assessment and Reduction Project model sampling effort in 2000 to 2004 (Great Lakes Environmental Center 2008) and during the 2007 to 2008 USEPA field effort, indicate that CSOs and SWOs are not a significant source for key contaminants in the Passaic River (LBG 2014). CSOs and SWOs contribute less than 3% of the solids entering the LPR.

Non-point sources, like groundwater flux and direct atmospheric deposition, are not believed to be major contaminant sources to the LPR. USEPA concluded in 2008 that chemical inputs from groundwater discharges are negligible throughout the LPR (correspondence between USEPA and

CSTAG [USEPA 2008]), and The Louis Berger Group concluded that the estimated groundwater contribution to the LPR is less than 2% of the long-term average river flow over Dundee Dam (LBG 2014). Atmospheric contributions of 2,3,7,8-TCDD to the LPRSA are expected to be small and diffuse relative to the contributions from dredging, erosion, and resuspension flux from historically contaminated sediments to the water column (Bopp et al. 1991; Chaky 2003; CSTAG 2008).

Additional details of ongoing sources can be found in Sections 7 and 10.

ES.3 Risks to Human and Ecological Receptors

Human Receptors

The objective of the Baseline Human Health Risk Assessment (BHHRA) was to identify potential unacceptable risks posed by site-related chemicals to human receptors in the LPR. Based on existing and potential future site uses and conditions, the BHHRA evaluated recreational anglers, swimmers, waders, boaters, and workers. Exposures were assumed to occur via direct contact with accessible surface sediment and surface water. The recreational angler was also assumed to eat fish or crab from the LPR.

The BHHRA was conducted using the empirical fish tissue, crab tissue, accessible surface sediment, and surface water data collected as part of the LPRSA RI. A total of 48 COPCs were selected for quantitative evaluation based on a conservative screening process. Dose-response values for COPCs were identified in accordance with USEPA guidance; both cancer and noncancer values were identified. Conservative assumptions were used to estimate the frequency and magnitude of each receptor's potential exposure to site media, including upper-bound fish and crab consumption rates identified by USEPA. For each receptor, the total potential cancer risk for each receptor was compared to the National Contingency Plan (NCP) risk range of 1 in 10^{-6} to 10^{-4} (one in one million to one in ten thousand). The total noncancer hazard index (HI) for each receptor was compared to the goal of protection of a HI equal to 1. Potential chemicals of concern (COCs) were identified as chemicals with potential cancer risks greater than 10^{-4}, and/or noncancer hazard quotient (HQ) greater than 1. Three COCs, 2,3,7,8-TCDD, PCBs, and methylmercury, were identified.

Consumption of fish and crab constitutes the predominant source of human health risk. Direct exposures to surface water and sediment do not pose human health risks in excess of NCP risk levels with the possible exception of accessible surface sediment in the RM 6 to RM 9 reach (particularly the East Bank) due to 2,3,7,8-TCDD. The primary human health risk drivers are 2,3,7,8-TCDD and PCBs. Other bioaccumulative compounds, including pesticides and mercury, also contribute to human health risk—but to a lesser extent. Background risks from consuming fish from the upstream area above Dundee Dam also exceed USEPA's risk management goals due to levels of PCBs, pesticides, and mercury in background fish.

The assumptions and approaches used in the BHHRA are health-protective, such that risks/hazards are more likely to be overestimated than underestimated.

Ecological Receptors

The objective of the Baseline Ecological Risk Assessment (BERA) was to identify unacceptable risks posed by site-related chemicals to ecological species in the LPR. Ecological receptors evaluated included benthic invertebrates, macroinvertebrates, mollusks, fish, birds, mammals, zooplankton, amphibians/reptiles, and aquatic plants. The potential for unacceptable risk was assessed using empirical and modeled data collected from a variety of chemical and biological sampling events and surveys conducted as part of the LPRSA RI. A step-by-step process included an initial screening level ecological risk assessment (SLERA), which identified media-specific chemicals of potential ecological concern (COPECs). Site-specific exposure data and a range of effect-level thresholds were used to derive risk estimates (expressed as HQs) to identify the potential for unacceptable ecological risk under baseline conditions using multiple lines of evidence (LOEs). COPECs with HQs greater than or equal to 1.0 based on effect-level toxicity reference values were identified as preliminary ecological COCs. Ecological risk drivers were identified based on a comparison to background concentrations and the uncertainty of the assessment used in the BERA. In addition, a weight-of-evidence approach was evaluated to draw conclusions about the benthic invertebrate community using a sediment quality triad approach.

Unacceptable risk to ecological species based on exceedances of a range of effect-level thresholds for various ecological receptor groups and LOEs is primarily driven by exposure to polychlorinated dibenzo-p-dioxins (PCDDs) and polychlorinated dibenzofurans (PCDFs), PCBs, and total DDx; these were the ecological risk drivers identified in the BERA. Some LOEs are stronger than others and should be weighted more heavily when used for management decisions. While there are statistically significant relationships between observed benthic community impairment and sediment chemistry/habitat conditions, the statistical relationships for individual contaminants are not strong.

Details on risks to human and ecological receptors are provided in Sections 8 and 9, respectively.

1 Introduction

1.1 Lower Passaic River Study Area Remedial Investigation Program Overview

The Lower Passaic River (LPR) is an Operable Unit (OU) of the Diamond Alkali Superfund Site. The Study Area (henceforth referred to as the Lower Passaic River Study Area [LPRSA]) comprises the tidally influenced 17.4-mile stretch of the Passaic River downstream of Dundee Dam (referred to as the LPR), its tributaries, and the surrounding watershed (Figure 1-1).

This LPRSA Remedial Investigation (RI) Report characterizes the distribution of contaminants in sediment, surface water, and biota, their fate and transport, and the risks they pose to human and ecological receptors. Its findings draw on data collected prior to and as part of the LPR Cooperating Parties Group (CPG)-led LPRSA RI and Feasibility Study (FS). It presents knowledge gained that will serve as the basis for identifying and evaluating remedial alternatives to prevent, mitigate, or otherwise respond to or remedy the release or threat of release of hazardous substances at or from the LPRSA.

1.2 Site Background

1.2.1 Site Description

The Passaic River originates in the Highlands of New Jersey (NJ) and flows through the Central Basin wetlands into Newark Bay. The Passaic River Basin is the third largest drainage system in NJ, draining over 950 square miles (Spitz et al. 2007). The 17.4-mile LPR[7] is the tidally influenced portion of the Passaic River that begins at Dundee Dam (river mile [RM] 17.4) and ends at Newark Bay (RM 0; see Figure 1-2). It is an integral part of the Greater Newark Bay Complex, along with Newark Bay, Hackensack River, Arthur Kill, and Kill Van Kull (see Figure 1-1). These waterbodies are connected through freshwater flows from the rivers to the ocean and by tidal flows that move water both inland and toward the ocean. The tidal flows also connect the Greater Newark Bay Complex to New York (NY) Harbor and Raritan Bay (also referred to as the NY/NJ Harbor Estuary or the Hudson-Raritan Estuary).

The LPR receives freshwater from the Upper Passaic River (UPR) above Dundee Dam, its three main tributaries (Saddle River, Third River, and Second River), and to a lesser extent, smaller tributaries, direct discharges from combined sewer overflows (CSOs), stormwater outfalls (SWOs), permitted municipal and industrial discharges, and direct runoff. There are no locks or dams within the LPR.

[7] The RI RMs used in this report differ from the U.S. Army Corps of Engineers (USACE) RMs of the LPR by approximately 0.3 mile due to the specification of the zero RM location. The USACE RM can be seen in Figures 1a and 1b of USACE 2010. In this RI Report, USACE RMs are designated by the prefix USACE, while the RI RMs have no such prefix. An approximate conversion to RI/FS RMs is to subtract 0.3 from the USACE RMs; the exact conversion varies along the river.

Tides are an important component of circulation and account for one-third of the river water volume below Dundee Dam at high tide under average flow conditions (USEPA 2008).

Adjacent land use is predominantly industrial and commercial between the mouth and RM 4. The LPR becomes less industrial and more commercial, residential, and recreational moving farther upstream and is increasingly residential and recreational above RM 8. Many municipalities and counties along the LPR have published master plans that call for the expansion and improvement of parks and open space along the river, which, if implemented, will lead to greater access to the river and improved ecological habitat in the future (Borough of Rutherford and CMX 2007; City of Newark 2010; City of Newark et al. 2004; Clarke Caton Hintz and Ehrenkrantz Eckstut & Kuhn 1999, 2004; Heyer Gruel 2002, 2003). The shift in the use of the waterfront, with increased public access and recreational use, will be upstream of approximately RM 3.6. The region between RM 0 and RM 2 will remain active for commercial use into the future, and the stretch from RM 2 to RM 3.6 will likely be developed into Portfields/Brownfields.

The LPR's physical characteristics have been altered by industrialization and urbanization. Most tidal marshes, wetlands, and mudflats were filled in or dredged, gradually transforming the LPR into a highly channelized river. Both banks of the lower 8 miles and a considerable length of the western bank upstream of RM 8 are dominated by hardened shorelines (e.g., sheetpile, riprap, and wood pilings) (MPI 2007), and limited areas of mudflats remain along the length of the LPR. Non-contiguous stretches of mudflat habitat are present along approximately 30% of the stretch above RM 8. Land use changes and physical alterations of the LPR shoreline have increased impervious surfaces and severely degraded the riverbank habitat and its ecological function (Iannuzzi et al. 2002). Downstream of RM 7 the riverbank comprises concrete, metal, or wood and/or riprap and supports limited vegetation (Windward 2014c). The eastern riverbank upstream of RM 7 primarily comprises vegetation and bulkhead, while the western riverbank is dominated by the presence of Route 21 and its hardened steep slopes, with only a few access points.

Chemical contamination has impacted LPR biota and limited the ecological value and habitat suitability of the LPR. Further discussion of the chemical releases and its impact on the biota of the LPR can be found in Sections 1.2.2.1 and 5.2, respectively. The historical urbanization and industrialization of the system has also resulted in the LPR exhibiting characteristics that are symptomatic of the "urban stream syndrome" (Walsh et al. 2005), including a higher frequency of flash floods, elevated nutrient levels, altered stream morphology, increased amounts of tolerant species, decreased amounts of sensitive species, and an overall decreased diversity, compared to streams not impacted by urbanization. Physical modifications to the river associated with urbanization in conjunction with releases of hazardous substances and discharges of pollutants have resulted in reduced ecological function.

1.2.2 Site History

The LPR is located within one of the major centers of the American Industrial Revolution. Early manufacturing was established near Paterson, NJ, during the post-colonial era. Beginning with cotton mills, the LPR watershed, concentrated along the river, grew to include manufactured gas plants; petroleum refineries; tanneries; ship building; smelting; pharmaceutical, electronic product, dye, paint, pigment, paper, and chemical manufacturing plants; and other industrial activity (MPI 2007). Major population centers such as Paterson and Newark transformed the watershed into a mix of residential, commercial, and industrial uses. As with many other urban river systems, the LPR has been subjected to a broad range of contaminant loadings from multiple sources (e.g., untreated industrial and municipal wastewater, CSOs/SWOs, direct runoff, and atmospheric deposition) for a long time.

Dated sediment cores show peak loading for most major contaminants occurred from the 1950s through the 1960s. This period coincides with the rapid infilling of the navigation channel (maintenance for a large part of the navigation channel ceased before 1950; see Section 1.2.2.3), resulting in relatively high contaminant concentrations in the accumulating sediment. Discharges to the LPR declined following the 1972 Federal Water Pollution Control Act amendments (Clean Water Act [CWA]) and subsequent regulations but still occur. The LPR remains non-compliant with federal and state water quality criteria and standards for many contaminants and non-chemical discharges such as pathogens and nutrients. Total Maximum Daily Loads (TMDLs) are in development for both nutrients and toxics (USEPA 2013a).

Numerous studies of the LPR have been conducted, which have resulted in an extensive database upon which to examine and understand the physical, chemical, and biological characteristics of the LPRSA. Comprehensive analyses of sediment, water chemistry and biota, ecological community surveys, physical and chemical fate and transport processes, hydrology, dredging history, anthropogenic shoreline and channel alterations, and geomorphology have yielded a good understanding of the contaminant patterns in the sediment, water column, and biota and important insights about sediment bed stability and erodibility. The knowledge gained provides a basis for crafting remediation strategies aimed at mitigating contaminant impacts and ultimately achieving CERCLA-compliant risk-based remediation goals protective of human health and ecological receptors.

1.2.2.1 Regulatory History

The LPR first became the focus of RIs because of contamination resulting from discharges from the former manufacturing facility located at 80 and 120 Lister Avenue in Newark, NJ (herein referred to as the Lister Avenue site). The Lister Avenue site, located at RM 3.1, was the home of various companies for more than 100 years. Kolker Chemical Works manufactured dichlorodiphenyltrichloroethane (DDT) and other pesticides at the Lister Avenue site in the 1940s. In 1951, the Diamond Alkali Company acquired Kolker Chemical Works. Between 1951 and 1969, the

Diamond Alkali Company (subsequently known as the Diamond Shamrock Chemicals Company, and later purchased by and merged into Occidental Chemical Corporation [OCC]) manufactured chemicals such as pesticides and phenoxy herbicides, including the primary components used to make the military defoliant Agent Orange. A by-product of the manufacturing was 2,3,7,8-tetrachlorodibenzo-*p*-dioxin (2,3,7,8-TCDD), which was released into the river. Investigators have since concluded that the Lister Avenue site was the dominant source of 2,3,7,8-TCDD and a significant source of DDT to the river (Bopp et al. 1991, 1998; Chaky 2003; Hansen 2002, Israelsson et al. 2014; Quadrini et al. 2015; Garland 2017).

In 1983, high levels of 2,3,7,8-TCDD were detected in on-site and off-site soils and groundwater at the Lister Avenue site. Based on these findings, in September 1984 the U.S. Environmental Protection Agency (USEPA) added the Diamond Alkali Superfund Site to the National Priorities List (NPL). USEPA also identified pesticides, volatile organic compounds (VOCs), and other hazardous substances in the groundwater at the site. In 1994, OCC (through the property owner Chemical Land Holdings [CLH], then known as Tierra Solutions Inc. [TSI], a subsidiary of Maxus Energy Corporation[8]) investigated a 6-mile stretch of the LPR (RM 1 to RM 7) under USEPA oversight. This investigation indicated that contaminated sediments moved upstream and downstream of this 6-mile stretch, leading USEPA, in 2002, to expand the investigation to include the 17.4-mile stretch of the LPR and Newark Bay as additional OUs.

The Diamond Alkali Superfund Site comprises four OUs:

- OU-1: The first operable unit addressed, through an interim remedy, contaminated soils, groundwater, and materials at the former Diamond Alkali manufacturing facilities at 80 and 120 Lister Avenue in Newark, NJ
- OU-2: The second operable unit addresses the contaminated sediments found in the lower 8.3 miles of the LPR[9] (also referred to as the Focused Feasibility Study [FFS] Area). The Record of Decision for OU-2 was issued on March 3, 2016.
- OU-3: The third operable unit addresses the Newark Bay Study Area.
- OU-4: The fourth OU addresses the entire 17 miles of the LPRSA; an RI/FS for OU-4 will serve as the basis for selecting a remedy for the sediments above (U.S. Army Corps of Engineers [USACE]) RM 8.3 and a river-wide remedy for surface water.

Subsequently, USEPA identified more than 100 industrial facilities within the LPRSA as potentially responsible for discharging contaminants into the river, including, but not limited to, dioxins and furans, polychlorinated biphenyls (PCBs), polycyclic aromatic hydrocarbons (PAHs), DDT and other pesticides, mercury, lead, and other metals (LBG 2014). Approximately 70 companies that owned or

[8] TSI and Maxus Energy Corporation both went bankrupt in 2017.
[9] As noted in Section 1.2.1, the 8.3-mile demarcation is based on the USACE RMs and not the RI RMs.

operated those facilities formed the CPG, which provided funding for USEPA to perform the RI/FS from 2004 to 2006 (see Figure 1-3 for CPG member locations). In 2007, the CPG entered into an administrative order on consent (AOC) to take over the performance of the LPRSA RI/FS from USEPA (2007). Accordingly, the goals and objectives of the RI, as outlined in the Settlement Agreement and Order on Consent and Statement of Work (USEPA 2007) are as follows:

1. Identify and quantify the hazardous contaminants present in sediment, water, and biota
2. Understand the vertical and horizontal distribution of hazardous contaminants in the LPRSA
3. To the extent practicable, identify sources of historical hazardous contamination
4. Quantify any significant continuing sources of hazardous contaminants
5. Understand the geomorphological setting and processes (e.g., resuspension, transport, deposition, and weathering) affecting the stability of sediment
6. Understand the key chemical and biological processes affecting the fate, transport, and bioavailability of hazardous contaminants
7. Identify the complete or potentially complete human and ecological exposure pathways for the hazardous contaminants
8. Identify current and potential future human and ecological risks posed by the hazardous contaminants
9. Collect data necessary to evaluate the potential effectiveness of natural recovery, in situ capping, sediment removal, and promising innovative technologies
10. Provide a baseline of data that can be used to monitor remedy effectiveness in all appropriate media (generally sediment, water, and biota)

1.2.2.2 Remediation History

The Lister Avenue site has undergone several remedial actions under the New Jersey Department of Environmental Protection (NJDEP) and USEPA oversight since its NPL listing in 1984 and subsequent expansion to include the LPR and Newark Bay (USEPA 2014a; TSI 2008). In 1987, USEPA selected an interim remedy for the Lister Avenue property. The remedial actions included construction of a slurry wall and floodwall around the properties, capping of the properties, and installation of a groundwater treatment system to reduce contaminated groundwater migration. Construction for the interim remedy began in April 2000 and was completed in December 2001 by OCC and TSI (USEPA 2014a). The interim remedy reduced risks associated with these properties.

Under a settlement agreement executed on June 23, 2008, OCC agreed to fund and perform the removal and disposal of 200,000 cubic yards (cy) of highly contaminated sediment located adjacent to the Lister Avenue site. Between 2011 and 2012, OCC (through TSI) removed 40,000 cy of the most elevated dioxin-contaminated sediments from the LPR in a 2-acre area in the immediate vicinity of the Lister Avenue site (Figure 1-4; also referred to as the Phase 1 removal action). An additional

removal of 160,000 cy of LPR sediments from an adjacent shoreline area on either side of the Phase 1 removal action (i.e., Phase 2 removal area) is planned but is currently not scheduled.

In 2013, under a settlement agreement executed on June 18, 2012, between USEPA and the CPG, the CPG removed approximately 16,000 cy of sediment from 5.6 acres of a mudflat centered on the eastern bank of the river at RM 10.9. This measure addressed the high concentrations of dioxins and other contaminants found at the surface of this mudflat.

1.2.2.3 Dredging History

Navigational dredging has been an important part of the LPRSA history and a significant factor in the trapping of sediments and associated contaminants. It was initiated in the late 1800s following construction of the Dundee Dam and lock system in 1858. The USACE first dredged the Passaic River for commercial navigation in 1874, initially dredging only smaller areas as needed. Numerous deepening and maintenance dredging activities took place between 1874 through the late 1920s (USACE 2007, 2010). No new channel construction was authorized after 1932; parts of the existing channel, however, were maintained for 50 more years. Authorized depths of the navigation channel are listed in Appendix A.

The last maintenance dredging conducted by USACE in 1983 removed more than 500,000 cy of sediments to a depth of 30 feet mean low water (MLW) between USACE RM 0 and USACE RM 1.9 (USACE 2010). The channel between USACE RM 1.9 and USACE RM 8.3 was last maintained in or before 1950 (i.e., before the peak loading years for most contaminants). Most of the channel upstream of USACE RM 8.3 was last dredged in the 1970s.[10] Dredging near the mouth of the LPR took place in the 1980s as part of the dredging of the Newark Bay Navigation Channel (TSI 2011).

Infilling and trapping of sediment-bound contaminants within the navigation channel has occurred to varying degrees since the cessation of maintenance dredging. Infilling was initially rapid (approximately 4 inches per year [LBG 2014]) and has since slowed. Infilling of the unmaintained navigation channel has been extensive, particularly downstream of RM 8. This is shown in Figure 1-5,[11] which contrasts the 2007 bathymetry with the authorized channel depths. The downstream sections often have 10 feet or more of sediment accumulation. Much of this infilling occurred during the years of peak contaminant discharge into the LPR, resulting in significant contaminant accumulation and subsequent burial (see Sections 3, 4, 6, and 10). Overall, the LPR has been an

[10] The stretches of the navigation channel from USACE RM 8.8 to USACE RM 9.9, USACE RM 10.3 to USACE RM 10.9, USACE RM 11.3 to USACE RM 12.4, USACE RM 12.7 to USACE RM 13.1, USACE RM 14.2 to USACE RM 14.3, and upstream of USACE RM 14.7 were last maintained before 1950.

[11] The extent and timing of the LPR dredging events in Figure 1-5 is based on a review of bathymetric information and channel history. The extent of the 1974 and 1976 events is based on pre- and post-dredging bathymetric surveys for a single, phased dredging project. The 1973 event is estimated based on aerial photography, which indicates a channel realignment during highway construction near RM 14 in the early 1970s. These estimates are more recent than those reported by Iannuzzi et al. (2002) and USACE (2010) and are thus used in place of the upriver dredging reported by those sources. More details for the dredging events can be found in Appendix A.

effective sediment and contaminant trap for more than 60 years (Chant et al. 2010; Bopp et al. 1991). Detailed evaluations of sediment erosion, deposition, and contamination patterns can be found in Sections 3 and 4.

1.3 Report Organization

This RI Report is organized into the following 12 sections:

- Section 1, Introduction: briefly describes the RI program overview and objectives and site background and history.
- Section 2, Study Area Investigation: summarizes the sediment, water column, and biota investigation activities performed in the LPRSA.
- Section 3, Overview of Hydrodynamics and Sediment Transport: discusses the transport of water and sediment in the LPR, which are important to understanding the fate and transport of contaminants.
- Section 4, Physical and Chemical Characteristics of the LPR Sediments: presents and discusses patterns in physical characteristics of the LPR sediment bed (sediment type distribution, geomorphology, etc.) and the association of these patterns with the levels and trends in contaminant concentration measured in the sediment.
- Section 5, Ecology and the Nature and Extent of Contaminants in Biota: presents the ecological setting and biological communities observed throughout the system, presents the structure of a conceptual food web for the system, and discusses the pathways by which contaminants are transferred through the food web.
- Section 6, Contaminant Fate and Transport in the Lower Passaic River: discusses the conceptual site model (CSM) of contaminant fate and transport (CFT) in the system.
- Section 7, Summary of Modeling Results for the Lower Passaic River Study Area: presents a summary of the development and application of numerical models to describe hydrodynamics, sediment transport, CFT, and contaminant bioaccumulation in the system.
- Section 8, Baseline Human Health Risk Assessment Summary: summarizes the Baseline Human Health Risk Assessment (BHHRA) conducted as part of the RI.
- Section 9, Baseline Ecological Risk Assessment Summary: summarizes the Baseline Ecological Risk Assessment (BERA) conducted as part of the RI.
- Section 10, Natural Recovery: discusses the recovery observed in sediment and biota contaminant levels.
- Section 11, Summary and Findings: presents a summary of the conceptual understanding of the system and findings derived from the data collected during the RI.
- Section 12, References: provides citations for all documents referred to throughout this RI Report.

2 Study Area Investigation

2.1 Introduction

This section describes the datasets used in the LPRSA RI. These datasets include USEPA-approved RI studies conducted by the CPG and RI/FS-related studies by the USEPA and its partner agencies. Since the 1980s, other parties have conducted studies that also help to understand the physical, chemical, and biological characteristics of the LPRSA and surrounding region (e.g., Newark Bay). Many of these studies were performed for specific purposes not related to the RI with varying study objectives, sampling protocols, and locations, and several studies have incomplete or missing documentation of sampling and analytical methods or quality control programs, including analytical data validation. The earliest of these studies was performed by IT Corporation (1986) between 1983 and 1985 for the Diamond Shamrock Chemicals Company, collecting sediment samples from the LPR.[12]

Datasets collected in 2000 and later (post-2000) were generally developed under a consistent set of objectives and protocols and provide spatial coverage throughout the LPR, though some earlier datasets are also relevant to the RI/FS and are incorporated into the analyses. The studies used in this RI are summarized in the following sections and by media in Tables 2-1 (sediments), 2-2 (water), 2-3 (biota tissue), 2-4 (biological communities and habitats), and 2-5 (bathymetry and physical characteristics). Data reports that provide details for CPG studies are provided in Appendix B, while data validation reports for these studies are provided in Appendix C. The BERA and BHHRA Reports are provided in Appendix D. The RI analytical chemistry database is provided in Appendix E. It should be noted that the pre-2000 datasets and some of the post-2000 datasets listed in Tables 2-1 through 2-5 were not collected by the CPG. As an example, data collected by the Joint Defense Group (JDG) in the TSI Phase 1 Removal Area, described in Table 2-1, were collected using the same protocols as the RI studies and were evaluated for the RI. TSI also collected samples in the Phase 1 Removal Area, and those data were reviewed in the context of the findings in this report.

2.2 Previous Investigations

2.2.1 Tierra Solutions Lower Passaic River Remedial Investigation Data

TSI performed remedial investigative studies for the region between RM 1 and RM 7 pursuant to a 1994 AOC with USEPA. These studies were conducted in 1995 and 1996 and included sampling water, sediments, and biota, as well as physical and process-related studies, such as sediment transport. Sediments were analyzed for contaminants, radiochemistry, and geotechnical properties (CLH 1995; see Table 2-1). Between 1999 and 2001, additional sampling was performed to

[12] LPR samples (RM 0.5 to RM 5.5) had median 2,3,7,8-TCDD concentrations of 800 to 900 nanograms per kilogram (ng/kg). Maximum 2,3,7,8-TCDD concentrations were 1,800,000 ng/kg at depths of 8 to 10 feet near RM 3; 15,600 ng/kg at depths of 4 to 5 feet between RM 0.5 and RM 2.5; and 32,000 ng/kg at depths of 8 to 10 feet between RM 3 and RM 5.5 (IT Corporation 1986).

characterize factors affecting ecological and human health risk, including investigations of surface water (i.e., total suspended solids [TSS] and other non-contaminant parameters), surface sediments (0 to 6 inches), and tissues (including bioaccumulation) and to survey ecological habitats (see Table 2-4). Bathymetric surveys were also performed (see Table 2-5; CLH 1999).

2.2.2 Other Data Sources

The USEPA's database for the LPR, the Passaic River Estuary Management Information System (PREmis), contains data from numerous studies conducted in the LPR and the region (including Newark Bay) dating back to the mid-1980s. Many of these datasets were collected for specific, non-RI purposes such as dredging or engineering studies performed by the USACE or for state or federal monitoring programs. Many of these studies have incomplete documentation of methods or quality control programs, including analytical data validation. While they were not used for the risk assessment because of this lack of documentation, some of these data have been used qualitatively to support a historical understanding of the nature and extent of contaminants in the LPRSA and to inform the CSM (see Tables 2-1 through 2-5).

2.3 Newark Bay Remedial Investigation Data

Similar to the LPRSA, the Newark Bay Study Area (NBSA) is an OU of the Diamond Alkali Superfund Site. TSI conducted two phases of sampling, in 2005 and 2007, as part of the NBSA RI (TSI 2004). Phase 1 consisted of sediment sampling, a bathymetric survey, and an assessment of the biologically active zone in the sediment column. Additional sediment sampling was conducted during Phase 2. Sediment samples were collected by coring and surface grabs, with a goal of characterizing the sediment column down to the 1940-time horizon (see Table 2-1). Both phases included sampling in the Hackensack River, Arthur Kill, and Kill van Kull—locations included nearshore zones, shoals, and channels. Further details are included in Table 2-1.

2.4 Lower Passaic River Study Area Remedial Investigation Data

Numerous studies have been conducted as part of the LPRSA RI under USEPA oversight. An overview of these studies, by media, is provided in the following subsections.

2.4.1 Bathymetry Surveys, Side Scan Sonar, Probing, and Sediment Characterization

Geophysical and bathymetric surveys performed in the LPR are listed in Table 2-5. Seven recent bathymetry surveys were performed between 2007 and 2012, using the same methodology and equipment (to the extent practicable) to provide comparable datasets. Depth-difference maps were calculated from paired surveys; these data were used to assess changes in bathymetry (AECOM 2010). The use of bathymetry as applied to specific analyses is discussed in Section 4, Appendix A, and Attachment B of Appendix M.

These surveys have been augmented with other datasets that are listed in Table 2-5. Bathymetric surfaces generated by digitizing point data from survey maps dating back to 1932[13] have been assembled to study the evolution of the LPR sediment bed over the years.

Sediment bed properties have been characterized in various studies using side scan sonar (SSS), probing, grain size, and other methods[14] for surface and subsurface sediment (below 6 inches) samples (Table 2-5). The bathymetric and sediment property data were used to support contaminant mapping and sediment stability evaluations. The SSS also included a debris/obstruction survey, which identified multiple features that could serve as obstructions to future dredging and capping operations. A gradiometer survey also identified magnetic signatures of numerous large shallow objects, large deep objects, and smaller shallow objects.

2.4.2 Contaminant Source Investigations

Potential external sources of contaminants to the LPR include the UPR (i.e., above Dundee Dam), Newark Bay, major tributaries (i.e., Saddle River, Third River, and Second River), and CSOs/SWOs and other point sources (e.g., industrial and municipal discharges). Several sampling programs have targeted freshwater inputs of solids and water column (total or dissolved phase), and solids-borne contaminants, by sampling surface sediments and water above the head-of-tide (HOT), at or above Dundee Dam and in the major tributaries. Sources of data for the UPR and the tributaries (above the HOT) are provided in Tables 2-1 and 2-2.

For USEPA's 2005 Small Volume Sampling Program, Malcolm Pirnie, Inc. (MPI), collected water column samples at the HOT of the major tributaries and at Ackerman Avenue Bridge (RM 17, intended to represent inputs from Dundee Dam) on November 10, 2005.

In the UPR, at Little Falls, water column contaminants were sampled four times (single-day events) between June 2000 and October 2001 under various flow conditions by the U.S. Geological Survey (USGS) for NJDEP's New Jersey Toxics Reduction Work Plan (NJTRWP) program, which is an element of the Contaminant Assessment and Reduction Project (CARP) (Bonin and Wilson 2006; Wilson and Bonin 2007). Contaminants were measured in water and on suspended solids.

Surface water and sediment samples were collected just above Dundee Dam, in Dundee Lake, to characterize the upstream boundary conditions for polychlorinated dibenzo-p-dioxin (PCDDs), polychlorinated dibenzofurans (PCDFs), PCBs, and other parameters of interest during the Chemical Water Column Monitoring (CWCM; December 2012 and June 2013) and Physical Water Column Monitoring (PWCM; October 2009 through November 2010) programs (Table 2-1). Additional surface sediment samples were collected above Dundee Dam in November 2012 as part of the Freshwater

[13] The accuracy of the methods and technologies used to generate these bathymetric datasets are discussed in Appendix A.
[14] Methods include magnetometer, fathometer, and gradiometer, as mentioned in Table 2-5.

Reference and Background Conditions Study (Table 2-1; Windward 2012a, 2019a). The sediment samples were collected at 24 Sediment Quality Triad (SQT) locations and at 16 chemistry-only locations. The objective of the November 2012 sampling event was to provide background concentrations and reference data to support the baseline risk assessment.

MPI collected surface sediment samples for radionuclide analysis (beryllium-7 and cesium-137 [Cs-137]) in Dundee Lake in 2005. They collected samples for geochronology and contaminants in Dundee Lake sediments using high-resolution coring at six locations in 2007 (Table 2-1).

CSO and SWO discharges are other potential sources of contamination to the LPRSA. TSI conducted a CSO sampling program in 1997 (Table 2-2). As part of the NJTRWP program, CSO and SWO outfalls were sampled during three wet weather events between 2001 and 2004 by the Great Lakes Environmental Center (2008). During winter 2008, MPI conducted high-flow storm event sampling during four events to capture the effects of CSO/SWO discharges. This study incorporated large-volume sampling and sediment traps to characterize solids-sorbed contaminant loadings. Locations included the major tributaries and Ackerman Avenue Bridge (RM 17) as well as CSO outfalls in Newark and SWO outfalls in Nutley, Belleville, Rutherford, and Lyndhurst (Table 2-2).

Evaluations of tributary and CSO/SWO inputs to the LPRSA are presented in Section 4.

2.4.3 Sediment Investigations

2.4.3.1 U.S. Environmental Protection Agency Sediment Data

Sampling programs that characterize the nature and extent of contaminants in LPRSA sediments have been described as low resolution, sampling relatively coarse intervals (i.e., typically 6 inches or greater) of the sediment column, or high resolution, sampling intervals on the scale of 1 inch (2.54 centimeters [cm]) to investigate short-term deposition and fine-scale gradients in chemical concentrations.

MPI, on behalf of USEPA, implemented several sediment sampling programs (Table 2-1). These studies collected surface sediment grabs and cores for sampling of low-resolution depth intervals and high-resolution depth intervals. High-resolution cores were used primarily for radiological dating, with a subset that was used to characterize contaminants. The more extensive low-resolution coring and sediment grab programs were used to characterize contaminant distribution and physical properties. While the primary focus of high-resolution sediment coring in 2005 and 2007 was radiological dating, analyses for contaminants were performed on a subset of the high-resolution cores. Further details are provided in Table 2-1.

2.4.3.2 Cooperating Parties Group Low Resolution Coring

CPG's Low Resolution Coring (LRC) program was conducted between 2008 and 2013 and included four sediment sampling programs to determine the nature and extent of contamination, including identification of potential source areas, and described physical characteristics of the LPR sediment. The program collected both low-resolution cores and high-resolution cores with finer segmentation of the samples. In addition, bathymetry surveys and a hydrodynamic field investigation (HFI) were also completed and are discussed in Appendix B.

The four LRC field programs are as follows: 2008 LRC, RM 10.9 Characterization with addenda, LRC Supplemental Sampling Program (SSP) (AECOM 2012a), and LRC Second Supplemental Sampling Program (SSP2) (AECOM 2013). The 2008 LRC field program was conducted to characterize surface and subsurface sediments throughout the LPR. Sediment probing was conducted between RM 8.5 and RM 12.3 to provide a more detailed assessment of the areal extent and thickness of sediment deposits in this reach. Sediment program locations and sample counts and descriptions of the analyses performed are provided in Table 2-1. Details regarding the sample locations, sampling protocols, segmentation schemes, and laboratory analyses employed during each of these sampling events are provided in Appendix B.

The 2011 RM 10.9 field program was conducted to characterize sediments collected from 54 cores within a deposit along the east bank for a time-critical removal action (AECOM 2011a). Low-resolution cores, high-resolution cores, and surface grab samples were collected (see Table 2-1 and Appendix B). An additional sampling program conducted in 2012 (Addendum A of the RM 10.9 Characterization Program [AECOM 2012b]) collected and analyzed sediment samples from 15 cores along the shoreline. Performed concurrently with the RM 10.9 Sediment Characterization Program, the HFI program was designed to address identified data gaps and to provide the data necessary to characterize current velocities and water levels at multiple locations within the RM 10.9 Study Area, including water flux data from the Third River (AECOM 2011b).

The 2012 LRC SSP and 2013 LRC SSP2 programs were conducted to fill data gaps identified by USEPA and CPG during the review of the 2008 LRC data. Low-resolution cores, high-resolution cores, and surface grab samples were collected between RM 4 and RM 13 during the LRC SSP and between RM 7 and RM 14 during the LRC SSP2 (see Table 2-1 and Appendix B). Additionally, as part of the LRC SSP2 program, sediment probing was performed to provide information on the sediment surface characteristics (e.g., armored, hard bottom, and sediment), the presence/absence of sediment, sediment thickness, and the general nature of the sediment (e.g., silt or sand) in seven areas between RM 8.3 and RM 14.0 of the LPR and in the Third River.

After an evaluation of the 2008 LRC program data, USEPA directed that all validated PCDD/PCDF data generated by the CPG as part of the USEPA-approved LRC Quality Assurance Project Plan

(QAPP) be adjusted to address what was characterized in reports prepared by USEPA's oversight consultant (MPI 2009) and a USEPA Office of Water consultant (CSC Environmental Solutions 2010, 2011) as a "disparity" or "systematic bias" between the split samples analyzed by the CPG's laboratory (Columbia Analytical Services) and USEPA's laboratory (Axys Analytical Services). It was agreed that a unique validation qualifier "F" would be assigned to adjusted results. This adjustment was only applied to 2008 LRC data. The CPG changed dioxin/furan laboratories for the subsequent three LRC field programs.

2.4.3.3 Surface Sediment Collection

Concurrent with studies of benthic communities, sediment toxicity, tissue contaminant concentrations, and bioaccumulation, surface sediment samples were collected in fall 2009 (Windward 2015). In addition, concurrent with sampling of benthic forage fish tissue contaminant concentrations, surface sediment samples were also collected in summer 2010 (Windward 2015). Locations, methods, and results are found in the data reports included in Appendix B.

In November 2012, surface sediment samples were collected from above Dundee Dam as part of the Freshwater Reference and Background Conditions Study (Table 2-1; Windward 2012a, 2019a). The sediment samples were collected at 24 SQT locations and at 16 chemistry-only locations. The objective of the sampling was to provide background concentrations and reference data to support the baseline risk assessments.

2.4.4 Surface Water Investigations

2.4.4.1 U.S. Environmental Protection Agency Water Column Data

MPI, on behalf of USEPA, undertook several water column sampling programs between 2005 and 2009 to characterize chemical and physical conditions within the LPR. These programs included small-volume (SV) sampling, high-volume (HV) sampling, high-flow storm event sampling, and PWCM (Table 2-2). The SV program was conducted in 2005 and aimed to capture a snapshot of the river conditions at select locations during an incoming tide. HV sampling was conducted in October 2005 to evaluate different sampling techniques (LBG 2014).

2.4.4.2 Physical Water Column Monitoring

The PWCM program was conducted between 2009 and 2012 (AECOM 2019a). The overall objective of the PWCM was to provide the data necessary to characterize estuarine dynamics and movement of suspended sediments in the LPR and Newark Bay. The sampling activities for the PWCM program included long-term mooring deployments, boat-based transect sampling, wet weather sampling, and high-flow/flood sampling (Table 2-2). Physical properties measured included currents, wave height, temperature, conductivity, turbidity, dissolved oxygen (DO), solids, and total organic carbon (TOC). A 120-day DO monitoring program was performed to characterize DO concentrations in LPRSA bottom

water and above Dundee Dam during periods of low freshwater flow to support the BERA (Windward 2012b). The Characterization Summary Reports provide detailed information for each PWCM event (Appendix B).

2.4.4.3 Chemical Water Column Monitoring

The CWCM program (also referred to as WCM/Chemical Data Collection) was conducted to characterize chemical concentrations associated with the movement of suspended sediments over a range of tides and flow regimes. Sampling took place in 10 events from August 2011 through July 2013. The CWCM program incorporated two types of sample collection methods: an HV program (AECOM 2012c) and an SV program (AECOM 2012d). The timing of events and the locations selected for the SV program were designed to provide spatial coverage in the LPRSA and NBSA and to capture features such as the limit of the saltwater incursion in the LPR under routine, high-flow and low-flow/spring tide conditions (Table 2-2; AECOM 2012c). The SV program included a location above Dundee Dam to support modeling, characterization of upstream loading to the LPRSA, and baseline risk assessments. The HV program characterized solid-phase and dissolved-phase concentrations of PCB congeners and PCDD/PCDFs in the LPRSA and the NBSA (Table 2-2). The Characterization Summary Reports provide additional detailed information for both CWCM programs (Appendix B). Additionally, results of these programs have been documented in two reports (AECOM 2019b, 2019c).

2.4.5 Ecological Investigations

Several ecological investigations supporting the BERA (Section 9 and Appendix D) and the BHHRA (Section 8 and Appendix D) were performed as part of the LPRSA RI/FS. The investigations included an SQT assessment (i.e., sediment toxicity, benthic community assessment, and sediment chemistry), bioaccumulation benthic invertebrate testing, and tissue analyses of fish and decapods. Other investigations included seasonal invertebrate, fish, and avian community surveys; habitat identification surveys; and an in situ caged bivalve study. A summary of ecological studies conducted within the LPRSA is provided in Table 2-4. Details are provided in data reports provided in Appendix B.

2.4.5.1 Toxicity and Bioaccumulation Testing

Surface sediment samples collected in 2009 from 98 SQT-designated locations were evaluated for sediment toxicity (Table 2-4; see Table 2-1 for sediment chemistry). Twenty-four SQT locations sampled in 2012 from the Passaic River above Dundee Dam were also evaluated for sediment toxicity (Table 2-4). Surface sediment samples from 20 locations were evaluated in laboratory bioaccumulation tests (Table 2-3; Windward 2018). Details on test methods and results are provided in Appendix B.

2.4.5.2 Fish and Decapod Tissue Collection

Fish and decapod (i.e., crab) tissue data were collected to evaluate ecological and human health risks throughout the LPRSA during August and September 2009 and between May and September 2010 (Table 2-3; Windward 2010a, 2011b). Details on survey methods and results are found in the community survey and tissue collection data reports included in Appendix B (see also Table 2-3). Species collected from the LPRSA included American eel, brown bullhead, common carp, channel catfish, largemouth bass, northern pike, smallmouth bass, white catfish, white perch, white sucker, and small forage fish (i.e., mummichog, gizzard shad, pumpkinseed, silver shiner, spottail shiner, mixed forage fish, and white perch), and blue crab. Crayfish were an initial decapod target organism, but few were collected during sampling efforts.

Fish tissue samples were collected from above Dundee Dam in 2012 to characterize contaminant concentrations in biota upstream of the LPRSA for use in the baseline risk assessments (Table 2-3). Species collected from above Dundee Dam included American eel, brown bullhead, common carp, channel catfish, northern pike, smallmouth bass, white perch, white sucker, and small forage fish (i.e., pumpkinseed, silver shiner, and banded killifish). Tissue samples were composited and submitted for chemical analysis.

2.4.5.3 Benthic Community Surveys

Benthic invertebrate community surveys were conducted in the LPRSA in fall 2009, as part of the 2009 sediment collection described in Section 2.4.3.1, and in spring (June) and summer (July/August) 2010 (Table 2-4; Windward 2014a, 2014b). These surveys evaluated the benthic invertebrate community through a qualitative assessment of seasonal changes in the benthic invertebrate community structure in the LPRSA (Table 2-4; Windward 2010b, 2015). Details on survey methods and results are found in the community survey reports included in Appendix B. The survey locations were co-located with samples collected for sediment chemistry and toxicity testing (discussed in Appendix D).

2.4.5.4 Fish Community Surveys

Fish community surveys were conducted concurrently with the fish and decapod tissue collection efforts in August and September 2009, January and February 2010, and again in June and July 2010 (Table 2-4; [Windward 2010a, 2010c, 2011b]). The primary objective of the fish community surveys was to assess the overall health of fish populations in the LPRSA using data on seasonal relative abundance, structure, and indices of the fish community. The results of the fish community survey and pathology evaluations, along with the remaining lines of evidence (LOEs) for fish and decapods, as specified in the USEPA-approved *LPRSA Human Health and Ecological Risk Assessment Streamlined 2009 Problem Formulation* (Windward and AECOM 2009), hereafter referred to as the Problem Formulation Document (PFD), were presented and interpreted in the BERA (see Appendix D). Additional details on survey methods and results are found in the community survey data reports included in Appendix B.

2.4.5.5 Avian Community Survey

Four seasonal bird surveys were conducted to characterize the seasonal use of river zones and habitats by the avian community throughout the LPRSA in summer (August) 2010, fall (October) 2010, winter (January) 2011, and spring (May) 2011 (Table 2-4; Windward 2011a, 2019b). Survey data were used in conjunction with previous site-specific avian community surveys (e.g., 1999 to 2000 LPRSA avian community surveys performed by TSI [BBL 2002; Ludwig et al. 2010; Iannuzzi and Ludwig 2004]) to identify exposure areas for bird populations for the BERA. Avian data were compared with habitat and shoreline condition data collected during a habitat identification survey to characterize avian habitat areas in the LPRSA. Additional details on survey methods and results are found in the community survey data report included in Appendix B.

2.4.5.6 Habitat Identification Survey

The 2010 habitat identification survey was conducted to characterize shoreline habitat types and shoreline conditions throughout the LPRSA and select tributaries (Table 2-4; Windward 2014c). The results were used in conjunction with results of previous habitat surveys, including the 1999 to 2000 habitat characterization survey conducted between RM 1 to RM 7 of the LPRSA (TSI 2002), the ecological benchmarking survey presented by Shisler et al. (2008), and the vegetation sampling, wetland delineation, and bio-benchmark surveys conducted by the USACE et al. (2008). Additional details on survey methods and results are found in the habitat identification survey and characterization report included in Appendix B.

2.4.5.7 Caged Bivalve Study

A 90-day in situ caged bivalve study was conducted in spring 2011 to evaluate the potential for caged bivalves to be used for long-term monitoring of chemicals near the bottom of the water column (Table 2-3, Windward 2019c). Two species of mussels were used in the in situ caged bivalve study: eastern elliptio (*Elliptio complanata*), a freshwater mussel (deployed from RM 10 to RM 17.4), and ribbed mussel (*Geukensia demissa*), an estuarine mussel (deployed from RM 0 to RM 10). Tissue samples from both species were collected prior to deployment and at the end of the exposure period and submitted for analytical chemistry analysis (Windward 2019c). Additional details on deployment methods and results are found in the caged bivalve study report included in Appendix B.

3 Overview of Hydrodynamics and Sediment Transport

The 17.4-mile LPR exhibits characteristics typical of a highly urbanized river system. Its large urban watershed and many industrial facilities have been a source of anthropogenic chemicals such as dioxin/furans, PAHs, PCBs, pesticides, and metals, as well as non-chemical stressors, including pathogens. The legacy contamination in the sediment bed continues to be a major contaminant source to the LPR. The river has a limited and impaired habitat for fish and shore birds as a result of centuries of industrial activities and development (e.g., contamination, channelization, shoreline hardening, dredging, and dam construction). Non-native species such as common carp have proliferated and influenced the food web. Along its lower portion (i.e., below RM 8), a majority of the river is highly industrialized; access to and human contact with the river's water and sediment is limited. Its upper portion, while still urban, does support some recreational use along the eastern shore (such as crewing activities), although access is limited to parks, public spaces, and some residences. Access to the western shore is limited to specific access points because of Route 21 located along the majority of the western bank of the river. As noted in Section 1.2, many municipalities and counties along the LPR have published master plans that call for the expansion and improvement of parks and open space along the river, which, if implemented, will lead to greater access to the river and improved ecological habitat (Borough of Rutherford and CMX 2007; City of Newark 2010; City of Newark et al. 2004; Clarke Caton Hintz and Ehrenkrantz Eckstut & Kuhn 1999, 2004; Heyer Gruel 2002, 2003). The increased access to the river may result in increased exposure to human receptors.

Contamination, SWO/CSO discharges, urban runoff, and natural sources of organic matter influence water and sediment quality and affect ecosystem health. The predominant source of organic matter is the upstream river flowing over Dundee Dam (Figure 3-1). Salinity gradients are one of the factors that affect the longitudinal distribution (i.e., from the mouth of the LPR to Dundee Dam) and composition of benthic communities. Their vertical distribution in sediments is generally limited by the shallow redox potential discontinuity (RPD) layer depth (Germano & Associates 2005), though several invertebrate species observed in the LPR can burrow into anoxic sediments below the RPD layer.[15] The ecology of fish and invertebrate communities is also impacted by contamination, high turbidity, brief periods of depressed DO, nutrient inputs, and variations in sediment grain size. Further discussion of the ecology and distribution of contaminants in biota is presented in Section 5.

This section presents the physical, hydrogeological, hydrological, and sediment characteristics pertinent to the fate and transport of sediments and contaminants so as to provide a basis for understanding contamination patterns and potential recovery. Although contaminant patterns and recovery are generally a function of source locations and history, they are also determined by the

[15] The RPD is the transition between oxygen-rich and oxygen-poor sediment layers.

evolution of the sediment deposits, their characteristics, the manner in which sediments are transported, and the stability of the sediment bed. Knowledge of these factors helps explain why contaminant concentrations vary in the way they do. It also provides a framework for crafting remediation strategies.

3.1 Physical Features

The LPR is a classic partially mixed coastal plain estuary of relatively shallow depth, gently sloping bottom, and expanding cross section from Dundee Dam to Newark Bay. It includes meanders reflective of its ancestral river channel. Its sediment dynamics, sediment transport, and geomorphological features reflect fluvial and estuarine processes influenced by navigational dredging and subsequent infilling after maintenance of the navigational channel ceased.

From Dundee Dam (RM 17.4) to approximately RM 14, the LPR behaves like a tidal river; that is, a freshwater stream influenced by tides. Within this stretch, the river cross section expands rapidly from approximately 200 square feet (ft^2) downstream of Dundee Dam (see Figure 3-6 of LBG 2014) to approximately 3,000 ft^2 at RM 14 (Figure 3-2). Between approximately RM 14 and RM 8, the LPR behaves more like a fluvial estuary, with a mix of freshwater and brackish waters and geomorphology strongly influenced by riverine processes in addition to tides. Here, the river cross section changes modestly, increasing to approximately 4,600 ft^2 near RM 9 before constricting down to approximately 3,000 ft^2 at RM 8. Downstream of RM 8, the LPR behaves like an upper estuary, that is, characterized by the mixing of freshwater and saltwater, and the strong influence of estuarine circulation. This region exhibits the expanding cross section typical of coastal plain estuaries, reaching almost 10,000 ft^2 at RM 1 and more than 80,000 ft^2 by the mouth at RM 0 (Figure 3-2). Note that the locations designated as transitions in the nature of the river are approximate, as the actual RM where conditions change varies with river flow and tidal forcing.

3.2 Hydrogeology

The LPRSA is on the bedrock unit known as the Passaic Formation. The bedrock surface of the Passaic Formation was shaped by the Late Wisconsin glaciation, whose retreating ice front produced 250-feet-thick glacial deposits comprising stratified sand, gravel, silt, and clay. These are, in turn, overlain by 10- to 20-foot-thick surficial deposits comprising artificial fill, alluvial, alluvial fan, swamp and marsh, stream terrace and estuarine sediments, windblown deposits, and talus of postglacial age. The riverbed is mainly alluvium (i.e., sand, silt, pebble/cobble gravel, and minor clay) underlain by Rahway Till (i.e., silty sand and sandy clayey silt) and glacial lake deposits (i.e., fine sand, pebble-gravel, and some silt) (Stanford 2002).

The hydraulic conductivities in the different sediment deposits govern groundwater flow within them. The sand and gravel in the glacial deposits are highly permeable with hydraulic conductivities ranging from 10^1 to 10^3 feet per day (ft/day), whereas the silt and clay deposits have a low

permeability of 10^{-5} to 10^{-3} ft/day. The fine sand and silt in lake bottom, alluvial, and estuarine deposits and the sandy silt in till have hydraulic conductivities of 10^{-3} to 10^{-1} ft/day (Stanford 2002). The estuarine and salt marsh units have variable hydraulic conductivities based on their silt and clay content. These impervious/semi-impervious boundaries surrounding the LPR restrict groundwater flow upward through the sediment bed or horizontally from the surroundings, likely making groundwater recharge an insignificant component of the flow balance of the system. Localized areas of groundwater recharge may, however, exist.

3.3 Hydrology and Hydrodynamics

The hydrodynamics of the LPR are governed by the freshwater discharge (also referred to in this document as freshwater flow or river inflow), tides, estuarine circulation, and changes in mean water level caused by storm surges in the Atlantic Ocean. River inflow enters over Dundee Dam and from several tributaries. Flow rates at the USGS station at Little Falls (1950 to 2014) and at Dundee Dam (2008 to 2014)[16] are shown in Figures 3-3a and 3-3b.

The highest inflow typically occurs in March (averaging 2,030 cubic feet per second [cfs] at Little Falls) due to snow melt and spring rains (Figure 3-4). The lowest flows generally occur between July and October (averaging 567 cfs at Little Falls). The annual average discharge is 1,140 cfs at Little Falls (equivalent to 1,200 cfs at Dundee Dam, based on drainage-area proration). Periods of note that are discussed further in Sections 3.4 and 4 include:

1. The consistently low-flow period (i.e., prolonged drought condition) extending from mid-1964 to the beginning of 1967 (Figure 3-3a), which corresponds with major industrial activity along the river, and to the peak production period at the Lister Avenue site (Silbergeld et al. 1993)
2. Two 1-in-25-year storm events in March 2010 and March 2011 (Table 3-1)
3. A 1-in-90-year storm event (Watson et al. 2014) in August 2011 caused by Hurricane Irene

Hurricane Sandy, which moved through the area on October 29, 2012, was not a significant flow event (flow peaked at approximately 6,000 cfs on November 1, 2012), though the associated storm surge caused flooding and property damage.

Water levels vary with tidal stage over a range between 0.9 and 2.2 meters (m) (3.0 to 7.2 feet) for neap and spring tides, respectively. The spring-neap period is 13.5 days.

Salinity exhibits a pronounced longitudinal gradient. The denser saline waters tend to flow beneath the freshwater discharge from Dundee Dam, resulting in turbulent mixing and a partially mixed water

[16] The USGS gage at Dundee Dam became active in April 2007.

column.[17] The baroclinic pressure gradient induced by this longitudinal salinity gradient generates a two-layer flow pattern known as estuarine or gravitational circulation, with a net down-estuary[18] flow in the upper layers of the water column and a net up-estuary flow near the bed. The net up-estuary flow provides a mechanism for water and solids originating from the lower portions of the LPR to move upstream. These dynamics are a defining component of sediment transport in the LPR and strongly influence contaminant patterns and ongoing natural recovery.

The interface between the fresh and brackish waters is called the salt front. Its location depends on the freshwater discharge, inter-tidal timing (spring/neap), intra-tidal timing (flood/ebb), and offshore water surface level fluctuations (set-up/set-down events). The salt front typically resides within the lower 10 miles and moves several miles during each tidal cycle (MPI 2007; Cañizares et al. 2009), but it can extend upstream beyond RM 14 under extreme low-flow conditions (SEI and HDR|HydroQual 2011).

Hydrodynamic modeling of the period from 1995 to 2004 (performed using a continuous simulation developed by USEPA Region 2 as part of the hydrodynamic model calibration and documented in the *Final Hydrodynamic Modeling Report* [HQI 2008]) indicates that the salt front is upstream of RM 5 when discharge at Dundee Dam is below the annual average of 1,200 cfs (Figure 3-5[19]; HQI 2008). The salt front is pushed downstream with increasing flow: near RM 3 at 2,000 cfs; below RM 2 at 6,000 cfs; and below RM 1 at 10,000 cfs. The location of the salt front is also a function of the tidal cycle, with tidal excursion lengths on the order of 2.5 to 4.5 miles from low to high tide.

During river flows less than a few hundred cfs, the salt front can extend upstream of RM 14.[20] Extreme droughts, such as those that occurred in the 1960s (e.g., September 1964 had a monthly mean flow of 29 cfs at Little Falls; Figure 3-3a) can result in extreme upstream limits of the tidal salt front, allowing for upstream migration of contaminated sediments from the lower portion of the LPR.

Various zones or river sections based on salinity and the location of the salt front (e.g., freshwater, transitional, and brackish) have been proposed. The boundaries for these sections are qualitative due to the variability in the location of the salt front. Salinity zones important for discussions on LPRSA ecology are included in Section 5.

[17] Saltwater is denser than freshwater, so it remains deeper in the water column as it moves upstream from a river mouth. Freshwater, being less dense, floats above the saltwater layer as it moves from upstream toward the river mouth. As the two layers mix, a wedge shape is formed in the saltwater intrusion (when viewing the river longitudinally).

[18] Upstream and up-estuary and downstream and down-estuary are used interchangeably in this document.

[19] The salt front is defined in Figure 3-5 as the location of 2 parts per thousand (ppth) salinity at the bottom of the water column.

[20] The salt front locations shown in Figure 3-5 are shifted somewhat upstream if a lower salinity threshold is used to define the salt front. For example, Sea Engineering and HDR|HydroQual (SEI and HDR|HydroQual 2011) presents a similar figure of model results using a salinity threshold of 0.5 ppth (instead of 2 ppth), which indicates salt front migration above RM 14 under extreme low-flow conditions.

3.4 Sediment Transport

The transport of sediment in the LPR is governed by the freshwater discharge, estuarine circulation, and tidal asymmetry. While freshwater discharge transports solids from upstream to downstream, tidal transport also moves downstream solids to upstream regions. The various features influencing tidal transport are discussed in the following subsections.

3.4.1 Estuarine Circulation

As described in Section 3.3, the baroclinic pressure gradient induced by the longitudinal salinity gradient in an estuary generates a two-layer flow pattern known as estuarine circulation. There is a net down-estuary flow in the upper layers of the water column and a net up-estuary flow near the bed. This net up-estuary flow provides a mechanism for water and solids originating from the lower portions of the LPR to move upstream.

The salt front typically coincides with the estuarine turbidity maximum (ETM), which is the region of an estuary with maximum turbidity that is associated with solids trapping (Dyer 1995; Chant et al. 2010). The ETM results from a combination of re-suspension of bottom sediments by tidal current stresses and the convergence of bottom water transport at the limit of salt intrusion (Sanford et al. 2001). The ETM collects flocculated material that settles at intermediate speeds, typically about 1 millimeter (mm) per second (Geyer 1993). The ETM migrates upstream and downstream, both seasonally and daily, due to tidally influenced movement of the salt wedge; therefore, the ETM is not a single point in space but is integrated over several miles, appearing spatially as a gradient that decreases with distance from the salt wedge.

A well-defined ETM has been confirmed by shipboard measurements of salinity and suspended sediment concentrations (SSCs) along longitudinal transects of the LPR and Newark Bay (Chant et al. 2010) and suspended sediment data collected during the fall PWCM program (Mathew et al. 2011). Transects showing salinity contours and SSCs under low-flow conditions (June 23, 2005, with discharge of 250 cfs at Little Falls) and high-flow conditions (a 16,000-cfs storm event on March 16, 2010) are shown in the upper and lower panels of Figure 3-6.[21] Both transects show higher SSCs in the vicinity of the salt front (defined by the 2 parts per thousand [ppth] isohaline) than at upstream or downstream locations. During the low-flow survey, both the salt front and the ETM are located at RM 7, with depth-average SSCs of approximately 100 milligrams per liter (mg/L). In contrast, during the high-flow survey, the salt front and the ETM are pushed to RM 0 with much higher depth-average SSCs of approximately 250 mg/L, a likely consequence of the higher river discharge. Higher river flow can contribute to elevated concentrations within the ETM via higher solids loading from Dundee Dam, as well as erosion (beyond that experienced under typical tidal currents during

[21] Datasets were generated by Dr. Robert Chant of the Institute of Marine and Coastal Science, Rutgers University. Salinity is represented by the red contours labeled in white text.

low-flow conditions) up-estuary of the salt front location. Around the slack phase of the tide, as flow velocities and shear stresses decrease, suspended sediments deposit from the water column, with the highest deposition fluxes expected within the ETM.

The estuarine circulation process, and the net upstream movement of suspended solids, extends to the salt front. The combination of estuarine circulation and tidal asymmetry (see Section 3.4.2) results in net suspended solids fluxes directed upstream within the salt front and directed downstream in the tidal river upstream of the estuarine regions during low to moderate flows. During high-flow conditions, tidal asymmetry and estuarine circulation can be disrupted such that net suspended solids fluxes are directed downstream in the tidal river upstream of the salt front as well as within the zone of salinity intrusion. Given the bi-directional nature of the suspended sediment fluxes as a function of the location of the salt front, the exchange between the LPR and Newark Bay is an important element of the sediment transport within the LPR.

3.4.2 Tidal Asymmetry and River Flow

SSCs vary within a tidal cycle and between tidal cycles (i.e., intra-tidal and inter-tidal variability, respectively) in response to fluctuations in flow velocities.

Within a tidal cycle, SSCs show systematic patterns with velocity, most notably within the salt front (see Figure 3-7, showing velocity, salinity, and suspended solids measurements from a low-flow period in October 2009 during which the salt front reached the RM 10.2 PWCM station). This period is associated with a tidal range of approximately 1.75 m (5.74 feet) and Dundee Dam flow of 256 cfs and is not affected by any significant transients in river flow or tidal stage during preceding days. On both flood and ebb tide, TSS concentrations increase as velocity increases, reaching a maximum around the time of maximum velocity, and decreasing thereafter to a minimum around slack water. More importantly, SSCs are typically higher during flood than ebb for all locations within the salt wedge under normal tidal and discharge conditions—this is the result of a process known as internal tidal asymmetry. In combination with a similar asymmetry in velocities, the asymmetry in suspended solids represents a net up-estuary flux (per tidal cycle) of suspended sediments within the salt front, a process known as tidal pumping. In contrast to the SSC measurements within the salt wedge, the freshwater station (RM 13.5) in Figure 3-7 shows little variability within the tidal cycle and consequently little tidal pumping.

The intra-tidal variability of SSCs described above is indicative of a pool of easily erodible sediment, termed a fluff layer, deposited on the bed during slack water and resuspended during the following flood or ebb tide (Maa et al. 1998; Van Kessel et al. 2011; El Ganaoui et al. 2004; Wang 2003; Droppo et al. 1998). The fluff layer consists of unconsolidated sediment that overlies a less erodible (consolidated) bed of sediment. The RI did not include field studies aimed at characterizing the fluff layer; its existence and nature are inferred from the intra-tidal variation in SSC and the extensive

sediment transport literature support that a fluff layer is a common characteristic of estuaries (Maa et al. 1998; Van Kessel et al. 2011; El Ganaoui et al. 2004; Wang 2003; Droppo et al. 1998). The evidence for the presence of the fluff layer is further described in Appendix M and its Attachments C and D. The role of this fluff layer in contaminant transport is discussed in Section 6.

The variability of SSCs between tidal cycles (inter-tidal variability) is demonstrated in Figure 3-8, based on PWCM SSC measurements during fall 2009. The temporal patterns of SSCs in the tidal stations (second through fifth panels) correspond well with the spring-neap tidal range (top panel, red line), whereas the correspondence is weak in the freshwater station at RM 13.5 (bottom panel)—consistent with the expectation of a sediment fluff layer resuspended and deposited by tidal currents within the salt wedge. SSCs also increase toward the end of the record when freshwater flow goes above 2,000 cfs at Dundee Dam (top panel, black line), indicating additional contributions from suspended solids loads entering at Dundee Dam and tributaries and/or erosion of more consolidated sediments. For instance, near-bottom daily-average SSC at RM 1.4 varies over the range of 10 to 20 mg/L during neap to spring and low-moderate flow conditions (October and November 2009). It is only when river flow stays consistently elevated above 2,000 cfs (at Dundee Dam) that near-bottom SSC at RM 1.4 exceeds the 10 to 20 mg/L range, reaching up to 40 mg/L. A similar correspondence between the spring-neap tidal range and SSCs is also noted in Figure 3-9, which presents the measurements of Sommerfield and Chant (2010) at RM 1.4.

The direction and magnitude of the net daily suspended sediment fluxes[22] as a function of daily freshwater discharge at Dundee Dam are shown in Figure 3-10 (negative fluxes indicate down-estuary flux). The net solids fluxes show the integrated effects of the tides, estuarine circulation, and freshwater discharge.

Solid fluxes at all predominantly estuarine locations are directed up-estuary below a certain discharge threshold (Figure 3-10). The net solids flux is consistently downstream in the freshwater station (RM 13.5; top left panel), and mostly downstream at RM 10.2 (top row, center panel). The discharge associated with the inflection in the direction of solids fluxes decreases with distance upstream. At RM 1.4, suspended sediment fluxes are directed up-estuary up to approximately 1,500 cfs (i.e., infilling regimes), with net export of suspended sediments from the LPR at higher discharges (i.e., exporting regimes). This finding at RM 1.4 follows from both the 2009 PWCM data (bottom middle panel) and the measurements of Sommerfield and Chant (2010; bottom right panel).

[22] The fluxes in Figure 3-10 (except the bottom right panel) were computed using paired measurements of suspended sediment (from acoustic backscatter measurements) and velocities from the moored acoustic Doppler current profilers during the fall 2009 PWCM program and are expressed in mass per unit width of the river. Both suspended sediment and velocity profiles have been extrapolated to the unmeasured depths at the near-bottom and near-surface of the water column. The bottom right panel contains fluxes calculated similarly from the measurements of Sommerfield and Chant (2010) at RM 1.4.

It is important to realize that the three significant processes (i.e., estuarine circulation, tidal asymmetry [pumping], and freshwater flow-induced flushing) transport sediment and induce a convergence around the ETM of fine sediments[23] originating from within the river and entering from above Dundee Dam, Newark Bay, and tributaries.

River flow determines the direction of net sediment transport. Conceptually, the following three sediment transport regimes are envisioned:

- Regime 1 – Low river flow (low-energy conditions) during which tidal asymmetry and estuarine circulation dominate and favor trapping of fine sediments, partly within the ETM and partly through settling elsewhere on the riverbed. This includes sediments entering the LPR over Dundee Dam, from tributaries, and from Newark Bay. Unconsolidated fine sediments in a bed fluff layer within the LPR may be resuspended and redeposited. The system, as a whole, imports sediments during this regime.
- Regime 2 – Moderate river flow (medium-energy conditions) during which river-induced advection dominates, and fine sediments that had accumulated in the water column (at the ETM) or in a bed fluff layer of unconsolidated fine sediments are flushed down river and mostly into Newark Bay. The system, as a whole, exports sediments during this regime, with solids potentially originating from above Dundee Dam, tributaries, and erosion that is primarily limited to the surficial fluff and unconsolidated sediment layers.
- Regime 3 – High river flow (high-energy conditions, possibly in conjunction with spring tide or rapid set-up/set-down) during which the riverbed may experience scour. The system, as a whole, exports sediments during this regime, with solids potentially originating from above Dundee Dam, tributaries, and in-river erosion of the consolidated sediment bed below the fluff layer (with potentially higher contaminant concentrations; see Section 6).

Evaluation of contemporary multi-beam bathymetry surveys and the suspended solids dynamics noted above suggests a transition between Regime 1 and Regime 2 behavior at freshwater flow rates of approximately 750 to 1,000 cfs and a transition from Regime 2 to Regime 3 behavior at about 6,000 to 7,000 cfs for the LPR above RM 1.5; below RM 1.5, a portion of the bed is also subject to scour due to ship traffic (Appendix M and Attachment B therein). It is noted that the above regime transition flow rates were likely higher historically because cross-sectional areas have been declining since the period of navigation channel maintenance (i.e., after 1950 in most of the lower 8 miles; see Section 1.2), and the resulting increase in velocities and bed shear stress for a given flow rate have likely caused scouring-favorable conditions to become more frequent, thereby reducing net solids import and deposition as the system approaches a large-scale morphodynamic equilibrium. However, this impact of infilling on the regime transition flow rates may in part have been offset by

[23] Primarily clays and silts (< 63 micrometer [µm]).

the channel deepening projects implemented in Newark Bay, Arthur Kill, and Kill van Kull as these have likely increased salinity intrusion into the LPR.

The integrated effect of the hydrograph and sediment dynamics on the LPR sediment bed is evaluated in sections that follow. Analyses of bathymetric data presented in Section 4 show that portions of the river have remained depositional through 2012, while other portions are subject to alternating erosion and deposition or net erosion (see also evaluations in Appendix M, Attachment B). These patterns have affected the trends in surface sediment contamination assessed between RM 1 and RM 7, with declines tending to occur in depositional areas and increases tending to occur in erosional areas (see Sections 4.2 and 10). These changes have roughly balanced over larger scales such that the averages of whole river surface sediment contaminant concentrations between RM 1 and RM 7 have not been meaningfully reduced in the period between 1995 and 2012 (see Section 10).

The frequency at which the LPR experiences Regime 3 conditions may change as precipitation patterns are altered by climate change. The New York City Panel on Climate Change concluded that total precipitation has increased at a rate of approximately 0.8 inch per decade from 1900 to 2013 (Horton et al. 2015). The coming changes are not well understood because of the complex relationships between ocean temperature and weather patterns and the associated uncertainty in climate model inputs (Monier and Gao 2015). The historical flow record at Little Falls since 1950 (Figure 3-3) does not indicate a clear trend in the decadal frequency of flows exceeding 7,000 cfs, although it is noted that 15 of the 20 highest-flow days over this period occurred between 2007 and 2011. A likely future increase in the frequency and magnitude of high-flow events (IPCC 2014) may alter the river's sediment dynamics from those experienced in the last several decades. The New York City Panel on Climate Change found that there has been a small but not statistically significant trend toward more extreme precipitation events in New York City since 1900 (Horton et al. 2015). The projected increase in precipitation within the LPR watershed may impact the extent of erosion that occurs in the river, and the evolving assessments of climate change are a factor to be considered in future evaluations. Sea level rise associated with climate change may also affect sediment dynamics, e.g., enhanced salinity intrusion and a deepening water column may promote sediment deposition while storm surge and flooding may become more prominent.

4 Physical and Chemical Characteristics of the LPR Sediments

LPR sediments contain a wide range of contaminant concentrations due to factors such as source location, nature of the sediments, spatial and temporal history of navigation channel dredging, and depositional/erosional history. This chapter explores the influence of such factors on observed concentration patterns, which are described in detail.

4.1 Introduction

The LPR is a classic partially mixed coastal plain estuary[24] with an expanding cross section from Dundee Dam to Newark Bay (Figure 4.1-1). It contains meanders reflective of its ancestral river channel.

To aid in the detailed investigation of the sediments that follows, the LPR is split into 10 reaches. Within each reach, the river characteristics are studied on the scale of individual geomorphic features. Breaking up the river in this fashion reflects its transitioning from tidal river to fluvial estuary, to the upper estuary of a larger coastal plain estuary. That said, definitive transition points do not exist, and the reach boundaries used herein were chosen considering factors such as geomorphology, changes in river orientation, locations of bridges, and tributary confluences. More importantly, these reaches were segmented to explain the relationship between geomorphic features, channel dredging, sediment type, and depositional/erosional history on the observed patterns of contaminants in sediments.

The discussions in the following subsections use multiple LOEs to investigate the river's sediment bed evolution and contaminant patterns. These include general geomorphic principles and site-specific datasets such as the 2005 SSS survey, single-beam bathymetry from surveys conducted between 1932 and 2007, multi-beam bathymetry and single-beam lateral transect data from surveys conducted between 2007 and 2012, Cs-137 vertical profile data, bottom shear stress predictions from a hydrodynamic model, and contaminant data in the sediment bed.[25] The coverage of the

[24] Coastal plain estuaries are estuaries formed due to the rising sea levels associated with melting ice after the last ice age. The melted waters entered low-lying coastal river valleys, and these estuaries are characterized by shallow river valleys with gently sloping bottoms, with increasing depth toward the mouth of the river (in the case of the LPR, the depth increases toward Newark Bay but is enhanced by navigational deepening).

[25] The use and applicability of bathymetry datasets are described in Appendix A. The analysis of all the Cs-137 data is described in Appendix I. Details of the model used for bottom shear stress predictions are presented in Appendix K.

datasets varies, with many single-beam datasets only available for a small fraction of the study area. Of note are the use and applicability of bathymetry and Cs-137 data, described as follows:

- Bathymetry
  - Bathymetry interpolated from single-beam data are, for the most part, used to understand large-scale changes in the river bottom, not for examining location-by-location changes that may be confounded by the interpolation of the transect data.
  - Where single-beam cross-channel survey lines are coincident from several surveys, they are used along with multi-beam data to study trends in sediment bed evolution. Plots for these transects use all available data from 1932 through 2012.[26]
  - The high-density bathymetry surfaces obtained from multi-beam data are used to identify where net erosion or net deposition occurred between surveys (2007 to 2008, 2008 to 2010, 2010 to 2011, and 2011 to 2012). During this 6-year period, the LPR experienced significant high-flow events in March 2010, March 2011, and August 2011 (including Hurricane Irene, a 90-year event that made landfall in New Jersey on August 28, 2011). The timing of these events relative to the bathymetry surveys is shown in Figure 4.1-2.
  - The main limitations in interpreting changes between the multi-beam surveys are instrument error and datum offsets between surveys. The instrument error for measurements averaged to the 5-foot x 5-foot scale used for differencing is about 2 inches (see Appendix A). Datum offsets range from about 1 inch between the 2010 and 2011 surveys to several inches between the 2008 survey and the 2007 and 2010 surveys (Attachment B of Appendix M). The 2008 survey was offset by 3 to 4 inches from the 2007 survey, whereas it was offset by 1.7 to 3.4 inches from the 2010 survey. Based on the comparison to the 2007 survey, the 2008 elevations were adjusted by 3.6 inches to approximately correct for the offset. Given the combination of instrument error and uncertainty in the magnitude of datum differences between surveys, the changes between consecutive surveys over the period 2007 to 2012 that are presented in this section were judged to be definitive evidence of erosion or deposition only if they were 6 inches or more.
  - An additional limitation in interpreting bathymetry changes between surveys is that they signify net change and can understate changes that occurred. For example, erosion during a high-flow event could be underestimated at locations where infilling occurred after the event but before bathymetry was measured.
  - Using the high-density multi-beam data to track bed elevation changes of at least 6 inches at the 5-foot by 5-foot scale, the sediment bed is mapped into four

[26] The development of these plots requires overlapping single-beam transects across multiple years and can result in different years of single-beam data being used at different locations, depending on how closely aligned the transects are.

bathymetry categories: Erosional from 2007 to 2012, Erosion and Deposition, Depositional from 2007 to 2012, and Change <= 6 Inches/Temporarily Depositional. The Erosional from 2007 to 2012 group comprises locations that experienced net erosion between 2007 and 2012. Locations with less than 6 inches net change or net deposition between 2007 and 2012, but with net erosion between any two consecutive surveys, are classified as Erosion and Deposition (i.e., these regions experienced deposition after the measured erosion). Locations that experienced net deposition between 2007 and 2012 and no survey-to-survey net erosion are grouped in the Depositional from 2007 to 2012 category, and all remaining locations are classified as Change <= 6 Inches/Temporarily Depositional (this category includes locations that experienced deposition between surveys but not between 2007 and 2012). The classification is shown in Figure 4.1-3a.[27] For only the RM 10.9 region, single-beam bathymetry data from 2004 and later were also used to classify the RM 10.9 point bar into bathymetry categories; the process used for this classification can be found in Figure 4.1-3b. Though the single-beam data included 2004, the names of the various categories are the same as those described above in this sub-bullet for consistency with the rest of the reaches.

  - Plots showing the change in sediment bed elevation at the location of a core are used to help interpret vertical profiles of contaminant concentrations in light of recent erosional or depositional events. An example of these plots is shown in Figure 4.1-4. The x-axis of this plot shows each year between 2007 and 2013, and the y-axis indicates the sediment surface elevation relative to the elevation when the core was collected, as judged from the next available bathymetry survey. Elevations are plotted for each of the years with a bathymetry survey (black line; note that the exact timing within the survey years is not shown). In the example shown, the 2007 elevation of the location of core 11B-0307 was approximately 1.7 feet higher than in 2011, when the core was collected. The plot panel is color coded with the 2,3,7,8-TCDD concentrations measured for each vertical core segment. This elevation history provides context for interpreting the profile of contamination at the time of sampling.

- Cs-137 data
  - Cs-137 profiles within sediment cores are used to support the understanding of the evolution of the sediment bed and its depositional environment, the profiles of contamination, and the observed changes in bathymetry. The lowest Cs-137 activities are found in areas that have not experienced sediment accumulation since the 1950s,

[27] As depicted in Figure 4.1-3a, the groupings were conducted sequentially. First, 5-foot by 5-foot locations falling under the Erosional from 2007 to 2012 group were identified. Next, locations falling in the Erosion and Deposition group were identified. Locations falling in the Depositional from 2007 to 2012 were then identified. The remaining locations were classified as Change <= 6 Inches/Temporarily Depositional. Area outside the spatial extent of any bathymetry survey between 2007 and 2012 were excluded from the groupings.

such as the most upstream parts of the LPR. Regions that have been net depositional with similar sediments since at least the 1950s contain well-defined buried peak Cs-137 activities. Some silt deposits of the LPR contain such cores. Regions that accumulated different types of sediment at different times or experienced some sediment removal (erosion or dredging) after the 1960s do not contain a well-defined peak; such profiles are often found in parts of the navigation channel that experienced maintenance dredging in the 1970s and 1980s. Regions that attained geomorphic equilibrium in the early 1960s often contain the maximum Cs-137 activity at the surface, such as those found in the upstream part of the RM 10.9 point bar. Because various conditions can impact the profiles and confound efforts to draw conclusions about historical deposition and erosion,[28] the Cs-137 data are only used in conjunction with other LOEs.

Overall, the sediment characteristics of the LPR are typical of a large estuary, with along-river trends that reflect sediment transport patterns influenced by the expanding cross section, tides, river inflow, and geomorphologic changes (Figures 4.1-5). The coarsest sediments are in the upper reaches, and finer sediments become more common as the river widens and deepens, especially downstream of RM 8. This change in sediment characteristics forms the basis of the upstream boundary of OU2. Along bends, the lower water velocities along the inner portion and the lateral circulation moving bottom water toward the inner portion result in the accumulation of finer sediments, and the higher water velocities along the outer portion prevent the accumulation of finer sediments and result in coarser sediments being present. Moving from the inner bend across the channel toward the outer bend, there is typically a gradual transition from finer to coarser sediments. The fine sediments along the inner bend tend to form point bars, most notably the RM 10.9 point bar, which was dredged and capped in 2013 and 2014 (excluding the utility corridor) to address elevated 2,3,7,8-TCDD, PCB, PAH, and mercury levels (2,3,7,8-TCDD levels, in some instances, exceeded 50,000 nanograms per kilogram [ng/kg]). Sediments tend to be coarse or absent (i.e., the bottom is Rock and Gravel) in the vicinity of structures such as bridge abutments and at tributary confluences; this is due to associated turbulence—particularly under higher flows—that prevents long-term accumulation of fine sediments or, in particularly high energy areas, any sediment.

The patterns of fine and coarse sediment are pertinent to the study of contamination because many of the contaminants tend to be found at highest concentrations in fine sediments.[29] This association reflects the higher amount of organic matter found in fine sediments (Figure 4.1-7 [30]) and the

[28] Such conditions include, among others, deposition of different types of sediments over the years, intermediate dredging, generally coarse sediments, erosion, and homogenization of sediments.

[29] As discussed later in this section, the association of HMW PAHs and LMW PAHs with fine sediments is weaker than the other contaminants evaluated herein.

[30] The amount of fine sediments in a sample is determined by the fraction of sediment passing through either the 63-micron sieve (#230) or the 75-micron sieve (#200), depending on the method used for grain size estimation. The figure compares the TOC distribution in post-2005 surface samples with >75% fine sediments to those with <25% fine sediments.

importance of organic carbon (OC) in sorbing many of the contaminants found in the river (Figure 4.1-8); the features of the box-and-whisker plot used in the figures are explained in Figure 4.1-6. The increasing occurrence of fine sediments moving downstream contributes to the large-scale longitudinal trend in contaminant concentrations. That trend also reflects the estuarine transport patterns that facilitate upstream as well as downstream movement of water, solids, and associated contaminants (discussed in Sections 3 and 6, respectively).

The spatial patterns of the other contaminants (Figures 4.1-9b through 4.1-9f) do differ from that of 2,3,7,8-TCDD, suggesting that they are impacted by upstream, downstream, and/or watershed sources. For example, total PCBs (Figure 4.1-9b) and total DDx (Figure 4.1-9c), although variable, exhibit surface sediment (0 to 0.5 foot) concentrations that decline less moving upstream of RM 12 to RM 14, indicating upstream sources.[31] Mercury concentrations (Figure 4.1-9d) do not decline into Newark Bay, suggesting a source downstream of the LPR. Also, note that the highest concentrations of these four contaminants are contained primarily in finer sediments.

The along-river patterns of PAHs are also dissimilar to 2,3,7,8-TCDD. Surface sediment concentrations of both high-molecular-weight (HMW) PAHs (Figure 4.1-9e) and low-molecular-weight (LMW) PAHs (Figure 4.1-9f) upstream of Dundee Dam are generally higher or comparable to those within the LPR, indicating upstream sources of PAHs are contributing to levels in the LPR. Moving into Newark Bay, mild declines in HMW PAH and LMW PAH concentrations are seen. These declines are less pronounced than those observed for 2,3,7,8-TCDD, indicating PAH levels in Newark Bay are likely influenced by downstream sources. The highest PAH concentrations in Newark Bay are generally observed in the lowermost portion of the bay, suggesting PAH sources may exist in this region. Note that there is insufficient information to quantify or further describe these external contaminant sources. Further, unlike the other contaminants, comparable amounts of PAHs are found in fine and coarse sediments, and the relationship of PAHs with OC is weaker than the other contaminants (Figures 4.1-8e and 4.1-8f). This is supported by studies at other sites that have found PAHs to be associated with coarser sediments (Wang et al. 2001, 2014).

Examining the data at a finer spatial scale, as is done in Section 4.2, reveals patterns in contaminant concentrations that are largely driven by variations in sediment type and depositional/erosional history. Concentrations generally correlate with sediment type, as discussed above, although the range of concentrations is large, particularly within fine sediments. That range seems to reflect geomorphic evolution and susceptibility to episodic erosion and cyclic erosion/deposition. The higher surface (0- to 6-inch) concentrations tend to be in fine sediments that have not been net depositional in the last few decades.

[31] Total DDx concentrations are not plotted for Newark Bay because the six components of total DDx are not available for Newark Bay data.

Concentrations tend to be lower in areas where net deposition continues or in areas of cyclic erosion/deposition where the surface sediments reflect the recent deposition of lesser contaminated solids. They tend to be lowest in areas of coarse sediment, although a complication to the interpretation of patterns arises from the protocols used in the sediment sampling programs. As noted in the Quality Assurance Project Plans in Appendix B, some of the sediment sampling programs (such as the SSP and SSP2; Section 2.4.3.2) targeted 80% core recovery. If a core with the required recovery could not be collected, up to two additional attempts were made at that location, after which single attempts were made in up to two additional locations. Achieving 80% core recovery is more difficult in coarse sediment than in fine sediments. Thus, attempting to meet this criterion can introduce a bias toward finer sediments in areas that are generally composed of coarse sediments. This may explain the frequency at which samples of fine sediment were collected in SSS-defined coarse sediment areas (Figure 4.1-10).[32] An implication of this finding is that coarse sediment areas can contain pockets of fine sediments not resolved by the SSS survey. It is also possible that erosion/deposition changed the nature of the sediments between the time of the SSS survey in 2005 and the time of core collection or that the sediment characteristics of the surface coring interval (6 inches) are different from the characteristics of the thinner surface interval measured by the SSS survey. To better understand the surface sediment characteristics, figures depicting the SSS information are bolstered with sediment probing data and the fraction of fine sediments in the core data. Additional details of the use of probing and percent fines data can be found in Section 3 of Appendix J.

The discussion of concentrations in the following sections typically compare the contaminant concentration to a numeric value, such as 1 ng/kg, or 100 milligrams per kilogram (mg/kg); these numeric values are used only for ease of comparison on a relative basis and are not based on risk or reference thresholds. The figures also present the data in concentration groups; the thresholds between these groups were selected for ease of presentation. Approximately equal fractions of the samples for each contaminant are contained by the corresponding group (that is, the lowest concentration group for 2,3,7,8-TCDD [0 to 100 ng/kg] contains approximately the same fraction of samples as the lowest concentration groups for total PCBs [0 to 0.5 mg/kg], total DDx [0 to 0.05 mg/g], mercury [0 to1 mg/kg], HMW PAHs [0 to 15 mg/kg], and LMW PAHs [0 to 2 mg/kg]). Overall, about 60% of the data is captured in the bottom three groups, while the remaining 40% is captured in the top three groups.

[32] Note that this figure only shows samples with available grain size data.

4.2 A Detailed Look at the River

As discussed in Section 4.1, the LPR has been divided into 10 longitudinal reaches that are examined in an effort to understand smaller-scale contamination patterns and the factors that contribute to them (Figure 4.2-1).

The reach boundaries are informed by physical and geomorphic features and were selected at natural breakpoints in the river (e.g., at the end of a major geomorphological feature, bridge abutment, or confluence of a tributary with the LPR). They should not be taken to construe a significant change in river behavior across boundaries. The reach boundaries are described below, and the sediment and contaminant patterns within each reach are discussed in the subsections that follow:

1. Dundee Dam (RM 17.4) to confluence with Saddle River (RM 15.6) – This reach extends from the upstream boundary of the LPR at Dundee Dam to the confluence of its first tributary—the Saddle River at RM 15.6.
2. Confluence with Saddle River (RM 15.6) to RM 14 – This reach extends from the confluence of the Saddle River to RM 14, where the LPR transitions from the second oxbow to a straighter section.
3. RM 14 to RM 12.5 – This reach extends from RM 14 to the beginning of the most upstream SSS-identified silt deposit of the LPR at RM 12.5.
4. RM 12.5 to confluence with Third River (RM 11.2) – This reach extends from RM 12.5 to the confluence of the second major tributary to the LPR—the Third River at RM 11.2.
5. RM 11.2 to RM 10.4 – This reach extends from the confluence of the Third River at RM 11.2 to the Avondale Bridge at RM 10.4.
6. RM 10.4 to RM 9.2 – This reach extends from the Avondale Bridge to the end of the silt deposit crossing into the channel at RM 9.2.
7. RM 9.2 to RM 7.8 – This reach extends from RM 9.2 to the WR Draw Railroad Bridge at RM 7.8. The upstream boundary of OU2 is located within this reach at RM 8.0 (USACE RM 8.3).
8. RM 7.8 to RM 5 – This reach extends from the WR Draw Railroad Bridge at RM 7.8 to RM 5, where the LPR turns approximately 90 degrees east.
9. RM 5 to Point-No-Point Conrail Bridge (RM 2.3) – This reach extends from RM 5 to the No-Point Conrail Bridge at RM 2.3, the approximate location where the navigation channel transitioned from a 30-foot authorized channel depth to a 20-foot authorized channel depth.
10. RM 2.3 to Mouth – This reach extends from the No-Point Conrail Bridge at RM 2.3 to the mouth of the LPR (RM 0).

The various figures presenting the physical and chemical characteristics of the LPR sediments in each reach are summarized in Table 4-1.

4.2.1 Dundee Dam (RM 17.4) to Confluence with Saddle River (RM 15.6)

The most upstream reach of the LPR (Figure 4.2.1-1) extends from Dundee Dam (RM 17.4) to the confluence of the first tributary, Saddle River (RM 15.6). It is oriented mostly in the northwest (NW) to southeast (SE) direction. River crossings include the Veterans Bridge at RM 17, the Monroe Street Bridge at RM 16.1, and the Garfield Highway (Wall Street Bridge) at RM 15.75. Most of the eastern and western shorelines are vegetated, except for a small stretch of sheetpile/bulkhead on the western bank at RM 16.2. The total area of the sediment bed in this reach is 60 acres.

Limited physical, bathymetry, and chemical data exist for this reach. The 2004 and 2007 bathymetry surveys are the only surveys that extend into it, with the 2007 bathymetry restricted to downstream of about RM 16.5. The SSS survey of 2005 includes the area downstream of RM 16.1. There are no Cs-137 data.

The cross-sectional area increases moving downstream (Figure 4.1-1), and the smallest cross-sectional areas in the LPR are contained within this reach. The area initially decreases from 1,600 ft^2 to about 1,280 ft^2 just downstream of the constriction around the Monroe Street Bridge, before increasing to 2,100 ft^2 by the confluence of the Saddle River. The narrow cross section has resulted in the highest shear stresses in the river (Figure 4.2.1-2).[33] The associated high velocities prevent the accumulation of fine sediments, and the bed is generally gravel and sand, with rock and coarse gravel around the confluence of the Saddle River[34] (Figure 4.2.1-3). The presence of the coarsest sediments around the confluence is the likely result of turbulence associated with the incoming tributary, particularly during high flows, which prevents fine sediment deposition; this is also observed around the confluence of other tributaries farther downstream. The lack of pre-2004 bathymetry datasets in this reach precludes an assessment of long-term changes to the river bottom, although a comparison of the 2004 and 2007 single-beam datasets indicates that it did not significantly change during those 3 years (Figure 4.2.1-4).

Contaminant Patterns

Only seven sediment samples were collected in this reach, and four were surface sediment grabs. Concentrations of 2,3,7,8-TCDD, total PCBs, total DDx, and mercury in all seven samples are lower than levels typically found farther downstream (Figures 4.1-9a through 4.1-9d), consistent with the lack of fine sediment accumulation and the limited upstream transport from the more urban downstream areas (the salt wedge rarely, if ever, reaches this far upstream). The overall concentrations measured in this reach are summarized in Table 4-2.

[33] The detailed reach-by-reach descriptions include maximum bottom shear stress predicted over a simulation spanning the 1989 to 2008 period with the higher-resolution hydrodynamic model described in Appendix L. These figures are used to qualitatively describe spatial variations in high-flow shear stress, in a relative sense.

[34] Finer sediments are present in the more downstream reaches as the cross-sectional area increases to reduce water velocities and thus increases the trapping of fine sediments.

Surface and at-depth 2,3,7,8-TCDD concentrations in this reach are below 1 ng/kg (Figure 4.2.1-5). Total PCB concentrations (Figure 4.2.1-6) are less than 0.5 mg/kg, except for the surface sediment grab sample just above RM 17 (LPRT17A), which has a concentration of 2.9 mg/kg. Total DDx concentrations (Figure 4.2.1-7) in the surface and subsurface sediments are less than 0.05 mg/kg, and mercury concentrations (Figure 4.2.1-8) are at or below 0.5 mg/kg through the reach. Unlike the other contaminants, HMW PAH levels in this reach are highest above RM 16.5 (61 mg/kg in the 0.5- to 1.5-foot segment of CLRC-096 at RM 17.1 [Figure 4-2.1-9]) and lower farther downstream. River-wide trends in HMW PAH concentration suggest the elevated levels observed above RM 16.5 likely originated from sources upstream of the Dundee Dam (Section 4.1). LMW PAH are always less than 10 mg/kg, except for the 0.5- to 1.5-foot section of CLRC-096 (21 mg/kg; Figure 4-2.1-10). As noted previously, PAHs in the LPR are also associated with coarser sediments (Figures 4.1-9e and 4.1-9f), and their concentrations could thus exhibit spatial patterns somewhat different than the other contaminants.

4.2.2 Saddle River (RM 15.6) to RM 14

This reach extends from the confluence of the Saddle River at RM 15.6 to RM 14, at the end of an oxbow. It is oriented N-S for the first half-mile and then enters two oxbows at RM 15 and RM 14.5. Two bridges cross this reach—the West Eighth Street Bridge at RM 15 and the Second Street Bridge at RM 14.4. The navigation channel begins just downstream of the West Eighth Street Bridge at RM 15. A minor tributary (Weasel Brook) enters at RM 14.25. Both shorelines are mostly vegetated upstream of the Second Street Bridge and sheetpiled/bulkheaded downstream of the bridge (Figure 4.2.2-1). The cross-sectional areas in this reach are higher than the previous reach, increasing from 2,100 to 2,900 ft^2 around RM 15.1, before decreasing around the first oxbow to 2,100 ft^2 at RM 14.7. The cross-sectional area then increases around RM 14.5 in the second oxbow to 2,550 ft^2 and stays roughly the same throughout the rest of the reach (Figure 4.1.1-1). The total area of the sediment bed in this reach is 55 acres.

The LPR was realigned downstream of the confluence of Weasel Brook at RM 14.25 in the late 1950s and 1960s to construct Route 21 along the western side of the river. The town of Wallington, New Jersey, relinquished an entire street for this realignment.[35] The longitudinal extent of the realignment is not known; consequently, its potential influence on sediment patterns is not considered here.

The most recent maintenance project of the federal navigation channel in this reach occurred in 1973 and targeted the region between RM 14.3 and RM 14. Upstream of RM 14.3, the navigation channel was last maintained before 1950. Bathymetry surveys indicate that the river channel deviates from

[35] http://www.wallingtonnj.org/content/history-cont-d.html

the navigation channel in several locations, especially on the inside of the oxbows (Figure 4.2.2-1), where infilling appears to have occurred.

The evolution of the sediment bed is studied using bathymetry data (single-beam surveys [1989, 2004, and 2007] and multi-beam surveys and associated single-beam transect measurements [2007, 2008, 2010, 2011, and 2012]), model-predicted bottom shear stress patterns, and Cs-137 core profile data. Its characteristics are described using results of the 2005 SSS survey and its ground-truthing data, probing surveys, and characteristics and contaminant concentrations of individual cores.

Bottom shear stresses in this reach follow expected trends. They are high around the confluence of the Saddle River and decrease as the LPR widens downstream of RM 15.25 (Figure 4.2.2-2). The high shear stresses prevent the accumulation of fine sediments at the confluence, resulting in a bed consisting of Rock and Coarse Gravel. The narrowing downstream of the West Eighth Street Bridge results in higher shear stresses. Through the second oxbow, lower water velocities along the inner bend result in lower shear stresses, and the higher water velocities along the outer bend, coupled with the confluence of Weasel Brook, result in higher shear stresses (Figure 4.2.2-2).

Sediment types correlate with water velocities and shear stresses; coarse sediments are more prevalent in regions subject to higher shear stresses, whereas finer sediments are found in regions with lower water velocities and correspondingly lower shear stresses.

Like the river bottom in the upstream reach, the sediment from Saddle River to the West Eighth Street Bridge is largely Gravel and Sand (Figure 4.2.2-3). Like other tributary confluence points, the area around the confluence of the Saddle River is Rock and Coarse Gravel.

In the first oxbow, the edges of the river are Rock and Coarse Gravel. Of note here along the inner bend is the beginning of the most upstream Sand deposit in the LPR. This deposit broadens as the river bends again at RM 14.5, and more structure is observed in the sediment types around this second bend. The first instance of Silt (via a Silt and Sand mixture) is observed along the inner bend, corresponding to the lower shear stress in this region where channel infilling appears to have occurred. The finer sediments transition to coarse sediments moving from the inner bend to the outer bend, with Rock and Coarse Gravel extending along the outer bend (consistent with the higher shear stress region noted previously). This general trend continues as the LPR bends at RM 14.25, with Silt and Sand along the inner bend giving way to Sand in the Channel and Gravel and Sand along the outer bend (Figure 4.2.2-3[36]).

[36] These figures also show locations where more than 20% fine sediments were detected. The 20% cutoff was based on the observation that samples with more than 20% fine sediment content contained higher 2,3,7,8-TCDD concentrations than samples with less than 20% fine sediments content (see Figure 3-7 of Appendix J).

Bathymetry data in this reach are mostly limited to the 1989, 2004, and 2007 single-beam surveys. Post-2007 multi-beam data are available downstream of RM 14.25. Comparison of the 1989, 2004, and 2007 single-beam surveys indicates that the shape of the LPR channel remained relatively unchanged during that period (Figure 4.2.2-4). However, the single-beam transect data in this reach suggests some erosion in the channel between 2004 and 2007 near RM 15, just downstream of the West Eighth Street Bridge (Figure 4.2.2-5a). A transect at RM 14.78 suggests the 2007 bed surface elevation is similar to that of the 2004 surface there (Figure 4.2.2-5b). The accumulation of sediment along the inner bend at RM 14.5 can be observed between the 1989 and 2004 bathymetries (darker green along the inner bend of the channel). Farther downstream at RM 14.21, a comparison of the 2012 transect with the 2004 transect indicates the accumulation seen between 2004 and 2007 has continued to 2012 (Figure 4.2.2-5c).

The recent multi-beam data between RM 14.25 and RM 14 indicate that the deposition suggested by the transect at RM 14.21 is part of a larger depositional region on the western side of the channel that has been net depositional between 2007 and 2012 (Figure 4.2.2-6).[37] Episodic erosion has been observed farther into the channel toward the eastern extent of the bathymetry surveys. Some of these regions experienced net deposition between 2011 and 2012 (a predominantly low-flow period). Parts of the reach experienced erosion between 2007 and 2008, 2008 and 2010, and 2010 and 2011. Most of the net deposition within this reach occurred between 2010 and 2011 (i.e., the period that included Hurricane Irene). It is possible that this area was the most upstream region in which larger particles (i.e., sands) transported during the high-flow event began to deposit.

The lack of deposition expected in the coarse sediments upstream of RM 15 is confirmed by the low Cs-137 activities detected in both Rock and Coarse Gravel (CLRC-089), and Gravel and Sand (CLRC-086) (Figure 4.2.2-7). Higher Cs-137 levels are present in the downstream Sand and Silt and Sand deposits (CLRC-085, CLRC-084, CLRC-083, and CLRC-082). Both CLRC-085 and CLRC-082 contain a well-defined[38] buried peak, suggesting a net depositional environment of similar sediments in those locations over many years and consistent with the infilling in the adjacent navigation channel areas suggested by present-day bathymetry (Figure 4.2.2-1). The two cores around RM 14.25 (CLRC-084 and CLRC-083) have Cs-137 levels at depth that indicate significant net deposition consistent with infilling of the navigation channel but do not contain a well-defined peak, likely due to the maintenance dredging in 1973. As discussed in the next section, this region also exhibits significant variability in fine sediment composition in the vertical sediment column.

Contaminant Patterns

Contamination patterns in this reach reflect the upstream extent of the salt front and the distribution of sediment types. The coarse sediments upstream of RM 14.75, which are generally beyond the

[37] Regions outside the extent of the multi-beam bathymetries are shown as gray in these figures.
[38] Well-defined here refers to the decreasing Cs-137 activities above and below the segment with maximum activity.

extent of the salt front, contain concentrations of 2,3,7,8-TCDD, total PCBs, total DDx, and mercury that are similar to those measured in the Dundee Dam to Saddle River reach (Figures 4.1-9a through 4.1-9d). Higher concentrations exist in the Silt and Sand deposit along the depositional inner bend around RM 14.5 (see Figure 4.2.2-8 for the distribution of 2,3,7,8-TCDD and total PCBs on the SSS-identified sediment types and Appendix K for similar figures of total DDx, mercury, HMW PAHs, and LMW PAHs). Outside the Silt and Sand deposit, concentrations of these contaminants are lower, reflective of the coarser sediments. PAH levels are similar to those measured in the Dundee Dam to Saddle River reach (Figures 4.1-9e and 4.1-9f), and concentrations of PAHs in the coarse upstream sediments of this reach are not greater in magnitude to those in the finer Silt and Sand deposit and in farther downstream sediments (see Appendix K Figures 8-1 and 9-1). The overall concentrations measured in this reach are summarized in Table 4-3. The rest of this section discusses the contaminant patterns in this reach in detail, focusing on the lower concentrations in the upstream extents, the elevated levels in the Silt and Sand deposit, and the lower levels outside the Silt and Sand deposit.

Upstream of RM 14.75, excluding the bottom two segments of CLRC-085 (RM 14.8), which have between 10 and 50 ng/kg, the collected five cores and seven grab samples have surface and at-depth 2,3,7,8-TCDD concentrations less than 10 ng/kg (Figure 4.2.2-9). Concentrations of total PCBs (Figure 4.2.2-10) at all locations are less than 0.5 mg/kg, except CLRC-085, which has levels between 0.5 and 1 mg/kg at the surface and various depths. Concentrations of total DDx (Figure 4.2.2-11) are generally below 0.05 mg/kg, except for the surface sample of CLRC-087 at RM 15.09 (0.18 mg/kg) and the segments below 1.5 feet of CLRC-085 (0.17 mg/kg between 3.5 and 5.5 feet, and 0.76 mg/kg below 5.5 feet[39]; RM 14.8). Subsurface concentrations of total DDx in CLRC-087, as well as the grab sample LPRT16A collected less than 5 feet away, are less than 0.05 mg/kg, suggesting the higher concentration in the surface sample of CLRC-087 is an exception in this region.

Mercury (Figure 4.2.2-12) concentrations are also lower upstream of RM 15 (i.e., less than 0.5 mg/kg) but higher in CLRC-085 (RM 14.8), with the highest concentrations in the reach measured in the 3.5- to 5.5-foot segment of this core (17.5 mg/kg). The surface concentration of mercury in this core is lower but still notable (5.5 mg/kg).

The downstream parts of this reach are within the upstream extent of the salt front under rare, extreme low-flow conditions (see Sections 3 and 6). Historical upstream transport of 2,3,7,8-TCDD has likely resulted in the accumulation of some elevated concentrations in the Silt and Sand deposit along the inner bend of the second (downstream) oxbow (Figure 4.2.2-8). This deposit is approximately 6.5 acres in area (12% of the overall 55 acres in the reach), and within it

[39] Depths below 5.5 feet are not shown on the maps.

concentrations are higher in the upstream portion (i.e., above RM 14.25). The grab sample 13B-0564 at RM 14.57 contains 800 ng/kg of 2,3,7,8-TCDD (Figure 4.2.2-9). Moving further downstream into the Silt and Sand deposit, both 13B-0563 and G0000172 at RM 14.46 exhibit contamination levels greater than 1,000 ng/kg (the 1.5- to 2.5-foot segment for 13B-0563, and the 0- to 2.5-foot segment of G0000172[40] have levels of 2,100 and 3,800 ng/kg, respectively). The surface concentration of 13B-0563, however, is notably lower (2.4 ng/kg). Further, the surface and 0.5- to 1.5-foot segments of 13B-0563 contain less than 5% fine sediments, while the 1.5- to 2.5-foot segment contains 91% fine sediments, suggesting historically accumulated 2,3,7,8-TCDD has since been buried under cleaner and coarser sediments at this location.

The Silt and Sand deposit also contains higher levels of total PCBs (Figure 4.2.2-10), total DDx (Figure 4.2.2-11), and mercury (Figure 4.2.2-12). The 1.5- to 2.5-foot segment of 13B-0563 and the 0- to 2.5-foot segment of G0000172 exhibit the highest total PCB concentrations within the reach (24 and 7.7 mg/kg, respectively). The highest total DDx concentration in the reach is also measured in the Silt and Sand deposit (0.38 mg/kg in the 0- to 2.5-foot segment of G0000172). Notably, the other core collected in the Silt and Sand deposit (13B-0563) has consistently low total DDx levels throughout the entire sediment column (less than 0.05 mg/kg at all depths), indicating the contamination within the deposit is spatially variable. Mercury levels are elevated within the Silt and Sand deposit, with both 13B-0563 and G0000172 exhibiting concentrations in the 10 to 15 mg/kg range.

Downstream of RM 14.25, contaminant concentrations are relatively low in both the Silt and Sand deposit and the adjacent Sand deposit. 2,3,7,8-TCDD levels in all 10 sampling locations are less than 100 ng/kg at all depths. Some buried contamination of total PCBs, total DDx, and mercury is observed in CLRC-084 and G0000171 within the Silt and Sand deposit at RM 14.2. Total PCB levels are less than 0.5 mg/kg at all depths in 9 of the 10 locations and are approximately 3 mg/kg in all segments below 1.5 feet in CLRC-084. Depths below 2.5 feet in this core also have higher total DDx (0.19 mg/kg) and mercury (between 2 and 2.5 mg/kg) levels. A similar concentration of total DDx is also found in the 1.5- to 2.5-foot segment of G0000171. In both samples, the top 1.5 feet are cleaner. This could possibly be due to a significant variation in the fine sediment composition; the fraction of fine sediments in the 1.5- to 2.5-foot and 2.5- to 3.5-foot segments of CLRC-084 are significantly higher than the 0.5- to 1.5-foot segments (72% and 62%, versus 0.3%, respectively), suggesting a coarse sediment layer has buried accumulated fine sediments, likely during infilling after the 1973 maintenance dredging.

[40] The entire 0- to 2.5-foot slice of G0000172 was analyzed and reported as one slice. The co-located core 13B-0563 has low surface contamination levels, suggesting that the high-contamination sediments in the 0- to 2.5-foot slice of G0000172 are likely located below a depth of 6 inches.

The correlation of total PCB, total DDx, and mercury with 2,3,7,8-TCDD can be seen in Figures 4.2.2-13a through 4.2.2-13c. The left panels of these plots suggest that higher levels of these three contaminants are found in locations that have higher 2,3,7,8-TCDD levels and vice versa. The relationship is stronger for the subsurface segments (middle panels) and the mass-per-area (MPA[41]; right panels). PAH patterns, however, vary from these three contaminants (Figures 4.2.2-13d and 4.2.2-13e); surface concentrations of HMW and LMW PAHs are not well correlated to 2,3,7,8-TCDD concentrations.[42] The relationship does, however, seem to be stronger in the subsurface sediments and on an MPA basis.

Like the Dundee Dam to Saddle River reach, HMW PAH levels (Figure 4.2.2-14) are generally similar in this reach to the farther downstream reaches of the LPR (Figure 4.1-9e), a possible result of the sources upstream of Dundee Dam and the association of PAHs with coarser sediments noted previously. Levels in the 50- to 80-mg/kg range are detected in three of the nine surface sediment samples upstream of RM 15, while subsurface concentrations are always less than 15 mg/kg. Downstream of RM 15, concentrations greater than 50 mg/kg are present in the deepest segment of CLRC-085 (87 mg/kg). Like the other contaminants, higher concentrations are also measured in the Silt and Sand deposit around the Second Street Bridge in 13B-0563 and G0000172 (90 mg/kg in the 1.5- to 2.5-foot segment of 13B-0563 and 71 mg/kg in the 0- to 2.5-foot segment of G0000172) and in CLRC-084 (53 mg/kg) and G0000171 (52 mg/kg). The higher levels are also present at the bottom of CLRC-082 (67 mg/kg).

LMW PAH levels (Figure 4.2.2-15) upstream of RM 15 are also comparable to levels downstream. The highest concentration in the reach is measured in the surface sediments of CLRC-086 (75 mg/kg; RM 15.09), and two additional surface samples upstream of RM 15 have concentrations in the 8- to 20-mg/kg range. Subsurface concentrations in this region are all lower than 2 mg/kg. Moving downstream, higher concentrations of LMW PAHs are also present in the bottom of CLRC-085 (27 mg/kg). Like the other contaminants, higher levels of LMW PAHs are present within the Silt and Sand deposit (27 mg/kg in the 1.5- to 2.5-foot segment of 13B-0563 and 19.6 mg/kg in the 0- to 2.5-foot segment of G0000172). Farther downstream, LMW PAH levels are between 10 and 15 mg/kg in the deeper segments of CLRC-084 and between 6 and 12 mg/kg in the top segments of G0000171.

To summarize, contaminant levels of 2,3,7,8-TCDD, total PCBs, total DDx, and mercury in this reach are highest within the upstream portion of the Silt and Sand deposit and are generally lower upstream of RM 15 than in the downstream portion of this reach. PAH patterns, on the other hand, do not demonstrate as large a spatial gradient moving upstream to downstream. Contamination levels are generally highest at-depth within the Silt and Sand deposit, suggesting some period of net

[41] MPA calculations are described in Appendix I.

[42] These figures also show the Spearman's rank correlation coefficient. However, the discussions and characterizations of these figures are based on a qualitative assessment of the correlations.

deposition. The sediment composition data suggest that in some of the locations within this deposit, coarse sediments have buried contaminated fine sediments.

4.2.3 RM 14 to RM 12.5

This reach extends from RM 14 to the beginning of the LPR's most upstream Silt deposit at RM 12.5. Two bridges cross this reach—the Gregory Avenue Bridge at RM 13.85 and the Douglas O. Mead Bridge at RM 13 (Figure 4.2.3-1). The river flows in the N-S direction, with a slight bend just downstream of the Douglas O. Mead Bridge (RM 13 to RM 12.5). The eastern shoreline is mostly vegetated, with some sheetpiling between RM 13.5 and RM 13.3. The western shoreline is intermittently sheetpiled/bulkheaded from the Gregory Avenue Bridge to RM 13.65, from RM 13.5 to RM 13.1, and from RM 12.9 to RM 12.8, and vegetated at other locations upstream of RM 12.8. Downstream of RM 12.8, the western shoreline has riprap/stone (Figure 4.2.3-1). The cross-sectional area continues to expand moving downstream, increasing from 2,900 ft^2 at the Gregory Avenue Bridge to 3,750 ft^2 at RM 13.2 (Figure 4.1-1). The cross-sectional area then decreases slightly and ranges between 3,500 and 3,650 ft^2 until RM 12.5. The total area of the sediment bed in this reach is 50 acres.

The federal navigation channel continues through this reach. The last maintenance project in this reach occurred in 1976, targeting the navigation channel between RM 13.9 and RM 12.8. The rest of the navigation channel was last maintained before 1950. Bathymetry data indicate that the present river channel is mostly aligned with the former navigation channel. Overall, the LPR has a classic straight river configuration in this reach, with a deep channel and shallower shoals (Figure 4.2.3-1).

The evolution of the sediment bed is studied using bathymetry data (single-beam surveys [1989, 2004, and 2007] and multi-beam surveys and associated single-beam transect measurements [2007, 2008, 2010, 2011, and 2012]), model-predicted bottom shear stress patterns, and Cs-137 core profile data. Its characteristics are described using results of the 2005 SSS survey and its ground-truthing data, probing surveys, and characteristics and contaminant concentrations of individual cores.

The relatively straight channel with uniform cross-section has resulted in fairly small longitudinal variations in maximum shear stress along most of this reach (Figure 4.2.3-2). Shear stresses are somewhat higher upstream of the Gregory Avenue Bridge at RM 13.85, due to the flow constriction and turbulence around the bridge pilings. Shear stresses are then lower and generally uniform until just downstream of RM 12.75, where higher shear stresses are observed along the western side of the river, corresponding to the area of riprap and stone along the western bank. Here, the inner bend exhibits lower shear stresses, as expected.

The deeper channel has finer sediments (Silt and Sand) than the shoals (Gravel and Sand) (Figure 4.2.3-3), likely reflecting the accumulation of finer sediments in the navigation channel after

the 1976 maintenance dredging. A crop of Rock and Coarse Gravel is observed on the outer bend downstream of RM 12.8, corresponding to the extent of riprap/stone along the shoreline (Figure 4.2.3-1) and the region of higher shear stresses noted above (Figure 4.2.3-2).

The 1989, 2004, and 2007 single-beam bathymetry surveys indicate that the shape of the LPR channel remained relatively unchanged over this period (Figure 4.2.3-4). A single-beam bathymetry transect at RM 13.4 indicates the bed elevation has not changed significantly between the 2004 and 2012 bathymetry surveys (Figure 4.2.3-5). A transect at RM 12.87 suggests the bed accumulated some sediment in the channel between 2004 and 2012 (Figure 4.2.3-5). More recent multi-beam bathymetry data show little evidence of measurable erosion or deposition, except between 2010 and 2011 (Figure 4.2.3-6). Some erosion is observed between 2008 and 2010 around the Gregory Avenue Bridge, where, as previously noted, higher shear stresses are expected, and in small slivers of the channel near RM 13.5.

The 2010 to 2011 period, which included Hurricane Irene and the March 2011 high-flow event, resulted in significant change (either erosion or deposition) for most of the channel with the greater fraction being depositional. The greatest erosion occurred around the Gregory Avenue Bridge and on the eastern half of the channel from the Gregory Avenue Bridge at RM 13.85 to RM 13.6. Erosion exceeding 1.5 feet was observed around the Gregory Avenue Bridge and in a small pocket on the outer bend at the western side of the channel about halfway between the Douglas O. Mead Bridge and RM 12.75. As observed on 3D relief maps of the LPR sediment surface (Figure 4.2.3-7[43]), these areas are mostly located on the side slopes of the channel.

Deposition was observed in the western half of the channel at RM 13.75, the entire channel from RM 13.65 to RM 13.55, a sliver on the eastern side of the channel between RM 13.5 and RM 13.3, a sliver on the western side of the channel between RM 13.25 and the Douglas O. Mead Bridge downstream of the bridge where the depositional region transitioned through the channel to the eastern side of the channel, corresponding to the inner bend around RM 12.75, and extended to RM 12.6. The six Cs-137 cores (Figure 4.2.3-8) in this reach contain higher Cs-137 activities than the cores collected in the coarser sediments upstream of RM 15, with a tendency for maximum activities to be in or near the deepest segment, indicating that the channel and the shoals have accumulated several feet of sediment over the long term.[44]

Contaminant Patterns

In addition to surface contamination, cores collected in this reach have contamination at depth, consistent with the sediment accumulation noted above. In general, the maximum concentration of

[43] Due to the absence of multi-beam bathymetry data for the Dundee Dam to RM 15.6 reach, and for most of the RM 15.6 to RM 14 reach, the 3D maps are only presented from this reach onward.

[44] A more detailed interpretation of depositional history at these locations is not possible given the lack of well-defined peaks.

2,3,7,8-TCDD, total PCBs, total DDx, and mercury occurs in subsurface segments, suggesting sediment accumulated beyond the 1950s and 1960s, when peak contaminant discharges occurred. The concentrations of these contaminants are generally higher than found farther upstream (Figures 4.1-9a through 4.1-9d) and exhibit somewhat of a longitudinal pattern, with higher levels more frequently encountered moving downstream. This pattern likely reflects this reach being a transition zone near the upstream limit of the estuarine circulation driven by the movement of the salt wedge. The highest contaminant levels in this reach are measured in fine sediments. Surface concentrations of 2,3,7,8-TCDD in coarse sediments here are higher than those measured in coarse sediments of the upstream reaches (Figure 4.1-9a) but are still lower than those measured in fine sediments (see Figure 4.2.3-9 for a distribution of 2,3,7,8-TCDD and total PCB concentrations on SSS-identified sediment types, and Appendix K for similar figures of total DDx, mercury, HMW PAHs, and LMW PAHs). Surface concentrations of total PCBs, total DDx, and mercury in coarse sediments are comparable to the levels in the coarse sediments of the upstream reaches (Figures 4.1-9b through 4.1-9d). PAH levels in this reach are similar to those in the upstream reaches (Figures 4.1-9e and 4.1-9f) and, like the rest of the river, are generally not lower in coarse sediments than in fine sediments (see also Appendix K Figures 8-2 and 9-2). The overall concentrations measured in this reach are summarized in Table 4-4.

Between RM 14 and RM 13.5, six grab samples and three cores were collected. Seven have surface sediment 2,3,7,8-TCDD levels below 25 ng/kg. The most downstream sample here at RM 13.54, LPT14B, contains 48 ng/kg (Figure 4.2.3-10). Of note is 13B-0561 collected in the right shoal at RM 13.74, which has a surface 2,3,7,8-TCDD concentration of 1,550 ng/kg even though it is surrounded by seven other samples with less than 25 ng/kg. Similarly, it has unusually high surface concentrations of total PCBs (Figure 4.2.3-11), total DDx (Figure 4.2.3-12), and mercury (Figure 4.2.3-13) for this region.[45] Though the subsurface levels of 2,3,7,8-TCDD are less than 100 ng/kg at this location, subsurface concentrations of other contaminants are comparable to their surface levels. Even though the location was mapped by SSS as Gravel and Sand, the surface segment consists of 25% fine sediments, and the at-depth segments contain 38% (0.5- to 1.5-foot) and 18% (1.5- to 2.5-foot) fines, suggesting the sample was collected in an area of fine sediments too small to have been delineated by the SSS survey. This is also seen in the probing data, which indicate multiple locations containing silt in the surface sediments in the eastern shoal between RM 13.85 and RM 13.7 in the region classified as Gravel and Sand by the SSS survey (Figure 4.2.3-3). The probing data in the rest of the channel and western shoal between RM 14 and RM 13.5 is mostly consistent with the coarser sediments identified by the SSS.

Between RM 13.5 and the Douglas O. Mead Bridge at RM 13, there are seven cores and one grab sample. Surface sediment 2,3,7,8-TCDD concentrations are less than 25 ng/kg in three samples and

[45] The surface segment of 13B-0561 contains 7.4 mg/kg of total PCBs, 0.4 mg/kg of total DDx, and 3.5 mg/kg of mercury.

between 25 and 100 ng/kg in four others (Figure 4.2.3-10). The notable exception to this pattern of relatively low concentrations is the left shoal sample 13B-0574 located at RM 13.5, which has a surface sediment 2,3,7,8-TCDD concentration of 465 ng/kg and concentrations between 650 and 700 ng/kg in deeper layers. Surface concentrations of the other contaminants are also higher in this sample relative to the rest of this region.[46] Like 2,3,7,8-TCDD, subsurface concentrations of these contaminants in this core are also higher than the concentrations measured upstream of RM 13. Also of note is the 2.5- to 3.5-foot layer of CLRC-078 at RM 13.25, which contains higher concentrations of 2,3,7,8-TCDD (447 ng/kg), total PCBs (3.97 mg/kg), and mercury (4.32 mg/kg) than elsewhere in the core and is higher than the concentrations generally observed in this region. Similar to CLRC-084 in the previous reach, the deeper sediment has a higher fine sediment content than the shallower sediments,[47] indicating the fine sediments have been buried under coarser materials

The association of contaminants with fine sediments is also seen in 12A-0486 on the western shoal at RM 13.01, just upstream of the Douglas O. Mead Bridge, where probing data support the presence of a spatially limited silt pocket (Figure 4.2.3-3). Here, the 0- to 0.5-foot and 1.5- to 2.5-foot layers have about 20% fines and contain higher contaminant levels than the intermediate layer (0.5 to 1.5 feet) has lower percent fines (8%).[48] The profiles suggest a combination of sediment type influence (middle layer typically lower than surface) and loading history (third segment typically highest). An association of contamination with fine sediments occurs for 13B-0572 on the eastern slope at RM 13.01; the 0.5- to 1.5-foot and 1.5- to 2.5-foot layers have fine sediment fractions of 30% and 38%, respectively, and show correspondingly elevated mercury levels (13.2 and 4.1 mg/kg, respectively).[49]

Between the Douglas O. Mead Bridge (RM 13) and RM 12.75, somewhat higher contamination levels are measured. A core collected in the inner bend (CLRC-077) just inside the boundary of the Silt and Sand deposit has a 2,3,7,8-TCDD concentration of 19,247 ng/kg in the 1.5- to 2.5-foot segment, with progressively lower concentrations toward the surface (2,095 ng/kg in the 0.5- to 1.5-foot segment and 585 ng/kg in the surface segment). The fine sediment content is high throughout the core and increases from the 1.5- to 2.5-foot segment to the surface (37%, 57%, and 95%), indicating a silt deposit that was not identified within the larger Silt and Sand deposit. The probing data between RM 12.8 and RM 12.7 indicate that most of the probed locations along the inner bend contain finer sediments than those mapped by the SSS. The probes identified sand along the Gravel and Sand

[46] While surface concentrations of total PCBs and total DDx are less than 0.5 and 0.05 mg/kg in the surrounding area, they are 2.15 and 0.7 mg/kg, respectively, in this core.

[47] The 2.5- to 3.5-foot layer has 40% fine sediments, while the 0- to 0.5-foot, 0.5- to 1.5-foot, and 1.5- to 2.5-foot layers comprise 5%, 12%, and 19% fine sediments, respectively

[48] 2,3,7,8-TCDD levels in the surface and 1.5- to 2.5-foot segments of 12A-0486 are 70 and 2,060 ng/kg, respectively; total PCB levels are 4 and 4.4 mg/kg, respectively; total DDx levels are 0.04 and 0.15 mg/kg, respectively; and mercury levels are 0.6 and 2.25 mg/kg, respectively. The 0.5- to 1.5-foot segment contains 51 ng/kg 2,3,7,8-TCDD, 0.2 mg/kg total PCB, 0.01 mg/kg total DDx, and 0.9 mg/kg mercury.

[49] Fine sediment composition for the surface segment of this sample is not available.

mapped shoals along the inner bend, as well as silt along the eastern boundary of the Silt and Sand and Gravel and Sand deposits here.

The small areal extent of the contamination in CLRC-077 is suggested by a nearby core in the same Silt and Sand deposit (13B-0571), which has a surface segment 2,3,7,8-TCDD concentration of 88 ng/kg despite having 47% fine sediment (Figure 4.2.3-10). Subsurface concentrations in 13B-0571 are 104 ng/kg in the 0.5- to 1.5-foot segment and 6 ng/kg in the 1.5- to 2.5-foot segment. The same is also true for total PCBs, total DDx, and mercury; the highest concentrations for all these contaminants in the inner bend is in the 1.5- to 2.5-foot segment of CLRC-077.[50]

Bathymetric survey data indicate that the 1.5- to 2.5-foot segment of CLRC-077, which contains the highest contaminant concentrations, remained buried over the period from collection in 2008 to the most recent bathymetric survey in 2012 (Figure 4.2.3-14). The changes in surface elevation indicate that the 0- to 0.5-foot layer may have been eroded and subsequently replaced with approximately 0.5 foot of new sediments.

Contaminant concentrations along the outer bend are lower than those in CLRC-077, with the highest 2,3,7,8-TCDD concentrations measured in the 1.5- to 2.5-foot segment and deeper than the 3.5-foot segment of 13B-0557[51] (279 and 339 ng/kg, respectively). The 1.5- to 2.5-foot segment also has the highest total PCB and total DDx concentrations in the outer bend (2.5 and 0.1 mg/kg, respectively). This core (13B-0557) was collected in 2013 in the area on the steep western shoal with greater than 1.5 feet of erosion (as observed in the 3D relief maps in Figure 4.2.3-7) after the consistent erosion that occurred here since 2007. The bathymetry data (Figure 4.2.3-14) suggest that the core surface here represents the minimum bed elevation since 2007. Unlike the other contaminants, elevated mercury levels are observed in the at-depth segments of the sample collected just upstream at RM 12.96 (13B-0558). Mercury concentrations in the 0.5- to 1.5-foot segment here are 6.89 mg/kg.

Within the channel between RM 13 and RM 12.75, two samples were collected at RM 12.8: core CLRC-076 and grab sample LPRT13F. CLRC-076 has higher contaminant concentrations at the surface than at depth.[52] The grab sample LPRT13F collected about 7 feet away exhibits much lower concentrations than the surface segment of CLRC-076; this sample has concentrations similar to the low at-depth concentrations of CLRC-076. Another oddity of the CLRC-076 surface segment is that it

[50] 13.9 mg/kg for total PCBs, 0.42 mg/kg for total DDx, and 9.79 mg/kg for mercury.
[51] No data are available for the 2.5- to 3.5-foot segment of this core.
[52] 2,3,7,8-TCDD levels in the surface are 296 mg/kg, while the at-depth levels are all less than 25 ng/kg. Similarly, while the surface total PCB, total DDx, and mercury levels are 8.8, 0.795, and 2.75 mg/kg, respectively, the at-depth concentrations are less than 0.05 mg/kg for total PCBs and total DDx and less than 1 mg/kg for mercury.

has a fairly low fine sediment fraction (6% at the surface and between 6% and 13% at all depths), which is associated with low contaminant concentrations elsewhere in this reach.

Downstream of RM 12.75, the highest 2,3,7,8-TCDD concentrations are measured in subsurface segments of G0000010, with 9,390 ng/kg in the 2.5- to 3.5-foot segment and 9,650 ng/kg below 3.5 feet (Figure 4.2.3-10). Levels of other contaminants are also elevated at these depths.[53] While there are no data for the surface segment of G0000010, CLRC-074, which is located a few feet away, has surface concentration data and exhibits a similar subsurface pattern to G0000010; contaminant levels are highest in the deepest segment (greater than 5.5 feet) and lower in the surface and 0.5- to 1.5-foot segments,[54] indicating burial has occurred here. Fine sediments comprise more than 40% of the sediments in the surface and subsurface segments of CLRC-074, and as observed in the probing data (Figure 4.2.3-3), the fine sediment deposit is located on the eastern boundary of the Rock and Coarse Gravel deposit here, suggesting another instance of a very small fine sediment deposit. The lower surface concentrations are further confirmed by the grab sample LPRT13E collected at the same location.[55] Although erosion at CLRC-074 has occurred since the core was collected in 2008, the highest contaminant levels have remained approximately 3 feet below the surface (Figure 4.2.3-14). All the other cores collected downstream of RM 12.75 have significantly lower contaminant concentrations in the surface and subsurface segments.

Like the previous reach, while surface concentrations, subsurface concentrations, and MPA of total PCBs, total DDx, and mercury are well correlated to 2,3,7,8-TCDD (Figures 4.2.3-15a through 4.2.3-15c), relationships are weaker for PAHs. Surface concentrations of HMW and LMW PAH are not well-correlated to 2,3,7,8-TCDD (Figures 4.2.3-15d and 4.2.3-15e). The subsurface concentrations appear better correlated, though there are still locations with comparable subsurface PAH levels at lower and higher subsurface 2,3,7,8-TCDD levels. Surface concentrations of the two PAHs in coarser sediments are higher than those in finer sediments, and concentrations do not have a longitudinal trend (Figures 4.1-9e and 4.1-9f).

HMW PAH levels (Figure 4.2.3-16) upstream of RM 13.5 are generally less than 30 mg/kg. Similar to the other contaminants, HMW PAH levels are higher in 13B-0561 (60 mg/kg in the surface and about 40 mg/kg in the subsurface segments). Concentrations greater than 100 mg/kg have also been measured in the grab sample 13B-0562 at RM 13.8 (139 mg/kg) and in the surface and 1.5- to 2.5-foot segments of CLRC-079 at RM 13.6 (156 and 192 mg/kg, respectively). The surface concentrations of LMW PAHs (Figure 4.2.3-17) in all three cores in this region, and two of the six grab

[53] Total PCB levels in the 2.5- to 3.5-foot segment and below 3.5 feet are 34 and 22 mg/kg, respectively; total DDx levels are 0.55 and 0.7 mg/kg, respectively; and mercury levels are 9.78 and 7.6 mg/kg, respectively.

[54] Concentrations in the surface segment here are 164 ng/kg 2,3,7,8-TCDD, 0.57 mg/kg total PCBs, 0.06 mg/kg total DDx, and 0.9 mg/kg mercury. Concentrations in the 0.5- to 1.5-foot segment are 120 ng/kg 2,3,7,8-TCDD, 0.75 mg/kg total PCBs, 0.08 mg/kg total DDx, and 1.27 mg/kg mercury. Concentrations in the deepest segment are 1,266 ng/kg 2,3,7,8-TCDD, 3.3 mg/kg total PCBs, 0.19 mg/kg total DDx, and 4.75 mg/kg mercury.

[55] 2,3,7,8-TCDD, total PCB, total DDx, and mercury concentrations of 79 ng/kg, 0.4 mg/kg, 0.04 mg/kg, and 0.83 mg/kg, respectively.

samples, are higher than 10 mg/kg, with the highest levels measured in the surface of CLRC-079 (65 mg/kg).

Between RM 13.5 and the Douglas O. Mead Bridge, most of the surface and subsurface HMW PAH measurements are between 15 and 30 mg/kg (Figure 4.2.3-16). The highest concentration here is measured in the surface of 13B-0573 at RM 13.27 (118 mg/kg). All other surface concentrations are between 15 and 40 mg/kg, except the surface segment of 12A-0486 at RM 13.01 (84 mg/kg). LMW PAH trends in this stretch (Figure 4.2.3-17) are similar to HMW PAHs, with the highest concentration measured in the surface of 13B-0573 (41 mg/kg). Like HMW PAHs, surface concentrations at other locations are lower than at 12A-0486 (15 mg/kg). The highest subsurface levels of both PAHs were measured in 13B-0560 (RM 13.49), which contained 87 mg/kg HMW PAHs and 30 mg/kg LMW PAHs in the 1.5- to 2.5-foot segment.

Downstream of the Douglas O. Mead Bridge, PAH trends again differ from the other contaminants. While the highest concentrations of the other contaminants were measured in the inner bend at CLRC-077, the highest PAH levels are measured elsewhere. For example, HMW PAH levels along the outer bend in 13B-0557 are between 30 and 40 mg/kg in the surface and subsurface segments, while levels along the inner bend are lower (Figure 4.2.3-16). The highest HMW PAH and LMW PAH levels are measured in the channel in the surface of CLRC-076 (209 and 33 mg/kg, respectively), which also has elevated levels of the other contaminants, and the surface of 12A-0485 (20.62 mg/kg). These concentrations are lower than the LMW PAH concentrations in CLRC-077 (5.69 mg/kg at surface and 6.94 mg/kg in the 1.5- to 2.5-foot segment, with all other depths having levels below 1.5 mg/kg). These findings could be because PAHs are not as preferentially associated with fine sediments as 2,3,7,8-TCDD, total PCBs, total DDx, or mercury (Figures 4.1-8 and 4.1-9).

PAH concentration patterns in the cluster of samples at RM 12.57 (G000010, CLRC-074, and LPRT13E) show similar deviations from the other contaminants. Concentrations of both PAHs are greatest at depth in the 2.5- to 3.5-foot segment of G000010 (49.5 mg/kg HMW PAHs and 12.3 mg/kg LMW PAHs). While levels of LMW PAHs are lower in the shallower segments (ranging widely between 2 and 8 mg/kg across all the depths of all three samples), concentrations of HMW PAHs at the surface and shallower subsurface segments are comparable to those in the 2.5- to 3.5-foot segment of G0000010 (e.g., the surface segment of G0000010 has an HMW PAH concentration of 40 mg/kg, and the 0.5- to 1.5-foot segments of G0000010 and CLRC-075 contain 42 and 38 mg/kg, respectively).

To summarize, concentrations of 2,3,7,8-TCDD, total PCBs, total DDx, and mercury in this reach increase longitudinally (i.e., moving downstream). The highest concentrations were found in fine sediment pockets that were not observed in the SSS. These small sediment pockets with higher contaminations were observed in the eastern shoal between RM 13.8 and RM 13.75, on the western shoal just upstream of the Douglas O. Mead Bridge at RM 13, on the eastern shoal on the inner bend between RM 12.8 and RM 12.7, and just next to the Rock and Coarse Gravel deposit at RM 12.57. Like

the upstream reaches, PAH levels in this reach do not show as much of a variation longitudinally and do not seem to be as closely associated with fine sediments.

4.2.4 RM 12.5 to Confluence with Third River (RM 11.2)

This reach extends from the upstream boundary of the first SSS-identified Silt deposit at RM 12.5 to the confluence with the Third River at RM 11.2. The total area of the sediment bed in this reach is 47 acres. Cross-sectional area initially decreases from 3,650 ft^2 at the upstream extent to 3,150 ft^2 at RM 11.8 (Figure 4.1-1). It then increases as the river bends west, with the cross-sectional area ranging between 3,700 and 4,200 ft^2 near the downstream extents. It is crossed by the Route 3 Bridge at RM 11.6 and the Lyndhurst Draw, which is a NJ Transit Railroad Bridge, at RM 11.4 (Figure 4.2.4-1). The reach runs mostly N-S, with a small bend centered at RM 12.3 shifting the orientation slightly west, and a larger bend downstream of the Route 3 Bridge, shifting orientation to NE-SW. The western shoreline runs along Route 21 and is sheetpiled or bulkheaded until just downstream of the Route 3 bridge and then vegetated for the remainder. The eastern shoreline is almost entirely vegetated, except for a small section around RM 12.2.

The federal navigation channel continues through this reach. Its last maintenance dredging in this reach occurred between RM 12.4 and RM 12.1 in 1976; the rest of it was last maintained before 1950. Bathymetry data indicate that the river channel is closely aligned to the navigation channel, except along the bend between the Route 3 Bridge and the Lyndhurst Draw, where deposition along the inner bend has shifted the river channel slightly eastward (Figure 4.2.4-1).

The evolution of the sediment bed is studied using bathymetry data (single-beam surveys [1932, 1948, 1976,[56] 1989, 2004, and 2007] and multi-beam surveys and associated single-beam transect measurements [2007, 2008, 2010, 2011, and 2012]), model-predicted bottom shear stress patterns, and Cs-137 core profile data. Its characteristics are described using results of the 2005 SSS survey and its ground-truthing data, probing surveys, and characteristics and contaminant concentrations of individual cores.

A thin sliver of SSS-identified Silt exists along the western inner bend from RM 12.5 to RM 12.15 (Figure 4.2.4-2) and constitutes the most upstream SSS Silt deposit within the LPR. This deposit is located mostly on the side slopes of the channel and is separated from the shoreline by a thin band of Rock and Coarse Gravel. Cs-137 profiles at the boundary of the Silt deposit and the Rock and Coarse Gravel deposit (G0000011-1A and G0000011-1D) do not show evidence of consistent deposition (Figure 4.2.4-3), but the magnitude of the Cs-137 activity there indicates that the area has been subject to several feet of historical deposition. Adjacent to the Silt deposit are two slivers

[56] The 1976 bathymetry dataset combines the post-dredge 1976 data (where available) with the 1975 bathymetry survey. In parts of the navigation channel maintained in 1974 (discussed in Section 4.2.7), the 1975 bathymetry survey represents a post-dredge survey.

designated by the SSS as Sand, and the remainder of the channel and eastern shoal down to the larger bend downstream of the Route 3 Bridge (RM 11.6) are a continuation of the Gravel and Sand from the previous reach. The Silt deposit occupies only 2 acres out of the 15.5 acres between RM 12.5 and RM 12.

The more significant bend downstream of the Route 3 Bridge exhibits the sediment trends observed in other bends, with the coarsest sediments along the outer bend, the finest sediments along the inner bend, and increasingly coarse sediments moving from the inner bend toward the outer bend (Figure 4.2.4-2). Consistent with this finding are the shear stress patterns (Figure 4.2.4-4), which show higher shear stresses along the outer bend and lower shear stresses along the inner bend. Cs-137 data in the bend indicate mixed trends with either well-defined buried peaks or surface peaks generally observed (Figure 4.2.4-3) and variations in the amount of accumulated sediment since the 1960s along both sides of the bend.

Similar to the region around the confluence of the Saddle River, a Rock and Coarse Gravel outcrop is present at the confluence of the Third River. The higher local shear stresses that likely exist here during Third River high discharge events are not reflected in the predicted maximum shear stresses (Figure 4.2.4-4), presumably due to the resolution of the hydrodynamic model in this region and the nature of the shear stress metric shown (see Section 7.3 for a discussion of model uncertainty and the model's limitations on representing small scale features). The bed composition in this region will also in part reflect the nature of the sediment load from the Third River.

Bathymetry data in this reach include the 1932, 1948, 1975, 1989, 2004, and 2007 single-beam surveys and the post-2007 multi-beam surveys. The 1932 and 1948 bathymetry surveys are only available for the downstream parts of this reach, with the 1932 survey beginning near the Lyndhurst Draw and the 1948 survey beginning around RM 11.25. A comparison of the single-beam datasets indicates that no major changes in the channel shape or elevation occurred during that period (Figure 4.2.4-5).

More recent multi-beam bathymetry data (Figure 4.2.4-6) suggest that upstream of the Route 3 bridge, the channel has mostly undergone less than 6 inches of change, with a narrow band of net erosion or erosion and deposition along the Silt deposit on the western side slopes of the channel (Figure 4.2.4-3) and a small area of net erosion on the eastern side slope of the channel. Most of the identified erosion occurred between 2008 and 2010, with some parts of the side slopes experiencing erosion of more than 1.5 feet. Much of this region (Silt deposit and the western slope) underwent subsequent infilling between 2011 and 2012 (generally a low-flow period).

The channel between the Route 3 bridge (RM 11.6) and the Lyndhurst Draw (RM 11.4) experienced significant erosion during Hurricane Irene, with most of the channel being more than 5 feet deeper in 2011 than in 2010. Some of the erosion near the Route 3 bridge may be associated with the constriction

of the channel at the location of the bridge; however, no recent bathymetry data are available at the location of the bridge. The erosion was restricted to the channel; some parts of the shoals along the inner bend experienced more than 5 feet of deposition after the 2010 survey (Figure 4.2.4-7). Farther downstream of the Lyndhurst Draw, the side slopes experienced erosion likely due to Hurricane Irene, but parts of the main channel were depositional. Two transects near the confluence of the Third River at RM 11.25 confirm this observation, with higher 2004 elevations compared to 2012 observed in the shoals near the confluence of the tributary and in the eastern side of the channel; elevations within the main channel are about the same across both years (Figure 4.2.4-8).

Contaminant Patterns

The salt front occasionally extends into and through this reach (Section 3.3), and the sediments generally contain higher levels of 2,3,7,8-TCDD, total PCBs, total DDx, and mercury here than in the upstream reaches (Figures 4.1-9a through 4.1-9d). PAH levels in this reach, however, tend to be lower than those in the upstream reaches (Figures 4.1-9e and 4.1-9f). Contaminant concentrations in the surface and 0.5- to 1.5-foot segment upstream of the Route 3 Bridge are highest in the 2-acre silt deposit between RM 12.5 and RM 12.15 (Figure 4.2.4-9; see Appendix K for similar figures of total DDx, mercury, HMW PAHs, and LMW PAHs). Farther downstream, concentrations are higher in the Silt and Sand deposit along the inner bend downstream of the Lyndhurst Draw, as well as in silt pockets along the outer bend. The latter concentrations are similar to those measured in the RM 10.9 deposit (discussed as part of the next reach). The overall concentrations measured in this reach are summarized in Table 4-5.

Upstream of the Route 3 Bridge, the highest concentrations are located within the RM 12.5 to RM 12.15 Silt deposit. Core 13B-0555, collected in 2013 from the upstream portion of this deposit (RM 12.46), has the highest levels of 2,3,7,8-TCDD (Figure 4.2.4-10), total PCBs (Figure 4.2.4-11), and total DDx (Figure 4.2.4-12) within the deposit, with at-depth levels similar to the surface levels.[57] This core also contains 14, 10, and 12.5 mg/kg of mercury in the 0–0.5 feet, 0.5- to 1.5-foot, and 1.5- to 2.5-foot segments, respectively, and 5.85 mg/kg in the 2.5- to 3.5-foot segment. The highest mercury concentrations (Figure 4.2.4-13) upstream of RM 7.8 in the LPR are found in the 0.5- to 1.5-foot segment of CLRC-073 at RM 12.31 (42 mg/kg).

Farther downstream, LPRC13A (RM 12.38) and 13B-0553 (RM 12.32) are located west of the other cores, and in the Rock and Gravel deposit along the western bank. Both locations contain lower contamination concentrations than the nearby eastern locations in the Silt deposit. The grab sample LPRC13A has lower contamination concentrations than the grab sample LPRT13C located just upstream and farther east. The former contains 2,3,7,8-TCDD, total PCB, total DDx, and mercury

[57] The surface segment of this core contains 17,600 ng/kg of 2,3,7,8-TCDD, 23 mg/kg of total PCBs, 0.4 mg/kg of total DDx, and 14.3 mg/kg of mercury. The 1.5- to 2.5-foot segment contains 15,250 ng/kg, 21 mg/kg, 0.49 mg/kg and 12.55 mg/kg of 2,3,7,8-TCDD, total PCB, total DDx, and mercury, respectively.

concentrations of 290 ng/kg, 0.6 mg/kg, 0.06 mg/kg, and 2.1 mg/kg, respectively, while levels in the latter are 490 ng/kg, 1 mg/kg, 0.1 mg/kg, and 2.6 mg/kg, respectively. Similarly, surface contaminant concentrations in 13B-0553 are lower than surface concentrations in nearby CLRC-073 that is located slightly east within the Silt deposit. Lower concentrations along the shoreline near silt areas are also observed elsewhere (e.g., along the RM 10.9 deposit discussed in the next section) and may in part reflect the absence of fine sediment accumulation due to wave action.

Downstream of 13B-0555 (RM 12.46) in the silt deposit, higher contaminations are found in the top 2.5 feet. Core 12A-0483, G0000169, and G0000166 have only 2.5 feet or less of recovered sediment. Cores CLRC-073 and 13B-0552 have much lower levels below 2.5 feet. The two most downstream cores in the Silt deposit (12A-0483 and 13B-0552) have coarser sediments below the surface, but still have higher contamination levels than outside the Silt deposit. For instance, the 1.5- to 2.5-foot segment of 12A-0483 contains 15% fine sediments and has 2 mg/kg of total PCBs and 4.5 mg/kg of mercury. Similarly, the 0.5- to 1.5-foot segment of 13B-0552 contains 14% fine sediments and has 795 mg/kg 2,3,7,8-TCDD and 2.5 mg/kg total PCBs.

The locations in the Silt deposit at which the cores were collected have experienced both erosion and deposition over the period from 2007 and 2012 (Figure 4.2.4-7; see cores 13B-0555, G0000169, CLRC-073, G0000166, 12A-0483, and 13B-0552). At some of these locations, the apparent erosion since the core was collected suggests that higher concentrations may have been exposed (note that the apparent bathymetry changes are subject to uncertainty due to sampling error and positioning error). An example is core CLRC-073 collected in 2008 (Figure 4.2.4-14). Between 2010 and 2011, it appears the location experienced erosion sufficient to expose the sampled 0.5- to 1.5-foot section. A similar outcome may exist at the location of core G0000166 collected in 2008. Here, subsequent erosion that occurred between 2008 and 2010 appears to have exposed higher concentration subsurface sediments; these sediments were then covered up between 2010 and 2011.

Outside the Silt deposit, contaminant concentrations at locations in the deeper channel are lower than concentrations on the side slopes and the shoals (Figure 4.2.4-7). This pattern extends downstream to the Route 3 Bridge. Cores in the channel (LPRT13D, 12A-0484, LPRT13A, CLRC-071, and 12A-0482) contain 2,3,7,8-TCDD concentrations less than 100 ng/kg in surface and subsurface sediments whereas levels on the eastern side slope are higher. While contamination levels on the eastern side slopes and eastern shoals are significantly lower than those in the Silt deposit, the grab sample LPRT12E on the eastern shoal at RM 11.74 has contamination levels higher than the surrounding region[58]. The fine sediment composition of this sample is 46%, suggesting another instance of a fine sediment pocket not captured by the SSS survey. The probing data here confirms

[58] 2,550 ng/kg 2,3,7,8-TCDD, 3.5 mg/kg total PCBs, 0.11 mg/kg total DDx, and 3.25 mg/kg mercury.

the limited spatial extent of the fine sediment deposit, with some Silt and Silt and Sand probes identified in the Gravel and Sand deposit between RM 11.74 and RM 11.7 along the eastern shoal.

Between the bridges, similar to other inner bends, contaminant concentrations are higher in the cluster of samples CLRC-069, B01-SD1, and LPRT12C collected in the finer Silt and Sand deposit in the inner bend at RM 11.52 than in the surrounding samples in the outer bend.[59] 2,3,7,8-TCDD concentrations greater than 500 ng/kg were measured in the surface and subsurface sediments in this cluster.[60] Concentrations of the other contaminants are also higher within these cores.[61] The two downstream samples within the same deposit contain lower levels of contaminants, with higher levels in the 1.5- to 2.5-foot segment of 13B-0548 (RM 11.46) than in the surface and 0.5- to 1.5-foot segments, a likely consequence of the higher percent fine sediment composition of the 1.5- to 2.5-foot segment (64%) than the surface (31%) and the 0.5- to 1.5-foot segment (28%).

While the region in the outer bend has been classified as Gravel and Sand by the SSS, the 0- to 0.5-foot and 1.5- to 2.5-foot segments of CLRC-70 contain 87% and 63% fine sediments, respectively, suggesting this core is part of a fine sediment deposit smaller than the resolution of the SSS survey. Probing data here suggest that the Silt deposit is limited to the region in the outer bend just around RM 11.5 (Figure 4.2.4-2). This core has higher total DDx levels in the surface (0.27 mg/kg) than other samples collected in Gravel and Sand deposits; the reason for this is unknown. Levels of the other contaminants are generally similar to the lower concentrations measured in the Gravel and Sand deposit of this reach, suggesting the elevated total DDx level is anomalous.

Though the inner bend exhibits higher surface and subsurface contaminant levels, the cores were collected at shoal locations that experienced significant post-2010 deposition (Figure 4.2.4-14). For example, the top 2 feet of cleaner sediments of B01-SD1 all deposited after 2011. This significant deposition has also resulted in burial of the more contaminated sediments in CLRC-069 (as observed in Figure 4.2.4-13, the core was collected in 2008 and has since experienced more than 3 feet of deposition of what are likely cleaner sediments with levels comparable to the top 2 feet of B01-SD1). A similar amount of deposition is also seen in B02-SD1 at RM 11.46. Some deposition also occurred on the right shoal, where CLRC-070 experienced a little more than 6 inches of deposition since core collection in 2008.

Between the Lyndhurst Draw and the downstream extent of this reach at RM 11.2, 2,3,7,8-TCDD levels are generally higher than 500 ng/kg in both surface and subsurface sediments on both sides of

[59] There are no samples available in the region that experienced more than the 5 feet of erosion noted previously.

[60] Surface 2,3,7,8-TCDD levels greater than 500 ng/kg are seen in LPRT12C (550 ng/kg), and CLRC-069 (1,751 ng/kg). Subsurface levels greater than 500 ng/kg are seen in the 0.5- to 1.5-foot segment of CLRC-069 (11,850 ng/kg) and in the 2.5- to 3.5-foot segment of B01-SD1 (4,135 ng/kg).

[61] The 0.5- to 1.5-foot segment of CLRC-069 contains 3 mg/kg of total DDx and 25 mg/kg of mercury, and the bottom (below 5.35 feet) segment of the same core contains 6 mg/kg of total PCBs.

the channel—all the samples here were collected in the shoals or on the side slopes; no samples were collected within the main channel[62]. The eastern Silt and Sand deposit continues until the end of this reach, with contaminant concentrations similar to those in the cluster of cores around RM 11.52.[63] Farther downstream on the western side, concentrations in 13B-0575 are highest in the surface and 0.5- to 1.5-foot segments.[64] Though 13B-0575 was collected in a location identified as Rock and Coarse Gravel around the Third River confluence, the fine sediment composition of these two segments (36% and 91%, respectively) suggests the core was collected in a fine sediment pocket. The probing data within the Rock and Coarse Gravel deposit at the Third River confluence suggest the presence of many such smaller Silt sediment pockets (Figure 4.2.4-2)

The cores collected on the western shoal contain surface and subsurface levels of 2,3,7,8-TCDD in excess of 10,000 ng/kg (Figure 4.2.4-10). Though the region has been classified as Gravel and Sand near the channel and Rock and Coarse Gravel near the banks, the cores here have varying amounts of fine sediments, suggesting the presence of multiple fine sediment pockets. From upstream to downstream, the surface segments of 13B-0578, 13B-0547, 12A-0481, and 12E-0369 contain 40%, 87%, 82%, and 18% fine sediments, respectively.[65] The grab sample 13B-0546 collected between 13B-0547 and 12A-0481 comprises 5% fine sediments, more indicative of the coarse sediments identified by the SSS survey in this region. The elevated contaminant concentrations seen here are similar in magnitude to those seen immediately downstream in the RM 10.9 point bar (discussed as part of the next reach).

The highest contaminant concentrations in this region are found in 13B-0547 and 12A-0481. The surface segment of 13B-0547 contains the highest 2,3,7,8-TCDD concentrations in this reach (51,100 ng/kg). A co-located sample 13B-0547-C5 has lower surface concentrations (1,075 ng/kg) but contains 23,125 ng/kg in the 0.5- to 1.5-foot segment. The 1.5- to 2.5-foot segments of the cores also indicate significant variability, with 38 ng/kg measured in 13B-0547 but 7,511 ng/kg measured in 13B-0547-C5. The surface segment of 13B-0547 also contains total PCB (16 mg/kg) and mercury (12.4 mg/kg) concentrations that are higher than most other measurements in this reach. Total DDx levels in the higher range of concentrations in this reach are found in the subsurface segments, with 1.17 mg/kg measured in the 1.5- to 2.5-foot segment of 13B-0547-C5.

[62] Sampling was biased toward the shoals in an effort to characterize the gradients in concentration between the shoreline and the channel side slope that were noted in the 2008 sampling efforts.

[63] For example, the 0.5- to 1.5-foot segments of CLRC-068 and G0000165 contain 1,478 and 10,700 ng/kg of 2,3,7,8-TCDD, 2.6 and 4.4 mg/kg of total PCBs, 0.24 and 0.48 mg/kg of total DDx, and 2.85 and 6.7 mg/kg of mercury, respectively.

[64] The surface segment contains 8,090 ng/kg 2,3,7,8-TCDD, 12 mg/kg total PCBs, 0.25 mg/kg total DDx, and 9 mg/kg mercury, while the 0.5- to 1.5-foot segment contains 3,420 ng/kg 2,3,7,8-TCDD, 5.8 mg/kg total PCBs, 0.2 mg/kg total DDx, and 3.4 mg/kg mercury.

[65] The 0.5- to 1.5-foot segments of these cores contain 24%, 90%, 44%, and 16%, while the 1.5- to 2.5-foot segments contain 57%, 69%, 34%, and 40% fine sediments, respectively.

2,3,7,8-TCDD concentrations in the surface and 0.5- to 1.5-foot segments of 12A-0481 are 23,200 and 35,600 ng/kg, respectively, but are significantly lower in the 1.5- to 2.5-foot segment (62 ng/kg). Total PCB, total DDx, and mercury levels in the surface and 0.5- to 1.5-foot segments (16 and 24 mg/kg total PCBs, 0.62 mg/kg total DDx in both segments, and 11.8 and 13 mg/kg mercury, respectively) are among the highest in the reach.

Like the upstream reaches, surface concentrations of total PCBs, total DDx, and mercury are well correlated to surface concentrations of 2,3,7,8-TCDD (Figures 4.2.4-15a through 4.2.4-15c). While subsurface concentrations and MPA of total PCBs and total DDx are also well correlated to 2,3,7,8-TCDD, the relationship is weaker for mercury. A weak relationship in surface concentrations and MPA levels is also observed for the PAHs (Figures 4.2.4-15d and 4.2.4-15e). Subsurface concentrations of the PAHs are not correlated to 2,3,7,8-TCDD. A further distinguishing fact is that unlike 2,3,7,8-TCDD, total PCBs, total DDx, and mercury, levels of HMW PAHs and LMW PAHs are lower in this reach than the upstream reaches (Figures 4.1-9e and 4.1-9f). While the RM 14 to RM 12.5 reach contained HMW PAH concentrations in the surface sediments generally in the 10 to 200 mg/kg range, this reach contains surface HMW PAH levels in the 1 to 50 mg/kg range. Surface LMW PAH concentrations in the RM 14 to RM 12.5 reach generally ranged between 1 and 65 mg/kg, whereas the highest surface LMW PAH concentration in this reach is 14 mg/kg.

Within the Silt deposit between RM 12.5 and RM 12.15, HMW PAH levels (Figure 4.2.4-16) are highest in the surface (35 mg/kg) and 0.5- to 1.5-foot segments (35 mg/kg) of 13B-0555, the surface of G0000169 (33 mg/kg), and surface of G0000166 (40 mg/kg). LMW PAH levels in the Silt deposit are higher in the surface and 0.5- to 1.5-foot segments of 13B-0555 (8 and 8.4 mg/kg respectively), and in the surface segment of G0000166 (9 mg/kg). Concentrations are lower at depth (Figure 4.2.4-16), and HMW PAH levels are generally comparable to levels outside the Silt deposit. The grab sample LPRT13A contains 35 mg/kg of HMW PAHs and 8.5 mg/kg of LMW PAHs, similar to the four samples cited above. This sample, located immediately downstream of the Silt deposit, has concentrations of 2,3,7,8-TCDD, total PCBs, total DDx, and mercury that are significantly lower than the levels within the Silt deposit.

Moving downstream, HMW PAH concentrations greater than 50 mg/kg are measured in the subsurface segments collected in Silt and Sand deposit along the inner bend downstream of the Route 3 bridge. The 0.5- to 1.5-foot and 1.5- to 2.5-foot segments of CLRC-069 contain 60 and 66 mg/kg, respectively. These are the two highest HMW PAH concentrations in this reach. The concentrations in the surface segment of this core and the nearby grab sample LPRT12C are lower (12 and 24.5 mg/kg, respectively). Concentrations are lower in CLRC-070, collected in the outer bend, with the highest concentration (11 mg/kg) measuring below 3.5 feet.

Downstream of the Lyndhurst Draw, HMW PAH levels are highest in the 0.5- to 1.5-foot segment of CLRC-068 (47 mg/kg) on the eastern shoal but are lower in all other surface and subsurface samples.

The remaining concentrations in this region are not elevated with respect to the parts of the reach upstream of the Lyndhurst Draw, a likely result of the diminished influence of the previously mentioned upstream source (noted in Section 4.2.1), and the differing PAH sorption properties.

LMW PAH concentration patterns (Figure 4.2.4-17) are similar to HMW PAHs. Concentrations of LMW PAHs are highest in the Silt and Sand deposit on the inner bend around the Route 3 bridge. The 0.5- to 1.5-foot segment of the most upstream core in this deposit (13B-0549 at RM 11.68) contains 9.7 mg/kg of LMW PAHs. Concentrations are higher in CLRC-069 at RM 11.52 (15.86 mg/kg, 15.66 mg/kg, and 11.5 mg/kg in the 0.5- to 1.5-foot, 1.5- to 2.5-foot, and 2.5- to 3.5-foot segments of this core). The surface segment and the co-located grab sample LPRT12C contain lower concentrations (2.8 and 4.3 mg/kg, respectively). The surface segment of 13B-0548 contains 14 mg/kg LMW PAHs. Like the other contaminants, concentrations are lower in CLRC-070 on the outer bend. Similar to HMW PAHs, concentration levels downstream of the Lyndhurst Draw are lower than the levels in the inner bend upstream of the Lyndhurst Draw. The highest LMW PAH concentrations here are measured in the 1.5- to 2.5-foot segment of 13B-0578 (12.4 mg/kg) and the 1.5- to 2.5-foot segment of CLRC-068 (9.7 mg/kg).

To summarize, higher concentrations of 2,3,7,8-TCDD, total PCBs, total DDx, and mercury have been measured in this reach than in the more upstream reaches, a likely result of the increasing influence of upstream tidal transport and the increased presence of fine sediments. Contamination patterns and sample sediment composition in this reach illustrate the limitations of the SSS mapping of sediment type and reinforce the finding that the higher concentrations are associated with finer sediments. Concentrations of 2,3,7,8-TCDD, total PCBs, total DDx, and mercury are all higher in the 2-acre Silt deposit between RM 12.5 and RM 12.15 than the coarser area around it. Farther downstream, concentrations are elevated in the Silt and Sand deposit on the inner bend around the Route 3 Bridge, and on both sides of the river downstream of the Lyndhurst Draw in samples with significant fine sediment content. PAH concentrations do not show the same marked differences, and PAH concentrations are generally lower than the concentrations measured in the upstream reaches. PAH levels in samples inside the Silt deposit are comparable to samples collected outside the Silt deposit. Further downstream, the highest PAH levels are measured in the Silt and Sand deposit around the Route 3 bridge, and unlike the other contaminants, concentrations in this deposit upstream of the Lyndhurst Draw are higher than concentrations farther downstream.

4.2.5 Third River (RM 11.2) to Avondale Bridge (RM 10.4)

This reach extends from the confluence of the Third River at RM 11.2 to the Avondale Bridge at RM 10.4 (Figure 4.2.5-1), over which there is an overall increase in cross section from 3,500 ft^2 at RM 11.2 to 4,200 ft^2 at RM 10.4. The western shoreline is sheetpiled and bulkheaded along Route 21, with some natural vegetation starting just upstream of RM 11 (Figure 4.2.5-1). The eastern shoreline is vegetated until RM 10.6 (including Riverside County Park near RM 10.9) and consists of

riprap/stone from RM 10.6 to the Avondale Bridge. The total area of the sediment bed in this reach is 36.5 acres.

The federal navigation channel runs through this reach, but it has not been maintained. The stretch between RM 11 and RM 10.6 was dredged in 1976; the remainder was last maintained in the late 1940s or earlier. Bathymetry surveys show that the portions of the present-day channel deviate from the delineated federal navigation channel (see, for example, the outer bend between RM 11 and RM 10.8 in Figure 4.2.5-1).

The reach contains an approximate 60-degree bend centered on RM 10.9, shifting the orientation from NE-SW to N-S at about the point bar along the inner (eastern) shoal. This point bar, which abuts Riverside County Park, was dredged and capped in 2013 and 2014 (excluding the utility corridor) following the finding of high surface contaminant levels (e.g., 2,3,7,8-TCDD in excess of 50,000 ng/kg). The high-density sediment data collected for remedial design of the removal area allow an in-depth examination of the physical and chemical characteristics of this point bar.

The evolution of the sediment bed is studied using bathymetry data (including post-dredge surveys [1932, 1948, and 1976], single-beam surveys [1989, 2004, 2007, 2012, and 2013], and multi-beam surveys [2007, 2008, 2010, 2011, and 2012]), model-predicted bottom shear stress patterns, and Cs-137 core profile data (mainly available within the point bar). Its characteristics are described using results of the 2005 SSS survey and its ground-truthing data, probing surveys, and characteristics and contaminant concentrations of individual cores.

The geomorphology along the bend at RM 10.9 is similar to that of the bend just upstream at RM 11.5 and follows a classic pattern. The channel moves to the outside as it enters the bend at RM 11.2, and then shifts back toward the center as the river straightens downstream of RM 10.8 (Figure 4.2.5-1). It is asymmetrical, being generally deeper with a steeper side wall along the outside of the bend (see Figures 4.2.5-2a and 4.2.5-1, which show cross sections at RM 10.9 and the bathymetry gradients at the channel edges, respectively). The shift of the channel toward the outside of the bend due to infilling along the inner bend after the maintenance of 1976 is evident by comparing the 1932 and 1976 bathymetry[66] surveys to more contemporary conditions (see, for example, the stretch between RM 11 and RM 10.75 in Figure 4.2.5-3). It also reflects net erosion along portions of the outer bend (see the outer bend between RM 11 and RM 10.75 in 1976 and the later years in Figure 4.2.5-3) that results from the higher shear stresses experienced there (Figure 4.2.5-4).

Most of the contemporary channel is shallower than when constructed/maintained, particularly along the inner bend. Much of the post-1976 infilling appears to have occurred prior to 1989 and has been

[66] The 1976 bathymetry in Figure 4.2.5-3 combines the post-dredge 1976 bathymetry where available with the 1975 survey.

followed by more widespread deposition between 1989 and 2004 (Figure 4.2.5-3). The inner bed deposition and the resulting thalweg migration are shown using additional surveys for transects at RM 10.91, RM 10.78, and RM 10.75 (Figure 4.2.5-2).

Like the other bends of the LPR, there is generally a transition from coarser sediments (i.e., Rock and Gravel) on the outer bend[67] to Sand in the channel and finer sediments along the inner bend point bar (Figure 4.2.5-5).

The RM 10.9 point bar is the major depositional area in this reach, reflecting lower shear stresses and the circulation patterns through the bend. Bathymetry cross sections at RM 10.91, RM 10.78, and RM 10.75 show that sediment has accumulated in the point bar since the earliest measurements in 1932, albeit with some intervening sediment removal during maintenance dredging (Figure 4.2.5-2). The accumulation proceeded in a manner consistent with the general understanding of point bar formation (i.e., expanding outward from the inner bend and upstream to downstream, as described below).

The point bar's lateral evolution is exemplified in a detailed examination of the changes in cross section at RM 10.91 (Figure 4.2.5-2). While infilling stopped in the mid-1970s or earlier to approximately 100 feet from the east bank, deposition was ongoing farther offshore as of 2004, with the point bar expanding into the channel following the 1976 dredging event. Similar patterns are observed at other transects that are shown in Figure 4.2.5-2, albeit some erosion is evident along the outer edge in more recent surveys (discussed further below). Lateral evolution may also be inferred from Cs-137 profiles (Figure 4.2.5-6); in the middle of the point bar, peak Cs-137 activities are near the surface, indicating that 1960s era sediments were at or near the surface prior to the removal action in 2013. Farther toward the channel, Cs-137 peaks are buried, indicating deposition beyond the 1960s.

The bathymetry changes also show the longitudinal evolution of the point bar. Figure 4.2.5-3 shows higher accumulation in the downstream portion of the deposit relative to the upstream portion since the 1976 dredging (the infilling between RM 11 and RM 10.75 after the 1976 maintenance is greater near RM 10.8 than near RM 11). The Cs-137 data are insufficient to illustrate the upstream to downstream evolution, but the process is supported by contaminant core data showing that peak concentrations are buried much deeper in the lower portion of the deposit that has been subject to more extensive recent deposition (as illustrated later in this section).

[67] Although these outer bend areas are classified by SSS as Rock and Gravel and, thus, are considered to be generally coarse, small pockets of finer sediments are present within these deposits—as indicated by probing and ground-truthing data in Figure 4.2.5-6 and previously noted for the preceding reaches. A total of 53% (21 of 39) of the probing/SSS ground-truthing data in this deposit indicate the presence of silt (includes Silt, Silt and Sand, and Gravel and Silt). This presumably reflects smaller-scale shear stress patterns and the history of erosion/deposition relative to survey/sampling periods.

Bathymetry differential plots for this reach are presented in Figures 4.2.5-7 through 4.2.5-9. Figure 4.2.5-7 shows the bathymetry categories defined here from a combination of multi-beam and single-beam data, the survey-by-survey multi-beam differentials are shown in Figure 4.2.5-8, and the corresponding differential plots for single-beam data are shown in Figure 4.2.5-9.[68] The analysis indicates that portions of the outer bend have experienced fairly recent erosion. The channel floor experienced a mix of deposition and erosion, presumably during Hurricane Irene as inferred between the 2010 and 2011 surveys in Figure 4.2.5-8, and to a lesser extent during the March 2010 high-flow event (as inferred between the 2008 and 2010 surveys in Figure 4.2.5-8). The deposition is largely focused between RM 11 and RM 10.8, which corresponds to the northernmost edge of the area dredged in 1976. Hurricane Irene also appears to have caused erosion along the eastern slope of the channel and the outer slope of the point bar (Figure 4.2.5-8b; see 2010 to 2011 panel). This outer edge of the point bar also underwent erosion between 2008 and 2010 (particularly the upstream edge near RM 11), a likely result of the high-flow event in spring 2010. Erosion below the top two vertical intervals of sediment typically analyzed for contamination rarely occurred; only 0.21 and 0.07 acre, respectively (0.9% and 0.3% of the total area in this reach), were subject to erosion beyond 1.5 feet. The interior of the point bar appears stable (Figures 4.2.5-7 and 4.2.5-9). Even in these areas, erosion may not be indicative of exposure of the deeper sediments collected in the cores, depending on the timing of core collection and the sequence of erosion and deposition (as discussed below).

The changes in bathymetry suggest that the edge of the point bar impinging on the channel is subject to lateral oscillation due to alternating erosion and deposition. The upper part of the bar's western edge was cut into by the extreme high flows and shear stresses of the 2010 and 2011 events and exhibits reformation during the more quiescent period between 2011 and 2012. Flows have remained relatively low (the maximum through October 2016 was 8,410 cfs on May 3, 2014) since the peak flow at Dundee Dam of 24,700 cfs during Hurricane Irene, and it is probable that the edge of the point bar has been accreting back into the channel.

Contamination Patterns

Contaminant inventory and peak concentrations within the sediment column in this reach are highest within the RM 10.9 point bar, as illustrated for 2,3,7,8-TCDD in Figure 4.2.5-10. Surface 2,3,7,8-TCDD and total PCB concentrations follow a predictable pattern with generally higher values in predominantly fine sediment areas and lower values in predominantly coarse sediments (Figure 4.2.5-11, left panel; see Appendix K for similar figures of total DDx, mercury, HMW PAHs, and LMW PAHs). The fine sediment point bar has higher concentrations than the coarser channel (except the narrow band of lower concentrations along the eastern shoreline, discussed further below). Lower concentrations are found within the coarse outer bend, except for two samples collected

[68] Single-beam bathymetry differentials are used in this reach to better understand the evolution of the RM 10.9 point bar, which is outside the spatial extent of the multi-beam surveys. The use of single-beam data for this purpose is discussed in Appendix A.

within the pockets of fine sediment previously noted in this region (orange points in the outer bend; cores 13B-0541 and 13B-0539). The same general patterns apply to the sediments 0.5 to 1.5 feet below the surface (right panel of Figure 4.2.5-11; see Appendix K for similar figures of total DDx, mercury, HMW PAHs, and LMW PAHs). Similar trends are observed for total PCBs (Figure 4.2.5-12), total DDx (Figure 4.2.5-13), and mercury (Figure 4.2.5-14). The overall concentrations measured in this reach are summarized in Table 4-6.

The highest levels of 2,3,7,8-TCDD (57,000 ng/kg), total PCBs (35 mg/kg), and total DDx (17 mg/kg) upstream of RM 7.8 have been measured in the RM 10.9 point bar (in the 0.5- to 1.5-foot segment of CLRC-067 at RM 10.94, the 1.5- to 2.5-foot segment of 11B-0340 at RM 11.01, and the 1.5- to 2.5-foot segment of 11B-0314 at RM 10.81, respectively). Contaminant concentration patterns within the point bar reflect its evolution. Surface concentrations decrease longitudinally within the point bar, due to the continuing evolution of the downstream portion in contrast to the upstream portion noted previously. This has also resulted in higher at-depth contaminant concentrations in the downstream portion of the point bar than in the upstream portion of the point bar. Laterally, surface concentrations are lower in the eastern bank, before increasing in the point bar, and then decreasing again toward and into the channel. Prior to the removal action in 2013, at-depth contaminant concentrations were higher near the center of the point bar than in locations closer to its edges; unlike the western edge, the central portion of the point bar does not appear to have been subject to maintenance dredging (as discussed further below).

The lateral trend is most evident downstream of RM 11, where the point bar widens. Along RM 10.95, the locations from the eastern shore through the point bar into the channel are 12E-0359, LPRH11B (a grab sample), 11B-0331, 11B-0333, and 11B-0336. The surface 2,3,7,8-TCDD concentrations in these cores increase from 12E-0359 and LPRH11B on the eastern shore to 11B-0331 and 11B-0333 in the point bar, before decreasing in 11B-0336 in the channel, and surface concentrations in 11B-0331 are greater than those in 11B-0333 (Figure 4.2.5-15). 2,3,7,8-TCDD concentrations in the 0.5- to 1.5-foot segments are higher in the point bar than in the eastern shore or in the channel. Concentrations in the deeper segments are higher in 11B-0333, which is located near the center of the point bar, and had thus accumulated more historically contaminated sediment, than in 11B-0331, which is located closer to the eastern edge of the point bar. Similar trends are also observed for total PCBs (Figure 4.2.5-12), total DDx (Figure 4.2.5-13), and mercury (Figure 4.2.5-14).

The lower concentrations and lower inventory along the eastern shore reflect a lack of historical fine sediment accumulation at the edge of the river. The inventory is similarly low in the channel including the region near the edge of the point bar, presumably due to the coarser nature of the sediments that tend to accumulate in this higher shear stress region and the maintenance dredging that occurred in 1976 (Figure 4.2.5-3 shows the post-dredge bathymetry alongside contemporary bathymetry, which is discussed further below). The slope of the point bar down to the channel is a

transition zone; here, accumulated sediments reflect more recent deposition and presumably also progressively coarser material. Concentrations are generally lower than in the center of the point bar (but higher than in the present-day channel; Figure 4.2.5-10b). The lower concentrations found in cores along the edge of the point bar tend to occur in areas that have filled in since the 1976 dredging, based on a comparison of the 2004 bathymetry to the 1976 post-dredge bathymetry in these areas (Figure 4.2.5-16). The higher chemical concentrations are found in cores that are generally located to the east of the 1976 dredging footprint.

The longitudinal contamination trends within the point bar are highlighted in Figure 4.2.5-17a, which compares 2,3,7,8-TCDD concentrations in an upstream center part of the point bar where little post-1960s infilling is indicated (purple hatched area) to a downstream part of the point bar (between RM 10.75 and RM 10.65) where far greater infilling has occurred (blue-green hatched area, which appears to lie within the 1976 dredging footprint [see Figure 4.2.5-16]; a similar comparison of total PCB concentrations can be found in Figure 4.2.5-17b). The purple area has high surface concentrations (right panel) and relatively shallow depths of contamination (left panel),[69] corresponding to the lack of burial after the significant 2,3,7,8-TCDD release of the 1950s and 1960s. On the other hand, the blue-green hatched area downstream has much lower surface concentrations with peak concentrations tending to occur at deeper depths. The strikingly different distributions of concentrations in these two areas can be seen in the right panels. Note that the lower concentrations observed in the blue-green area are not due to a general lack of fine sediment (as was noted for the channel and outer bend); rather, the fine sediments that accumulated tend to have lower concentrations, which is attributed to the timing of the deposition (i.e., post-1976).

Similar patterns are evident for total PCBs and mercury; within the RM 10.9 removal area between RM 11 and RM 10.85, 15 of the 21 cores have higher surface total PCB levels than the maximum surface concentration measured in the point bar between RM 10.76 and RM 10.65 (1.76 mg/kg in G0000160 at RM 10.76). Seventeen of the 21 cores have higher mercury concentrations in the surface than the maximum between RM 10.75 and RM 10.65 (2.2 mg/kg in 11B-0309 at RM 10.76). Though the maximum total DDx surface concentration was measured at the surface of 11B-0302 at RM 10.68 (0.75 mg/kg), the next highest total DDx value in the surface sediments between RM 10.75 and RM 10.65 is significantly lower (0.11 mg/kg) and is lesser than 19 of the 21 surface samples in between RM 11 and RM 10.85. At-depth levels are also consistent with 2,3,7,8-TCDD. In the downstream region, all total PCB concentrations greater than 4 mg/kg are below 3.5 feet. Excluding the surface sample noted before, all total DDx concentrations greater than 0.5 mg/kg are in or below

[69] The phrase *depth of contamination* denotes the depth below which concentrations are always less than or equal to 50 ng/kg 2,3,7,8-TCDD. The distinction between shallow and deep depths of contamination is at 5 feet; the purple hatched area contains no concentrations greater than 50 ng/kg below 5 feet. On the other hand, the downstream blue area contains low surface concentrations but levels greater than 50 ng/kg below 5 feet. The thresholds of 50 ng/kg and 5 feet have been chosen only for illustrative purposes.

the 3.5- to 5.5-foot segment, and all mercury levels greater than 5 mg/kg are 2.5 feet or deeper, excluding the 1.5- to 2.5-foot segment of 11B-0308.

The overlay of 2,3,7,8-TCDD concentration with contemporary patterns of sediment erosion/deposition is evaluated using 3D relief maps (Figures 4.2.5-18). Surface 2,3,7,8-TCDD concentrations tend to follow bathymetry as it reflects the evolution of the bed; as previously noted, higher concentrations are found mainly in the interior of the point bar and the upper portion of its side slope and are more prevalent in the upstream portion of the bar due to depositional history. These areas have not experienced appreciable deposition along the interior of the point bar and have exhibited some erosion along the side slopes. This suggests that these areas have in recent years recovered slowly, if at all, and that contaminant mobilization along the side slopes during extreme high flows experienced in 2010 and 2011 may have acted as a source to other areas and contributed to inhibited recovery. Near-surface 2,3,7,8-TCDD concentrations (0.5- to 1.5-foot, Figure 4.2.5-18) reinforce the potential for contaminant mobilization in erosional side slope areas along the inner bend as they follow a similar pattern.

Elevation changes at the locations of cores collected are shown in Figure 4.2.5-19. Within the RM 10.9 point bar, eight cores were collected in locations where more than 1.5 feet of erosion was observed in the recent multi-beam bathymetric surveys.[70] Of these eight cores, six were collected in 2011 post-Hurricane Irene, one (11B-0353) was collected just before Hurricane Irene, and one was collected in 2008. At all locations, the bed surface elevation was highest in 2008 and all experienced erosion between 2008 and 2010, presumably a result of the March 2010 high-flow event. Additional erosion occurred at four of the eight locations between 2010 and 2011 post-Hurricane Irene (11B-0349 at RM 11.07, 11B-0346 at RM 11.05, 11B-0343 at RM 11.03, and 11B-0342 at RM 11.01). The seven 2011 cores were all collected when the locations reflected the minimum elevation observed between 2007 and 2012 (Figure 4.2.5-19). Thus, the erosion evident from the 2007 to 2012 elevation changes is not indicative of erosion into the sub-surface layers measured in 2011. Additionally, all seven locations experienced deposition between 2011 and 2012, meaning that the surficial sediments present in 2012 were likely at concentrations reflective of those seen in the downstream portion of the point bar at locations that have experienced ongoing deposition. Erosion between 2008 and 2010 at the location of the core collected in 2008 (G0000163 at RM 11.09) removed approximately 1.5 feet of sediment and penetrated into the layer of higher 2,3,7,8-TCDD concentrations below the top 0.5 foot of sediment, exposing and potentially mobilizing the deeper contamination. From 2010 to 2012, this location experienced deposition of approximately 1.5 feet of material, returning the bed surface to the 2008 elevation.

[70] These cores are 11B-0353 (RM 11.11), 11B-0352 (RM 11.09), G0000163 (RM 11.09), 11B-0349 (RM 11.07), 11B-0346 (RM 11.05), 11B-0343 (RM 11.03), 11B-0345 (RM 11.03), and 11B-0342 (RM 11.01). The discussion here focuses on cores covered by only multi-beam surveys. Cores 12E-0368 and 12E-0369 were collected in locations on the edges of bathymetry cells and thus have considerable uncertainty associated with the pre-Irene 2011 bathymetry (and are not included in this discussion).

The potential for contaminant mobilization appears less in the downstream portion of the point bar (below approximately RM 10.75) due to the lower concentrations that exist there (Figure 4.2.5-18). It is lower still in the main channel throughout this entire reach due to its much lower and less variable concentrations, consistent with the coarser sediments that have accumulated there (some of which have been recent as indicated by the light blue areas in Figure 4.2.5-18). In the opposite side slope and shoal, the contaminant data are limited but, as previously discussed, fine sediment accumulation there has been limited, particularly compared to the inner bend, with some portions of the outer bend exhibiting net long-term scour (Figure 4.2.5-3). Thus, although some of these areas exhibited erosional or temporarily erosional behavior in the recent bathymetric surveys, their potential for inhibiting recovery in other areas via contaminant erosion is considerably less.

Like the upstream reaches, surface concentrations of total PCBs, total DDx, and mercury are well correlated to surface concentrations of 2,3,7,8-TCDD (Figures 4.2.5-20a through 4.2.5-20c). While subsurface concentrations and MPA of these contaminants are also well correlated to 2,3,7,8-TCDD, the relationship for subsurface concentrations is weaker for mercury. A comparison of surface contamination levels of HMW PAHs and LMW PAHs to 2,3,7,8-TCDD indicates that, like the other contaminants, higher PAH concentrations correspond to higher 2,3,7,8-TCDD concentrations (Figure 4.2.5-20). However, like the upstream reaches, higher PAH concentrations are also found in coarser sediments, which contribute to some locations containing lower 2,3,7,8-TCDD concentrations but higher PAH concentrations (see also Appendix K Figures 8-4 and 9-4). The differences are greater at depth, with substantially less concordance observed in subsurface concentrations and contaminant inventory levels relative to 2,3,7,8-TCDD.

The lack of association of PAHs with fine sediments is seen in the surface segment of 11B-0352 at RM 11.09, which contains the highest HMW PAH (Figure 4.2.5-21) and LMW PAH (Figure 4.2.5.22) levels upstream of RM 7.8 (510 and 171 mg/kg, respectively). This segment contains only 13% fine sediments and is located outside the point bar. Levels of 2,3,7,8-TCDD (150 ng/kg), total PCBs (0.4 mg/kg), total DDx (0.04 mg/kg), and mercury (0.8 mg/kg) here are significantly lower than those in the point bar and like those measured in coarse sediments elsewhere in the LPR. Other locations outside the point bar that contain elevated PAH levels but lower amounts of the other contaminants include, but are not limited to, the surface segment of 13B-0542 on the outer bend at RM 11.02 (100 mg/kg of HMW PAHs and 56 mg/kg of LMW PAHs but only 10 ng/kg of 2,3,7,8-TCDD, 0.2 mg/kg of total PCBs, 0.001 mg/kg of total DDx, and 5.6 mg/kg of mercury, despite containing 49% fine sediments) and the grab 12E-0364 on the eastern bank at RM 11.1 (114 mg/kg of HMW PAHs and 39 mg/kg of LMW PAHs but only 171 ng/kg of 2,3,7,8-TCDD, 0.13 mg/kg of total PCBs, 0.02 mg/kg of total DDx, 0.34 mg/kg of mercury, and 22% fine sediments).

The lateral and longitudinal trends noted for the other contaminants are not evident for the PAHs. Along the transect at RM 10.95 (comprising, from east to west, the locations 12E-0359, LPRH11B [a

grab sample], 11B-0331, 11B-0333, and 11B-0336), like the other contaminants, HMW PAH surface concentrations increase from the eastern bank (2.5 mg/kg in 12E-0359 and 2.9 mg/kg in LPRH11) into the point bar (54 mg/kg in 11B-0331 and 21 mg/kg in 11B-0333). However, unlike the other contaminants, rather than decreasing into the channel, concentrations are highest in the surface segment of 11B-0336 (462 mg/kg—the second highest HMW PAH concentration measured upstream of RM 7.8). LMW PAHs also exhibit similar patterns, with the highest concentration in the surface segment of 11B-0336 (136 mg/kg, also the second highest LMW PAH concentration measured upstream of RM 7.8). Longitudinal trends also look similar for the PAHs, with surface concentrations between RM 10.76 and RM 10.65 in a similar range to those between RM 11 and RM 10.85 within the RM 10.9 removal area. This can be further observed in Figures 4.2.5-17c and 4.2.5-17d, which suggest not much variation in the depth of contamination of the PAHs in the upstream and downstream areas, compared to those of 2,3,7,8-TCDD and total PCBs (Figures 4.2.5-17a and 4.2.5-17b).

To summarize, the high-density sampling data collected as part of the remedial design for the RM 10.9 removal provide a detailed evaluation of the characteristics of the point bar and the nature and extent of contaminants, and the data confirm the conceptual understanding of the relationship between geomorphic features, dredging, and depositional/erosional history on the observed patterns of contaminants in sediments. Concentrations of 2,3,7,8-TCDD, total PCBs, total DDx, and mercury follow similar patterns to those observed in the upstream reaches, with higher levels detected in fine sediments than in coarse sediments. Concentrations are highest within the RM 10.9 point bar, with the maximum 2,3,7,8-TCDD, total PCB, and total DDx concentrations upstream of RM 7.8 measured here. Patterns within the point bar reflect trends in its evolution. Laterally, concentrations are lowest along the eastern bank and increase moving into the point bar, before decreasing into the channel. At-depth concentrations are higher near the center of the point bar than toward its edges. Longitudinally, concentrations of these contaminants are higher in the surface sediments in the upstream center region of the point bar than the downstream regions, consistent with the evolution of the point bar, which attained equilibrium in the 1960s in the upstream regions but underwent deposition until more recently in the downstream region—particularly in the portion subject to maintenance dredging in the 1970s. The slope of the point bar down to the channel is a transition zone with sediments reflecting more recent deposition of coarser material since the 1976 dredging event. Like the upstream reaches, PAH concentration patterns are dissimilar to the other contaminants; higher PAH concentrations are also measured in coarse sediments. Though the highest HMW PAH and LMW PAH levels upstream of RM 7.8 were also measured in this reach, the sample where these levels were detected is in coarse sediments outside the point bar and contains lower levels of the other contaminants. The lateral trends are also not evident for PAHs, with concentrations in the channel often higher than concentrations within the point bar. Longitudinal trends are also not as evident as for the other contaminants.

4.2.6 Avondale Bridge (RM 10.4) to RM 9.2

This reach extends from the Avondale Bridge to the end of a large Silt deposit at RM 9.2. Flow is in the N-S direction, with gentle meanders around RM 10.0 and RM 9.6, where a minor unnamed tributary enters. The western shoreline is mostly sheetpiled/bulkheaded, excluding a vegetated stretch between approximately RM 10.2 and RM 10. Route 21 continues along the western shoreline. The eastern shoreline is sheetpiled/bulkheaded upstream of RM 10.25 and vegetated farther downstream (Figure 4.2.6-1). The cross-sectional area varies between 4,000 and 4,300 ft^2 from Avondale Bridge to RM 10.1, with the width of the river increasing from 300 feet at Avondale Bridge to 455 feet at RM 10.1, as the western bank turns sharply farther west. The river then narrows to 3,730 ft^2 (width of 390 feet) at RM 9.8, before expanding again to 4,350 ft^2 (width of 450 feet) at RM 9.6 and narrowing again to 3,930 ft^2 (with 350 feet) at RM 9.4. The total area of the sediment bed in this reach is 50 acres.

The federal navigation channel continues through this reach. The last maintenance dredging in this reach occurred within the navigation channel between RM 10 and RM 9.6 in 1976; the rest of the navigation channel was last maintained before 1950. Bathymetry data indicate that the river channel is closely aligned with the navigation channel, except between RM 10 and RM 9.75, where deposition along the eastern shoal has shifted the thalweg slightly west (Figure 4.2.6-1).

The evolution of the sediment bed is studied using bathymetry data (single-beam surveys [1975, 1989, 2004, and 2007] and multi-beam surveys and associated single-beam transect measurements [2007, 2008, 2010, 2011, and 2012]), model-predicted bottom shear stress patterns, and Cs-137 core profile data. Its characteristics are described using results of the 2005 SSS survey and its ground-truthing data, probing surveys, and characteristics and contaminant concentrations of individual cores.

The bed is composed of various sediment types (Figure 4.2.6-2). The channel and eastern shoal are Gravel and Sand to RM 10.2 where the river widens considerably. The western shoal from the top of the reach to RM 10 is Rock and Coarse Gravel partially covered by Silt. This upper portion of the reach appears to be influenced by the Avondale Bridge, which bifurcates the channel and orients flow toward the western side of the river. A Cs-137 core collected at the edge of the channel in the Gravel and Sand region at RM 10.03 (CLRC-061) has low Cs-137 activities at all depths, indicative of a general lack of accumulation (Figure 4.2.6-3). The single-beam surveys do not indicate any significant changes in the shape of the LPR channel in that time, except a slight eastward migration of the thalweg in 1989 between RM 10.05 and RM 9.95—near the upstream extent of the 1976 maintenance dredging there (the 1975 survey was before this maintenance; Figure 4.2.6-4). The thalweg seems to have shifted back west by 2004. Multi-beam bathymetry data (Figure 4.2.6-5) indicate that upstream of RM 10.2, the western edge of the channel extending into the shoal experiences cyclic erosion and deposition. Net deposition occurred between 2007 and 2008 and

between 2011 and 2012. Most of this Silt deposit experienced more than 1 foot of sediment accumulation. Between 2008 and 2010, and 2010 and 2011, the same Silt deposit experienced erosion, with the parts within the channel experiencing more than 1.5 feet of erosion. Despite this erosion, most of this deposit within the channel was net depositional between 2007 and 2012.

The widening eastern shoal between RM 10.2 and RM 10 experiences lower shear stresses (Figure 4.2.6-6), and a Silt deposit starts here and extends downstream to the bottom of the reach, crossing the channel to the western shoal at RM 9.6 (Figure 4.2.6-2). This deposit accounts for approximately 27.5 of the 50 acres in this reach (55% of the reach). The silt accumulation here in the navigation channel likely reflects infilling since the 1976 maintenance dredging. Two Cs-137 cores on the upper part of this deposit (Figure 4.2.6-3) in the shoal exhibit a peak at the surface (G0000016-13A and G0000016-13D at RM 10.05), while a third exhibits low Cs-137 activity throughout (CLRC-062 at RM 10.03). These patterns suggest a lack of sediment accumulation since the 1960s or earlier, which would be consistent with the evolution of the RM 10.9 point bar. Coarser sediments exist at the confluence of the unnamed tributary, similar to the region around the confluence of other tributaries. A Cs-137 core (CLRC-060 at RM 9.57) indicates net deposition within the Silt deposit downstream of the confluence. As the LPR meanders here, the sediment distribution is similar to other bends, with the coarse sediments (Gravel and Sand) along the outer (eastern) bend and Silt along the inner bend and the channel. Just upstream of RM 9.25, a Sand deposit begins in the channel and continues into the downstream reach. The riverside portion of the Silt deposit along the edge of the channel downstream of RM 10.2 to just downstream of RM 10 was subject to cyclic erosion and deposition, similar to the edge of the RM 10.9 point bar.

Cyclical erosion and deposition occurred in the rest of this reach between 2007 and 2012. Transects comparing the 2004 and 2012 elevations at RM 9.97, RM 9.91, and RM 9.43 suggest that there was little net change in the bed elevations at those locations during that time (Figure 4.2.6-7). Some of the cyclical erosion and deposition between those years can be observed in Figure 4.2.6-5. Deposition occurred along the western edge of the channel and sporadically in the main channel downstream of RM 9.5 between 2007 and 2008. These areas that experienced deposition between 2007 and 2008 experienced erosion between 2008 and 2010. This period also eroded most of the channel between RM 9.9 and RM 9.75. Between 2010 and 2011, the parts of the main channel that eroded between 2008 and 2010 accumulated sediment, while the eastern side of the channel between RM 10 and RM 9.6 experienced erosion. Most of this region upstream of RM 9.5 that experienced erosion between the prior two periods accumulated sediment between 2011 and 2012. Overall, between 2007 and 2012, areas of net erosion downstream of RM 10 occurred on the western and eastern sides of the channel, while areas of net deposition occurred toward the center of the channel. The areas that experienced net erosion along the western side of the channel, and areas on the eastern side of the channel downstream of RM 9.3, include regions that experienced erosion of more than 1.5 feet.

Contaminant Patterns

2,3,7,8-TCDD, total PCB, total DDx, and mercury contamination in this reach follow expected patterns. Higher concentrations are found in the silt deposit, and in silt pockets within coarse sediment deposits. Concentrations in the channel are lower than concentrations in the shoal (Figure 4.2.6-8; see Appendix K for similar figures of total DDx, mercury, HMW PAHs, and LMW PAHs). Concentration patterns within the point bar at RM 10.1 follow similar trends to those in the RM 10.9 point bar and decrease longitudinally upstream to downstream and laterally from the shoal into the channel. The overall concentrations measured in this reach are summarized in Table 4-7.

Between the Avondale Bridge and RM 10, concentrations of 2,3,7,8-TCDD (Figure 4.2.6-9), total PCBs (Figure 4.2.6-10), total DDx (Figure 4.2.6-11), and mercury (Figure 4.2.6-12) are lowest in the channel and highest in the shoals (Figure 4.2.6-13). Throughout the two cores collected in the main channel at RM 10.31 and RM 10.27 (13B-0537 and 12A-0479) 2,3,7,8-TCDD concentrations are below 100 ng/kg. Total PCB, total DDx, and mercury levels in these cores are below 0.3, 0.03, and 0.7 mg/kg, respectively. The cluster of cores collected in the channel between RM 10.1 and RM 10 (13B-0531, 13B-0532, 13B-0529, 13B-0530, and CLRC-061) exhibit similar concentrations. 2,3,7,8-TCDD levels are less than 100 ng/kg, excluding the 0.5- to 1.5-foot segment of 13B-0530, which contains 399 ng/kg. The same segment also contains 2.12 mg/kg of total PCBs, while all other samples, excluding the surface segment of CLRC-061 (0.77 mg/kg), contain less than 0.5 mg/kg total PCBs. Total DDx levels in these cores are less than 0.1 mg/kg. Mercury concentrations are at or below 1 mg/kg, excluding the surface of 13B-0530 (2.5 mg/kg) and the surface and the 2.5- to 3.5-foot segments of CLRC-061 (1.6 and 1.05 mg/kg, respectively).

The Silt on the western side slopes and western shoals upstream of RM 10.1 was sampled at four locations (12A-0480, CLRC-063, 12A-0478, and 13B-0535). These cores show that this region is characterized by a relatively thin layer of silt overlying coarser sediments. A core at 12A-0480 recovered 1.7 feet of sediment, and the surface contaminant concentrations were much higher than its single subsurface segment (e.g., 2,3,7,8-TCDD concentration of 1,860 and 230 ng/kg). CLRC-063 exhibits concentrations of 2,3,7,8-TCDD ranging from 840 to 1,190 ng/kg in the top 2.5 feet and less than 50 ng/kg of 2,3,7,8-TCDD below that. The surface segment of 12A-0480 is 68% fines, whereas it is approximately 22% in the subsurface segment. Similarly, core CLRC-063 has 2.5 feet of sediments characterized as greater than 90% fines overlying a sediment with 18% fines. Both locations have also accumulated sediment between 2011 and 2012 (Figure 4.2.6-14). 12A-0480 was collected in 2012, after sediment accumulation, suggesting the elevated surface concentrations are from recently deposited sediments. The 2.5 feet of sediment collected in 12A-0478 contain 52% to 90% fines. The highest concentration here is in the 1.5- to 2.5-foot segment, which comprises 90% fines.

Contamination levels in this segment are the highest across all four cores.[71] 13B-0535 contains higher contaminant levels in the surface than at depth[72]; the pattern is, in part, reflective of the 42% fine sediments in the surface but less than 20% fine sediments at depth.

The cores on the eastern side of the channel upstream of RM 10.1 (13B-0538 and 13B-0536) were collected in a region classified by the SSS survey as Gravel and Sand. However, both contain high fines content indicating they were collected in fine sediment pockets too small to be delineated by the SSS survey.[73] The contaminant levels in these cores are higher than those observed in other Gravel and Sand designated areas, reflective of the high percent fines content of these cores.[74] The bottom segment of this core has lower 2,3,7,8-TCDD, total PCBs, and total DDx than the already low levels in the channel[75]; however, mercury levels are higher than those in the channel (4.6 mg/kg). Mercury patterns also differ from the other contaminants in 13B-0536; while the surface concentrations of the other contaminants are higher than the subsurface levels, mercury concentrations are highest in the bottom (16.6 mg/kg).

Moving downstream, contaminant concentrations are higher in the eastern silty shoals than in the channel. Like the RM 10.9 point bar, concentrations decline from upstream to downstream. 2,3,7,8-TCDD levels greater than 10,000 ng/kg were measured in cores 13B-0534, 13B-0533, and 13B-0528, and the grab sample G0000159. The 0.5- to 1.5-foot segments of 13B-0533 and 13B-0528 contain levels greater than 30,000 ng/kg, with 13B-0528 containing the maximum concentration in this region (32,300 ng/kg). These cores also have segments with total PCB, total DDx, and mercury concentrations greater than 20, 2, and 15 mg/kg, respectively.

Immediately downstream of these cores, lower concentrations were found in the cluster of CLRC-062, G0000158, and G0000168. Surface segment 2,3,7,8-TCDD concentrations are 2,670 ng/kg in G0000158 and 108 ng/kg in G0000168. The surface has less than 30 ng/kg in all the other samples in this cluster. The highest total PCB level here is in the surface of G0000168 (2 mg/kg), and CLRC-062 contains between 1 and 2 mg/kg of total PCBs at various depths; all other samples contain less than 0.5 mg/kg of total PCBs. Total DDx levels are greater than 0.8 mg/kg in the surface segments of all three cores, but excluding the 0.5–1.5 segment of CLRC-062, are less than 0.02 mg/kg in all other

[71] 8,040 ng/kg 2,3,7,8-TCDD, 8.6 mg/kg total PCBs, 0.7 mg/kg total DDx, and 7 mg/kg mercury

[72] 882 ng/kg 2,3,7,8-TCDD, 1.25 mg/kg total PCBs, 0.09 mg/kg total DDx, and 2.7 mg/kg mercury in the surface, but less than 10 ng/kg 2,3,7,8-TCDD, 0.005 mg/kg total PCBs, 0.005 mg/kg total DDx, and 0.6 mg/kg mercury at depth.

[73] The fine sediment content of the surface, 0.5- to 1.5-foot, 1.5- to 2.5-foot, and bottom segments are 71%, 93%, 78%, and 26%, respectively, in 13B-0538 and 59%, 89%, 90%, and 82%, respectively, in 13B-0536.

[74] In 13B-0538, 2,3,7,8-TCDD levels in the upper three segments exceed 10,000 ng/kg, with the highest level (14,500 ng/kg) measured in the surface segment. Total PCB levels in these segments are higher than 15 mg/kg, with the highest concentration also measured in the surface segment (23.8 mg/kg). Total DDx levels in the upper two segments are higher than 0.5 mg/kg, with the highest concentration in the 0.5- to 1.5-foot segment (0.85 mg/kg), while mercury levels are higher than 20 mg/kg in the upper two segments, with the highest levels in the 0.5- to 1.5-foot segment (23.3 mg/kg).

[75] 0.871 ng/kg 2,3,7,8-TCDD, 0.002 mg/kg total PCBs, and 0.0002 mg/kg total DDx

samples. Mercury levels are greater than 10 mg/kg in all the subsurface segments of CLRC-062 and 9.3 mg/kg in the surface. Levels in the other two cores are lower.

Contaminant concentrations in 13B-0526 at RM 9.99 are higher than those measured just upstream.[76] The surface concentrations are lower than the subsurface levels, except for total DDx, which has a surface concentration of 1.4 mg/kg. Across the river, on the silty eastern shoal, 13B-0527, located toward the downstream extent of the RM 10.1 point bar, continues the longitudinally decreasing concentrations in the point bar—2,3,7,8-TCDD levels are less than 30 mg/kg at all depths. Total PCB, total DDx, and mercury levels in this core are below 0.1, 0.01, and 0.5 mg/kg, respectively.

Farther downstream, on the western shoal, two grab samples were collected at RM 9.85 (13B-0568) and RM 9.64 (13B-0523). Though the location of the former was classified by the SSS survey as Rock and Coarse Gravel, the sample contains 90% fine sediments, indicating it was collected in a small fine sediment pocket. The grab sample at 13B-0523 was collected within the SSS-identified Silt deposit but is located close to the boundary of the deposit. The lack of sediment recovery here is indicative of the generally coarse nature of the area. The grab sample at 13B-0568 contains 2,340 ng/kg 2,3,7,8-TCDD, 4.9 mg/kg total PCBs, 0.26 mg/kg total DDx, and 5.9 mg/kg mercury. 13B-0523 contains lower levels of these contaminants, with 435 ng/kg 2,3,7,8-TCDD, 1.1 mg/kg total PCBs, 0.1 mg/kg total DDx, and 2.7 mg/kg mercury.

Along the silty eastern shoal, the highest concentrations of all four contaminants are found near the confluence of the minor unnamed tributary. The highest 2,3,7,8-TCDD levels are found in the 2.5- to 3.5-foot segment of CLRC-060 (2,547 ng/kg). Total PCB concentrations in the subsurface segments of G0000155 are between 7.4 and 8 mg/kg. Total DDx and mercury levels in the same segments are around 0.4 and 6.5 mg/kg, respectively. While total DDx levels, like total PCBs, are higher than the other cores, higher mercury levels are found below 3.5 feet in 13B-0524 (7.5 mg/kg). The lowest concentrations of all contaminants are measured at depth in the cores collected near the confluence (12A-0476 and G0000154). The higher surface and 0.5- to 1.5-foot contamination levels of 12A-0476 are likely due to the higher fine sediment content there (43% and 26%, respectively, compared to less than 20% farther below). A sample in the channel at RM 9.51 (CLRC-059) has data available for only total PCBs and mercury (and not the other contaminants) and contains lower levels of both contaminants than the shoals (0.006 mg/kg total PCBs and 0.02 mg/kg mercury).

Downstream of RM 9.5, nine cores and four grab samples were collected. Concentrations are lowest in the two grab samples 13B-0517 and 13B-0518 and in the core 13B-0521. While the two grabs were collected in SSS-identified Sand or on the boundary of SSS-identified Silt and SSS-identified Sand, and have correspondingly low fine sediment contents (less than 20% in each case), core

[76] The 0.5- to 1.5-foot segment contains 32,900 ng/kg 2,3,7,8-TCDD, 20.8 mg/kg total PCBs, 0.72 mg/kg total DDx, and 12 mg/kg mercury, and the 1.5- to 2.5-foot segment contains 16,800 ng/kg 2,3,7,8-TCDD, 22 mg/kg total PCBs, 0.61 mg/kg total DDx, and 12.15 mg/kg mercury.

13B-0521 was collected in SSS-identified Silt but contains 3% fine sediments in the surface and 0.5- to 1.5-foot segment, as well as 13% fine sediments in the 1.5- to 2.5-foot segment, suggesting that a small coarse sediment pocket was missed by the SSS survey within the larger fine sediment deposit.

Contaminant levels are higher in G0000152, G0000151, and the triad of cores at RM 9.3—12A-0475, 13B-0519, and 12A-0474. The bottom segment of 12A-0474 contains 17,600 ng/kg 2,3,7,8-TCDD, 33 mg/kg total PCBs, 1 mg/kg total DDx, and 16 mg/kg mercury—the highest in this region. The subsurface segments of G0000151 were reported as a composite (for the map, the at-depth segments have been assumed to have equal concentrations of each contaminant). This composite segment contains 10,400 ng/kg 2,3,7,8-TCDD, 22 mg/kg total PCBs, 0.5 mg/kg total DDx, and 11.5 mg/kg mercury.

Like the previous reaches, surface concentrations of total PCBs, total DDx, and mercury are well correlated to surface concentrations of 2,3,7,8-TCDD (Figures 4.2.6-15a through 4.2.6-15c). Subsurface concentrations and MPA are also well correlated, though mercury exhibits a weaker correlation than the other contaminants.[77] Like the previous reaches, surface PAH concentrations here are not as well correlated to 2,3,7,8-TCDD as the other contaminants (Figures 4.2.6-15d and 4.2.6-15e). Subsurface PAH concentrations and MPAs are better correlated to 2,3,7,8-TCDD. Further, PAH concentrations in this reach are higher in finer sediments (Figures 4.1-9e and 4.1-9f; see also Appendix K Figures 8-5 and 9-5); both observations are perhaps merely due to the increased areal extent of fine sediments in this reach, which has resulted in fewer samples collected in coarse sediments.

HMW PAH (Figure 4.2.6-16) and LMW PAH (Figure 4.2.6-17) concentrations upstream of RM 10.1 are higher in the shoals than the channel; both 13B-0537 and 12A-0479 contain lower PAH concentrations than the samples collected in the shoals. The highest PAH concentrations here are in the bottom segment of 13B-0536 (93 mg/kg HMW PAHs and 38 mg/kg LMW PAHs).

Farther downstream, like the other contaminants, PAH levels are generally higher in the eastern shoal between RM 10.1 and RM 10 than the channel. The exception is the surface segment of 13B-0529, which contains higher HMW PAH and LMW PAH concentrations than the samples in the shoal (77 and 29 mg/kg, respectively). As discussed above, this segment contains significantly lower concentrations of the other contaminants relative to the shoals.

Between RM 10 and RM 9.5, the highest HMW PAH concentration of 118 mg/kg is in the surface segment of 13B-0524 at RM 9.74. This segment also contains 40 mg/kg of LMW PAH; the segments deeper than 3.5 feet of this core contain the maximum HMW PAH and LMW PAH concentration (193 and 44 mg/kg, respectively) in this region. This too is unlike the other contaminants, which exhibit

[77] Variations in correlations of subsurface concentrations and MPA could be due to a temporal variability in the sources.

higher concentrations in the vicinity of the confluence of the minor tributary than the more upstream cores.

Downstream of RM 9.5, HMW PAH patterns are higher in G0000152, G0000151, and 12A-0474, like the other contaminants. The highest concentration here is measured in the surface segment of 12A-0474 (92.6 mg/kg). Unlike the other contaminants, a comparable concentration is also measured at the bottom of CLRC-058 (92 mg/kg).[78] The maximum LMW PAH concentration in this region is also detected in this segment (30.5 mg/kg). Patterns of LMW PAH concentrations excluding this segment are similar to the other contaminants and are higher in G0000152, G0000151, and in the triad of cores at RM 9.3 (12A-0475, 13B-0519, and 12A-0474) than the rest of the cores.

In summary, concentrations of all the contaminants in this reach correlate with fine sediment content. They are generally low in the channel and higher in the side slopes and shoals. One of the key features within this reach is the point bar formed by the widening of the river starting at RM 10.2. This point bar, on the eastern shoal between RM 10.2 and RM 10, has higher contaminant levels than the shoals farther downstream and the adjoining channel. Concentrations within the point bar also decrease from upstream to downstream, similar to the RM 10.9 point bar.

4.2.7 RM 9.2 to WR Railroad Drawbridge (RM 7.8)

This reach is mostly straight with two minor bends and two bridge crossings—the Lance Corporal Osbrany Montes de Oca Memorial Bridge (formerly the Belleville Turnpike Bridge) at RM 8.5 and the WR Railroad Drawbridge at RM 7.8. The Second River, a major tributary to the LPR, enters in this reach at RM 8.05. The upstream boundary of OU2 is located within this reach at RM 8.0 (USACE RM 8.3).

The western shore is mostly sheetpiled or bulkheaded along Route 21, with small stretches of vegetation near the Lance Corporal Osbrany Montes de Oca Memorial Bridge (RM 8.5) and just downstream of the confluence of the Second River (around RM 8). The eastern shore is vegetated throughout (Figure 4.2.7-1). The total area of the sediment bed in this reach is 53 acres.

The reach is oriented NE–SW to RM 8.5, where just downstream of the Lance Corporal Osbrany Montes de Oca Memorial Bridge it begins an approximately 23-degree bend that shifts it to N-S by RM 8.25. At RM 8.1, it bends approximately 35 degrees in the opposite direction, shifting back to NE-SW from RM 7.9 to RM 7.8. The cross-sectional area expands from 3,800 ft^2 at RM 9.2 to a maximum of 4,500 ft^2 at RM 8.8. It then drops to 4,000 ft^2 at the constriction of the Lance Corporal Osbrany Montes de Oca Memorial Bridge and to 3,000 ft^2 at RM 8, before expanding to 3,700 ft^2 at the WR Draw railroad bridge.

[78] The bottom segment of CLRC-058 is the 5.5- to 7.5-foot segment. The stacked COPC maps only show depths down to 5.5 feet.

The federal navigation channel continues through this reach, and bathymetric surveys show that the channel generally corresponds with the delineated navigation channel (Figure 4.2.7-1). Downstream of RM 8.4, the navigation channel was last maintained in 1974, while the upstream stretch was last maintained in 1950 or before.

The evolution of the sediment bed in this reach is studied using bathymetry data (including a post-dredge survey from 1975 [single-beam], single-beam surveys [2004, 2007, and 2012], and multi-beam surveys [2007, 2008, 2010, 2011, and 2012]), model-predicted bottom shear stress patterns, and Cs-137 core profile data. The bed's sediment types are described using the 2005 SSS survey results and associated ground-truthing data, probing surveys, and characteristics of cores collected for contaminant analysis.

Sediment accumulation in the channel is evident throughout this reach by comparing bathymetry maps from 1975 to those from 2004 and 2007 (Figure 4.2.7-2). A prominent feature in this comparison is the buildup of sediment downstream of the confluence of the Second River at RM 8.05, in the form of a delta resulting from the Second River sediment load (Figure 4.2.7-2c). The shallow deposit seen on the 1975 map generally corresponds with the area mapped by the 2005 SSS as Rock and Coarse Gravel (Figure 4.2.7-4c). The expansion evident in the 2004 and 2007 maps (after the channel was last dredged in 1974) extends the shoal into the channel and downstream and migrates the thalweg toward the outer bend (eastern shore). The shoal here was mapped as Sand and Gravel, with a silty-sand deposit beginning about 200 feet downstream of the confluence (Figure 4.2.7-4), suggesting that coarse sediment from the Second River is responsible for the buildup. This evolution is similar to those observed at other upstream confluences. Single-beam and multi-beam data along a transect at RM 8.03 indicate a stable cross-section (Figure 4.2.7-3a).

Overall, the sediment characteristics continue the patterns observed in upstream segments. The channel is mostly Sand or Gravel and Sand, with the shoals containing a mixture of sediment types (Figure 4.2.7-4). Silt pockets exist in the shoals along both banks between RM 9.1 and RM 8.8, where the river is widest and has the greatest cross section. The Silt deposits formed due to the lower velocities and shear stresses in this region of expanded cross section. Two core Cs-137 profiles measured in these pockets (CLRC-056 and CLRC-057) show well defined Cs-137 profiles, confirming this area is a historically net depositional environment (Figure 4.2.7-5). A small area of Silt upstream of the major deposits extending from the shoal into the channel was delineated from probing data near RM 9.05. Its shape and incursion on the channel would require further study to characterize it more precisely. As the river narrows moving downstream of RM 8.7 (corresponding to increased flow velocity and shear stress [Figure 4.2.7-6]), the shoals contain coarser materials (i.e., Gravel or a mixture of Gravel and Sand [Figure 4.2.7-4]).

Sediment patterns along the RM 8.5 to RM 8.25 bend are similar to those observed in the bend centered at RM 10.9, with the eastern inner bend shoal consisting of a fine sediment point bar

beginning just downstream of the Lance Corporal Osbrany Montes de Oca Memorial Bridge (Figure 4.2.7-4). A Cs-137 profile measured near RM 8.4 (CLRC-055) in the upstream portion of the point bar exhibits maximum Cs-137 activity at the surface, suggesting this portion has not experienced net deposition since the 1960s (Figure 4.2.7-5), a finding consistent with the general process of point bar evolution observed in the RM 10.9 point bar. The point bar terminates at the shore with a narrow band of coarse sediments (Rock and Coarse Gravel), presumably due to shallow water turbulence that prevents long-term accumulation of fine sediments. Moving to the western outer bend shoal from the sandy channel, there is progressively coarser material with Rock and Coarse Gravel along the bank (Figure 4.2.7-4). Probing data in the Rock and Coarse Gravel along the outer bend suggests the presence of silt at some locations.

The coarse deposit along the western shoal transitions into a finer deposit as the river bends in the opposite direction at RM 8.1. The finer sediments on the inner bend western shoal are interrupted by the previously mentioned Rock and Coarse Gravel deposit at the confluence with the Second River. The channel is coarser than found upstream, being composed of Gravel and Sand, likely reflecting the higher velocities in this constricted cross-section. The eastern shoal along the outer bend is composed of Rock and Coarse Gravel, which extends up to RM 8.3 (Figure 4.2.7-4b). A larger Silt deposit begins at approximately RM 7.9 where the river widens and extends downstream into the next reach. The Cs-137 profiles in this deposit show evidence of deposition, similar to Silt deposits in general (Figure 4.2.7-5). Comparison of the 2007 and 2012 bathymetry data along a transect at RM 7.83 in this Silt deposit suggests recent sediment accumulation (Figure 4.2.7-3b). Overall, silt deposits comprise 8 acres (15%) of the sediment bed of this reach.

Bed elevation changes analyzed using multi-beam bathymetry surveys indicate erosion and deposition patterns similar to those seen upstream. Net deposition or change<= 6 inches predominates between the 2007 and 2008 surveys and the 2011 and 2012 surveys (both low-flow periods), and net erosion or <= 6 inches change predominates between the 2008 and 2010 surveys and the 2010 and 2011 surveys (for which erosion is likely attributable to the March 2010 and March 2011 high-flow events and to Hurricane Irene in August 2011; Figure 4.2.7-7). The portions of the channel that experienced net erosion or erosion followed by deposition (Figures 4.2.7-8 and 4.2.7-9) from 2007 through 2012 comprise approximately 23% of the reach. Erosion was common on the side walls of the channel, which exist from the edges of the navigational channel to the outer limit of the multi-beam bathymetry coverage (Figure 4.2.7-9). The channel erosion occurred mostly in areas that experienced deposition in the low-flow period between 2007 and 2008 (Figure 4.2.7-7). Most of the erosion produced bathymetry changes of less than 1 foot.

Deeper erosion occurred between RM 9.2 and RM 9.1 (2008 through 2010 survey differential) and just downstream of the Lance Corporal Osbrany Montes de Oca Memorial Bridge at RM 8.5 (2010 through 2011 survey differential). The pocket of deeper erosion downstream of RM 9.2 appears to be

in a region of post-1975 sediment accumulation (Figure 4.2.7-2). The net erosional areas downstream of the RM 8.5 bridge abutments could potentially be due to the flow constriction and secondary flows generated by these abutments. Consistent with the deposition downstream of the Second River since 1975, a large area of deposition in this region also occurred between 2007 and 2012, (Figures 4.2.7-7, 4.2.7-8, and 4.2.7-9). Many of the areas that experienced erosion experienced either preceding or subsequent deposition such that the 2007 elevations were regained by 2012 (Figure 4.2.7-7).

Contamination Patterns

The sediment contamination patterns are qualitatively similar to those observed in the preceding upstream reaches, as demonstrated by the 2,3,7,8-TCDD core profiles (Figure 4.2.7-10) and contamination patterns of 2,3,7,8-TCDD and total PCBs on surface and near-surface sediments (Figure 4.2.7-11; see Appendix K for similar figures of total DDx, mercury, HMW PAHs, and LMW PAHs). Although the data are sparse, contaminant inventory at depth tends to be higher in the shoals than in the channel (Figure 4.2.7-10). The overall concentrations measured in this reach are summarized in Table 4-8.

Upstream of RM 8.75, the highest surface concentrations of 2,3,7,8-TCDD, total PCBs (Figure 4.2.7-12), and mercury (Figure 4.2.7-14) in the channel were measured in LPRT10A at RM 9.07 at the boundary of the Silt deposit there.[79] The highest surface concentration of total DDx (Figure 4.2.7-13) was measured at CLRC-056 (0.14 mg/kg; RM 8.99). Subsurface concentrations are highest in the Silt deposit at CLRC-056, with concentrations in the subsurface segments increasing with depth.[80] The elevated subsurface contaminant levels compared to the surface levels suggest burial and are supported by the Cs-137 profile here (Figure 4.2.7-5). The third core in the channel in this region (12A-0472) was collected in coarse sediments and contains lower contaminant levels (surface and subsurface sediments contain less than 25 ng/kg 2,3,7,8-TCDD, 0.2 mg/kg total PCBs, 0.03 mg/kg total DDx, and 0.25 mg/kg mercury).

Upstream of RM 8.75, the highest contaminant concentrations are found in the Silt deposits within the shoals (e.g., 16,000 ng/kg 2,3,7,8-TCDD in LPRT09F at RM 8.8, and buried levels of 8,700 ng/kg 2,3,7,8-TCDD, 17 mg/kg total PCBs, 1 mg/kg total DDx, and 14 mg/kg mercury in the 0.5- to 1.5-foot or 1.5- to 2.5-foot segments of CLRC-057 on the eastern silty shoal at RM 8.99). Bathymetry data at this location suggest that this location experienced more than 1.5 feet of deposition between 2007

[79] 310 ng/kg 2,3,7,8-TCDD, 0.9 mg/kg total PCBs, and 1.8 mg/kg mercury

[80] 2,3,7,8-TCDD levels in this core are 247 ng/kg in the surface and 126 ng/kg in the 0.5- to 1.5-foot segment but increase to 364 ng/kg in the 1.5- to 2.5-foot segment, 2,585 ng/kg in the 2.5- to 3.5-foot segment, 8,400 ng/kg in the 3.5- to 5.5-foot segment, and 13,561 ng/kg in the 5.5- to 7.5-foot segment (not shown in figure). Total PCBs are higher in the subsurface segments (5.15 mg/kg in the 1.5- to 2.5-foot segment, 4.4 mg/kg in the 2.5- to 3.5-foot segment, 25 mg/kg in the 3.5- to 5.5-foot segment, and 14.6 mg/kg in the 5.5- to 7.5-foot segment) than in the surface (0.74 mg/kg), as are total DDx (increasing from 0.14 mg/kg in the surface to 0.26 mg/kg between 1.5 and 2.5 feet and 0.6 mg/kg below 3.5 feet), and mercury (increasing from 1.1 mg/kg in the surface to 5.3 mg/kg between 1.5 and 2.5 feet and 20 mg/kg between 3.5 and 5.5 feet).

and the time of core collection (Figure 4.2.7-15). Levels in the samples collected outside the Silt deposit are sometimes higher than the contaminant concentrations measured in coarse sediments in the other reaches (e.g., LPRT10B contains 740 ng/kg of 2,3,7,8-TCDD); however, the probing data here indicate the presence of fine sediments (Figure 4.2.7-4a), suggesting they likely represent small pockets of fine sediment in a larger SSS mapped coarse sediment deposit. The sample LPRT10B itself contains 29% fine sediments. Elevations of other sampling locations upstream of RM 8.75 also indicate recent deposition (the highest elevations at 13B0515, CLRC-056, and 12A-0472 were all measured in the most recent bathymetry available at those locations).

Similar trends continue between RM 8.75 and the Lance Corporal Osbrany Montes de Oca Memorial Bridge at RM 8.5. Concentrations within the Silt deposit on the eastern shoal are higher at depth than in the surface (e.g., core 13B-0511). Core 13B-0511 was also collected after the location experienced erosion between 2008 and 2011 (Figure 4.2.7-15); the location since experienced deposition before core collection in 2013. Of note in this region is core 13B-0509 at RM 8.56, which contains higher contaminant concentrations in the surface sediments (16,200 ng/kg 2,3,7,8-TCDD, 6.7 mg/kg total PCBs, 0.26 mg/kg total DDx, and 5.4 mg/kg mercury) than other locations within coarse sediments. Subsurface levels of some contaminants are also similarly higher (10.4 mg/kg mercury in the 2.5- to 3.5-foot segment). Though the fine composition of the surface segment is not available, the 0.5- to 1.5-foot and 1.5- to 2.5-foot segments contain 62% and 81% fine sediments, respectively. Additionally, the probing data here specify the presence of silt, indicating the core was collected in a small silt deposit that could not be detected by the SSS. This location experienced erosion since 2007, and the elevation during core collection in 2013 was a foot lower than that in 2007.

Downstream of the bridge, surface sediment contaminant patterns in the RM 8.5 point bar are similar to those in the RM 10.9 point bar and reflect upstream to downstream point bar evolution as noted previously. Concentrations of 2,3,7,8-TCDD decline moving upstream to downstream, though the absence of data in the downstream half of the point bar precludes confirming whether that trend continues throughout (Figures 4.2.7-10 and 4.2.7-11). Surface concentrations in the most upstream core of the point bar (G0000150 at RM 8.48; 3,250 ng/kg 2,3,7,8-TCDD, 3 mg/kg total PCBs, 0.27 mg/kg total DDx, and 8.2 mg/kg mercury) are higher than those in the surface of the most downstream sample (LPRC09A; 260 ng/kg 2,3,7,8-TCDD, 0.8 mg/kg total PCBs, 0.08 mg/kg total DDx, and 1.9 mg/kg mercury). The location G0000150 also experienced erosion between 2007 and the year of core collection (2008; Figure 4.2.7-15).

While coarser sediments are found on the outer bend, corresponding to the higher shear stresses there, the core 12A-0468 was collected within a fine sediment pocket (in the region of the silt probes within the Rock and Coarse Gravel deposit noted previously) and has correspondingly higher contaminant concentrations than other locations in coarse sediments. 2,3,7,8-TCDD levels in the

surface and 0.5- to 1.5-foot segments are 8,370 and 2,650 ng/kg, respectively. Corresponding levels of total PCBs (5 and 1.8 mg/kg, respectively), total DDx (0.5 and 0.4 mg/kg, respectively), and mercury (5 and 11 mg/kg, respectively) are further reflective of the impact of fine sediments on contamination levels in the LPR. The remainder of the locations sampled until RM 8 contain lower contamination concentrations, consistent with the coarse sediments present here. The elevation in 2012 at these locations was also the highest since 2007 (Figure 4.2.7-15).

The grab sample LPRT09B at the confluence of the Second River contains only 1% fine sediments but has higher levels of total PCBs and total DDx than coarse sediments elsewhere, suggesting that at this location some contamination was also found in coarse sediments. Three locations were sampled in a transect at RM 7.97. From east to west, these locations are CLRC-052, CLRC-051, and CLRC-050. CLRC-052 was collected in a region identified by the SSS as Rock and Coarse Gravel. Though the fine sediment composition of CLRC-052 was 32%, the general lack of sediment accumulation here is indicated by the fact that only a grab sample could be collected. Fine sediments in CLRC-051 are less than 10% throughout the entire core. The 1.5- to 2.5-foot segment of CLRC-050 contains 32% fine sediments, but the segments above this contain about 11% fine sediments each. The surface contamination levels are reflective of the coarse sediments and lack of sediment recovery, with lower 2,3,7,8-TCDD, total PCBs, and mercury concentrations similar to those measured in other coarse sediments detected here. Total DDx levels, however, are higher in the surface of CLRC-051 (0.57 mg/kg); the reasons for the anomalous value are unknown. Similarly, high concentrations are also measured in the subsurface segments of CLRC-050. The 1.5- to 2.5-foot segment of CLRC-050 contains the highest 2,3,7,8-TCDD, total DDx, and mercury levels in this transect, likely due to the higher fine sediments here. This segment contains 987 ng/kg of 2,3,7,8-TCDD, 1.12 mg/kg of total PCBs, 0.58 mg/kg of total DDx, and 7.3 mg/kg of mercury. Total PCB levels in CLRC-050 are highest in the 0.5- to 1.5-foot segment (3.13 mg/kg); the reason for the higher levels in coarser sediments is not known.

Concentrations in the cluster of cores farther downstream (CLRC-049, LPRT08E, and 12A-0465) are lower, corresponding to the low percent fine composition of the sediments here (fine composition is uniformly less than 10%). These cores are, however, located with the SSS mapped silt deposit (Figure 4.2.7-11), suggesting they might have been collected in a coarse sediment pocket in a larger fine sediment deposit. Total DDx levels in the subsurface segments of CLRC-049 (1 mg/kg between 0.5 and 1.5 feet, and between 0.2 and 0.3 mg/kg farther below until 3.5 feet), however, suggest that some total DDx in this reach is associated with coarser sediments.

HMW PAH and LMW PAH patterns (Figures 4.2.7-17 and 4.2.7-18, respectively) exhibit less concordance with 2,3,7,8-TCDD than the other contaminants (Figure 4.2.7-16), as has been noted in previous reaches. Upstream of RM 8.75, concentrations are highest in CLRC-056 and CLRC-057, with more than 50 mg/kg HMW PAHs measured in the subsurface segments of CLRC-057 and 22 mg/kg

LMW PAHs measured in the 3.5- to 5.5-foot segment of CLRC-056. Concentrations are lower in the other sampled locations and do not show a consistent trend. Farther downstream, like the other contaminants, concentrations are higher in 13B-0509 than the rest of the region between RM 8.75 and the Lance Corporal Osbrany Montes de Oca Memorial Bridge.

PAH patterns between RM 8.5 and RM 8 are similar to the other contaminants. At the point bar, concentrations in the most upstream core (G0000150) are higher than levels in the most downstream location (LPRC09A). Along the outer bend, PAH concentrations in 12A-0468 are higher than surrounding cores. Downstream of RM 8, like the upstream reaches, higher concentrations are measured intermittently in the coarse sediments.

In summary, the sediment contamination patterns between RM 9.2 and 7.8 are qualitatively similar to those observed in the preceding reaches with inventory higher in the shoals than in the channel. Levels in the samples collected outside the Silt deposit are sometimes higher, indicative of small pockets of fine sediment. Higher concentrations of 2,3,7,8-TCDD, total PCBs, total DDx, and mercury in the surface and subsurface are mostly limited to the fine sediment deposits. Some deviation from this is seen with total DDx, which is present in higher concentrations in coarse sediments downstream of RM 8. Patterns in the point bar at RM 8.5 are similar to those seen in the RM 10.9 point bar, with concentrations declining longitudinally within the point bar. Like the upstream reaches, PAH levels are not as well correlated with 2,3,7,8-TCDD or with fine sediments.

4.2.8 RM 7.8 to RM 5

This reach extends from the WR Railroad Drawbridge to the beginning of an approximately 90-degree turn at RM 5 (Figure 4.2.8-1). It is oriented NE-SW until RM 6.25, where it bends slightly to flow in the N-S direction. At RM 5.4, it bends slightly east. River crossings in this reach include the Fourth Avenue Bridge (RM 6.07), Clay Street Bridge (RM 5.82), Route 280 Bridge (RM 5.61), Newark Drawbridge (RM 5.56), and Bridge Street Bridge (RM 5.42). The total area of the sediment bed is 140 acres.

The western shoreline is mostly sheetpiled/bulkheaded, except for a small vegetated stretch between RM 7.25 and RM 7.2. The eastern shoreline is vegetated until RM 6.75 and sheetpiled/bulkheaded downstream of RM 6.25. Smaller extents of sheetpile/bulkhead, riprap/stone, and vegetation comprise the eastern shoreline between RM 6.75 and RM 6.25 (Figure 4.2.8-1). The cross-sectional area expands from 3,700 ft^2 at the WR Railroad Drawbridge to 5,000 ft^2 at RM 7.75 and is between 5,000 ft^2 and 5,750 ft^2 for the rest of the reach. The width expands from 400 feet at RM 7.75 to 600 feet at RM 7.45. It then decreases to 425 feet at RM 7 and continues decreasing to 315 feet at the Newark Drawbridge (RM 5.56), before expanding to 415 feet at the end of the reach.

The federal navigation channel continues through this reach but was last maintained here before 1950. Bathymetry data suggest the channel generally corresponds with the delineated navigation channel. A slight westward migration of the thalweg toward the outer bend can be seen around RM 6.25, reflecting the presence of a wide shoal along the inner bend.

The evolution of the sediment bed is studied using bathymetry data (single-beam surveys [1949/1950, 1966, 1989, 1995, 2004, and 2007] and multi-beam surveys and associated single-beam transect measurements[81] [2007, 2008, 2010, 2011, and 2012]), model-predicted bottom shear stress patterns, and Cs-137 core profile data. Its characteristics are described using results of the 2005 SSS survey and associated ground truthing data, probing surveys, and characteristics and contaminant concentrations of individual cores.

Shear stresses and sediment types in this reach reflect the river shape and the unmaintained navigation channel. Shear stresses (Figure 4.2.8-2) are lower than those in the upstream reaches, due to the larger cross-sectional area and lower water velocities. Shear stresses are lowest upstream of RM 7.2, where the river is wider, and highest within the flow constriction at the Fourth Avenue Bridge (RM 6.07). The lower shear stresses and lack of maintenance dredging have resulted in significant fine sediment accumulation—as reflected in 71% of the 140 acres of sediment being classified as Silt (Figure 4.2.8-3). Gravel and Sand were found intermittently along the shoals between RM 7.05 and RM 6, and Silt and Sand were found in the shoals downstream of RM 5.42, except for a small Rock and Coarse Gravel outcrop on the eastern shoal around RM 5.15. Near the Clay Street Bridge (RM 5.82) and Bridge Street Bridge (RM 5.42), the SSS characterized the bed as Rock and Coarse Gravel, Gravel and Sand, and Sand, likely due to turbulence around the bridge piers. The region between the bridges is mostly Silt and Sand.

A broad shoal exists along the eastern shoreline on the inside of the bend that forms the jog between RM 7.5 and RM 7.0. Sediment types here are like those in other point bars and bends. A narrow band of Rock and Gravel lies along the eastern bank (like that seen at the RM 10.9 point bar and likely due to wave action preventing sediment accumulation), a silty shoal extends into the channel, and coarser Silt and Sand lie along the outer bend.

Significant geomorphological changes have occurred in the reach since the first bathymetry surveys in 1949/1950 below RM 6.8 and in 1966 above RM 6.8 (Figure 4.2.8-4). Most of the channel experienced infilling, except for the region just below WR Railroad Drawbridge, the region between RM 7.0 and RM 6.8, and the region around the downstream two bridges. The evolution of the shoals is less informed by the bathymetry surveys because of limited coverage prior to 1995. The data are sufficient to see that the point bar centered at RM 7.3 expanded downstream and toward the

[81] The multi-beam surveys downstream of RM 7.8 also included bank-to-bank single-beam transects

channel and reached a somewhat stable configuration by 2004. In the region containing the bridges, the shoals expanded somewhat.

The Cs-137 data in this reach (Figure 4.2.8-5) provide further insights on the geomorphological changes. Two high-resolution cores collected in the shoal at RM 7.79 (G0000014-26A and G0000014-26B), where bed evolution could not be evaluated from bathymetry changes, have Cs-137 peaks that are 25 to 35 inches below the sediment surface, indicating net deposition since the mid-1960s. In contrast, the core just downstream of RM 7.5 in the point bar (CLRC-048) has no detectable Cs-137 below the surface and very low activity in the surface segment, suggesting this upper portion of the point bar reached a stable configuration before the 1950s. The nearby core in the channel (CLRC-048) has detectable Cs-137 at depth and a peak in the surface segment, suggesting net accumulation until the mid-1960s. The core at RM 7.0 collected at the channel edge of the point bar (CLRC-045) has a peak about 12 inches below the surface, suggesting that the downstream portion of the point bar evolved later than the upstream portion. Its neighboring core in the channel (CLRC-044) has a profile like the RM 7.5 channel core, suggesting the infilling in this area occurred largely before the mid-1960s. The three cores at RM 6.75 (276, 277, and 278) have relatively high Cs-137 concentrations at depth suggesting significant sediment accumulation, but ragged profiles, perhaps indicating alternate periods of erosion and deposition. Cs-137 data between RM 6.5 and RM 6.0 mostly contain well-defined buried peaks, consistent with long-term deposition.

The Cs-137 data between the Fourth Avenue Bridge and Bridge Street Bridge support the lack of sediment accumulation there; many samples here contain either low activities of Cs-137 or peaks at or near the surface. Interspersed in this region are cores with buried peaks or with no clearly identifiable peaks. Downstream of the Bridge Street Bridge, consistent with the historical sediment accumulation upstream of the bridges noted above, the Cs-137 profiles contain well-defined buried peaks, except for core 256 at RM 5.15. Though this sample does not contain a well-defined Cs-137 maximum, the decrease in activities below 5 feet is consistent with sediment accumulation.

Recent multi-beam data (Figure 4.2.8-6) show a pattern of alternating erosion and deposition between RM 7.7 and RM 7.45 on the eastern portion of the channel; however, single-beam transects at RM 7.63 show little to no elevation difference between 2007, 2008, 2011, and 2012 surveys (Figure 4.2.8-7a), suggesting some smaller portions of this region might not have experienced this alternating erosion and deposition. The other major erosional areas upstream of the Fourth Avenue Bridge comprise a band along the western side of the channel between RM 7.2 and RM 6.85 and most of the eastern half of the channel between RM 6.85 and RM 6.25. A transect at RM 6.44 (Figure 4.2.8-7b) shows that the highest elevation here was in 2004. The first two of the erosional regions noted above are located on the side slopes (Figure 4.2.8-8), while the last is located within the main channel.

The region between the bridges mostly experienced 6 inches or less change, as observed in both the multi-beam bathymetry (Figure 4.2.8-6) and in a transect collected at RM 5.9 (Figure 4.2.8-7c). Downstream of the Bridge Street Bridge, much of the channel, particularly the western half, experienced erosion between 2010 and 2011 (Figures 4.2.8-6 and 4.2.8-8). Some portions experienced net erosion of more than 1 foot. A transect collected at RM 5.1 indicates that the maximum bed elevation here was measured in 2004 (Figure 4.2.8-7d).

Contaminant Patterns

Surface contaminant levels in this reach are like those generally found throughout the RM 2 to RM 12 stretch of the river (Figure 4.1-9a through 4.1-9f). Concentrations of 2,3,7,8-TCDD, total PCBs, total DDx, and mercury are higher in finer sediments than coarser sediments. PAH concentrations, however, do not follow a similar trend. Despite similar sediment types, surface contaminant concentrations are typically higher in the shoals than in the channel (Figure 4.2.8-9; see Appendix K for similar figures of total DDx, mercury, HMW PAHs, and LMW PAHs). This presumably reflects differences in sediment transport patterns and long-term deposition and erosion, including the aforementioned channel infilling. The region between the bridges contains lower contaminant concentrations, reflective of the general lack of sediment accumulation and coarser sediments there. The overall concentrations measured in this reach are summarized in Table 4-9.

The cores collected in the shoal at RM 7.79 (G0000014 and C01-SD1) contain higher concentrations at depth than in the surface segment for 2,3,7,8-TCDD (Figure 4.2.8-10), total PCBs (Figure 4.2.8-11), total DDx (Figure 4.2.8-12), and mercury (Figure 4.2.8-13)[82]; burial of historical sediments at this location was previously noted for the Cs-137 cores collected here (Figure 4.2.8-5). Farther downstream, at RM 7.62, there appears to have been less burial in the shoals. Both shoal cores have relatively high concentrations in the surface segment and 0.5- to 1.5-foot segments. In contrast, the core collected in the channel here (12A-0463) has relatively low concentrations. This core contains less than 15% fine sediments in all segments, indicating it was collected in a coarse sediment pocket within the SSS-identified Silt deposit.

Contamination patterns within the point bar on the eastern shoal between RM 7.5 and RM 7.05 reflect its development.[83] The concentrations of 2,3,7,8-TCDD, total PCBs, and total DDx are highest in the surface segments.[84] Within the surface segments, concentrations are lower in the upstream

[82] Concentrations of total PCBs, total DDx, and mercury in G0000014 are highest in the 2.5- to 3.5-foot segment. 2,3,7,8-TCDD concentrations are only available for the 2.5- to 3.5-foot segment and in none of the shallower segments. Concentrations of 2,3,7,8-TCDD in the co-located C01-SD1, however, are lower in all segments (between 500 and 1,000 ng/kg) than in the 2.5- to 3.5-foot segment of G0000014 (6,220 ng/kg).

[83] From upstream to downstream, the locations within the point bar are CLRC-048, LPRT08C, 13B-0507, 12A-0460, LPRT10B, 13B-0503, 12A-0459, and 12A-0458.

[84] Subsurface concentrations are less than 25 ng/kg 2,3,7,8-TCDD, 0.5 mg/kg total PCBs, and 0.005 mg/kg total DDx in all the samples except 12A-0458, which is located at the downstream extent of the point bar.

parts of the point bar (CLRC-048 at RM 7.45 contains 61 ng/kg 2,3,7,8-TCDD) than farther downstream (12A-0460 at RM 7.32 contains 34,100 ng/kg 2,3,7,8-TCDD, and 12A-0459 at RM 7.22 contains 22,400 ng/kg 2,3,7,8-TCDD). Surface concentrations of total PCBs and total DDx also follow similar trends. The low concentrations in CLRC-048[85] suggest that the upstream parts of this point bar evolved before the release of 2,3,7,8-TCDD (i.e., before the 1950s), a timing also supported by the previously noted low Cs-137 activities in this location. Mercury patterns within the point bar are an exception, with the highest concentrations measured in the 0.5- to 1.5-foot and 1.5- to 2.5-foot segments of CLRC-048 (12.3 and 11.4 mg/kg, respectively). The variation in mercury patterns could be due to temporal differences in loading compared to the other contaminants. The more recent development of the downstream portions of the point bar is consistent with higher subsurface contamination levels in 12A-0458.

The two locations sampled on the boundary between the shoal and the channel (13B-0506 at RM 7.32 and 13B-0502 at RM 7.23) contain coarser sediments than the locations in the point bar[86] and contain correspondingly lower contamination levels. Core 13B-0502 contains higher concentrations at depth that may have been covered as the point bar expanded into the channel, as seen in Figure 4.2.8-14, which overlays 2,3,7,8-TCDD data on 1949/1950, 1966, and 2004 bathymetries. As observed in Figure 4.2.8-15b, the lower surface concentration in this core appears to be due to post-2008 deposition of cleaner sediments.

The two sampled locations on the outer bend between RM 7.5 and RM 7.05 contain 2,3,7,8-TCDD levels exceeding 10,000 ng/kg (13B-0504 at RM 7.32 and 12A-0461 at RM 7.23).[87] The higher levels here reflect lack of deposition on the outer bend side slopes (Figure 4.2.8-8). Higher concentrations are also found for total PCBs, total DDx, and mercury.

The channel in this region shows contamination levels reflective of its historical evolution (Figure 4.2.8-14). The highest levels are buried; the two locations sampled in the channel—130B-0505 and 130B-0501—contain the maximum concentrations in the 1.5- to 2.5-foot segments for 2,3,7,8-TCDD, total PCBs, total DDx, and mercury. As observed in Figure 4.2.8-14, both locations have accumulated sediment since 1966.

Farther downstream to approximately RM 6.8 (the upstream extent of the 1949/1950 bathymetry), contaminant concentrations continue to be lower in the channel than in the shoals. The highest

[85] The lower concentrations in CLRC-048 are not due to a lack of fine sediments. The 0- to 0.5-foot, 0.5- to 1.5-foot, and 1.5- to 2.5-foot segments of CLRC-048 contain greater than 70% fine sediments.

[86] The surface segment of 13B-0506 contains 28% fine sediments, and the bottom segment of 13B-0502 contains 32% fine sediments. All other segments of these cores contain less than 15% fine sediments.

[87] Location 13B-0504 contains 28,200 and 22,500 ng/kg 2,3,7,8-TCDD in the surface and 0.5- to 1.5-foot segment, respectively. Location 12A-0461 contains 19,500 ng/kg 2,3,7,8-TCDD in the 0.5- to 1.5-foot segment.

levels here were measured in CLRC-045[88] at RM 7 on the eastern edge of the channel. The next highest values were measured on the western shoal (CLRC-043, RM 7). Significantly lower concentrations were measured in the channel (12A-0457 and 12A-0455) with the exception of mercury; mercury levels in the channel cores are comparable to the lowest levels in the top 3.5 feet of these two cores (e.g., the surface segment of 12A-0455 contains 8.4 mg/kg of mercury). As noted previously for CLRC-048, the variation in mercury concentrations could be due to temporal differences in loading compared to the other contaminants.

Downstream of RM 6.8, where the navigation channel widens and significant deposition occurred between 1949/1950 and 1966 (Figure 4.2.8-4 and 4.2.8-14), high subsurface concentrations are observed within the channel. Except 12A-0449 at RM 6.34, all locations between RM 6.8 and RM 6.07 contain higher concentrations at depth than in the surface.[89] Of note here is location 12A-0454 in the channel at RM 6.62; this location experienced more than 2 feet of erosion between 2010 and 2011, before accumulating a few inches of sediment when it was sampled in 2012. Despite the significant erosion, the deepest and most contaminated segment (1.5- to 2.5-foot) was not exposed to the surface (Figure 4.2.8-15).

Along the bend between RM 6.5 and RM 6.07, the eastern side of the channel (inner bend) has accumulated sediment, with a point bar extending into the channel. The western side, like the outer bends in other parts of the river, has not accumulated sediments. This has resulted in higher surface concentrations (e.g., CLRC-040) than found on the eastern side (CLRC-041 and CLRC-042).[90,91] A similar trend is also observed farther downstream between 12A-0449 and 12A-0450[92]; however, this variation could also be due to the greater fine sediment content of the former (44% versus 13%). The decreasing deposition moving east to west at RM 6.5 has resulted in shallower depths of maximum contaminant concentration in that direction; while the maximum 2,3,7,8-TCDD concentration in the western most core (CLRC-040) is present in the 1.5- to 2.5-foot segment (36,000 ng/kg), the

[88] 2,3,7,8-TCDD levels in the surface, 0.5- to 1.5-foot, 1.5- to 2.5-foot, and 2.5- to 3.5-foot segments of CLRC-045 are 13,250, 50,400, 10,100, and 1,420, respectively. Total PCB levels are 19, 33, 3.6, and 1 mg, respectively. Total DDx levels are 0.95, 1.3, 3.7, and 1.6 mg/kg, respectively. Mercury levels are 13.4, 14.2, 26.4, and 9.9 mg/kg, respectively.

[89] Location G000029 at RM 6.72 is excluded here—the surface segment of this core was not separately analyzed for contaminants. The 0.5- to 1.5-foot and 1.5- to 2.5-foot segments contain 19,400 and 10,075 ng/kg 2,3,7,8-TCDD, respectively, and lower amounts in the deeper segments. A similar pattern also holds for total PCBs but not for total DDx and mercury, suggesting a temporal variation in loading. This location is also on the side slope of the channel and was thus subject to less deposition than other locations within the main channel.

[90] The core CLRC-040 contains 1,364 ng/kg 2,3,7,8-TCDD, 2.5 mg/kg total PCBs, 0.4 mg/kg total DDx, and 2.3 mg/kg mercury in the surface segment. The cores immediately east—CLRC-041 and CLRC-042—contain 383 and 610 ng/kg 2,3,7,8-TCDD, 0.32 and 1.3 mg/kg total PCBs, 0.17 and 0.25 mg/kg total DDx, and 1.6 and 1.7 mg/kg mercury, respectively.

[91] The location CLRC-042 was sampled in 2008. Erosion between 2010 and 2011 here would have exposed the 1.5- to 2.5-foot segment, which contains 1,040 ng/kg 2,3,7,8-TCDD level (Figure 4.2.8-14).

[92] The core 12A-0449 contains 15,900 ng/kg 2,3,7,8-TCDD, 28.5 mg/kg total PCBs, 0.4 mg/kg total DDx, and 14.2 mg/kg mercury. The core immediately east (12A-0450) contains 144 ng/kg 2,3,7,8-TCDD, 1 mg/kg total PCBs, 0.17 mg/kg total DDx, and 1.2 mg/kg mercury.

corresponding depths moving east are 2.5 to 3.5 feet (CLRC-041, 48,900 ng/kg) and 3.5 to 5.5 feet (CLRC-042, 28,300 ng/kg). Similar trends are also observed for total PCBs, total DDx, and mercury.

Downstream of the Fourth Avenue Bridge, core CLRC-038 shows evidence of burial, with the highest concentrations measured at 1.5 feet; the deposition occurred after 1949/1950 and continued after 1966 (Figure 4.2.8-14). This depositional region includes core 12A-0448, which shows similar patterns. The rest of the channel down to the Bridge Street Bridge (RM 5.42) contains lower concentrations than the regions upstream of the bridges; 2,3,7,8-TCDD levels are less than 250 ng/kg, total PCB concentrations are less than 1 mg/kg, total DDx concentrations are less than 0.1 mg/kg, and mercury concentrations are less than 2 mg/kg. Higher concentrations are found on the side slopes of the channel (CLRC-036 and CLRC-037, just downstream of the Newark Drawbridge). Both locations experienced post-1966 deposition (Figure 4.2.8-15) and contain higher subsurface contamination levels than at the surface.

Downstream of the Bridge Street Bridge (RM 5.42), where the channel was depositional and accumulated sediment since 1949/1950 and after 1966, two locations were sampled within the channel—CLRC-034 and 12A-0447. The former contains the maximum concentration in the deepest sampled depth (1.5 to 2.5 feet), consistent with other depositional locations within the channel. The latter contains higher concentrations in the surface segment., which may reflect erosion during Hurricane Irene (Figures 4.2.8-15g indicates erosion occurred in the 2010 to 2011 period, which is also consistent with the bathymetric comparison in Figure 4.2.8-14f). The surface segment of this core, despite containing the highest contaminant concentrations,[93] is also the coarsest segment (8% fines), suggesting some variability in the concentration on fine sediments for this sample. The remaining locations sampled downstream of the Bridge Street Bridge (RM 5.42) were in the shoals and side slopes of the channel and, like the rest of the channel upstream of the Fourth Avenue Bridge (RM 6.07), contain higher surface concentrations than the main channel.[94]

Surface concentrations of total PCBs, total DDx, mercury, HMW PAHs, and LMW PAHs are well correlated to those of 2,3,7,8-TCDD (Figure 4.2.8-16), though the correlation is weaker for the PAHs (see also Appendix K Figures 8-7 and 9-7). While subsurface concentrations and MPA are also correlated, mercury and the PAHs exhibit greater variability, with elevated mercury and PAH concentrations observed in locations with lower 2,3,7,8-TCDD subsurface concentrations. As noted previously, the variation in mercury patterns could be due to a temporal variation in sources. Further, as noted in Figure 4.1-9d, the highest mercury concentrations in the LPR-Newark Bay region are found in Newark Bay, suggesting a downstream source of mercury to the LPR, especially to the lower reaches. The variability in PAH patterns may also reflect source differences as well as differences in

[93] The surface segment of 12A-0447 contains 2,660 ng/kg 2,3,7,8-TCDD, 1.3 mg/kg total PCBs, 0.12 mg/kg total DDx, and 3.5 mg/kg mercury.

[94] The low-resolution core G000027 on the eastern slope of the channel was not segmented into a 0- to 0.5-foot segment and is thus excluded in this discussion.

the nature of the compounds, with PAHs also present in coarser sediments (noted previously in Section 4.1).

Like the previous four contaminants, HMW PAH (Figure 4.2.8-17) and LMW PAH (Figure 4.2.8-18) patterns in this reach show evidence of burial, with higher concentrations found in the subsurface sediments. Upstream of the RM 7.5 to RM 7 point bar, concentrations are higher in the shoals than in the channel. Within the point bar, like mercury, concentrations of both PAHs are highest in CLRC-048.[95] Similar concentrations are also found buried in the channel in CLRC-047.[96] Concentrations are lower farther downstream in the point bar, and in the channel, except for LMW PAH in the 0.5- to 1.5-foot segment of 13B-0505 (RM 7.32; 33 mg/kg).

Farther downstream, outside the point bar down to RM 7, concentrations of both PAHs are lower in the surface sediments than in the subsurface sediments. The highest concentrations here are measured in the grab sample LPRT08A on the western shoal (88 mg/kg HMW PAHs and 59 mg/kg LMW PAHs) and in the 2.5- to 3.5-foot segment of CLRC-045 on the eastern shoal (83 mg/kg HMW PAHs and 24 mg/kg LMW PAHs).

Between RM 7 and RM 6.5, like the other contaminants, the highest PAH concentrations are buried at depth. The exception is 12A-0455[97] at RM 6.86, which, like mercury, contains higher PAH concentrations in the surface and 0.5- to 1.5-foot segments than the rest of the surrounding locations.

Like the other contaminants, the cluster of cores collected in the channel at RM 6.5 show PAH contamination at depth, with the highest concentrations here found in the 0.5- to 1.5-foot segment of CLRC-041 (116 mg/kg HMW PAHs and 49 mg/kg LMW PAHs). The core CLRC-040 contains between 55 and 65 mg/kg of HMW PAHs in all segments between 0.5 and 5.5 feet and between 20 and 25 mg/kg of LMW PAHs in all segments between 0.5 and 3.5 feet. However, unlike the previously discussed contaminants, surface concentrations in CLRC-040 (on the western side of the channel, which, as noted previously, has not accumulated as much sediments as those in the eastern side, where the point bar expanded into the channel) are lower than those in CLRC-041,[98] suggesting the depositing sediments on the inner bend were relatively more contaminated with respect to PAHs. Farther downstream, PAH patterns in 12A-0449 and 12A-0450 are like the other contaminants.

[95] The 0.5- to 1.5-foot and 1.5- to 2.5-foot segments of CLRC-048 contain 112 and 63 mg/kg HMW PAHs, respectively, and 53 and 26 mg/kg LMW PAHs, respectively.

[96] The 2.5- to 3.5-foot and 3.5- to 5.5-foot segments of CLRC-047 contain 95 and 56 mg/kg HMW PAHs, respectively, and 52 and 22 mg/kg LMW PAHs, respectively.

[97] The surface segment of 12A-0455 contains 210 mg/kg HMW PAHs and 54 mg/kg LMW PAHs. The 0.5- to 1.5-foot segment contains 93 mg/kg HMW PAHs and 46 mg/kg LMW PAHs.

[98] Surface concentrations of HMW PAHs in CLRC-040 and CLRC-041 are 30.5 and 46 mg/kg, respectively. LMW PAH concentrations here are 8.25 and 14 mg/kg, respectively.

PAH concentrations in the region of the bridges and downstream of the Bridge Street Bridge are lower than those measured upstream of the bridges. Like the other contaminants, concentrations are mostly higher at depth, suggesting burial of historically contaminated solids.

In conclusion, contaminant patterns in this reach reflect the predominance of fine sediments and the deposition that occurred in much of the channel. Subsurface levels are frequently higher than surface levels, suggesting the historical contamination has been buried under more recent cleaner solids. Shoals and channel side walls tend to have higher concentrations than the channel. Surface concentrations are highest in historically depositional shoal areas with little contemporary net deposition.

4.2.9 RM 5 to Point-No-Point Conrail Bridge (RM 2.3)

This reach extends from RM 5 to the Point-No-Point Conrail Bridge at RM 2.3, the approximate location where the navigation channel authorized depth changes from 20 feet to 30 feet. It begins with a roughly N-S orientation, turns sharply east at RM 4.75, and flows in the W-E direction until RM 3.75, where it bends NE until RM 3.25, before again bending east and flowing in the W-E direction through the end of the reach at RM 2.3. River crossings in this reach include the Amtrak Dock Bridge (RM 4.74), Jackson Street Bridge (RM 4.35), New Jersey Turnpike (RM 2.4), and Point-No-Point Conrail Bridge at the downstream extent (RM 2.3) (Figure 4.2.9-1). The Lister Avenue site, the predominant source of 2,3,78-TCDD and a major source of total DDx, is located along the southern shoreline near RM 3.2. The total area of the sediment bed in this reach is 175 acres.

Due to the orientation of the river in this reach, the cardinal directions used to describe this reach are different than the other reaches; the right shoreline looking upstream, referenced as the eastern shoreline of the previous reach, is the northern shoreline here, and left shoreline looking upstream, referenced as the western shoreline of the previous reach, is the southern shoreline here. Both shorelines are sheetpiled/bulkheaded down to the Jackson Street Bridge (RM 4.35). The southern shoreline is vegetated between RM 4.35 and RM 3.75, and downstream of RM 2.8, and mostly sheetpiled/bulkheaded from RM 3.75 to RM 2.8, except for some riprap/stone between RM 3.67 and RM 3.5 and between RM 3.35 and RM 3.3. The northern shoreline is vegetated between RM 4.35 and RM 3.15, sheetpiled/bulkheaded between RM 3.15 and RM 2.7, and composed of riprap/stone farther downstream (Figure 4.2.9-1).

The navigation channel was here last maintained before 1950 and has experienced significant deposition. Shoals have impinged on the channel along the inner bends around RM 3.75 and RM 3.25 and moved the thalweg toward the outer bends (Figure 4.2.9-1).

The evolution of the sediment bed is studied using bathymetry data (single-beam surveys [1949/1950, 1966, 1989, 1995, 2004, and 2007] and multi-beam surveys and associated single-beam

transect measurements [2007, 2008, 2010, 2011, and 2012]), model-predicted bottom shear stress patterns, and Cs-137 core profile data. Its characteristics are described using results of the 2005 SSS survey and associated ground truthing data, probing surveys, and characteristics and contaminant concentrations of individual cores.

The cross-sectional area expands from 5,600 ft^2 at RM 5 to 7,950 ft^2 at RM 2.3. A smaller cross section of 5,000 ft^2 exists as the river bends at RM 4.4. Shear stresses are lower than in the upstream reaches, due to the expanding cross-sectional area and resultant lower water velocities (Figure 4.2.9-2). The lowest shear stresses are on the inner bends at RM 3.75 and RM 3.25.

The channel is mapped as Silt (Figure 4.2.9-3). Coarser sediments exist in the region of the smaller cross section centered at RM 4.4. A small Rock and Coarse Gravel deposit exists on the outer bend at RM 4.75, around the piers of the Amtrak Dock Bridge, which transitions to a Silt and Sand deposit on the two shoals until the constriction ends around the Jackson Street Bridge at RM 4.35. In the bend downstream of RM 4.35, trends are like other bends further upstream—a thin sliver of coarse sediments (Rock and Coarse Gravel) is found near the shore on the inner bend, which transitions to Silt that extends across the shoal and most of the channel, and then to Silt and Sand and Rock and Coarse Gravel toward the outer bend. A similar trend is observed as the river bends around RM 3.5, with a nearshore thin Rock and Coarse Gravel sliver on the inner bend soon giving way to Silt on the shoal and in the channel, and Silt and Sand on the outer bend. Downstream of RM 3.15, where the river flows straight in a W-E direction, the entire river bottom is mapped as Silt.

The channel throughout the reach accumulated sediment between 1949/1950 and 1966 and then also after 1966 (Figure 4.2.9-4). The deposition after 1966 seems greatest upstream of the Amtrak Dock Bridge. Of note is the expansion of the inner bend point bars, which can be seen by comparing the 1949/1950, 1966, and 1989 bathymetries between RM 4 and RM 3.75 and between RM 3.5 and RM 3.

Consistent with the infilling evident in the bathymetry comparisons, 64 of the 72 Cs-137 cores collected in this reach show evidence of a long-term net deposition (Figure 4.2.9-5). The remaining eight contain either low activities of less than 0.05 picocuries per gram all through or below the surface, suggesting little to no net sediment accumulation at those locations since the early 1950s.

Recent multi-beam bathymetry data indicate that most of the channel experienced erosion between 2010 and 2011 (Figure 4.2.9-6), the period that included a large flow event in March 2011 and Hurricane Irene. Portions of the channel side slopes abutting the point bars experienced more than 1.5 feet of erosion (Figure 4.2.9-7). Erosion also occurred between 2008 and 2010 but was more restricted spatially. Most of the channel experienced 6 inches or less change in bed elevation between 2007 and 2008, 2008 and 2010, and between 2011 and 2012 (the last period lacked significant high-flow events). A single-beam transect at RM 4.46 indicates that the lowest elevation in

the channel was measured in 2011 (Figure 4.2.9-8a). Toward the northern side of the channel, the elevation was lowest in 2004, suggesting some of that region experienced deposition between 2004 and 2007. At the immediate downstream location (RM 4.83), the 2004 elevation is higher than 2007, suggesting post-2004 erosion (Figure 4.2.9-8a, lower panel); there is, however, little overlapping bathymetry data at this location. The post-2004 erosion is also seen in transects collected at RM 4.21, RM 3.94, RM 3.46, RM 3.09, RM 2.8, and RM 2.61 (Figures 4.2.9-8b through 4.2.9-8e). These transects also indicate that the lowest elevation here was measured in 2011 or 2012, corresponding to the net erosion between 2010 and 2011 and little to no change between 2011 and 2012 indicated by the multi-beam data.

Contaminant Patterns

Surface contamination concentrations for 2,3,7,8-TCDD, total PCBs, total DDx, mercury, HMW PAHs, and LMW PAHs are similar overall to those in the RM 7.8 to RM 5 reach (Figures 4.1-9a through 4.1-9f). Due to infilling, concentrations within the channel are higher in subsurface sediments than in the surface sediments. The few samples collected in the small Rock and Coarse Gravel outcrop on the outer bend between RM 4.25 and RM 3.75 contain low surface concentrations of 2,3,7,8-TCDD and total PCBs (Figure 4.2.9-9; see Appendix K for similar figures of total DDx, mercury, HMW PAHs, and LMW PAHs). The overall concentrations measured in this reach are summarized in Table 4-10.

Between RM 5 and the Amtrak Dock Bridge (RM 4.74), the locations sampled in the channel have their highest levels of 2,3,7,8-TCDD (Figure 4.2.9-10), total PCBs (Figure 4.2.9-11), total DDx (Figure 4.2.9-12), and mercury (Figure 4.2.9-13) in deep segments, reflecting the post-1966 deposition. A core from the western shoal (12A-0445) had its highest concentration in the surface segment.[99]

In the bend between the Amtrak Dock Bridge and the Jackson Street Bridge (RM 4.35), concentration patterns are like those in other bends. Post-1966 deposition occurred mostly along the inner bend, resulting in the expansion of the shoal into the channel (Figure 4.2.9-14). A transect of cores at RM 4.63 (from the inner bend to the outer bend, 12A-0441, 12A-0442, 12A-0443, and 12A-0444) shows that surface concentrations are lower in the shoals and side slopes of the inner bend and the inner half of the channel than in the shoals on the outer bend[100] (the location on the side slopes can be seen in the 3D maps in Figure 4.2.9-7). Similar trends are also observed in the subsurface sediments. A transect of cores farther downstream at RM 4.52 (from the inner bend to the outer bend, 12A-0438, 12A-0439, and 12A-0440) also exhibits this trend.

[99] The low-resolution core G000022 on the western shoal was not segmented into a 0- to 0.5-foot segment and is thus excluded in this discussion. Note that the 0.5- to 1.5-foot segment of this core contains the lowest concentrations, and the highest levels are measured in the bottom segment.

[100] Surface concentrations of 2,3,7,8-TCDD in 12A-0441, 12A-0442, 12A-0443, and 12A-0444 are 299, 122, 56.7, and 10,800 ng/kg, respectively. The same trend is also observed for other contaminants and in the deeper segments. 12A-0443 contains less than 15% fine sediments at all depths and comprises the least contamination.

Downstream of the Jackson Street Bridge (RM 4.35), the highest concentrations are found below the surface segment within the channel, reflective of deposition. Relatively low concentrations exist in the Gravel and Sand deposit along the southern shoal. Location CLRC-031, collected in the channel in 2008, experienced a foot of erosion between 2008 and 2010 that likely exposed the more contaminated 0.5- to 1.5-foot segment (Figure 4.2.9-15).

As the LPR bends between RM 4 and RM 3.5, infilling has buried the highest contamination, though recent erosion may have exposed deeper sediments at some locations. The highest surface levels here were measured in 12A-0427[101] at RM 3.64. This core was taken in 2012, after the location experienced about 1 foot of erosion between 2008 and 2010 and more than 3 feet of erosion between 2010 and 2011 (Figure 4.2.9-15). The erosional region here includes CLRC-028 (RM 3.52), whose more contaminated 1.5- to 2.5-foot segment may have been exposed in 2011.

Between RM 3.25 and RM 3, contamination levels are lower on the northern shoal than on the southern shoal, except mercury in core 12A-0421, which exceeds 10 mg/kg in all depth intervals. The southern shoal here, which corresponds to the region around the Lister Avenue discharge, contained the highest concentrations of 2,3,7,8-TCDD and total DDx in the LPR; maximum 2,3,7,8-TCDD and total DDx concentrations of 6,149,170 ng/kg and 17,150 mg/kg, respectively, were measured in the 5.5- to 7.5- foot segments of HRC-04H at RM 3.13. The highly contaminated sediments within the 2-acre area immediately adjacent to the Lister Avenue site (see Figure 1-3 for the footprint) were removed as part of the Phase 1 remediation that occurred between 2011 and 2012.

In the southern shoal (but outside of the Lister Avenue dredge footprint), burial has resulted in all concentrations greater than 10,000 ng/kg 2,3,7,8-TCDD and 4 mg/kg total DDx being found below 1.5 feet of sediment. The impact of the burial is seen in the fact that 9 out of the 15 locations sampled in the southern shoal contain less than 650 ng/kg of 2,3,7,8-TCDD in the 0.5- to 1.5-foot segment[102] and 11 out of the 15 contain less than 2 mg/kg total DDx in the 0.5- to 1.5-foot segment.

From RM 3 to the downstream extent of the reach, all the sediment is mapped as Silt. Like the rest of the Silt areas of the reach, the highest contamination is found in the subsurface sediments, and surface concentrations in the shoals are greater than those in the channel (the highest surface concentrations of 2,3,7,8-TCDD are found in 12A-0413 and CLRC-022, on the northern and southern shoal, respectively; Figure 4.2.9-10). Many of the locations sampled in the channel experienced a foot or more of erosion between 2007 and 2011 (Figure 4.2.9-15); however, all but three of these locations were sampled in 2012, suggesting that even after the erosional events, the higher subsurface contamination was not exposed. The other locations were sampled in 2008 (CLRC-025 at

[101] 11,700 ng/kg 2,3,7,8-TCDD, 21 mg/kg total PCBs, 0.65 mg/kg total DDx, and 16 mg/kg mercury

[102] These cores were not segmented into a 0-0.5 feet segment, and the analysis here thus does not include a discussion of surface contamination

RM 2.84, CLRC-023 at RM 2.61, and CLRC-024 at RM 2.61), and the 0.5- to 1.5-foot segment may have been exposed in those locations.

Surface concentrations of total PCBs, total DDx, mercury, HMW PAHs, and LMW PAHs are well correlated to those of 2,3,7,8-TCDD (Figure 4.2.9-16), though the correlation is weaker for the PAHs. Subsurface concentrations and MPA of total PCBs and total DDx are also correlated with 2,3,7,8-TCDD, but mercury and the PAHs are less so; elevated mercury and PAH concentrations exist in samples with lower 2,3,7,8-TCDD subsurface concentrations (see also Appendix K Figures 8-8 and 9-8). As noted previously, the variation in mercury patterns could be due to sources whose history of releases differs from other contaminants. Also, this reach contains the predominant source of 2,3,7,8-TCDD and a major source of total DDx to the system, resulting in extremely high local levels of these two contaminants. The variability in PAH patterns is likely influenced by the difference in nature of the compounds, with PAHs also present in coarser sediments (noted previously in Section 4.1). The upstream extent of this reach (RM 5 to RM 3.5) contains some of the highest LMW PAH levels in the LPR, and unlike the rest of the river, LMW PAH levels here are often higher than HMW PAH levels, suggesting a possible LMW PAH source.

Between RM 5 and the Amtrak Dock Bridge, the highest PAH concentrations are found in the subsurface sediments. The highest levels here were found in CLRC-033 (RM 5), which contains 375 mg/kg HMW PAHs (Figure 4.2.9-17) and 380 mg/kg LMW PAHs (Figure 4.2.9-18) in the 3.5- to 5.5-foot segment. Farther downstream, along the bend between the Amtrak Dock Bridge and the Jackson Street Bridge, PAH concentration patterns are like the other contaminants, with the highest surface concentration measured in the location sampled on the outer bend.[103] All locations here show evidence of burial, indicating that the PAH concentrations that deposited here have decreased over time.[104] Farther downstream, surface concentrations in 12A-0440 on the outer bend are higher than those in 12A-0438 and 12A-0329. The surface segment of 12A-0440 contains 342 mg/kg HMW PAHs and 894 mg/kg LMW PAHs, the latter being the highest level in this reach. The subsurface sediments contain even higher amounts of PAHs.[105]

Between the Jackson Street Bridge and RM 4, the highest concentrations continue to be buried at depth. The highest concentration here was found in the bottom segment of 12A-0436 on the northern shoal.[106] Unlike the other contaminants, concentrations in the Gravel and Sand deposit are

[103] Location 12A-0444 on the outer bend contains 59 mg/kg HMW PAHs and 32 mg/kg LMW PAHs in the surface sediments. The locations on the inner bend and the inner half of the river—12A-0441, 12A-0442, 12A-0443—contain 45, 32, and 21 mg/kg HMW PAHs, respectively, and 7, 5, and 3 mg/kg LMW PAHs, respectively, in the surface sediments.

[104] Location 12A-0444 contains 147 and 359 mg/kg HMW PAHs, and 147 and 300 mg/kg LMW PAHs in the 0.5- to 1.5-foot and 1.5- to 2.5-foot segments, respectively.

[105] The 0.5- to 1.5-foot segment of 12A-0440 contains 1,991 mg/kg HMW PAHs and 5,478 mg/kg LMW PAHs. The 1.5- to 2.5-foot segment contains 1,441 mg/kg HMW PAHs and 4,232 mg/kg LMW PAHs.

[106] 1,118 mg/kg HMW PAHs and 2,123 mg/kg LMW PAHs

not lower than those in the channel, with the bottom segment of 12A-0434 containing 989 mg/kg HMW PAHs and 950 mg/kg LMW PAHs.

Farther downstream to RM 3.5, like other contaminants, the highest surface PAH concentrations were measured in 12A-0427.[107] This sample, as noted before, was collected in a location that experienced about 1 foot of erosion from 2008 to 2010 and more than 3 feet of erosion between 2010 and 2011. Surface concentrations are lower than subsurface concentrations at all other locations here.

As the LPR bends again between RM 3.5 and RM 3, PAH concentrations are lower than the more upstream parts of the reach. The highest surface concentrations were found in 12A-0422 and 12A-0421.[108] Excluding the former, concentrations are greater at depth, indicative of burial. Concentrations are lower on the southern shoal, where concentrations of 2,3,7,8-TCDD and total DDx were higher due to the Lister Avenue site discharge.

From RM 3 to the downstream extent of the reach, surface concentrations of both PAHs are lower than those measured upstream of RM 3.5. Surface levels of HMW PAHs are less than 50 mg/kg in this region, and those of LMW PAHs are less than 8 mg/kg. The highest HMW PAH levels here are measured below 2.5 feet in CLRC-022 (RM 2.64) on the southern shoal.[109] The highest LMW PAHs are measured at depth in CLRC-023 (RM 2.61).[110]

In summary, contamination concentrations in this reach reflect long-term deposition in the unmaintained navigation channel. Surface concentrations are generally lower than subsurface concentrations. However, many parts of this reach experienced erosion between 2008 and 2010 and between 2010 and 2011, which would have likely exposed more contaminated subsurface sediments. Concentration patterns along bends follow expected trends, with the inner bend containing lower surface concentrations due to the accumulation of sediments. The highest 2,3,7,8-TCDD and total DDx levels in this reach were found in the southern shoal between RM 3.5 and RM 3, proximate to the Lister Avenue site discharge. Like the previous reach, a weaker correlation is observed between mercury concentrations and 2,3,7,8-TCDD concentrations, possibly due to the nature of the sources and the increased influence of Newark Bay as a downstream source. PAH concentrations in this reach are higher upstream of RM 3.5 than farther downstream, and LMW PAH concentrations here are the highest in the LPR, suggesting a possible local source of LMW PAHs. Like the reaches upstream of RM 7.8, PAH concentrations in this reach are similar in a coarser Gravel and Sand deposit and in a finer Silt deposit, likely due to the differences in the nature of the compounds noted in Section 4.1.

[107] 213 mg/kg HMW PAHs and 63 mg/kg LMW PAHs

[108] Location 12A-0422, in the channel, contains 97 mg/kg HMW PAHs and 21 mg/kg LMW PAHs. Location 12A-0421, on the outer shoal, contains 60 mg/kg HMW PAHs and 39 mg/kg LMW PAHs.

[109] The 2.5- to 3.5-foot and 3.5- to 5.5-foot segments of CLRC-022 contain 211 and 93 mg/kg HMW PAHs, respectively.

[110] The 5.5- to 7.5-foot segment (not shown on the maps) of CLRC-023 contains 33 mg/kg LMW PAHs.

4.2.10 RM 2.3 to Mouth

This reach extends from the Point-No-Point Conrail Bridge at RM 2.3 to the mouth of the LPR (RM 0) (Figure 4.2.10-1). The river bends sharply between RM 2.25 and RM 2 and flows in the N-S direction to the mouth. River crossings in this reach include the Pulaski Skyway (RM 1.74), Lincoln Highway Bridge (RM 1.56), and Abandoned Central Railroad Bridge (RM 0.89). The cross-sectional area increases from 7,950 ft^2 at RM 2.3 to 9,700 ft^2 at RM 1 and then expands dramatically to 18,700 ft^2 at RM 0.5 and more than 70,000 ft^2 by the mouth (Figure 4.1-1 and Figure 3.1-2). The total area of the sediment bed in this reach is 353 acres.

The western shoreline is sheetpiled/bulkheaded between RM 2.3 and RM 2.02 and is vegetated down to the Lincoln Highway Bridge (RM 1.56; Figure 4.2.10-1). Between RM 1.56 and RM 1.25, it is mostly riprap/stone, except for a small stretch of sheetpile/bulkhead. The rest of the western shoreline is sheetpiled/bulkheaded down to the mouth. The eastern shoreline consists of riprap/stone to RM 1.95 and is sheetpiled/bulkheaded down to approximately the Abandoned Central Railroad Bridge (RM 0.89). The rest of the eastern shoreline is riprap/stone.

The navigation channel in this reach has been unmaintained above RM 1.85 since before 1950. Between RM 1.85 and RM 1.65, it was last maintained in 1957, and downstream of RM 1.65 was last maintained in 1983. The authorized channel depth in this reach is 30 feet, transitioning from the 20 feet in the previous reach at the upstream extent. The lack of maintenance around RM 2 has expanded the shoal on the inner bend (western bend) into the channel, and the formation of the point bar here has shifted the thalweg east (Figure 4.2.10-1). The more recent maintenance downstream has resulted in the river channel aligning closely with the navigation channel.

The evolution of the sediment bed is studied using bathymetry data (single-beam surveys [1989, 1995, 2004, and 2007] and multi-beam surveys and associated single-beam transect measurements [2007, 2008, 2010, 2011, and 2012]), model-predicted bottom shear stress patterns, and Cs-137 core profile data. Its characteristics are described using results of the 2005 SSS survey and its ground truthing data, probing surveys, and characteristics and contaminant concentrations of individual cores.

The large cross-sectional area in this reach has resulted in the lowest shear stresses in the LPR (Figure 4.2.10-2). Shear stresses are lowest downstream of RM 0.9, where the river expands dramatically to the mouth. Like other bends, shear stresses are higher along the outer bend between RM 2.3 and RM 1.75 than along the inner bend. Most of the sediment is mapped as Silt (Figure 4.2.10-3). Thin slivers of Rock and Coarse Gravel are found on the eastern shoreline, likely due to shoreline hardening and resultant wave action preventing sediment accumulation. Like other outer bends, the outer bend around RM 2 is somewhat coarser, being mapped as Silt and Sand. A band of Silt and Sand is also found to the west of the channel downstream of RM 0.9. Note that the

SSS survey does not extend across the river to the eastern shoal as it widens downstream of RM 0.9 near Kearny Point.

Historical bathymetry in this reach (Figure 4.2.10-4) indicates that the point bar on the inner bend around RM 2 was mostly formed by 1989, and the higher shear stresses on the outer bend there deepened the channel after 1989 (compare the 1989 and 1995 bathymetry panels). Farther downstream, the 1983 maintenance dredging has resulted in little sediment accumulation after 1989 down to RM 1.3 (presumably the channel filled in between 1983 and 1989). Most of the historical deposition after 1989 occurred downstream of RM 1.15.

Recent multi-beam bathymetry (Figure 4.2.10-5) indicates that most of the channel experienced alternating episodes of net erosion and net deposition between 2007 and 2010. Much of the net erosion occurred during the low-flow periods (2007 to 2008 and 2011 to 2012), and the net deposition occurred in the high-flow periods (2008 to 2010 and 2010 to 2011). The largest areas that experienced this behavior are on the side slopes of the channel between RM 2.3 and RM 1.75 (see location of side slopes on the 3D maps of Figure 4.2.10-6) and in the channel between RM 1.35 and RM 0, and a lot of the erosion exceeded 1.5 feet. A transect at RM 2.27 (Figure 4.2.10-7a) shows that the western side slope initially accumulated sediment here between 2004 and 2007. Other transects in this reach at RM 1.99, RM 1.8, and RM 1.63 show that at the locations of the transects the bed experienced little change between the survey years (Figure 4.2.10-7b through 4.2.10-7d). Some of the erosion during low-flow periods in the region downstream of RM 1.5 has been attributed to navigation scour associated with ship traffic (see the discussion in Appendix L on sediment transport model development).

Cs-137 cores in this reach reflect the deposition associated with Silt deposits and the more recent maintenance of the navigation channel. Between RM 2.3 and RM 2 (Figure 4.2.10-8), Cs-137 profiles show evidence of a well-defined peak at depth or increasing activity with depth, suggesting net deposition over the past decades. Similar trends are observed farther downstream to the Pulaski Skyway (RM 1.74). The core collected in the channel at RM 1.68 (211B) contains the maximum Cs-137 activity at the surface, perhaps due to deposition of sediments eroded from upstream after the local Cs-137 containing sediments had been removed by maintenance dredging. The core on the eastern shoal (210) contains low activities throughout, a likely result of the lack of deposition in the SSS-mapped Rock and Coarse Gravel deposit. The core on the eastern shoal (212) contains the highest activity at depth, consistent with a net depositional environment. None of the cores collected downstream of RM 1.25 in the channel contain a well-defined buried peak, an expected result of the 1983 maintenance here.

Contaminant Patterns

Surface contamination levels of 2,3,7,8-TCDD, total PCBs, total DDx, HMW PAHs, and LMW PAHs in this reach are generally lower than the RM 5 to RM 2.3 reach and tend to decline into Newark Bay, due to the sedimentation in the expanded cross section and dilution associated with the upstream tidal transport of water and solids from Newark Bay (Figure 4.1-9a through 4.1-9f). Mercury levels do not show such a decline, a likely result of the levels in Newark Bay being similar to or higher than those in the LPR. All the sampled locations in this reach are within the SSS-identified Silt regions (Figure 4.2.10-9; see Appendix K for similar figures of total DDx, mercury, HMW PAHs, and LMW PAHs). The overall concentrations measured in this reach are summarized in Table 4-11.

Between RM 2.3 and the Pulaski Skyway (RM 1.74), the highest concentration of 2,3,7,8-TCDD (Figure 4.2.10-10), total PCBs (Figure 4.2.10-11), total DDx (Figure 4.2.10-12), and mercury (Figure 4.2.10-13) are found in the subsurface sediments.[111] Surface concentrations are lower along the inner bend here, where the development of the point bar has resulted in surface concentrations more reflective of newly depositing solids.

The 1983 maintenance dredging below RM 1.65 and subsequent infilling has likely resulted in lower contaminant concentrations in the channel, with average surface 2,3,7,8-TCDD, total PCB, total DDx, and mercury concentrations of 275 ng/kg, 1.1 mg/kg, 0.14 mg/kg, and 1.9 mg/kg, respectively.[112] Concentrations are higher at depth, consistent with deposition over time and may in some cases reflect historical sediment accumulation below the maintained depths. The shoals upstream of RM 0.75 contain lower surface concentrations than subsurface levels, consistent with historical deposition here. The higher surface contaminant concentrations outside the channel are also seen downstream of RM 0.75, where the LPR expands significantly.

Of the 24 locations sampled within the spatial extent of the multi-beam bathymetry in this reach, 17 of these were sampled in 2008. Of these 17, excluding CLRC-021 (RM 1.93), CLRC-019 (RM 1.46), and CLRC-004 (RM 0), elevations in 2012 were greater than or equal to the 2008 elevation, indicating the subsurface contamination has been buried farther since sample collection (Figure 4.2.10-14). The remaining seven cores were collected in 2012, and experienced alternating episodes of erosion and deposition between 2007 and 2012 (e.g., cores 12A-0411, 12A-0408, 12A-0410, 12A-0406, 12A-0405, and 12A-0402).

[111] The highest 2,3,7,8-TCDD concentration was found in the 3.5- to 5.5-foot segment of CLRC-021 (RM 1.93; 237,762 ng/kg). The highest level of total PCBs was found in the 0.5- to 1.5-foot segment of 12A-0408 (RM 1.97; 13.4 mg/kg). The highest total DDx concentration was found in the 5.5- to 7.5-feet segment of CLRC-021 (4 mg/kg), and the highest mercury concentration was found in the 2.5- to 3.5-foot segment of 12A-0408 (16 mg/kg).

[112] The maximum concentrations are also lower than the channel in the upstream reaches—the highest 2,3,7,8-TCDD surface concentration in the channel here is 478 ng/kg (12A-0406; RM 1.67). The highest total PCB, total DDx, and mercury levels are 2.1 mg/kg (CLRC-019; RM 1.46), 0.5 mg/kg (CLRC-019; RM 1.46), and 4.93 mg/kg (12A-0402; RM 0.24), respectively.

Surface concentrations of total PCBs, total DDx, mercury, HMW PAHs, and LMW PAHs are correlated to those of 2,3,7,8-TCDD (Figure 4.2.10-15), though the correlation is weaker for the PAHs. The relatively recent maintenance dredging and subsequent infilling may have caused the better correlation in subsurface concentrations and MPA of mercury, HMW PAHs, and LMW PAHs with those of 2,3,7,8-TCDD than in the upstream reaches.

Concentrations of HMW PAHs (Figure 4.2.10-16) and LMW PAHs (Figure 4.2.10-17) decline into Newark Bay. The highest HMW PAH and LMW PAH concentrations in this reach were measured in the surface segment of 12A-0408 on the outer bend at RM 1.97.[113] Concentrations of both PAH groups in the bend are mostly higher in the surface sediments than in the subsurface sediments (see also Appendix K Figures 8-9 and 9-9).

Downstream of the Lincoln Highway Bridge, the surface segments of CLRC-019 and 12A-0405 contain 122 and 111 mg/kg HMW PAHs, respectively; all other concentrations measured (at all depths) in this reach are less than 80 mg/kg HMW PAHs. The same segments also contain 21 mg/kg and 46 mg/kg LMW PAHs, respectively. Levels greater than 20 mg/kg LMW PAHs were measured at multiple locations in the 5.5- to 7.5-foot segment (not shown on the maps),[114] suggesting a possible historical source of LMW PAHs that has since been buried under cleaner sediments.

To summarize, surface contamination levels in this reach decrease into Newark Bay to varying degrees, except for mercury, which reflects the relatively high levels in Newark Bay. The impact of historical deposition is evident, with lower concentrations of all contaminants except PAHs generally measured in the surface than at depth.

[113] 359 mg/kg HMW PAHs and 104 mg/kg LMW PAHs

[114] These locations and concentrations are as follows: G0000004 (RM 1.42; 39.5 mg/kg), CLRC-020 (RM 1.46; 34 mg/kg), CLRC-021 (RM 1.93; 30 mg/kg), CLRC-014 (RM 1.02; 26 mg/kg), G0000005 (RM 2.18; 24 mg/kg), and CLRC-017 (RM 1.06; 22 mg/kg).

5 Ecology and the Nature and Extent of Contaminants in Biota

Shoreline and aquatic habitats within the LPR are impaired as a result of shoreline development and physical changes within the river caused by urbanization (i.e., loss of wetlands, dredging, channelization, and dam construction), particularly in the portions of the LPR below RM 8 (Windward 2014c). Heavy urbanization has resulted in extensive habitat loss, namely wetlands, small tributaries, submerged aquatic vegetation (SAV), and emergent woodlands (Windward 2014c). The ecology has been further impaired by a variety of environmental factors influenced by urbanization, including turbidity, organic inputs, chemical contamination, DO, and invasive and/or non-native species. The construction of Dundee Dam at RM 17.4 in 1858 altered the downstream freshwater flow characteristics and blocked the upstream migration of various fish species to spawning habitat.

Urbanization has influenced the biological communities and their structures in the river. The benthic invertebrate community, which forms the basis of the ecological food web, was observed in 2005 to be disturbed in many locations (particularly below RM 8) by significant physical erosion and deposition or organic enrichment (Germano & Associates 2005). Benthic omnivore fish—the numerically dominant group among LPR fish—consume instream detritus, invertebrates, surface sediment, and settling solids coming from impervious surfaces, CSOs, and urban runoff from the surrounding watershed.[115] These food web interactions between organisms and interactions between organisms and sediment affect the bioaccumulation of contaminants from sediment into biota tissue.

The ecological habitat and the biological communities of the LPR are discussed in more detail in Sections 5.1 and 5.2, respectively. A general overview of bioaccumulation in the LPR food web is discussed in Section 5.3. Tissue chemistry results for six contaminants—2,3,7,8-TCDD, total PCBs, HMW PAHs (based on Human Health Risk Assessment [HHRA] risk only), LMW PAHs (based on HHRA risk only), total DDx, and mercury—are presented in Section 5.4. Overall key findings are summarized in Section 5.5.

5.1 Ecological Habitat

The distributions of shoreline habitat and vegetation types from various surveys since 1999 (Iannuzzi and Ludwig 2004; USACE et al. 2008; Windward 2014c) are provided in Figures 5-1 and 5-2. Shoreline habitat is limited in the LPRSA due to the physical development associated with urbanization along the banks of the river, particularly in the lower portion of the LPRSA (below RM 8) (Table 5-1). While some plant communities may exist adjacent to the bulkhead or riprap in the lower portion of the LPRSA, these are mostly narrow strips of vegetation of minimal ecological significance. The prevalence of degraded complex and functional ecological habitats and hardened shorelines may

[115] Constituents of urban runoff (both organic and inorganic particles and chemicals) from impervious surfaces form flocculants, which then settle out in urban water bodies (Droppo et al. 2002).

adversely affect the abundance, diversity, and reproductive success of biological populations in the system.

General shoreline habitat within the LPR is categorized based on geomorphological features (i.e., mudflats), the type of riparian vegetation (aquatic or mixed vegetation), and man-made structures (i.e., riprap and bulkhead) along the banks of the LPR (Table 5-1). Currently, 70% of the riverbank downstream of RM 7 consists of bulkhead and/or riprap, which supports a limited amount of vegetation (Windward 2014c). Farther upstream, the riverbank is dominated by mixed vegetation, generally over steep banks (Table 5-1). Natural habitat areas along the shoreline, including wetlands, are limited to small patches or isolated areas due to development. Available mudflats provide key foraging habitat for shorebirds, and the nearshore shallow areas provide key foraging areas for small forage fish and other prey species. Table 5-1 provides a summary of each mudflat in the LPRSA, and Table 5-2 provides a summary of mudflat area per reach (additional details can be found in the BERA [Appendix D]).

Riparian vegetation along the LPR is greatly limited due to extensive urbanization in the watershed. Development of the uplands below RM 8 is extensive, and very little riparian habitat exists (Windward 2014c). In the lower portions of the LPR, where most of the shoreline has been industrially developed, the plant community is less diverse and characterized primarily with scrub-shrub vegetation such as groundsel tree frequently intermixed with individual or small stands of trees (Windward 2014c). Where vegetation does exist along the shoreline below RM 8, the vegetation is in very narrow patches adjacent to bulkhead structures (Table 5-1). Farther upriver, where the shoreline is flanked by wider urban green spaces and parks, mixed forest becomes more prevalent and diverse (Table 5-1). Riparian vegetation in the LPR includes both native and non-native plant species; only 20% to 57% of herbaceous plant species and 60% to 80% of shrubs observed along the LPRSA during the 2007 and 2008 vegetation surveys were native species (USACE et al. 2008; Windward 2014c). Invasive species in the LPRSA such as purple loosestrife (*Lythrum salicaria*) and Japanese knotweed (*Fallopia japonica*) can displace native plants.

The LPR has limited aquatic vegetation. During the 2010 habitat survey of the LPRSA (Windward 2014c), approximately 1% of the shoreline was classified as containing aquatic vegetation, most of which was emergent rather than SAV. Such vegetation was limited to protected fringes of intertidal mudflats. Mudflats were found along 35% of the total LPRSA shoreline and were more prevalent below RM 8 (Figure 5-1); 90% of the left[116] bank mudflats (looking upstream) were below RM 8, and 62% of the right bank mudflats (looking upstream) were below RM 8, although the areal extent of mudflats was predominately on the right bank (91% of the total area) due to the inclusion of the expansive Kearney Point mudflats (Table 5-1).

[116] Left and right bank mudflats are based on the orientation of looking upstream on the LPR.

5.2 Biological Communities

Most of the biological communities observed in the LPR, which include benthic infaunal invertebrates, mollusks, and other macroinvertebrates; fish; birds; mammals; amphibians; and reptiles, are typical of estuarine environments of the Northeastern United States. While some species within the LPR are pollution-tolerant, the biological communities include species that are found in both degraded and relatively unimpacted habitats.[117] The LPR and its ecological community are influenced by alterations to the salinity regime and chemical contamination, as well as a variety of other environmental factors influenced by urbanization including turbidity, organic inputs, DO, and invasive and/or non-native species. This section provides an overview of the findings of several surveys of the biological communities in the LPR; additional details can be found in the data reports (Appendix B) and the BERA (Appendix D).

5.2.1 Benthic Infaunal Invertebrate Community

Benthic invertebrates are an integral member of a fully functioning aquatic system and have a marked impact on ecosystems because they sort, rework, and oxygenate sediment (Bolam et al. 2002) and alter biogeochemical fluxes (e.g., nutrient cycling through processing of detritus) (Covich et al. 1999). Furthermore, benthic invertebrates provide a source of sustenance to many fish and wildlife species, particularly large-bodied individuals such as decapods (e.g., crabs) or mollusks (e.g., bivalves).

Because salinity exerts the primary influence on benthic community structure, the LPR benthic invertebrate community can be described in terms of the following three salinity zones[118]:

- Tidal freshwater zone: RM 17.4 to RM 13
- Fluvial estuarine salinity zone: RM 13 to RM 4
- Upper estuarine salinity zone: RM 4 to RM 0

A primary influence on the benthic community composition is salinity; benthic community data are general consistent with salinity zones described above (Figures 5-3 and 5-4). Other habitat characteristics (such as grain size) and urban stressors (such as high organic inputs) can affect the type of benthic community that is possible in the LPR. In addition, sediment chemical concentrations have the potential to impact the benthic community.

Numerically, the majority of individuals in the LPR are annelid worms, with oligochaetes dominating the tidal freshwater and fluvial estuarine benthic salinity zones, and polychaetes dominating the

[117] "Tolerant" species are those that can survive in systems exposed to environmental stress. These species are often adaptable to changing conditions, allowing them to thrive in less stressed systems as well.

[118] Benthic salinity zones are based on the movement of the salt wedge and the evaluation of interstitial and overlying salinity data collected during the fall 2009 benthic invertebrate community survey (see Appendix D for details). These designations are based on the benthic ecology's response primarily to salinity changes in the LPR. See Section 9 for more information on the salinity zone designations.

upper estuarine benthic salinity zone (Figure 5-3). Other major taxa include bivalves, chironomids, crustaceans, gastropods, and turbellarians.

The LPR benthic community is exposed to resuspended sediments in near-bottom particulate (i.e., the sediment fluff layer as described in Section 3.4) and shallow bedded sediment (0 to 15 cm), both of which contain nutrients and food sources. Germano & Associates (2005) described LPR sediments as highly dynamic in terms of erosion and deposition and resulting in different stages of invertebrate community succession throughout the river. For example, during the sediment profile imaging (SPI) survey, species associated with early successional stages (e.g., small polychaete worms) were more frequently observed in the LPR at many locations, particularly in the "brackish" portion of the LPR.

Organic contaminant loading may also drive the observed community succession throughout the LPR. As stated in Germano & Associates (2005), "given the obvious elevated levels of organic enrichment and high resultant SOD [sediment oxygen demand] at many of the brackish water stations, it is considered likely that these taxa [early successional polychaete worms] are among the long-term numerical dominants in this part of the river." Evidence of larger, deeper-dwelling species (e.g., oligochaete worms and bivalves) associated with late successional stages was more frequently observed in the freshwater portion of the LPR. The late-successional, dominant invertebrates that Germano & Associates (2005) observed farther upstream in the LPR are "relatively tolerant to elevated levels of organic loading." Though this may suggest that benthic habitat in the tidal freshwater portion of the LPR is also impacted, Germano & Associates (2005) also noted that LPR tidal freshwater conditions are "more varied and capable of supporting a more advanced benthic community" relative to downstream habitat conditions. Physical drivers of benthic community succession (i.e., scour during high flows and burial thereafter) are likely to reduce bioturbation, which also hinders the establishment of a deep-dwelling community (Rhoads et al. 1978; Rhoads and Germano 1986), particularly in channelized, urban waterbodies, which experience more frequent and more intense pulses of freshwater discharge (Lake 2000; Walsh et al. 2005).

The depth of sediment oxygenation in the LPR (e.g., shown in Figures 5-6 and 5-7) is influenced by high levels of organic inputs, and that may in turn affect invertebrate community succession, structure, and composition. In addition to legacy organic chemical contamination in bedded sediments, the LPR experiences a high degree of organic and inorganic sediment enrichment from CSOs/SWOs, permitted industrial discharges, and non-point source urban runoff. Flow over Dundee Dam is the largest external source of OC to the LPR (LBG 2014), though the flow of OC over Dundee Dam may decrease over time as a result of potential infrastructure improvements (unrelated to site remediation). The presence of highly enriched organic sediment in the LPRSA was confirmed by the 2005 SPI data (Germano & Associates 2005) and by sediment samples collected between 2009 and 2012 (Windward 2018, 2014a, 2014b). The high level of several organic inputs into the LPR are part of

the ongoing urban condition. Organic inputs like CSO discharges could potentially be reduced as system improvements are implemented; however, these potential future changes are uncertain, and their relative impact on organic inputs cannot be quantitatively determined.

In addition to potentially reducing survival, growth, or reproduction, chemical contamination in sediments may alter the depth of invertebrate burrowing and bioturbation of sediments (and the depth of oxygenation) by causing sediment avoidance behaviors. Sediment avoidance by infauna has been observed in laboratory experiments (e.g., Oakden et al. 1984; Keilty et al. 1988), and it is possible that such behaviors also occur in the field.

The TOC content in sediment directly influences the benthic community structure and function and can affect burrowing depth (Pearson and Rosenberg 1978; Borja et al. 2008). Although organic matter is an important food source for benthic organisms and can have other positive ecological impacts such as providing a source of cover, excess organic matter can cause changes in the benthic community structure (affecting species richness and abundance) (Diaz and Rosenberg 1995) through the depletion of oxygen and the buildup of toxic biological waste products, such as ammonia. Approximately 60% of LPR surface sediment samples collected in 2009 and 2010 exceeded 3.5% TOC (ddms 2013; Windward 2015), a level of enrichment generally associated with reduced benthic invertebrate richness in marine and estuarine habitats (Hyland et al. 2005) (Section 4.1).

Reduced DO and increased fluxes of biological wastes (e.g., ammonia and nitrate/nitrite) are also correlated with community impairment and dominance by tolerant taxa under higher TOC conditions across fresh and saline habitats (Pearson and Rosenberg 1978; Hilsenhoff 1987, 1998; Pelletier et al. 2011; Nilsson and Rosenberg 2000). Specifically, higher organic loading in sediments increases the sediment oxygen demand (SOD), resulting in decreased DO in overlying water and porewater and a reduced depth of oxygenated sediment (Valente et al. 1992; Germano & Associates 2005). The SPI data collected by Germano & Associates (2005) also indicated that sediments tend to be organically enriched, as evidenced by methane generation at many locations (44% site-wide) throughout the LPR (in addition to a generally shallow RPD depth).

5.2.2 Macroinvertebrates and Mollusks

Several decapod species and a limited number of bivalves and gastropods observed in the LPR (Windward 2010a, 2011b) are evaluated in the BERA (Appendix D). All decapods identified were classified as epibenthic omnivores; a very small number of other invertebrates encountered were either bivalves (n=2 organisms) or gastropods (n=1). Of all epibenthic invertebrates caught during the recent fish surveys, 93% were decapods from the omnivore guild. The most common decapod was blue crab (60% of total decapods), a target ecological receptor found in all reaches of the LPR. Blue crab were found in higher numbers in the lower portions of the LPR than in the upper portions

of the LPR. Crayfish were also target organisms in the freshwater reaches but were not found to be abundant.

5.2.3 Fish

Forty-five estuarine or freshwater fish species were identified throughout the LPR during fish surveys conducted in 2009 and 2010 (Windward 2010a, 2011b). Earlier fish community surveys conducted in 1999 and 2000 that were limited to approximately the lower 7 miles of the LPR encountered many of the same species (Iannuzzi and Ludwig 2004). Recent fish surveys taken over a 1-year period (Windward 2010a, 2010d, 2011b) indicate most estuarine fish (e.g., white perch and American eel) are tolerant of brackish salinities as well as freshwater and move throughout the river as far upstream as Dundee Dam. Freshwater fish in the LPR (e.g., channel catfish, largemouth bass, and smallmouth bass) are excluded from certain portions of the LPR because of the salinity gradient; these species generally follow the salt wedge, so their location in the LPR changes accordingly.

The fish identified in the 2009 and 2010 surveys were classified into the following five general feeding guilds based on a review of their feeding habits (FishBase 2013):

- Benthic omnivore (e.g., mummichog and common carp): feed near the river bottom and consume primarily benthic invertebrates and detrital material
- Invertivore/omnivore (e.g., brown bullhead and channel catfish): consume a varied diet of invertebrates (aquatic and terrestrial), plant material, small crustaceans, small fish, and other small organisms
- Planktivore (e.g., Atlantic menhaden): filter feeding fish that consume primarily plankton and other suspended materials, as well as benthos and benthic detritus
- Invertivore/piscivore (e.g., American eel and white perch): consume a diet composed primarily of small fish and various aquatic/terrestrial invertebrates
- Piscivore (e.g., largemouth bass and smallmouth bass): consume primarily small fish

Of the total fish caught during the recent surveys,[119] the majority of fish (88%) were classified as benthic omnivores or invertivores/omnivores. The remaining fish caught were classified as planktivores (8%), invertivores/piscivores (3%), or piscivores (1%) (Figure 5-8). These data indicate that the LPR fish community is primarily a benthic-dominated food chain.

The presence of invasive/non-native species affects the biological community, as adaptable invasive species successfully compete for necessary resources with native species, resulting in localized paucity or extinction of sensitive species (Carey and Wahl 2010; Colnar and Landis 2007; Buhle and Ruesink 2009). The lack of natural predators and diseases that kept invasive species in check in their

[119] Total fish collected is based on fish caught during the three fish community seasonal surveys conducted in August to September 2009 (late spring/early summer), January to February 2010 (winter), and June to July 2010 (late spring/early summer), as well as the fish collected as part of the small forage fish sampling efforts from June to August 2010.

original habitat allows invasive species to grow and persist at very high rates and densities in their new environment (Van Clef 2009). The common carp is a prevalent invasive/non-native species in the LPR and is adapted to the conditions observed in the LPRSA. Common carp were found to accumulate substantial biomass (average weights of carp collected were 2.7 kg [approximately 6 pounds]) and were found in large numbers from approximately RM 5.5 to RM 17.4 (Windward 2010a, 2011b).

5.2.4 Birds

The LPR provides a limited and fragmented habitat for avian species. There are limited mudflats for sediment-probing birds and some riparian habitat for species inhabiting the shoreline. Significant marsh habitat is largely absent from the LPR shoreline; marsh habitat is present at Kearny Point near the mouth of the LPR. As discussed in the BERA (Appendix D), 49 aquatic or semi-aquatic bird species were observed during the four seasonal surveys conducted in the LPR in 2010 and 2011 (Windward 2011b, 2019b). Several bird species are observed in the LPR year-round and may breed in nearby areas with suitable breeding and nesting habitat (e.g., Kearney Marsh) (Walsh et al. 1999; Butler 1992; Antonucci et al. 2008; Boyle 2011; USFWS 1997; Kerlinger 1997). Gulls, geese, and ducks were the most commonly observed during the 2010 and 2011 surveys, with numbers and relative abundances of species varying by season (Figure 5-9). Shorebirds, wading birds (including herons/egrets), and other bird species (including piscivorous birds such as osprey, belted kingfisher, and double-crested cormorants) are also present. The frequency of observance of these birds is not necessarily an indication of chemical exposure; due to different foraging and feeding behaviors, some infrequently observed bird species may be exposed to more contamination than commonly observed species may be.

5.2.5 Mammals

No surveys specifically targeting water-associated mammals have been conducted to date in the LPR, but few mammalian species were observed during other surveys or sampling events conducted in or near the LPR across multiple seasons and years. Examples of surveys wherein mammals were observed (and noted) include the 2010 habitat and avian surveys. Combined, these efforts included approximately 4,500 hours of habitat, avian, and aquatic species surveys (including observations during sunrise and sunset), during which there was little evidence of mammals. Examples of domestic (e.g., dogs) and urban-dwelling (e.g., rats and feral cats) mammals sighted in water or on the banks of the LPR during previous surveys are summarized in the BERA (Appendix D); species potentially present in the LPRSA but that have not been observed are also summarized in Appendix D. Without having conducted a survey targeting water-associated mammals (i.e., using appropriate trapping or tracking methods), there is uncertainty associated with the conclusion that mammal presence is limited.

Potential foraging areas for mammals include mudflats and patches of shoreline vegetation identified in habitat surveys (Iannuzzi and Ludwig 2004; Windward 2014c), and in patches of forested banks above RM 9.5. No current reports, either anecdotal or from surveys, were found of river otter (*Lutra canadensis*) in the LPRSA. The only recent report of river otter in the LPRSA was an individual observed during the late 1990s in the Hackensack Meadowlands that was believed to have escaped from captivity in a local zoo (Kiviat and MacDonald 2002). Mink tracks were photographed near Dundee Dam in August 2010 during a survey of the avian community in the LPR (Windward 2011a), but a geographic information system (GIS) analysis conducted for the BERA (Appendix D) indicated insufficient riparian tree and shrub cover in the LPRSA to provide the habitat necessary for a breeding population of mink.

5.2.6 Amphibians and Reptiles

Surveys were not conducted specifically for amphibians and reptiles in the LPR. No amphibian species and few reptile species have been directly observed during previous sampling events in the LPR. Conditions in the LPRSA may provide limited suitable habitat for some amphibian and reptile species, specifically in the small patches of marsh in the estuarine portion of the river and the wooded shorelines and riverfront parks in the freshwater section above RM 9.5. A list of the species that could potentially be present in the LPR is presented in the BERA (Appendix D).

5.2.7 Threatened, Endangered, and Special Status Species

Nine aquatic bird species and the wood turtle (*Glyptemys insculpta*) listed by the State of NJ as present or potentially present in the LPR are either endangered, threatened, or of special concern (Appendix D). One fish species (American eel) is under evaluation by the U.S. Fish and Wildlife Service for listing as threatened.

5.3 Bioaccumulation in the Ecological Food Web

The ecological food web in the LPR reflects an urbanized system. Urbanization results in increased inputs of TOC, particulates, nutrients, and contaminants (Droppo et al. 2002; Walsh et al. 2005), which can result in diminished habitat quality, complexity, or availability (Eitzmann and Paukert 2010; Layman et al. 2007) and potential toxicity to ecological receptors from chemical contamination. As discussed in Section 5.2, the LPR benthic community is dominated numerically by deposit feeders and detritivores (e.g., annelids, chironomids, and bivalves). These species, which consume a mixture of particulates (or fluff), detritus, and sediment, form the base of the food chain for higher trophic levels (e.g., fish).

A simplified LPR ecological food web is shown in Figure 5-10. The fish community is primarily a benthic-dominated food chain. The fish species that are the most common in the LPRSA appear to be those that feed on benthic invertebrates (rather than on smaller fish) or those that feed

opportunistically depending on what prey is abundant. Benthic omnivores (which constitute 88% of the LPR fish population, including catfish, carp, suckers, small forage fish, and small American eel[120]) feed near the river bottom and consume primarily benthic invertebrates and detrital material. Sediment is consumed incidentally to a small degree while foraging for invertebrates or grazing on detritus. Invertivores (such as small white perch, which constitute a much smaller fraction of the LPR fish population) have a varied diet consisting of invertebrates, plant material, small crustaceans, and other small benthic organisms. Thus, it is expected that the bioaccumulation of contaminants in LPR fish tissues generally reflects the contaminant concentrations in benthic invertebrate tissues, which in turn reflect the concentrations of contaminants in detritus and surface sediment (0 to 15 cm). Contaminant concentrations in biota are discussed in Section 5.4.

5.4 Lower Passaic River Biota Tissue Chemical Concentrations

This section presents the tissue chemistry results for six contaminants in LPR biota. These six contaminants were selected as key chemicals driving human health and/or ecological risks: 2,3,7,8-TCDD, total PCBs (sum of congeners), HMW PAHs (key chemical based on human health risk only), LMW PAHs (key chemical based on human health risk only), total DDx, and mercury. Biota tissue summarized in this section are as follows:

- LPRSA fish (i.e., American eel, brown bullhead, common carp, channel catfish, largemouth bass, northern pike, smallmouth bass, white catfish, white perch, and white sucker) and decapod (i.e., blue crab) tissue collected from August to September 2009
- LPRSA small forage fish (i.e., mummichog, gizzard shad, pumpkinseed, silver shiner, spottail shiner, mixed forage fish, and white perch) tissue collected from June to August 2010
- Bioaccumulation worm tissue[121] based on 28-day laboratory exposure to LPSRA surface sediment collected in fall 2009
- Caged bivalve tissue[122] exposed to LRPSA water in situ for 90 days from March to June 2011
- UPR fish (i.e., American eel, brown bullhead, common carp, channel catfish, northern pike, smallmouth bass, white perch, white sucker, and small forage fish [banded killifish, pumpkinseed, and silver shiner]) tissue collected in October 2012.

A summary of results for these key contaminants and other contaminants in the LPRSA and UPR as identified in the baseline risk assessments is presented in Appendix F data tables and figures.[123] Figure 5-11 presents the elements of the box and whisker plots for the biota tissue figures presented

[120] Small (juvenile) American eel feed primarily on lower-trophic-level prey (e.g., annelids, polychaetes, insect larvae and nymphs, crustaceans, bivalves, and gastropods), while larger (adult) American eel are more piscivorous.

[121] Bioaccumulation tests were collected on estuarine worms exposed to sediment collected from RM 0 to RM 5.5 and freshwater worms exposed to sediment collected from RM 6.5 and to RM 15.

[122] Ribbed mussel tissue was analyzed from estuarine LPR sampling areas between RM 1 and RM 3, and eastern elliptio mussel tissue was analyzed from freshwater sampling areas between RM 10.5 and RM 14.5.

[123] Regional tissue data were evaluated and presented in the risk assessments (see the BHHRA and BERA in Appendix D).

in Figures 5-12 through 5-17. Data reduction rules, including the method used to convert fillet and carcass to whole-body concentrations, are presented in the BERA (Appendix D).

5.4.1 2,3,7,8-TCDD

2,3,7,8-TCDD was detected in 99% of the fish, blue crab, bioaccumulation worm, and caged bivalve tissue samples. The following general trends are presented in Figures 5-12a (whole body) and 5-12b (fish fillet) and Table 1 of Appendix F:

- Detected fish tissue concentrations ranged from 0.32 to 1,400 ng/kg wet weight (ww) for whole-body and from 0.31 to 730 ng/kg ww for fillet samples; concentrations were higher in fish whole-body samples than in fish fillet samples of the same species. The highest whole-body concentrations were measured in carp (mean of 410 ng/kg ww), white catfish (mean of 170 ng/kg ww), and white perch (mean of 120 ng/kg ww).
- Whole-body tissue concentrations of 2,3,7,8-TCDD in blue crab were generally within the range of whole-body concentrations in small forage fish (e.g., mummichog) and higher trophic level fish (including smallmouth bass and American eel) (Figure 5-12a). Blue crab tissue concentrations ranged from 0.82 to 210 ng/kg ww, with the lowest concentrations measured in muscle tissue and highest concentrations measured in hepatopancreas tissue (Figure 5-12c).
- Concentrations in bioaccumulation estuarine worm tissue (1.8 to 19 ng/kg ww; based on 28-day laboratory exposure to sediment collected between RM 0 and RM 5.5) were much lower than those measured in fish and blue crab (Figure 5-12d). Concentrations in bioaccumulation freshwater worm tissue (0.50 to 140 ng/kg ww) were lower than most whole-body fish samples but higher than those measured in estuarine worm tissue samples.
- Concentrations in both the caged estuarine mussels (ribbed mussel) and freshwater mussels (eastern elliptio mussel) were much lower than those measured in fish, blue crab, and bioaccumulation worm tissue (Figure 5-12e). Mussel tissue concentrations ranged from 0.077 to 3.6 ng/kg ww.

Concentrations of 2,3,7,8-TCDD in the LPR were higher than those measured in fish from the UPR (see Appendix F). The spatial variation of 2,3,7,8-TCDD in biota tissue is presented in Figures 1 through 5 of Appendix F.

For some LPR fish species, 2,3,7,8-TCDD concentrations in whole-body tissue samples were generally consistent across LPR Reaches 1 through 8 (e.g., see catfish in Figure 1 of Appendix F).[124] However, whole-body tissue samples from other species, such as American eel, white perch, mummichog,

[124] Eight reaches of the LPRSA were defined as 2-river mile segments starting at the mouth of the LPRSA and ending at Dundee Dam; reaches were defined as follows: Reach 1 – RM 0 (mouth of LPRSA) to RM 2; Reach 2 – RM 2 to RM 4; Reach 3 – RM 4 to RM 6; Reach 4 – RM 6 to RM 8; Reach 5 – RM 8 to RM 10; Reach 6 – RM 10 to RM 12; Reach 7 – RM 12 to RM 14; and Reach 8 – RM 14 to RM 17.4 (Dundee Dam).

small forage fish, and carp, exhibited generally higher 2,3,7,8-TCDD concentrations in the middle reaches of the LPR (approximately Reaches 3 through 7) than in the upper and/or lowest reaches.[125]

5.4.2 Total Polychlorinated Biphenyls

Total PCBs were detected in all biota tissue samples. The following general trends are presented in Figure 5-13 and Table 2 of Appendix F:

- Detected fish tissue concentrations ranged from 170 to 7,900 microgram per kilogram (µg/kg) ww for whole-body and from 48 to 15,000 µg/kg ww for fillet samples. Total PCB concentrations were higher in fish whole-body samples than in fish fillet samples of the same species—with the exception of carp, which had similar concentrations in fillet and whole-body samples. Similar to 2,3,7,8-TCDD, the highest total PCB concentrations in fish were measured in carp (mean whole-body carp tissue concentration was 4,100 µg/kg ww). Whole-body tissue concentrations of total PCB in small forage fish were generally lower than concentrations measured in other fish, including large benthic fish and higher trophic level fish (Figure 5-13a). In fish fillet tissues, total PCB concentrations in benthic fish, American eel, and white perch were generally higher than those in higher trophic level freshwater fish (i.e., largemouth bass, smallmouth bass, and northern pike) (Figure 5-13b).
- Whole-body tissue concentrations of total PCBs in blue crab were generally within the range of whole-body concentrations in small forage fish (e.g., mummichog, shiners, and mixed forage fish) (Figure 5-13a). Blue crab tissue concentrations ranged from 11 to 1,400 µg/kg ww, with the lowest concentrations measured in muscle tissue and highest concentrations measured in hepatopancreas tissue (Figure 5-13c).
- Concentrations in bioaccumulation estuarine worm tissue (26 to 130 µg/kg ww) were much lower than those measured in fish and blue crab (Figure 5-13d). Accumulations in bioaccumulation freshwater worm tissue (55 to 530 µg/kg ww) were similar to small forage fish but were higher than estuarine worm tissue samples.
- Concentrations in both the caged estuarine and freshwater mussels were much lower than those measured in fish, blue crabs, and bioaccumulation worm tissue (Figure 5-13e). Mussel tissue concentrations ranged from 2.6 to 30 µg/kg ww.

Concentrations of total PCBs in tissue were similar for the UPR and LPR for some fish species (i.e., channel catfish, smallmouth bass, and northern pike); for other fish species (i.e., American eel, common carp, brown bullhead, white sucker, and white perch), total PCB concentrations in the LPR were higher than those measured in the UPR (see Appendix F). In general, those fish species most closely linked to bottom sediments (e.g., benthic omnivores) have higher exposures in the LPR, while mostly non-benthic taxa have similar exposures in the UPR and the LPR.

[125] Common carp was not found in Reaches 1 or 2, and white catfish was not found in Reach 1.

The spatial variation of total PCBs in biota tissue is presented in Figures 6 through 10 of Appendix F. Total PCB tissue concentrations in smallmouth bass whole-body samples were consistent across those reaches where samples were collected (i.e., Reaches 4, 5, and 8). However, whole-body samples collected from other species exhibited generally higher individual total PCB concentrations in the middle reaches of the LPR than in the upper and/or lowest reaches. For example, total PCB concentrations in American eel whole-body tissue samples ranged higher in samples collected from Reaches 3 and 4 than in other reaches; mummichog/banded killifish whole-body tissue samples collected from Reaches 3 through 5 had higher total PCB concentrations than did samples from other reaches; white catfish whole-body tissue samples collected from Reaches 3 and 5 had higher individual total PCB concentrations than did samples collected from other reaches; total PCB concentrations in white perch and white sucker whole-body tissue samples ranged higher in samples collected from Reaches 4 and 5 than in other reaches; and common carp individual whole-body tissue total PCB concentrations were higher in Reaches 3 through 7.

5.4.3 High-Molecular-Weight and Low-Molecular-Weight Polycyclic Aromatic Hydrocarbons

The detection frequency of HMW PAHs and LMW PAHs was greater than 85% in most biota samples, with the following exceptions: HMW PAHs were not detected in one smallmouth bass fillet and LMW PAHs were not detected in two largemouth bass and two smallmouth bass fillets (detection frequency of HMW PAHs was 67%). The following general trends are presented in Figures 5-14 and 5-15 and Tables 3 and 4 of Appendix F:

- Detected fish tissue concentrations of HMW PAHs ranged from 3.1 to 1,000 µg/kg ww for whole-body and from 1.3 to 100 µg/kg ww for fillet samples. LMW PAHs ranged from 15 to 470 µg/kg ww for whole-body and from 2.4 to 370 µg/kg ww for fillet samples. HMW PAH concentrations were higher in fish whole-body samples than in fish fillet samples of the same species. HMW PAH median concentrations in whole-body tissues in small forage fish (i.e., mummichog, shiners, and mixed forage fish) were higher than in large benthic fish (i.e., common carp, white sucker, white catfish, and channel catfish) and most higher trophic level fish (i.e., American eel, northern pike, and largemouth bass) (Figure 5-14a). Fillet fish tissue concentrations of HMW PAHs decreased generally with increasing trophic level (Figure 5-14b). Clear patterns of LMW PAHs in fish tissues were not as apparent as for HMW PAHs; variable ranges of LMW PAHs were measured in small forage fish, large benthic fish, and higher trophic-level fish (Figures 5-15a and 5-15b).
- Whole-body tissue concentrations of HMW PAHs in blue crab were less than small forage fish concentrations but similar to other fish tissues, whereas LMW PAHs in blue crab were less than most fish tissue concentrations (Figures 5-14a and 5-15a). Blue crab tissue HMW PAH and LMW PAH concentrations ranged from 0.91 to 690 and 1.8 to 620 µg/kg ww, respectively,

with the lowest concentrations measured in muscle tissue and highest concentrations measured in hepatopancreas tissue (Figures 5-14c and 5-15c).

- HMW PAH concentrations in estuarine worms (ranging from 58 to 140 µg/kg ww) were similar to those observed in most fish, whereas HMW PAH concentrations in freshwater worms were the highest HMW PAHs measured in any biota (ranging from 1,100 to 4,900 µg/kg ww) (Figure 5-14d). LMW PAH concentrations in estuarine worms (ranging from 5.3 to 12 µg/kg ww) were lower than those observed in fish, whereas LMW PAH concentrations in freshwater worms were more variable (Figure 5-15d). LMW PAH concentrations in four of the five freshwater worm samples (ranging from 71 to 220 µg/kg ww) were similar to those measured in fish, but the highest freshwater estuarine worm LMW PAH concentration was the highest biota concentration measured for LMW PAHs (940 µg/kg ww).
- HMW PAH concentrations in both the caged estuarine and freshwater mussels (ranging from 28 to 230 µg/kg ww) and LMW PAH concentrations in the estuarine mussels (44 to 140 µg/kg ww) were within the range of concentrations observed in fish (Figures 5-14e and 5-15e). LMW PAH concentrations in freshwater mussels were lower than those observed in fish (ranging from 12 to 17 µg/kg ww).

PAHs are metabolized in fish (they do not bioaccumulate like organic chemicals or mercury), which complicates the evaluation of PAH levels in fish tissue. For most species, UPR and LPR tissue PAH concentrations overlapped substantially. However, HMW PAHs appeared to be higher in American eel and white perch samples from the LPR than in samples collected from the UPR. For LMW PAHs, concentrations in American eel, white perch, and brown bullhead tended to be higher in LPR samples than in UPR samples. As discussed in Section 4.4, PAH concentrations in the sediment were elevated in the UPR compared to the LPR, indicating potential PAH sources from above Dundee Dam, lateral sources that feed into the LPR, and potential sources within the LPR.

The spatial variation of HMW PAHs and LMW PAHs in biota tissue is presented in Appendix F, Figures 11 through 15 and Figures 16 through 20, respectively. As shown in those figures, spatial trends in fish tissue sample concentrations of HMW PAHs were inconsistent across Reaches 1 through 8 of the LPR, in that concentrations varied by reach without a clear pattern. Blue crab tissue concentrations were a clear exception, as HPAH concentrations were higher in Reaches 1 to 4 than in Reaches 5 to 8. Bioaccumulation in worms and mussels showed an opposite trend (higher concentrations in upper reaches), although the change in trend may be due to species differences. For LMW PAHs, tissue concentrations were again variable across reaches for most species. LMW PAH concentrations in blue crab tissues showed a spatial trend similar to that of HMP PAH concentrations in blue crab tissues. Observable trends in crab tissue PAH concentrations may be related to the relatively low PAH metabolism of invertebrates relative to that of fish, for which tissue PAH concentration trends were not observable.

5.4.4 Total DDx

Total DDx was detected in all fish tissue samples, in all blue crab samples except for one muscle tissue sample, in all freshwater worm samples, in two of the five estuarine worm samples, and in seven of the eight caged bivalve samples. General trends are presented in Figure 5-16 and Table 5 of Appendix F:

- Detected fish tissue concentrations ranged from 20 to 1,100 µg/kg ww for whole-body and from 2.7 to 1,600 µg/kg ww for fillet samples. Total DDx concentrations were higher in fish whole-body samples than in fish fillet samples of the same species with the exception of carp, which had similar concentrations in fillet and whole-body samples. Similar to 2,3,7,8-TCDD and total PCBs, the highest total DDx concentrations were measured in carp samples (the mean whole-body carp tissue concentration was 510 µg/kg ww and ranged from 110 to 1,100 µg/kg ww). Whole-body tissue concentrations of total DDx in small forage fish were generally lower than concentrations measured in other fish, including large benthic fish and higher trophic level fish (Figure 5-16a). In fish fillet tissues, total DDx concentrations in benthic fish, American eel, and white perch were higher than those in largemouth bass and smallmouth bass (Figure 5-16b).
- Whole-body tissue concentrations of total DDx of blue crab were generally within the range of whole-body concentrations in small forage fish (e.g., mummichog, shiners, and mixed forage fish; Figure 5-16a). Blue crab tissue concentrations ranged from 5.7 to 510 µg/kg ww, with the lowest concentrations measured in muscle tissue and highest concentrations measured in hepatopancreas tissue (Figure 5-16c).
- Concentrations in bioaccumulation estuarine and freshwater worm tissue were both lower than those in fish and blue crab tissues, although total DDx concentrations in freshwater worm samples (3.6 to 33 µg/kg ww) were higher than in estuarine worm (1.8 to 3.6 µg/kg ww) samples (Figure 5-16d).
- Concentrations in both caged estuarine and freshwater mussels were much lower than those measured in fish and blue crab tissue (Figure 5-16e). Mussel tissue concentrations ranged from 2.3 to 6.9 µg/kg ww.

With the exception of carp and white perch, for all fish species for which data were available from both the LPR and the UPR above Dundee Dam, LPR tissue concentrations of total DDx were similar to those measured in fish tissue from the UPR (see Appendix F). Total DDx concentrations in one channel catfish sample from Reach 8 and two brown bullhead samples (one each from Reaches 3 and 4) exceeded the range of concentrations in the UPR for those species. Because only concentrations in these three samples exceeded the range of UPR concentrations, a spatial difference (between the LPR and UPR) in channel catfish tissue total DDx is possible but uncertain. Insufficient data are available for some species to make such a comparison (e.g., small forage fish species and Northern pike).

The spatial variation of total DDx in biota tissue is presented in Figures 21 through 25 of Appendix F. Tissue samples from fish species generally exhibited higher total DDx concentrations in individual samples from particular LPR reaches. For example, common carp whole-body concentrations were highest in Reach 4 but showed a decreasing trend in total DDx from Reaches 3 to 8. For several species, including American eel, small forage fish, catfish, white perch (excluding one high concentration in Reach 1), and freshwater worm, total DDx concentrations were greatest in the middle reaches (i.e., Reaches 3 to 5). Blue crab hepatopancreas tissue concentrations were highest in the lower reaches (Reaches 1 to 3). White catfish had relatively high concentrations in Reaches 4, 5, and 8, with little discernible spatial trend.

5.4.5 Mercury

Total mercury was detected in all biota tissue samples. The following general trends are presented in Figures 5-17 and 5-18 and Table 6 of Appendix F:

- Detected fish tissue concentrations ranged from 30 to 680 µg/kg ww for whole-body and from 41 to 990 µg/kg ww for fillet samples. Total mercury concentrations were higher in fish fillet samples than in fish whole-body samples of the same species. Mercury concentrations in whole-body and fillet tissues generally increased with increasing trophic level in fish, with lower mercury concentrations in small forage fish (i.e., mummichog, shiners, and mixed forage fish) and higher concentrations in piscivorous fish (i.e., American eel, northern pike, largemouth bass, and smallmouth bass) (Figures 5-17a and 5-17b). Exceptions to this general trend were in pumpkinseed (n=1), which had a higher concentration (and was larger in size) than did other small forage fish, and white catfish, which had higher concentrations than did other larger benthic fish. Higher mercury concentrations in white catfish are not unexpected because fish can make up a large portion of that species' diet.
- Whole-body tissue concentrations of total mercury in blue crab were higher than those measured in small forage fish and in some large benthic fish (e.g., common carp and brown bullhead) (Figure 5-17a). Blue crab tissue concentrations ranged from 32 to 320 µg/kg ww, with the lowest concentrations measured in hepatopancreas tissue relative to the other tissue types (muscle, whole body, and carcass) (Figure 5-17c), which is different than trends seen across blue crab tissue types for the chemicals described above.
- Concentrations in bioaccumulation estuarine and freshwater worm tissue were generally both lower than those in fish and blue crab tissues, although total mercury concentrations in freshwater worm samples (7.6 to 150 µg/kg ww) were higher than in the estuarine worm (21 to 25 µg/kg ww) samples (Figure 5-17d).
- Concentrations in both the caged estuarine and freshwater mussels were much lower than those measured in fish and blue crab tissue (Figure 5-17e). Mussel tissue concentrations ranged from 8.7 to 35 µg/kg ww,

- Methylmercury composed the majority of the total mercury concentration in most fish and blue crab tissue samples (Figure 5-18a and 5-18b) but only a small percentage in bioaccumulation worm tissue samples (Figure 5-18c). Methylmercury contributed 35% in estuarine mussel tissue and 62% in freshwater mussel tissue samples (Figure 5-18d).

For species for which whole-body data were available from both the LPR and the UPR above Dundee Dam, LPR fish tissue concentrations of total mercury are either similar to or less than concentrations measured in fish tissue from the UPR (Figure 5-19; see also Appendix F).

The spatial variation of total mercury in biota tissue is presented in Figures 26 through 30 of Appendix F. As shown in those figures, total mercury concentrations in tissue samples were generally consistent across Reaches 1 through 8 of the LPR for many tissue samples. However, tissue samples from a few fish species exhibited higher individual sample total mercury concentrations in particular LPR reaches. For example, higher individual sample total mercury concentrations were observed in American eel tissue samples collected from LPR Reaches 3 through 5, as well as white catfish samples collected from LPR Reaches 3 and 5. Concentrations in blue crab tissue samples collected in Reaches 1 and 2 were generally greater (although highly variable) than concentrations in samples collected in Reaches 3 through 8. Potential spatial differences among caged mussel tissues showed an opposite trend: concentrations were greater in Reaches 6 through 8 than in Reaches 1 through 3, possibly due to species differences (i.e., freshwater mussel versus estuarine mussel).

5.4.6 Summary

Organic chemicals, including 2,3,7,8-TCDD, total PCBs, and total DDx, are generally highest in large benthic omnivorous fish, with the highest concentrations found in carp. The same chemicals are also observable in the tissues of fish and invertebrates at lower trophic levels. Tissue concentrations of 2,3,7,8-TCDD, total PCBs, and total DDx tend to be highest in fish samples from the middle reaches of the LPR (e.g., Reaches 3 to 5) and lowest in fish tissue samples from above Dundee Dam. However, this is not true for all species. The close association of carp and other large benthic omnivorous fish with surface sediments influences their accumulation of organic chemicals. HMW and LMW PAHs are also generally higher in the benthic omnivores, and concentration ranges in fish from the LPR mostly overlap with concentration ranges in fish from above Dundee Dam. Mercury concentrations in LPR fish tissue generally increase with increasing trophic level in fish and are similar or even lower than those measured in fish collected above Dundee Dam.

5.5 Key Findings

The key findings regarding the overall LPR ecology and biota distribution of chemicals are summarized as follows:

- The ecology of LPR fish and invertebrate communities may be impacted by chemical contamination, turbidity, DO, nutrient inputs, and grain size. In addition, the highly urbanized setting of the LPR has resulted in a loss of ecological habitat, which has, in turn, impacted the LPR ecology and ecological food web and exposure to chemical contaminants.
- The LPR benthic community is dominated numerically by small deposit feeders and detritivores (e.g., annelid worms, chironomids, and bivalves). The taxonomic composition of the community (e.g., dominated numerically by annelid worms) is typical of disturbed, urban systems.[126]
- The oxygenated depth of sediment in the LPR is influenced by legacy chemical contamination, a high level of organic inputs from the numerous CSOs/SWOs, and non-point source urban runoff. Flow over Dundee Dam is the largest external source of OC to the LPRSA; however, the flow of OC over Dundee Dam may be reduced to some extent in the future.
- While salinity is the primary influence on the benthic community, other non-chemical stressors (e.g., TOC, sediment grain size, and other habitat characteristics) affect benthic community function and structure. Chemical contamination also has the potential to impact benthic community function and structure; the effects of chemical contamination on benthic invertebrate communities are discussed in Section 9.4.
- Organic chemicals, including 2,3,7,8-TCDD, total PCBs, and total DDx, were generally highest in large benthic omnivorous fish, with the highest concentrations found in common carp. Total PCBs, 2,3,7,8-TCDD, and total DDx are also observable in the tissues of fish and invertebrates at lower trophic levels. Concentrations of these chemicals tend to be highest in samples from the middle reaches (e.g., Reaches 3 to 5) and lowest in samples from above Dundee Dam. PAHs were also generally higher in the benthic omnivores, and concentration ranges in fish from the LPR overlap with concentration ranges in fish from above Dundee Dam. Conversely, mercury biota tissue concentrations generally increased with trophic level, and LPR mercury fish tissue concentrations were similar or even lower than those measured in fish collected above Dundee Dam.
- Concentrations of 2,3,7,8-TCDD in many LPR fish tissue samples exceeded UPR fish tissue concentrations by one or more orders of magnitude.
- Comparisons of biota tissue concentrations to risk thresholds are discussed in Sections 8 and 9 as part of the HHRA and BERA, respectively.

[126] Less stressed systems may also be dominated by pollution-tolerant taxa to some extent.

6 Contaminant Fate and Transport Processes in the Lower Passaic River

6.1 Overview of Contaminant Transport

Contaminants in the water column and the sediment bed exist mainly in three phases: 1) freely dissolved; 2) sorbed to dissolved or colloidal organic matter; and 3) sorbed to particulate matter (including both inorganic and organic material). Partitioning among these phases is important because transport processes affect each phase differently and because it influences the bioavailability of the contaminant.[127] A general schematic of contaminant transport processes in a coupled surface water and sediment system such as the LPR is shown in Figure 6-1. These include advection, dispersion, settling, and turbulent mixing in the water column; volatilization and atmospheric deposition at the air-water interface; deposition, resuspension (erosion), diffusion, and advection at the sediment-water interface; and, within the sediments, vertical particle mixing, porewater diffusion, and advection (Figure 6-1). The LPR flow transports dissolved and sorbed contaminants within and through the river toward Newark Bay and potentially to the lower portions of its tributaries.[128] Volatilization transfers contaminants between the dissolved phase in the water and the air, and atmospheric deposition may also contribute mass to the water column. Settling particles carry sorbed contaminants toward and into the sediment bed, which may include a "fluff" layer of unconsolidated sediments overlying a consolidated parent bed (see Section 3.4). Resuspension transports sorbed contaminants from the sediment bed and can cause the water column concentration to change dramatically on hourly timescales because the hydrodynamic and shear stress conditions in a tidal system such as the LPR are continually changing. Contaminant mobilization from the sediment to the water column due to erosion is generally limited to the unconsolidated fluff layer during low-shear stress conditions and likely extends into the underlying bed during higher-shear stresses. Dissolved contaminants[129] may be transported within the sediment bed and between the sediment and the water column via diffusion or porewater advection associated with hyporheic flow, groundwater flow, or bioirrigation. Bioturbation acts similarly on sorbed contaminants by mixing bedded sediments. A combination of these transport processes mediate the transfer of contaminant mass between the fluff layer and the underlying bed. Fluff solids and associated contaminants may gradually be incorporated into the underlying bed if shear stresses are insufficient to periodically resuspend the entire fluff layer. This process is not well understood (Reimers et al. 2004), but in addition to consolidation, it may be biologically mediated via ingestion

[127] The uptake pathways of dissolved and sorbed contaminant phases in the LPR foodweb will be described in Appendix P (summary of the bioaccumulation model), which will be developed and finalized at a later date in coordination with USEPA. .

[128] The transport of contaminant from the LPR to the tributaries is expected to occur primarily during low flows and would be limited to the HOT. Tributary surface sediment chemistry data are considered in Section 10.2.2.

[129] Dissolved contaminant refers here to the freely dissolved phase as well as the contaminant bound to dissolved or colloidal organic matter.

of fluff solids by epibenthic organisms and subsequent fecal production (Lauerman et al. 1997; Thomsen 1999; Jones et al. 2009) or the result of advective transport into the bed via hyporheic flow[130] (O'Connor and Harvey 2008; Boano et al. 2014).

Of the above transport processes, advection, erosion, and deposition have the largest influences on the contaminant mass balance in the water column, whereas the contribution of volatilization, atmospheric deposition, and groundwater flow are expected to be small.[131] The relative contribution of the processes transporting contaminants within the bed and across the sediment-water interface is difficult to quantify but is expected to vary vertically and likely also temporally and spatially along the river.[132]

6.1.1 Sorption and the Tie Between Contaminant Transport and Sediment Transport

For neutral hydrophobic organic chemicals in surface water systems, OC is believed to be the main sorbent and models typically treat sorption this way (e.g., Karickhoff 1984; Seth et al. 1999; Hawthorne et al. 2011). Similarly, OC has been found to be the principal sorbent for mercury (Karlsson and Skyllberg 2003) and other metals (Turner et al. 2004). Sorption of neutral hydrophobic organic chemicals to mineral surfaces has been found to be relatively weak (Mader et al. 1997), and even in sediments with extremely low OC content, OC appears to be the main sorbent (Piatt et al. 1996).

Sorption processes are specific to both the sorbate (i.e., the contaminant) and the sorbent (e.g., particulate matter). Sediment desorption studies have found that the rates of exchange between the dissolved and sorbed phases can vary dramatically on timescales of a few hours to several hundred days (e.g., Carroll et al. 1994; Sormunen et al. 2009). The sorptive exchange can be modeled by splitting the sorbed contaminant mass into a resistantly bound fraction (the mass bound to sorption sites with very slow desorption rates) and a reversibly sorbed fraction characterized by an equilibrium distribution or partitioning coefficient (the amount of mass sorbed to sites with desorption rates that are rapid enough to be approximated as undergoing instantaneous

[130] The potential transport of colloids and very fine sediments by hyporheic flow is described in Boano et al. (2014) and references therein.

[131] Contaminant mass balances in Section 7 and Appendix O demonstrate the relative importance of processes resolved by the model. Although volatilization is expected to be more important for compounds that are of lower molecular weight and hydrophobicity, the predicted mass balance indicates that volatilization and atmospheric deposition fluxes are several orders of magnitude smaller than those of advection, deposition, and erosion for each of the nine modeled COPCs. Groundwater flow is not modeled, as its contribution to the LPR is expected to be small based on the local hydrogeology and post-construction monitoring at the RM 10.9 early action area (see Sections 3 and 10).

[132] For example, bioturbation and bioirrigation will be active to the depth that benthic fauna can burrow and may vary in time and space due to factors such as sediment properties and ambient conditions. Likewise, contaminant transport at the sediment-water interface may be controlled by diffusion across a thin boundary layer and vary with layer thickness and partitioning at the interface. Given the uncertainty, exchange processes within the bed and at the sediment-water interface are typically represented in CFT models using lumped mass transfer coefficients meant to represent the aggregate transport without resolving the contributing processes.

partitioning) (DiToro 1985; see Appendix G for additional detail). In this framework, the hydrophobicity of the chemical (characterized by a K_{ow} or K_{oc}), the fraction of mass not resistantly bound (f_E [fraction equilibrium]), and the amount of carbon available for sorption determine the fraction dissolved (f_D; the ratio of the dissolved chemical mass to total chemical mass per volume).

When sediment particles are resuspended, the reversibly sorbed fraction exchanges mass with the dissolved phase, dissolved OC (DOC), and other suspended particulate matter (including sediment particles of a different origin and organic particles such as algae—their relative uptake of the desorbed mass depends on their relative contribution to the water column carbon pool). In contrast, the resistantly sorbed chemical remains sorbed to the particle and will be transported and re-deposited along with it. Re-equilibration of contaminant mass among the resistant and reversible sorption sites occurs for particles that remain in the bed for long periods of time (e.g., months to years), whereas particles in the fluff layer participating in intratidal resuspension and deposition have insufficient time in the water column to re-equilibrate and may be depleted in the contaminant mass fraction available for desorption upon resuspension. The fraction of dissolved mass in the water column, f_D, has been measured for dioxins, furans, and PCBs in the LPR and Newark Bay as part of the hv-CWCM program (see Section 2.4). It is very low for 2,3,7,8-TCDD (0.012 to 0.19 with a mean of 0.06) and 1,2,3,4,6,7,8-HpCDF (less than 0.01), while it is higher and more variable for tetrachlorobiphenyl (tetra-CB), ranging from 0.18 to 0.80 with a mean of 0.4 (Table 6-1).[133] These values mean that most of the 2,3,7,8-TCDD and 1,2,3,4,6,7,8-HpCDF in the water column is sorbed to the particles even at the modest particulate organic carbon (POC) concentrations observed during the hv-CWCM program (about 1 mg/L, with a maximum of 2.5 mg/L). To assess potential exchange between the dissolved and particulate phases in the water column, the fraction of mass not resistantly bound (f_E) was estimated using the hv-CWCM data together with the DiToro model (DiToro 1985; as discussed with USEPA Region 2). The f_E values predicted by this model generally mirror the fraction dissolved (Table 6-1; also, Appendix G).[134] With the majority of the 2,3,7,8-TCDD (mean f_E of 0.1) and 1,2,3,4,6,7,8-HpCDF (mean f_E less than 0.01) resistantly bound to particles with desorption timescales of weeks to months (Appendix G), the exchange between sorbed and dissolved phases of these contaminants is rate-limited during resuspension events and most of the contaminant transport is expected to track the transport of solids. Tetra-CB shows a larger range of values of f_D and f_E (means of 0.42 and 0.55, respectively; Table 6-1), implying a greater exchange with the dissolved phase and a potentially greater influence of dissolved contaminant transport. However, over longer periods of time, the contaminant transport may still be expected to largely track the transport of solids; model simulations of these compounds (see Section 7.2.3) indicate that the net longitudinal contaminant loading associated with the particulate fraction is substantially larger than

[133] The selection of contaminants in Table 6-1 reflects the primary calibration COPCs used in the RI/FS CFT model. Additional information about the data and calculations are given in Appendix G along with properties for other measured contaminants.

[134] As discussed in Appendix G, the f_E values derived from hv-CWCM data in Table 6-1 are qualitatively consistent with the findings of literature desorption experiments.

that of the dissolved phase when integrated over a range of flow conditions and suspended solids concentrations. Although hv-CWCM data are only available to describe the partitioning of dioxins, furans, and PCBs in the LPR, particulate phase transport is expected to be important for each of the LPR contaminants discussed in preceding sections given their hydrophobic and persistent nature, albeit to varying degrees. For example, LMW PAHs are less hydrophobic than HMW PAHs and are likely to have a larger dissolved component, meaning a greater influence of dissolved transport processes. The importance of particulate phase transport is also suggested by the correlation between volumetric contaminant concentrations and suspended solids concentrations for the other contaminants within the LPR (Figure 6-2, which shows sv-CWCM data). Although this relationship varies in space and time (note the scatter among different stations), the association of elevated contaminant concentrations with elevated suspended solids concentrations implies that the net flux will be strongly impacted by sediment transport processes. Factors contributing to the observed water column response are considered in Section 6.2 and Appendix H.

The expectation that the transport of the highly sorptive principle LPR contaminants (i.e., 2,3,7,8-TCDD, PCBs, PAHs, DDx, and mercury) will largely mirror that of solids (albeit to varying degrees) implies that the conceptual sedimentological regimes introduced in Section 3.4 may qualitatively be extended to contaminant transport, as follows:

- During low river flow (low-energy conditions; Regime 1), fine sediments and associated contaminants are trapped in the LPR, partly within the ETM and partly by settling elsewhere on the riverbed. This includes sediment and contaminants entering the LPR over Dundee Dam, from tributaries, and from Newark Bay. Upriver net solids transport and infilling, which vary with freshwater inflow and tidal range, may move contaminants upstream. Longitudinal gradients in bed contaminant concentrations and boundary influences may also influence the net contaminant transport via tidal pumping. Contaminant concentrations in the water column primarily reflect concentrations in the mm-scale unconsolidated fluff layer (or "mobile pool") believed to dominate tidal resuspension during low-energy conditions (see Section 3.4). The highest contaminant concentrations are expected to coincide with the high suspended solids concentrations within the ETM, where chemical deposition flux is presumably also highest. The potential influence of the dissolved phase on the net longitudinal transport is likely largest during this flow regime in which the net solids fluxes are lowest, but this effect will be COPC-specific per the preceding discussion of chemical exchange within the water column.
- During moderate river flow (medium-energy conditions; Regime 2), fine sediments and contaminants in the water column and fluff layer are flushed downstream toward Newark Bay, and the ETM also shifts downstream. The sediment bed generally remains stable. Water column concentrations and the loading to Newark Bay reflect a blend of resuspended concentrations and upstream/watershed loadings.

- During high river flow (high-energy conditions[135]; Regime 3), the riverbed may scour and cause buried sediments with potentially higher contaminant levels to be exposed or resuspended to the water column. The net contaminant flux is likely in the downstream direction and into Newark Bay, but it also likely varies in magnitude by contaminant depending on its distribution within the sediment bed and boundary contaminant loadings.

Over time and most intensely during high-flow events, the aforementioned dynamics disperse sediments, causing fine sediments and the associated contaminants to preferentially accumulate in areas of lower shear stress. This redistribution process allows areas of elevated surface concentration to act as contaminant sources to lower concentration areas. Subsurface sediments may potentially also be redistributed during high-energy events, although erosion beyond the top 6 inches appears to be limited (see detailed discussion of deposition/erosion patterns in the reach-by-reach evaluations presented in Section 4). Although transport of the LPR's principal contaminants is strongly tied to the transport of solids, the net contaminant flux is influenced by contaminant-specific considerations, including boundary loadings, sediment concentration gradients, and partitioning behavior. Solids and contaminant fluxes during each of the above flow regimes and the relative contribution of dissolved and particulate loads are assessed in Section 7.2.3 using model results, as there are not sufficient measurements to construct reliable contaminant mass balances using data alone.

6.2 Short-Term Contaminant Fate and Transport

Insights into short-term transport are gained from the eight sampling events comprising the 2011 to 2013 sv-CWCM program, which covered a range of flow and tidal conditions. Details about this program, including sampling stations[136] and the hydrologic conditions during the sampling events, are provided in Appendix B. The hydrologic conditions are also summarized in Figure 6-3. Within the framework of the conceptual sedimentological regimes,[137] the program comprises four low-flow events (Regime 1) and four moderate-flow events (Regime 2).

As discussed in Section 10, 2,3,7,8-TCDD concentrations in the LPR are not significantly influenced by external sources (e.g., flow over Dundee Dam, tributaries, CSO/SWOs, and tidal inflows from Newark

[135] As noted in Section 3, spring tides or offshore set-up/set-down events may be a compounding factor to further enhance shear stresses during the flow-based conceptual regimes.

[136] The nomenclature in this and subsequent sv-CWCM figures is as follows: "T000" refers to the station at RM 0, "T014" refers to the station at RM 1.4, and "T10.2" refers to the station at RM 10.2. "TTR1" and "TTR2" are the floating stations designed to follow the salt front. TTR1 was located at LPR RM 6.7 (when flows were greater than 1,000 cfs) or approximately 1 mile downstream of the toe of the salt wedge (when flows were less than 1,000 cfs). TTR2 was located at LPR RM 4.2 (when flows were greater than 1,000 cfs) or halfway between the toe of the salt wedge and upstream of RM 1.4 up to RM 4.2 (when flows were less than 1,000 cfs). More generally, TTR1 can be defined as the station near the limit of the salt intrusion, and TTR2 is within the salt wedge (Appendix B). For the two events designated as high-flow monitoring in February/March and June 2103, stations "T067" at RM 6.7 and "T042" at RM 4.2 were reported in place of TTR1 and TTR2, respectively. In the data evaluations presented herein, unless otherwise noted, the T067 data are aggregated with TTR1 data and the T042 data are aggregated with TTR2 data.

[137] As described in Appendix M (Attachment B), Regime 1 applies for flows below 750 to 1,000 cfs, and Regime 3 applies for flows above 6,000 to 7,000 cfs.

Bay). As such, 2,3,7,8-TCDD is useful for interpreting contaminant dynamics associated with sediments. Consequently, the discussion below focuses mainly on 2,3,7,8-TCDD, with observations for other contaminants described mainly in a relative sense and in less detail. The evaluation is organized along the following select themes:

- Tidal resuspension and deposition
- Longitudinal transport trends
- Influence of flow and tidal forcing
- Relationship between water column and sediment bed concentrations

More detailed evaluations of station- and event-specific responses are provided in Appendix H, which includes statistical analyses of the sv-CWCM dataset.

In the evaluations that follow, contaminant concentration patterns from the sv-CWCM dataset are evaluated on both a volumetric basis and solids-normalized basis (i.e., the total volumetric contaminant concentration divided by the suspended solids concentration). The solids-normalized concentrations are considered in lieu of true estimates of the contaminant concentration on particulates (i.e., the volumetric concentration of the particulate phase divided by the suspended solids concentration) because particulate phase concentrations were not measured during the sv-CWCM program for most of the contaminants evaluated below (mercury is the lone exception; see Appendix G). Solids-normalized concentrations are deemed relevant given the hydrophobic nature of the contaminants and the observed correlation between volumetric concentration and suspended solids concentrations, but it is recognized that they are biased high as estimates of particulate concentration, to an extent that depends on the COPC-specific contaminant behavior and likely also on the concentration of suspended solids (dissolved fractions will tend to be higher at low suspended solids concentrations, for a reversibly sorbed contaminant).

6.2.1 Tidal Resuspension and Deposition

The importance of tidal resuspension/deposition on LPR water column concentrations is indicated by Figure 6-4, which presents the distributions of the sv-CWCM 2,3,7,8-TCDD data across all LPR stations over six of the eight events.[138] Volumetric concentrations (Figure 6-4a, left column) tend to be higher in near-bottom samples than in near-surface samples (top left panel) at the upper end of the distribution, and concentrations tend to be higher at mid-tide (flood and ebb combined) than at slack tide (left middle and bottom panels), particularly for near-bottom samples. The differences among these distributions are notably less when concentrations are solids-normalized, for both the surface and bottom samples (Figure 6-4a, right panels), which suggests that differences in suspended solids concentrations explain much of the differences between tidal phases. Additional insight is

[138] Figures 6-4 and 6-5 exclude the February/March and June 2013 events because sampling was not conducted to capture the various tidal stages for these monitoring events; these were instead designed to capture higher-flow conditions.

gained when sample pairs are plotted against each other (Figure 6-5). The difference between surface and bottom, as well as between slack tide and mid-tide, tends to be greater at high concentrations than at low concentrations on a volumetric basis, and forms a tighter band around the 1:1 line when solids normalized. These behaviors are consistent with a strong influence of sediment resuspension and deposition on intratidal variations in 2,3,7,8-TCDD concentrations, which is expected given the observed intratidal variations in suspended solids (Figure 3-7) and is supported by model mass balances during low-flow conditions (see Section 7.2.3).

Although solids normalizing explains a substantial portion of the variability in volumetric comparisons of 2,3,7,8-TCDD sv-CWCM concentrations, it does not explain all of it. Figure 6-4 indicates that near-bottom solids-normalized 2,3,7,8-TCDD concentrations across all stations varied by about 1.5 orders of magnitude (10 to 600 ng/kg) with a few exceptions, including one mid-tide sample at TTR1 with a concentration in excess of 10,000 ng/kg (Figure 6-5). Likewise, while solids-normalization better aligns the data with the 1:1 line, considerable variability remains about this line. Although some of this remaining variability may reflect the influence of the dissolved phase, given dissolved fractions of less than 20% for 2,3,7,8-TCDD (Table 6.1 and Appendix G), it more likely reflects vertical and temporal variability in the mix of solids present in the water column at each station (i.e., surface versus bottom and mid-tide versus slack tide). Solids originating recently from above Dundee Dam, tributaries, Newark Bay, and the upper few miles of the LPR will tend to have much lower 2,3,7,8-TCDD concentration than sediments resuspended within the remainder of the LPR (see Sections 4.1 and 10.3), and the sediment resuspended from within the LPR can be expected to vary in concentration depending on its time history (bedded sediment versus fluff layer solids and high-concentration versus low-concentration areas) and sorptive capacity (OC content).

Similar behaviors are noted for the other contaminants (Figures 6-4b to 6-4f and 6-5b to 6-5f) in that concentrations tend to be higher in bottom samples and during mid-tide on a volumetric basis (left panels). However, the variability in water column concentrations and the degrees of separation between the volumetric (left panels) and solids-normalized distributions (right panels) varies. For PCBs, HMW PAHs, DDx, and mercury, the range of water column concentrations is about two orders of magnitude on a volumetric basis and one order of magnitude on a solids-normalized basis, which is somewhat less than for 2,3,7,8-TCDD. LMW PAHs exhibit less variable concentrations (about one order of magnitude on both a volumetric and solids-normalized basis). LMW PAHs and, to a lesser degree, total DDx and PCBs tend to have solids-normalized concentrations that are higher in the surface relative to the bottom and at slack tide relative to mid-tide, perhaps reflecting a greater influence of the dissolved phase.

Overall, the data evaluations in Figures 6-4 and 6-5 indicate that tidal resuspension/deposition is a driving factor for water column contaminant levels, and contaminant-specific influences such as

spatial patterns in bed concentrations, boundary loadings, and partitioning behavior also play a role. Other factors contributing to the water column response are considered in subsequent sections.

6.2.2 Longitudinal Transport Trends

The longitudinal patterns in water column contaminant concentration are presented by event on a volumetric basis (Figure 6-6) and on a solids-normalized basis (Figures 6-7). To illustrate the large-scale longitudinal trends of the data, the floating stations TTR1 and TTR2 samples are grouped with the closest fixed station location (i.e., into bins centered on RM 1.4, RM 4.2, RM 6.7, or RM 10.2), and non-detects are set to half of the detection limit. Also shown is the approximate range of the salt front (defined here by the 2 ppth isohaline[139]) and the prevailing mean flow and tide conditions over the events (see Figure 6-3 for more information on conditions before and during the events). The mean flow conditions were used to group the events in Figures 6-6 and 6-7: low-flow events (Regime 1, with flows less than 1,000 cfs) are in the top row, and moderate-flow events (Regime 2) are in the bottom row. It is noted that the February/March and June 2013 events consisted of two sub-sampling periods aimed at capturing the rising and falling limbs of the hydrograph during a higher-flow event, which were separated by 4 and 10 days, respectively; these periods are combined in Figures 6-6 and 6-7, and the aggregated dataset is weighted toward the more intensely sampled rising limb. For reference, salinity and suspended solids are presented in a similar fashion in Figure 6-8. Additional versions of these figures are included in Appendix H, including versions with unbinned data and versions in which surface and bottom samples are binned separately.

The relative importance of upstream boundary influences and the contributions from LPR sediments may be assessed from the change in concentration between the Dundee Dam station and the RM 10.2 and RM 6.7 plotting bins (showing data from those stations and floating station data that are nearest to them; Figure 6-6). For 2,3,7,8-TCDD, concentrations measured at the Dundee Dam station were mostly below the detection limit (Figure 6-6a, open symbols). Moving to RM 10.2 and RM 6.7, there is a substantial increase in the water column 2,3,7,8-TCDD concentration for all events, which indicates a strong influence of the LPR sediments (the only detected concentration at Dundee Dam occurred during the June 2013 sampling event, which had moderate-flow conditions and the highest flow of the eight sv-CWCM events; here, five of six samples were non-detect and the detected sample was a factor of 2 to 3 lower than the downstream mean). A similar pattern holds for mercury (Figure 6-6f) and PCBs (Figure 6-6b). Conversely, the concentrations at Dundee Dam are more similar to those in the LPR for HMW PAHs, LMW PAHs, and DDx (Figures 6-6c to 6-6e), indicating an upstream boundary

[139] The range of the salt front in Figures 6-6 and 6-7 is based on longitudinal extrapolation of salinity measurements to the 2 ppth isohaline for the first six sv-CWCM events (range of low-slack and high-slack estimates, visually assessed) and CPG model results for the last two events (range of the daily mean predicted positions). It is meant only as a guide; the sparseness of the dataset means that the salt front location is not well resolved and the estimate is a rough approximation. It is also noted that the data were collected over several days, during which the salt front location would be variable. Nevertheless, the salt front location is qualitatively consistent with expectations.

source influence for these contaminants. Solids-normalized Dundee Dam concentrations (Figure 6-7) are similar to or higher than those in the LPR for LMW PAHs, HMW PAHs, and total DDx and somewhat lower than those in the LPR for PCBs and mercury. Available 2,3,7,8-TCDD solids-normalized concentrations were all non-detect,[140] which indicates an increase between Dundee Dam and the LPR stations, consistent with the previously noted assumption that 2,3,7,8-TCDD is not controlled by upstream sources (see evaluation of external sources in Section 10).

The highest volumetric 2,3,7,8-TCDD concentrations occur within the LPR, though the location varies (Figure 6-6a). The peak tends to occur in the vicinity of the estimated salt front position, though it is noted that this position is uncertain due to data limitations, and some separation between the data and the salt front bands is also introduced by binning concentration values to the nearest fixed station (visible in Figure 6-8a; see Appendix H for unbinned equivalent figures). The occurrence of the peak concentrations within the estuarine portion of the LPR is expected given the elevated suspended solids there and the influence of tidal resuspension on volumetric concentrations (see Section 6.2.1, discussed further below). There is a decline of concentration moving farther downstream within the LPR and across Newark Bay to levels 1 to 2 orders of magnitude lower than the peak. Similar observations generally apply to the other contaminants (Figures 6-6b to 6-6f), although the distributions are flatter to varying degrees. Relative to 2,3,7,8-TCDD, the decline from the LPR to Newark Bay is generally less for total PCBs, HMW PAHs, DDx, and mercury (on the order of 5 to 20) and notably less for LMW PAHs (on the order of 2 to 5). These smaller declines moving into Newark Bay relative to 2,3,7,8-TCDD may indicate a stronger downstream boundary influence or differences in partitioning behavior (e.g., the dissolved phase may play a larger role for LMW PAHs, which would reduce the influence of settling).

Solids-normalized trends within the LPR are similar to volumetric trends for 2,3,7,8-TCDD (Figure 6-7a), but distributions are somewhat flatter, consistent with the prior observation that concentration variability is reduced upon solids-normalizing. Similar to the surface sediment trends (Figure 4.1-9), there is a fairly steady decline in the solids-normalized concentration moving from the peak within the LPR into Newark Bay, particularly for the moderate-flow events (bottom row: August 2011, June 2012,[141] June 2013, and, to a lesser degree, February/March 2013). This suggests a declining influence of exported, settling LPR solids moving across Newark Bay, which is supported by the concurrent decline in suspended solids during these moderate-flow events (Figure 6-8b; note that such declines may result from a combination of settling and dilution). For the other contaminants, a mix of trends in the solids-normalized concentration is seen. Mercury and HMW PAHs show a decline similar to that of 2,3,7,8-TCDD though somewhat more muted; total PCB and DDx distributions are fairly flat through Newark Bay; and LMW PAHs show a flat to increasing pattern

[140] The single detected 2,3,7,8-TCDD concentration did not have a paired suspended solids measurement.
[141] 2,3,7,8-TCDD was not sampled for in Newark Bay during this event, but a similar decline is noted in the lower LPR.

across the bay. Relative to 2,3,7,8-TCDD, the patterns suggest a stronger downstream source for LMW PAHs, DDx, and total PCBs, though it may also reflect the influence of a stronger dissolved component.

With regard to longitudinal transport within the LPR, it is noted that when the six sv-CWCM events that studied tidal effects are aggregated, the highest mean concentrations within the LPR occurred at the floating tidal stations (TTR1 and TTR2; i.e., the stations near the salt front and within the salt wedge, respectively[136] [Appendix B]). This suggests the potential for net upstream contaminant transport within the salt wedge during low flows, associated with the upstream transport of solids and the movement of the ETM that typically occurs near the salt front. As discussed in Section 3.4, the upstream transport occurs due to asymmetry in the tidal currents and vertical mixing, which gives rise to higher suspended solids flux on flood than on ebb. A comparison of near-bottom mid-tide 2,3,7,8-TCDD concentrations indicates that they tend to be higher on flood tide than ebb tide, consistent with the response of the solids to the flood-dominant tidal currents. See Appendix H for additional discussion and supporting evaluations.

Figures 6-4 through 6-6 also show the available New Jersey Surface Water Quality Standards (NJAC 7:9B) and USEPA National Recommended Water Quality Criteria for 2,3,7,8-TCDD, total PCBs, and mercury (corresponding standards for total DDx, LMW PAHs, and HMW PAHs were not available, although they are available for some of the underlying constituents such as 4,4-DDT and benzo[a]pyrene). Brief observations on the water column data in relation to these benchmarks[142] are as follows:

- 2,3,7,8-TCDD: All sv-CWCM measurements collected within the LPR with concentrations above the reported detection limit exceeded the USEPA and NJDEP human health benchmark of 0.005 picogram per liter (pg/L) (Figures 6-4a, 6-5a, and 6-6a; standard is noted in footer but not shown). Reported detection limits were higher than this benchmark and thus preclude a comparison of non-detect samples to the benchmark.
- Total PCBs: Approximately 60% of bottom samples and 57% of surface samples within the LPR exceeded the USEPA and NJDEP aquatic life benchmark of 14 ng/L (Figure 6-4b and 6-5b), and exceedances were mainly limited to the LPR (Figure 6-6b). All measurements exceeded the human health benchmark of 0.064 ng/L (Figures 6-4b; standard is noted in footer but not shown).
- Mercury: Approximately 45% of bottom samples and 30% of surface samples in the LPR exceeded the NJDEP human health benchmark of 50 ng/L (Figures 6-4f and 6-5f), and

[142] The percent exceedances quoted here are based on the data at the LPR stations for all eight sampling events and differ slightly from the frequencies shown in Figure 6-4 because those figures show only the six events for which the tidal stages were sampled (i.e., not including the February/March and June 2013 events).

exceedances tended to occur within the LPR and upper Newark Bay (Figures 6-6f). Only a single measurement within the LPR exceeded the USEPA aquatic life benchmark of 770 ng/L.

Discussion of LPR water column contaminant levels from a human health and ecological risk perspective may be found in Sections 8 and 9 and Appendix D.

6.2.3 Influence of Flow and Tidal Forcing

Although LPR water column contaminant concentrations are influenced by changes to the freshwater flow and tidal forcing (Figures 6-4 through 6-7), the nature of that influence is complex. The volumetric and solids-normalized contaminant concentrations show no evident relationship to the event-mean freshwater flow at Dundee Dam or to the event-mean tidal forcing (Figure 6-9). Although two of the higher-flow "Regime 2" events (August 2011 and June 2012, with mean flows of 2,530 and 1,330 cfs, respectively) have higher median and mean[143] concentrations than any other event, the other two higher-flow sampling events (February/March and June 2013, with mean flows of 2,200 and3,180 cfs, respectively) have distributions comparable to the four low-flow events; i.e., on a total distribution basis, there is not an evident difference between the flow regimes. Moreover, these events are similar to the August 2011 event in both flow and tidal range, yet the concentration distributions are lower—particularly for the February/March 2013 event. While the elevated concentrations in June 2012 may be attributable to the combination of elevated flow and strong tidal forcing, a global flow (or tide) relationship to concentration is not apparent. The LMW PAH data differ somewhat from those of the other COPCs in that the February/March 2013 event has modestly higher concentrations than the three low-flow events sampled for this COPC, but a global flow relationship is not suggested given the similarity of the August 2011 event to the low-flow events (the June 2012 and June 2013 higher-flow events were not sampled for this COPC).

The lack of clear relationship may be because greater flow dilution and upstream solids loading mask increases in contaminant flux to the water column due to erosion. It may also reflect the conditions immediately before the sampling events. The February/March and June 2013 moderate-flow events were preceded by other Regime 2 events of similar magnitude, which may have caused fluff layer concentrations to have been depleted during these events relative to the other two Regime 2 events (August 2011 and June 2012), which were preceded by lower flows (Regime 1). Lastly, the comparison may also be influenced by differences in the sample collection for the February/March and June 2013 events, which were designed to capture both the rising limb and falling limb of the hydrograph during a freshwater discharge event. Although removing the falling limb samples from the distributions has nominal impact to the comparison in Figure 6-9 (most samples were collected during the rising limb), the data from these events indicate a higher range in volumetric

[143] The means for the August 2011 and June 2012 events are strongly influenced by a single outlier in each case.

concentrations on the rising limb than the falling limb and therefore do suggest a concentration response to freshwater flow.

Although the high-flow regime was not sampled during the sv-CWCM program, the data allow for a qualitative assessment of whether Hurricane Irene's impact on the bed (as discussed in Section 10.4.1) had a measurable impact on water column contaminant levels. This event, which caused freshwater flows of up to 24,700 cfs at Dundee Dam, occurred approximately 1 week after the August 2011 sv-CWCM event. Subsequent sampling events, spanning February 2012 through June 2013, do not indicate a systematic shift in water column concentrations between the pre- and post-Irene events (Figure 6-9). Bathymetric data indicate that portions of the LPR experienced erosion during Irene. Core data indicate that subsurface sediments with elevated concentrations were likely exposed or eroded at some locations (see Section 4.2), and an increase in the mean 0- to 15-cm bed concentration is suggested by model results (see Section 7.2.3) and a comparison of pre- and post-Irene datasets (see Section 10.4.1). However, a sustained increase to the flux of contaminants from the bed to the water column is not suggested by the sv-CWCM data distributions. The lack of evident impacts of Irene on water column concentrations may be because impacts were attenuated during the approximate 6-month lag between Irene and subsequent sv-CWCM sampling events. The pre- and post-Irene comparison may also be influenced by the fact that the pre-Irene event was one of the higher-flow CWCM sampling events. Model results indicate an increase in the post-Irene water column concentrations between RM 0 and RM 8, which was not fully attenuated by the end of the sv-CWCM period (see Section 7.2.3).

The variability in the water column concentrations and their longitudinal distribution indicate that water column transport is a mechanism for redistributing contaminants at the sediment-water interface and, during high flows, contaminants in the near-surface sediments of areas that are subject to scour. The flow influence on contaminant fluxes within the LPR and to Newark Bay is characterized using the model in Section 7.3.2, which includes results for low-, moderate-, and high-flow conditions. Additional investigation into the factors driving the water column response is discussed in Section 6.2.5, and station-specific evaluations are included in Appendix H.

6.2.4 Relationship Between Water Column and Sediment Bed Concentrations

This section compares contaminant levels on suspended solids with surface sediments, in order to assess mass exchange between the sediment bed and the water column. Solids-normalized water column concentrations are compared to surface sediment (0 to 6 inches) concentrations between RM 1 and RM 7. The comparison is restricted to this interval to focus on the estuarine portion (the salt front is typically upstream of RM 7; Figure 3-5) where the greatest tidal resuspension occurs (as a consequence of tidal asymmetry and estuarine circulation; see Sections 3.1 and 3.4). Additional reasons that this reach is of interest include: 1) it contains much of the sv-CWCM data collected

within the LPR; and 2) it is studied in the context of natural recovery (see Section 10) and CFT model calibration (Appendix O) because it has data from the mid-1990s as well as contemporary RI data. The sediment concentration data are disaggregated into channel and shoal; this was done to see if either better match the distribution of water column concentrations. All sv-CWCM data are used in the top row panels, whereas the middle and bottom row panels restrict the sv-CWCM dataset to low-flow (Regime 1) and moderate-flow (Regime 2) events.[144] Unfortunately, for the COPCs examined, the differences between the shoal and channel concentration distributions are not large enough to judge their relative importance to the concentrations in the water column (Figure 6-10). Median concentrations are closely matched. The principal difference is the greater variability in the channel exemplified for most of the COPCs in greater percentages of high and low concentrations. For example, the channel has more 2,3,7,8-TCDD concentrations greater than 1,000 ng/kg (17% versus 8%) and more concentrations less than 100 ng/kg (15% versus 5%). Similarly, for PCBs the channel has more concentrations greater than 1.5 mg/kg (35% versus 10%) and more concentrations less than 0.5 mg/kg (10% versus 5%).

For 2,3,7,8-TCDD (Figure 6-10a), water column concentrations exhibit less variability than the sediments, with a substantially flatter distribution and lower median. With the exception of two data points at the extreme upper tail of the water column distribution during moderate-flow events, there is strong divergence of the distributions in the upper 10% when compared to the shoal distribution and upper 20% when compared to the channel. These observations hold for both moderate- and low-flow events, although the middle of the distributions is closer if only higher-flow events are used.

Patterns vary among the remaining contaminants (Figure 6-10b through 6-10f). Total PCBs and DDx are similar to 2,3,7,8-TCDD, and the discrepancy at the upper tail—particularly in the channel—is even stronger for HMW PAHs. LMW PAHs and mercury show less discrepancy between the bed and water column; water column mercury concentrations are within a factor of 3 of the bed at the upper end of the distribution, whereas the difference is a factor of 5 to 10 for LMW PAHs. Moreover, the water column distribution is mostly higher than the channel sediment distribution for these two contaminants, particularly for moderate-flow events. These tendencies could indicate a stronger external source influence for LMW PAHs and mercury and may also reflect differences in partitioning behavior as contaminants from the bed and external sources are mixed in the water column.

Although the differences between the RM 1 to RM 7 bed and water column data suggest that the solids being eroded and resuspended do not typically reflect the most elevated 0- to 6-inch

[144] The "low flow" data in Figure 6-10 comprise the February, March, August, and December 2012 events for which event-mean flows were in the range of approximately 300 to 650 cfs. The "moderate" data comprise the August 2011, June 2012, February/March 2013, and June 2013 events. The four low-flow events correspond to sedimentological Regime 1, whereas the higher-flow events correspond to Regime 2 (see Sections 3.4 and 6.1 for definitions).

sediment concentrations, those concentrations may still be contributing (along with low-concentration areas and external loadings) and may be important to the water column through redistribution of near-surface contaminant mass.

Several factors may be contributing to the noted differences between the water column solids-normalized concentrations and the 0- to 6-inch sediment concentrations in RM 1 to RM 7, including the following:

- Vertical gradients within the 0- to 6-inch surface sediment interval of the parent bed resulting in lower concentrations at the surface, a steep concentration gradient between the parent bed and the overlying fluff layer, or a combination of both.
- Spatial covariance of lateral and/or longitudinal sediment concentration gradients and the solids flux:
  - High covariance between resuspension flux and lower concentrations such that the dominant solids flux comes from areas with lower concentrations (i.e., material that deposits is typically re-eroded).
  - High covariance between solids flux and areas with high 0- to 6-inch concentrations but steep vertical gradients.
  - Low spatial covariance, meaning exchange with the sediment over a large area (e.g., a tidal excursion) such that the water column reflects an averaging across the spectrum of 0- to 6-inch sediment concentrations in RM 1 to RM 7.
- Horizontal and vertical mixing within the water column, which control the extent to which water column concentrations within RM 1 to RM 7 reflect locally resuspended sediment versus sediment/contaminants originating outside of RM 1 to RM 7; these mixing patterns may be influenced by COPC-specific partitioning behavior in the water column.
- Related to the previous bullet, boundary solids (from Dundee Dam, tributaries, or Newark Bay) diluting or elevating particulate concentrations within RM 1 to RM 7 in a COPC-specific manner; for example, Dundee Dam solids would likely dilute LPR 2,3,7,8-TCDD concentrations but may elevate LMW PAH concentrations (per Figures 6-6 and 6-7).

For 2,3,7,8-TCDD, the fourth explanation seems least likely given the relatively low external solids loading during low flow and the aforementioned correlation between total 2,3,7,8-TCDD concentration and TSS (suggesting a bed source), though it may play a larger role approaching RM 1 as the influence of the Newark Bay loading increases. Regarding the second explanation, spatial covariance of solids flux and concentration likely contributes to some extent; even though the inside/outside shoal segregation did not generally remove the bed to water column concentration discrepancy, a more localized control of water column concentration is plausible. However, the favored conceptual model is that lower LPR water column concentrations are primarily caused by the spatial integration of fluxes across a range of sediment concentrations (which are subsequently

mixed in the water column) coupled with the influence of vertical gradients on local bed flux. The existence of vertical gradients in the mean concentration is consistent with the CFT model calibration results (see Section 7.2.3 and Appendix O) and is expected, given the strong bed mixing that would be needed to maintain a uniform concentration in a 0- to 6-inch sediment layer undergoing exchanges at the sediment-water interface. The vertical gradients may include a sharp concentration drop between the bedded sediments and the unconsolidated fluff layer, although model results indicate that this effect is COPC-specific (see Figures 7-23a and 7-23b).

6.2.5 Statistical Evaluation of sv-CWCM Dataset

To further examine the relationships of water column contaminant concentrations to various physical variables, statistical evaluations of the sv-CWCM data across all LPR stations were performed for each COPC, including the following:

- Analysis of variance (ANOVA) of mean concentration differences when data are binned by sampling depth interval, tidal phase, event, and station, on both volumetric and solids-normalized bases
- Linear regression of concentration versus river mile, flow, tidal range, salinity, TSS, and POC[145]
- Multivariate linear regression of concentration versus the above parameters

The main findings of the above evaluations are described briefly below; details are provided in Appendix H along with additional evaluations.

Mean concentrations for various data groupings are summarized on a volumetric and solids-normalized basis in Appendix H (Figures 1-1a through 1-1f and 1-2a through 1-2f, respectively). These figures indicate that on a mean basis:

- Volumetric bottom concentrations are statistically higher than surface concentrations for all contaminants when LPR data are aggregated across sampling stations and events (ANOVA with $p<0.05$ threshold), and the degree to which this holds when data are binned by flow regime (low and moderate flow) or by station varies by contaminant (Appendix H, Section 2.1).
- Volumetric concentrations at mid-tide are statistically higher than at slack tide for all contaminants when LPR data are aggregated across sampling stations, events, and depths, and the degree to which this holds true when data are binned by flow regime or by station varies by contaminant (Appendix H, Section 2.2).
- There are statistically significant differences in concentration among LPR stations when data are aggregated across sampling events and depths, with concentrations tending to be higher

[145] As described in Section 5 of Appendix H, TSS and POC were log-transformed in the regression analyses contaminant concentrations as this improved the goodness of fit.

at the TTR1, TTR2, and RM 10.2 stations than at the RM 1.4 and RM 0 stations (Appendix H, Section 3).

- There are statistically significant variations in volumetric concentration among sampling events for 2,3,7,8-TCDD, PCBs, and mercury (not for PAHs or DDx) when data are aggregated across all LPR stations and depths, and the degree to which this holds true when data are binned by flow regime or by station varies by contaminant (Appendix H, Section 4).
- Solids-normalization generally reduces the concentration differences between surface and bottom (Appendix H, Section 2.1), mid-tide and slack tide (Appendix H, Section 2.2), among stations (Appendix H, Section 3), and among events (Appendix H, Section 4); however, statistically significant differences remain for some data binning and contaminant combinations.

The regression analyses in Appendix H (Section 5) indicated that for all the evaluated contaminants, variability in water column concentrations across all LPR stations and events was best explained by variations in TSS and POC (Appendix H, Tables 5-1 and top row of Tables 5-2a through 5-2f). Salinity had the next highest correlation with concentration for all contaminants, followed by river mile. Flow and tidal range were typically the least correlated variables globally, though somewhat stronger for PAHs and DDx. For all contaminants, a multivariate regression of all LPR data yielded somewhat higher R^2 values than for TSS or POC alone (Table 5-2), ranging from 0.54 for 2,3,7,8-TCDD to 0.84 for HMW PAH. The regression analysis also indicated that stratifying the data by flow regime and station shifted the relative importance of the explanatory variables somewhat, in a COPC-specific manner. Using 2,3,7,8-TCDD as an example, at low flows, salinity has greater relative importance as an explanatory variable (but remains weaker than TSS and POC), and at moderate flows the relative importance of TSS and POC increases. Also, for 2,3,7,8-TCDD, salinity is only a statistically significant explanatory variable at the RM 1.4 and RM 0 stations ($p<0.05$), and at RM 0 it is the dominant explanatory variable.

Overall, the analysis is consistent with observations discussed earlier in Section 6.2 and supports the importance of the particulate phase to contaminant transport for the LPR RI COPCs, though it also reveals other nuances. Additional evaluations of station-specific and flow-regime-specific responses are included in Appendix H, and contaminant dynamics are evaluated quantitatively using the calibrated CFT model in Section 7.2.3.

6.3 Long-Term Contaminant Fate and Transport

The contaminant distribution within the sediment bed can be used to infer long-term transport patterns that cannot be discerned in short-term observations of the type discussed in Section 6.2. Section 6.3.1 reviews observed sediment contamination patterns within the LPR and Newark Bay and interprets them in terms of fate and transport processes. The evaluation of natural recovery of LPR sediments (and also biota) follows in Section 10.

6.3.1 Historical Patterns of 2,3,7,8-TCDD

The evaluation of historical transport patterns focuses mainly on 2,3,7,8-TCDD because it has a known dominant source from which the contaminant was dispersed over time. Moreover, it is the only contaminant not significantly influenced by external sources (see Section 10). As such, its patterns in the river provide a means to understand transport of hydrophobic contaminants.

Consistent with the discussion of surface sediment 2,3,7,8-TCDD concentration patterns in Section 4.1 (Figure 4.1-9a), the estimated 2,3,7,8-TCDD mass inventory within the sediments[146] (Figure 6-11, top panel) has a longitudinal pattern indicating transport as far as approximately RM 14 (11 miles upstream of the Lister Avenue site source at RM 3.1) and downstream across Newark Bay. Although the mass estimates and concentrations indicate a significant drop off in net upstream transport between RM 12 and RM 14, they also suggest that it extended as far upstream as RM 14.5, where there is a small deposit (see Figure 4.2.2-9) that accounts for more than 99% of the estimated mass in the RM 14 to RM 17.4 bin in Figure 6-11. The transport of 2,3,7,8-TCDD upstream to approximately RM 14 and downstream into Newark Bay has also been suggested by evaluations of TCDD ratios and other dioxin/furan fingerprints (e.g., Israelsson et al. 2014; Quadrini et al. 2015).

The mass inventory pattern in Figure 6-11 further indicates that the lower miles of the LPR and Upper Newark Bay have been effective contaminant traps. Approximately 74% of the estimated 2,3,7,8-TCDD mass in the LPR and Newark Bay was trapped in the lower 6 miles of the LPR, and 56% was trapped within approximately 1 mile of the Lister Avenue site source (i.e., the RM 2 to RM 4 bin).

The decline in mass inventory moving upstream and the low inventory above RM 14 likely reflect a declining potential for upstream contaminant transport and trapping. It is not simply due to the upstream decline in surface area because the mass inventory pattern persists on an MPA basis (Figure 6-11, bottom panel). The major upstream transport modes (estuarine circulation and tidal pumping) vary moving upstream and eventually decay at the salt front, which marks the limit of the net landward bottom flow associated with the estuarine circulation and the density gradients that induce the flood-dominant internal tidal asymmetry (e.g., Jay and Musiak 1996 and Burchard and Baumert 1998; see discussion in Sections 3.4). Figure 6-12 shows that the salt front rarely extends

[146] The bars in the top panel of Figure 6-11 reference the left axis and indicate the mass inventory in each spatial bin based on an interpolation of MPA estimates from vertical integration of core profiles designated to be "complete." The dashed blue line indicates the total mass integrated longitudinally from Dundee Dam moving downstream, referencing the right axis (i.e., the blue line shows the summation of the bars moving from left to right). The bottom panel shows the MPA implied by the top panel, calculated by dividing the mass in the top panels by the area of the corresponding 2-mile bin. The analyses and calculations involved in the development of this plot are described in Appendix I. Note that the estimates provided herein do not account for mass removal from the TSI Phase 1 footprint area in 2012 and the RM 10.9 point bar in 2013 to 2014, as they are intended to describe the historical trapping of contaminant.

above RM 14,[147] although it may have extended beyond this point with greater frequency between 1961 and 1965 during the time of peak 2,3,7,8-TCDD loading due to a prolonged period of low flow (see Section 3.3). It has been suggested that salt front intrusion was also greater during this period because less infilling had occurred in the lower river navigation channel (Chant et al. 2010; Cañizares et al. 2009), but this effect is uncertain as it may have been offset by shallower depths in Newark Bay prior to the deepening of the channel in lower Newark Bay and the Kills associated with the Harbor Deepening Project, which has had a pronounced effect on circulation and solids loading to Newark Bay (Sommerfield and Chant 2010). A decreasing contaminant trapping potential moving upstream of RM 4 is indicated by the generally decreasing prevalence of fine-grained deposits, especially above RM 14 (see SSS in Figure 4.1-5). Likewise, there is a decrease of average surficial fine sediment fraction with distance upstream (Figure 6-13), most notably within the navigation channel boundaries under contemporary conditions.[148] The declining trapping of fine sediment moving upstream is consistent with the narrowing cross-sectional area (Figure 3-2), thereby gradually favoring higher shear stresses and less long-term deposition. Historically, the decrease in cross-sectional area moving upstream of RM 4 was enhanced relative to contemporary conditions due to the deeper and wider navigation channel that existed below RM 7.8, which has seen greater subsequent infilling (trapping) since the time of the Lister Avenue site discharge relative to upstream areas (Figure 1-5). It is also noted that the 2,3,7,8-TCDD mass inventory above RM 7.8 has, in some reaches, been impacted by maintenance dredging in the 1970s (Figure 1-5, influencing about 3 miles in total); consequently, the historical contaminant trapping upstream of RM 7.8 may not be fully reflected in Figure 6-11.

The 2,3,7,8-TCDD distribution downstream of RM 2 also reflects transport and trapping potentials integrated over time, as well as navigation channel dredging. Relative to the LPR upstream of RM 4, more favorable trapping conditions existed in the expanded cross sections of the lower miles of the LPR (Figure 3-2) and upper Newark Bay, as indicated by the greater historical infilling of the navigation channel (Figure 1-5) and higher fine-sediment fraction (Figure 6-13) moving downstream, particularly below RM 2. The mass spatial pattern in Figure 6-11 indicates greater contaminant mass trapping occurred downstream of RM 2 than above RM 4; the mass distribution has a downstream skew (about 29% of the total mass below RM 2 compared to only 15% above RM 4) despite the more extensive and more recent navigational dredging below RM 2 (Figure 1-5; USACE 2010; Somerfield and Chant 2010) and not accounting for mass losses to the Kills or the Hackensack River.

[147] The estimated salt front intrusion frequencies in Figure 6-12 are approximate in nature and for discussion purposes only. Flow relationships from Chant et al. (2010), LPRSA CPG model results (regression of values in Figure 3-5), and SEI and HDR|HydroQual 2011 (visual inspection of figure therein) were used to estimate flows at which the 2 ppth or 0.5 ppth isohalines could reach the segment boundaries considered in Figure 6-11. The flows were converted into cumulative frequencies using the historical flow record at Little Falls. Also shown are the observed frequencies of 0.5 ppth and 2 ppth in the maximum daily salinity record at five PWCM moorings.

[148] This lateral gradient may have been less historically before channel infilling; also note the present-day channel deviates in some areas from the authorized navigation channel used here to bin the data in Figure 6-13.

The strong trapping of solids and contaminant in the lower miles of the LPR and upper Newark Bay has contributed to a declining transport moving across Newark Bay, as suggested by the declining MPA (Figure 6-11), surface sediment concentrations (Figure 4.1-9a), and solids-normalized water column concentrations (Figure 6-7a) moving from RM 2 across Newark Bay. The settling and concurrent mixing of LPR solids with solids originating from other sources can be expected to cause the sediment bed to gradually reflect a declining fraction of solids and contaminant originating from the LPR.[149] However, it should be noted that the longitudinal trend in MPA and surface sediment concentration is influenced by 2,3,7,8-TCDD mass removal due to navigation channel dredging subsequent to the peak 2,3,7,8-TCDD discharges. Current transport conditions are likely different, given the channel infilling within the LPR and upper Newark Bay and the channel deepening in lower Newark Bay. The dredging history may also impact the comparison of 2,3,7,8-TCDD patterns with those of the other contaminants considered in the next section.

With regard to the lateral distribution of 2,3,7,8-TCDD, the general association between surficial 2,3,7,8-TCDD concentrations and finer-grained sediments above RM 4 (Figure 4.1-9a) and the higher average surficial fine sediment content outside of the channel in this region (Figure 6-13) causes the highest surficial concentrations to be generally found in the present-day shoals, although shoal concentrations are highly variable as described in detail in Section 4.2. The lateral distribution of contaminant mass inventory is, however, subject to additional factors such as deposition history (both the depth and nature of the deposited sediments) and the timing of the deposition in relation to the contaminant loading. Historical channel infilling and subsequent maintenance dredging are likely to have strongly influenced the lateral distribution in some regions, and the mass distribution between the shoals and the present-day channel does not necessarily mirror the mean fine sediment distribution suggested by Figure 6-13 (note also that the present-day channel has in some places shifted away from the authorized navigation channel used to bin data in this figure (e.g., along the RM 10.9 point bar [see Figure 4.2.5-14b]). In the contaminant mass interpolation summarized in Figure 6-11, the integrated 2,3,7,8-TCDD mass between RM 4 and RM 14 is evenly split between the shoal and the present-day channel,[150] even though the mean 2,3,7,8-TCDD surface concentrations are considerably higher in the shoal.[151] The integrated mass downstream of RM 2 (including Newark Bay) is slightly higher in the shoals relative to the channel (54% versus 46%), despite the considerably

[149] As discussed in Israelsson et al. (2014), the decreasing influence of the LPR moving across Newark Bay is conceptually consistent with two solids transport considerations. First, while episodic high-flow events contribute to more widespread transport of LPR sediments into Newark Bay, the probability of a hydrologic event capable of delivering significant amounts of LPR solids to a given location should generally decrease moving across the Bay. Second, there is under most conditions a net northward (landward) solids transport along the navigation channel in Newark Bay toward the LPR due to a combination of tidal pumping and gravitational circulation (Chant 2006; Pecchioli et al. 2006; Sommerfield and Chant 2010).

[150] In the contaminant concentration mapping performed as part of the RI (see Appendix J), the shoals as defined by USEPA's "broad shoals" and "margins" geomorphic regions (SEI and HDR|HydroQual 2011) are used as an interpolation group boundary within the LPR (one of several). The contaminant mass interpolation uses the same boundaries (see Appendix I).

[151] For example, mapped concentrations characterized by Conditional Simulation 37 (a random realization of the concentration field implied by the 2005 to 2013 data; see Appendix J) yield an RM 4 to RM 14 average 2,3,7,8-TCDD concentration of about 2,500 ng/kg in the shoal versus about 800 ng/kg in the channel.

larger fractional area of the shoals (68% of the total area) and similar average surficial fine sediment fraction (Figure 6-13). As noted above, the navigation channels in this region have been heavily dredged and thus the channel mass is presumably significantly low biased relative to the historical accumulation of 2,3,7,8-TCDD.

6.3.2 Historical Patterns of Other Contaminants

The longitudinal patterns of total PCBs, PAHs, total DDx, and mercury mass (Figure 6-14) are considered below, building on the transport insights gained from 2,3,7,8-TCDD. It is noted that the core counts used to develop the mass interpolations (shown in blue in Figures 6-11 and 6-14, top panel) vary somewhat by contaminant due to data availability and the core selection criteria described in Appendix I. Differences in core coverage introduce some inherent uncertainty in the comparison of interpolated mass distributions across contaminants, particularly in the case of DDx as noted below.

The estimated total PCB mass inventory is shown in Figure 6-14a. The upstream and downstream source influences suggested by the surface sediment PCB data (see Section 10.2.1; Figure 4.1-9b) are supported by comparing the estimated PCB mass inventory pattern (Figure 6-14a) to that of 2,3,7,8-TCDD (Figure 6-11); the PCB center of mass is shifted toward upper Newark Bay (top panels), and the MPA distribution within the LPR is more uniform (bottom panels). The farther downstream center of mass (67% of PCB mass in Newark Bay versus 18% for 2,3,7,8-TCDD) is consistent with expectations for a more spatially distributed source with downstream influences, which may have caused the PCB distribution to better reflect the historical sediment infilling patterns discussed previously. Relative to PCBs, the 2,3,7,8-TCDD source was highly localized at RM 3, and the efficiency of the lower few miles of the LPR as a contaminant trap during peak discharges has likely limited 2,3,7,8-TCDD accumulation in Newark Bay despite the sediment infilling that occurred there. The differences in mass distribution of the two contaminants may also reflect differences in the time history of their loading; assuming the PCB loading was more evenly distributed in time than 2,3,7,8-TCDD, its inventory would be less strongly impacted by the maintenance dredging events below RM 2 that have occurred since the peak 2,3,7,8-TCDD loading. Another feature of the PCB mass distribution relative to that of 2,3,7,8-TCDD is the less pronounced decline in mass inventory above RM 12, which is consistent with a greater upstream source influence for PCBs.

The estimated mass inventories of PAHs (Figure 6-14b for HMW PAHs and Figure 6-14c for LMW PAHs) also suggest regional and local sources. The pattern for HMW PAHs is similar to that of PCBs but with somewhat greater relative mass upstream of RM 14, perhaps indicative of a stronger upstream source. Similar to PCBs, the center of mass for HMW PAHs is shifted toward Newark Bay (67% of mass for both PCBs and HMW PAHs), presumably reflecting the absence of a dominant point source and the predominant influence of the historical sediment infilling patterns. The LMW PAH mass distribution has similar features as HMW PAHs, but the center of mass is shifted upstream (52%

of total mass in Newark Bay) due to high concentrations in RM 4 to RM 6, which may indicate the presence of a localized source as previously noted in Section 4.2.9.

The total 4,4′-DDx mass distribution[152] (Figure 6-14d) should be treated with caution as it is based on a lower core count than the other contaminants, particularly between RM 2 and RM 6. The interpolated pattern is similar to that of 2,3,7,8-TCDD in that it has strong accumulation in the vicinity of the Lister Avenue site source, but the relative mass fraction in this region is much higher (88% of LPR/Newark Bay mass is in the RM 2-4 bin versus 56% for 2,3,7,8-TCDD). Peak total DDx concentrations in sediment cores collected adjacent to the Lister Avenue site in 2011 range as as high as 160,000 mg/kg—16% of the sampled layer being pure product (DDT).[153] It may be that the physical characteristics of DDT and 2,3,7,8-TCDD waste and pure product released to the river differ such that more of the DDT was sequestered close to the point of release. The differences between them may also reflect differing numbers of cores used in the mass calculation (i.e., some cores from the 1995 dataset that had relatively low concentrations of other contaminants did not have DDx data, which might have limited the spatial influence of high concentration cores adjacent to the Lister site). Zooming in on the mass outside of the RM 2-4 bin (Figure 6-15) indicates that the remaining mass inventory is distributed similar to PCBs, HMW PAHs, and mercury but not 2,3,7,8-TCDD. This perhaps reflects upstream and downstream external source influences of this widely used pesticide (supported in Section 10 based on DDx surface sediment data).

The mercury mass distribution (Figure 6-14e) appears most similar to that of total PCBs and HMW PAHs but with a stronger skew toward accumulation in Newark Bay (80% of total mass versus 67% for PCBs and HMW PAHs), consistent with the likely downstream source influence noted in Section 10. An upstream influence is also indicated by the less-pronounced decline in mass inventory above RM 12, relative to 2,3,7,8-TCDD.

[152] Due to data availability in the older core datasets, the mass inventory in Figure 6-14d is based on the sum of 4,4′-DDx (see Appendix I).

[153] These product-level concentrations are consistent with the observations of a mountain of solid DDT in the LPR that was visible during low tides while DDT was being produced at the Lister Avenue site (Centanni and Andreini 1988; Scureman and Burton 1988).

7 Summary of Modeling Results for the Lower Passaic River Study Area

7.1 Overview of Modeling Framework

A suite of coupled models was developed to simulate the important processes affecting contaminant movement in the LPR and support the LPRSA RI/FS. The modeling framework comprises five individual models: a hydrodynamic (HD) model, a sediment transport (ST) model, an organic carbon (OC) model, a contaminant fate and transport (CFT) model, and a bioaccumulation model. Together these models simulate contaminant movement and bioaccumulation in fish and crab tissue for the LPR and, through parameterization and calibration, provide predictions that reasonably match measured data. Several of the components were originally developed by USEPA, based in part on the model suite previously developed for the CARP of the NY/NJ Harbor Estuary Program, and have been adapted during the course of the LPRSA RI/FS.[154] The models are subject to the requirements of the May 2007 Settlement Agreement and Order on Consent and Statement of Work (USEPA 2007) as well as the modeling work plan developed by the USEPA (HQI 2006a, 2006b), and their application to the LPRSA RI/FS is subject to USEPA approval. The characteristics of the five models and their development are summarized below and described in detail in Appendices L through P. Section 7.2 presents several insights that are gained from application of the models. Section 7.3 summarizes some uncertainty and limitations associated with the models.

The HD model describes flow within the LPR and the adjacent NBSA, the Hackensack River, Kill van Kull, and Arthur Kill. It was developed using the Estuarine Coastal Ocean Model (ECOM; Blumberg and Mellor 1980, 1987) and is built upon the model developed by HDR|HydroQual (HQI; 2008) and accepted by USEPA. The original model development by HQI (2008) included four calibration periods that span the major data collection efforts between 1995 and 2004 within the LPR and Newark Bay, and the model was calibrated to measurements of water surface elevation, current velocity, temperature, and salinity. HQI (2008) presents the calibration and validation results, and it concludes that the model is adequately calibrated and ready for use with the other LPR model components. After receiving the model from USEPA, the CPG modeling team conducted extensive tests and additional model validation using LPR RI/FS datasets (e.g., the PWCM data described in Section 2.4). Under USEPA oversight, the CPG also refined some aspects of the model, including an update to the model's input bathymetry to better represent the geometry of the LPR and the development of a truncated model grid suitable for use in LPR RI/FS simulations (Figure 7-1; this grid is also used by the ST, OC, and CFT models). HD model inputs include water surface elevations, water temperature, and salinity boundary conditions at the southern end of the Arthur Kill and the eastern end of the Kill

[154] In some cases, changes have been made to process representations of the underlying model frameworks, as documented below and in the supporting model appendices. These changes have been discussed with USEPA in conjunction with their model oversight.

van Kull (extracted from model simulations using the larger full grid of the region); freshwater discharge boundary conditions at Dundee Dam, the Hackensack River, several LPR tributaries, and CSO/SWOs; and wind and heat flux forcing throughout the domain. Boundary inputs were provided by USEPA, including those at the Kills which reflect USEPA's regional CARP model output. Additional details on the HD model and its development are provided in Appendix L.

The ST model incorporates the flows calculated by the HD model, and it calculates the erosion, deposition, and transport of sediments within the LPR and NBSA. The ST model framework is the same one used by USEPA in the FFS (LBG 2014) and the March 2016 Record of Decision for the Lower 8.3 Miles (USEPA 2016). It involves an implementation of the SEDZLJ bed model (Jones and Lick 2000) within the computational framework of the ECOM HD model. The SEDZLJ bed model describes the interaction between the bed and the water column (deposition and erosion, including entrainment and bedload transport) and allows for the parameterization of erodibility of bed sediments based on measurements on sediment cores conducted using Sedflume (McNeil et al. 1996; Jepsen et al. 1997; Roberts et al. 1998). During the course of its application to the LPR as part of the FFS, SEDZLJ was further developed by USEPA to include a bed consolidation model developed by Sanford (2008), which calculates the evolution of sediment density and erosion properties for deposited sediments in time and over depth. The combined HD and ST modeling framework is referred to as the ECOM-SEDZLJS model. Under USEPA oversight, this framework was modified by the CPG in a few respects, most notably by the inclusion of a sediment fluff layer (i.e., a thin, easily erodible sediment layer overlying less erodible parent bed layers; see Section 3), and the inclusion of the erosion and suspended sediment loading due to navigation scour in selected portions of the western side of the LPR below RM 1.5.[155] ST model inputs include suspended solids concentrations (SSCs) entering the domain at each boundary, the sediment types and classes to be represented, initial conditions for grain size distribution and density in the sediment bed, and parameterization of the erosion and deposition formulations in the model. In addition, as mentioned previously, the model framework was also extensively modified by both USEPA and CPG to represent various features and processes relevant to sediment transport dynamics in the LPR. Model application occurred in parallel with data analysis and model development. For instance, tests with the model setup initially developed using Sedflume measurements from the LPR showed erosion depths and SSCs significantly larger than measured values during both low-flow and high-flow periods. This led to a more comprehensive analysis of the Sedflume data, which identified certain biases in the data, which, in turn, resulted in a calibration strategy to appropriately parameterize the erodibility inputs derived from the Sedflume data. Subsequent model test runs showed that the revised approach tended to perform well during high-flow conditions but not during low-flow conditions. This, in turn, led to the formulation, implementation, and data-based parameterization of a fluff layer in the ST

[155] The empirical representation of navigation scour in the LPR is described in Appendix M. The areas subject to scour are shown in Figure 34 of Appendix M.

model, consistent with the expectation that this thin layer of unconsolidated sediments dominates intratidal suspended solids dynamic during low-flow conditions (see Section 3.4 and Appendix M). Therefore, even though the various model inputs and parameters have been defined to a large extent by data from the LPR, with minimal adjustment during calibration, the CPG's ST model represents the product of a collaborative effort under USEPA oversight related to data collection, data analyses, model development, and model calibration. The ST model includes two cohesive classes (clay and silt) and three non-cohesive classes (fine-medium sand, coarse sand, and gravel). The ST model was applied to the 1995 through 2013 period, covering discharge conditions ranging from low-flow conditions to an extreme event (Hurricane Irene, a 1-in-90-year storm event). The model was calibrated and validated to a number of datasets, including SSCs and solids fluxes measured as part of the PWCM program, SSCs measured during the CWCM program and during extreme high-flow conditions, and short-term bathymetric changes between periodic bathymetric surveys conducted as part of the LPR RI/FS, as well as long-term bathymetric changes following the 1949 dredging within the lower 8 miles of the LPR. Additional details on the ST model and its development are provided in Appendix M.

The CPG OC model incorporates the results of the HD and ST models together with carbon boundary loadings to simulate the fate and transport of two carbon fractions in the water column; algae-associated (or biotic) carbon and sediment-bound detrital (or abiotic) OC. Algae-associated carbon enters at the boundaries, but growth and respiration within the model domain are not simulated. It is subject to settling and deposition to the bed. Detrital carbon is treated as a conservative substance subject to bed-water exchange via resuspension and deposition. The OC model is a USEPA-approved simplification of the full eutrophication model (Sediment Transport-System Wide Eutrophication Model [ST-SWEM]) originally proposed by the USEPA Region 2 (HQI 2006a) and applied in the FFS (LBG 2014). Model inputs include external carbon loadings from the various inflows into the LPR (set to the same values as the USEPA FFS eutrophication model [USEPA 2016]) and the OC content of the sediment bed for detrital carbon (set using RI/FS sediment OC measurements). Detrital carbon is assumed to be associated with only the cohesive fraction of sediments (clays and silts). DOC is not calculated dynamically in the model but instead specified as temporally constant values that vary longitudinally across the domain, based on observed spatial patterns. Comparisons of CPG OC model predictions to measurements have indicated some differences primarily in the concentrations of algal carbon during summer months, likely due to the effects of algal growth, which are not incorporated in the model; however, these differences were demonstrated to have a nominal impact on associated CFT model test simulations. Additional details on the OC model and its development are provided in Appendix N.

The CFT model calculates contaminant concentrations in the sediment and overlying water column based on the predicted spatial and temporal dynamics of flow, sediments, and carbon. It has been built using the RCATOX modeling framework developed by HQI, which was previously applied by

USEPA to the LPR as part of the regional CARP model of the NY/NJ Harbor Estuary (HQI 2007) and on a finer scale in the FFS (LBG 2014; USEPA 2016). The RCATOX model framework includes mechanistic descriptions of the major fate and transport processes affecting the LPR contaminants, including partitioning between the dissolved and particulate phases; exchanges between the sediment bed and water column due to resuspension, deposition, and porewater diffusion; vertical mixing and diffusion within the sediment bed; and advection, settling, and volatilization within the water column (see Section 6.1 and Figure 6-1 for more discussion of these processes). Under USEPA oversight, the RCATOX framework was modified and/or parameterized by the CPG to reflect several additional processes during CFT model development.

The most notable modifications and parameters are as follows:

- A sediment fluff layer was added to better represent the intra-tidal contaminant erosion and deposition fluxes.
- A kinetic sorption framework was added to account for resistantly sorbed chemical so as to avoid over-specifying desorption from resuspended sediments.[156]
- A revised cohesive erosion velocity formulation was adopted to better represent the impact of vertical gradients in sediment composition on the erosion flux of contaminants.
- Sediment mixing intensity was specified as variable over the upper 10 cm in consideration of available literature (Dauer et al. 1987); this assumption is supported by the results of the SPI survey for the LPR (Germano & Associates 2005).
- The contaminant loading associated with navigation scour was added for consistency with the ST model, representing this term as a reduction of bed contaminant inventory and a corresponding release of contaminant mass to the water column.

As agreed to by USEPA, the CFT model has been calibrated for 2,3,7,8-TCDD, tetra-CBs, and 1,2,3,4,6,7,8-HpCDF, which were selected as the primary calibration chemicals of potential concern (COPCs).[157] In addition, the model has been supplemented with six secondary calibration COPCs: 1,2,3,7,8-PeCDD, 2,3,4,7,8-PeCDF, PCB-126, PCB-167, total 4,4′-DDx (i.e., sum of 4,4′ isomers only), and mercury. This suite of COPCs was selected for several reasons, including human health and ecological risk, the desire to calibrate across a wide range of sorption properties, the need for a high frequency of detected concentrations in sediment and water to constrain the calibration, and the ability to correlate un-modeled chemicals of interest to modeled chemicals (e.g., for risk estimation). The details of the selection criteria applied are described in Anchor QEA's December 2016

[156] Over-predicting contaminant mass transfer from resuspended sediments may cause an artificial reduction of predicted surface sediment concentrations by transferring resistantly sorbed contaminant mass to non-settling forms of carbon. Support for resistant phase sorption of the modeled contaminants is discussed in Section 6.1 and Appendix G.

[157] The CFT model has been calibrated to fewer COPCs than originally envisioned in the USEPA LPR Modeling Workplan (HQI 2006a; Section 5.6).

memorandum. The primary COPCs[158] best met all the criteria and thus were the focus of the calibration efforts, whereas secondary COPCs were added as a check on model behavior and parameterizations or if deemed necessary for characterizing future risks in future FS analysis of alternatives. In considering potential FS needs, it was recognized that predictions of the nine modeled COPCs can be used to estimate the concentrations of several other COPCs and toxicity equivalence (TEQ) values that may be needed in the FS by applying correlations derived from bed and water column data. In particular: total PCBs can be estimated from tetra-CB predictions; total DDx can be estimated from total 4,4′-DDx predictions; PCB-105 and PCB-118 can be estimated from PCB-167 predictions; total PCDD/PCDF TEQ can be estimated from 2,3,7,8-TCDD, 1,2,3,7,8-PeCDD, and 2,3,4,7,8-PeCDF predictions; total PCB TEQ can be estimated from PCB-126 and PCB-167 predictions combined with PCB-105 and PCB-118 estimates from PCB-167; and methyl mercury can be estimated from mercury predictions. Initial efforts to develop these correlations from the data were presented in Anchor QEA (2016) and subsequently updated correlations, along with accompanying analyses, will be documented in a separate document to be reviewed by USEPA once finalized.[159]

A main input to the model is the contaminant initial condition for the sediment bed, which was defined for two time horizons in support of the CFT model calibration periods: a "1995 mapping" (i.e., based on 1995 to 1999 sediment data) was used to initialize water year (WY) 1996 to WY2013 calibration runs and a "2010 mapping" (i.e., based on 2005 to 2013 sediment data collected for the RI/FS) was used to initialize WY2012 to WY2013 calibration runs. Contaminant loadings at the boundaries were applied directly from USEPA inputs from the FFS model (USEPA 2016) but have been mapped to the more finely resolved CFT grid used by the CPG (see Figure 7-1). Scaling factors were applied to the Dundee Dam and/or the Kills boundaries for select COPCs during the calibration process, based on measurements at the boundaries, model-data agreement, and consideration of the uncertainty in the boundary conditions (see Section 3 of Appendix O for details). The CFT model was jointly calibrated to the water column data from the sv-CWCM program and to surface sediment data collected between 2005 and 2013. Calibration to water column data was primarily judged using the WY2012 to WY2013 simulation, which encompasses seven of the eight sv-CWCM events and uses a sediment initial condition based on the "2010 mapping." Calibration to the surface sediment data was judged using the WY1996 to WY2013 simulation, and it focuses on the region between RM 1 and RM 7, which is the longitudinal extent of the data in the "1995 mapping" used to specify initial conditions for this simulation period. Additional details on the CFT model and its calibration

[158] The December 2016 memorandum identified PCB-167 as a primary COPC. In subsequent interactions with USEPA, it was agreed that this COPC could be demoted to a secondary COPC due to concerns about the historical sediment data accuracy.

[159] The initial regressions presented in the December 2016 memorandum to USEPA were subsequently discussed in USEPA/CPG meetings. During a call on August 1, 2018, it was agreed that CPG would provide the updated regressions in a separate document once the FS needs were more clearly defined. Details of the final regression analysis, including the underlying selection of modeled COPCs, will be included in a separate document and referenced in the FS as appropriate.

are provided in Appendix O, and the development of the mappings for model initial conditions is described in Appendix J.

The modifications and calibrations of the HD, ST, OC, and CFT models have been performed under USEPA oversight, and the current level of accuracy in these models has been deemed acceptable by USEPA for the RI/FS (USEPA 2018). However, USEPA has noted that a "high degree of caution should be applied when using those predictions to compare remedial alternatives" given the uncertainties of modeling this complex system and the limits that these uncertainties and data gaps place on the accuracy of models' predictions. A discussion of the uncertainties and limitations is provided in Section 7.3.

Lastly, the bioaccumulation model, which is currently undergoing calibration, predicts contaminant concentrations in the tissue of fish and invertebrates that comprise the food web of the LPR, based on the CFT model's predictions of chemical concentrations in water and sediment. The Arnot and Gobas model (Arnot and Gobas 2004) was selected as the basis for the LPR bioaccumulation modeling effort, consistent with USEPA's LPRSA Modeling Work Plan (HQI 2006a). It is a mechanistic model that includes ecological elements (e.g., food web structure and exposure assumptions) and chemical elements (e.g., biotic chemical uptake, depuration processes, and chemical properties) and is appropriate for modeling hydrophobic organic chemicals (e.g., dioxins/furans and PCBs). The model assumes that the flux of chemicals between water and organisms, between ingested media (i.e., sediment and other organisms) and organism tissue, and between different tissue types (e.g., lipid and non-lipid organic matter) are governed by fugacity relationships (Arnot and Gobas 2004). It is based on several fundamental assumptions regarding the routes of chemical uptake and elimination, the partitioning of chemicals within organisms, and the exchange of chemicals between an organism and the environment. Several critical aspects of the LPRSA impact the bioaccumulation of chemicals in the food web: the presence of a nutrient-rich near-bottom particulate layer in the LPR, a fish community that is dominated by benthic fish,[160] and the influence of urbanization on the LPR food web.[161] The bioaccumulation model includes model compartments (i.e., species or species groups) representing 15 trophic groups, selected to reasonably replicate the LPR food web while not unnecessarily complicating the model. Model calibration for human health risk assessment (HHRA) target species will be prioritized, namely for blue crab, common carp, white perch, catfish (both white catfish and channel catfish), American eel, and freshwater bass. Calibration will be performed for three non-overlapping different spatial units—RM 0–6, RM 6–14.7, and RM 14.7–17.4, which were selected based on habitat and food web characteristics—for the three modeled chemicals (i.e.,

[160] The dominance of benthic fish causes the bioaccumulation of contaminants for most species to reflect the concentrations in benthic invertebrate tissue, which, in turn, reflects concentrations in the near-bottom particulate layer and sediment.

[161] The ecological setting of the LPR is typical of urban systems, with severely reduced habitat quality and increased urban inputs, which affect benthic invertebrate habitat and community structure and, thus, the entire food web. Watershed urbanization is known to result in a reduction of benthic diversity and to ultimately collapse the food web to a smaller number of urbanization-tolerant taxa (Eitzmann and Paukert 2010; Pearson and Rosenberg 1978).

2,3,7,8-TCDD, tetra-CB [as a surrogate for total PCBs], and 1,2,3,4,6,7,8-HpCDF). Additional details on the bioaccumulation model and its development will be provided in Appendix P (a summary of the bioaccumulation model that will be developed and finalized at a later date in coordination with USEPA).

7.2 Insights into LPR Dynamics from Model Predictions

7.2.1 Hydrodynamics

The location of the salt front as a function of discharge was analyzed using the HD model application documented in HQI (2008) and presented in Figure 3-5 and previously summarized in Section 3.3. For purposes of this analysis, the salt front was nominally defined as the location of the 2 ppth isohaline at the bottom of the water column; other details about the simulation and processing of results are presented in Appendix L. The results indicate that the salt front is situated up-estuary of RM 5 when discharge at Dundee Dam is below the annual average of 1,200 cfs (HQI 2008). The salt-front location is pushed down-estuary with increasing flow and, at 2,000 cfs, it is found on average near RM 3. During a 1-year return flow of approximately 6,000 cfs, the salt front is pushed below RM 2, while a 5-year return flow of approximately 10,000 cfs pushes the salt front below RM 1 (where the river widens rapidly). The location of the salt front is also a function of the tidal cycle, with tidal excursion lengths on the order of 2.5 to 4.5 miles from low to high tide.

7.2.2 Sediment Transport

7.2.2.1 Sediment Fluxes and Loadings

Figure 7-2 shows the water column and bed-water exchange mass fluxes calculated by the ST model within the LPR during the WY1996 to WY2013 long-term calibration period. The results are presented on a total basis in Figure 7-2a and separately for the ST model's cohesive and non-cohesive fractions in Figures 7-2b and 7-2c, respectively. The loadings to the LPR from Dundee Dam, loadings from the tributaries (Second River, Third River, Saddle River, and McDonald Brook), loadings from the CSOs/SWOs, advective transport over various reaches, advective transport into and out of the LPR, and the bed-water exchange fluxes (erosion, deposition, and navigation scour in selected areas of the LPR) are shown.

On an annualized basis over the duration of the long-term calibration period, the total solids loading to the LPR from above Dundee Dam, tributaries, and CSOs/SWOs is approximately 29,400 metric tons per year (MT/year) or 80 MT/day, of which Dundee Dam contributes about 21,400 MT/year (59 MT/day), the tributaries about 6,400 MT/year (17 MT/day), and the CSOs/SWOs about 1,600 MT/year (4.4 MT/day) (Figure 7-2a). Net export from the LPR to Newark Bay during this same period amounts to 19,200 MT/year (53 MT/day), resulting in net trapping of 10,200 MT/year (28 MT/day) within the LPR. However, the trapping dynamics vary with the hydrograph, with the low-flow

periods such as WY2002 showing net sedimentation within the LPR and high-flow periods such as WY2007 and WY2010 showing net erosion in the LPR (Figure 7-3). Consequently, the exchange between the LPR and Newark Bay is also hydrograph-dependent, with low-flow years such as WY2002 exhibiting a net import of solids from Newark Bay into the LPR, and high-flow years such as WY2007 and WY2010 showing net export from the LPR. The hydrograph influence on the trapping behavior and solids fluxes is further illustrated by contrasting the aggregated mass balance over a low-flow solids import period in June 2005 (Figures 7-4 and 7-5) and a high-flow solids export period in March 2010 (Figures 7-6 and 7-7) (these periods encompass the periods discussed in Section 3.4 and shown in Figure 3-6). Using the sedimentological regimes developed in Section 3.4, the low-flow period corresponds to Regime 1 (below about 750 to 1,000 cfs, per Appendix M) and the high-flow period corresponds mainly to Regime 3 (above about 6,000 to 7,000 cfs). In addition, the 5-month period preceding the high-flow period (October 2009 to March 10, 2010, encompassing the period shown in Figure 3-8 of Section 3.4) is included (Figures 7-8 and 7-9) to illustrate trapping and solids flux behavior during moderate flows (Regime 2) and when conditions oscillate between the low and moderate regimes (referred to as the moderate-flow period in the following text).

Non-cohesive transport (Figure 7-2c) within the LPR (in terms of external loadings as well as advective fluxes) is generally 1 to 2 orders of magnitude lower than equivalent cohesive transport terms (Figure 7-2b). In contrast, the gross erosion and deposition fluxes are considerably higher for non-cohesives, particularly in the RM 2 to RM 8 bins and RM 8 to RM 14.8 bins. This reflects the strong influence of high-flow events on primarily bedload transport in these reaches, as illustrated by the much higher non-cohesive than cohesive erosion/deposition fluxes during the high-flow period in Figures 7-6b and 7-6c; conversely, cohesive erosion/deposition fluxes are higher during low flows (Figures 7-4b and 7-4c). The moderate-flow period exhibits mixed behavior; the gross non-cohesive erosion/deposition fluxes are somewhat higher upstream of RM 8, and the gross cohesive erosion/deposition fluxes are higher downstream of RM 8 (Figures 7-8b and 7-8c).

Spatially within the LPR, the upper miles (above RM 8) are net erosional[162] and the lower miles (below RM 8) are net depositional with respect to cohesive sediments during the long-term calibration period (Figure 7-2b). Non-cohesive sediments follow a similar pattern (Figure 7-2c), with the exception that there is more trapping in the RM 2 to RM 8 bin relative to the region below RM 2, a result likely related to the lower shear stress regimes below RM 2; cohesive deposition is expected to preferentially dominate deposition in lower shear stress areas, whereas non-cohesive deposition occurs in relatively higher shear stress areas. As expected, these spatial patterns also exhibit hydrograph-dependent variability, with the high-flow periods being typically erosional above RM 2 and above RM 8 for the cohesive and non-cohesive fractions, respectively (e.g., as in Figures 7-6b

[162] The RM 14.8 to Dundee Dam reach is treated as unerodable hard-bottom in the sediment transport model per discussions with USEPA. The nominal amount of erosion indicated in Figure 7-2b reflects the resuspension of material that was accumulated during the model's "spin-up" period.

and 7-6c), and the low-flow periods being depositional for both sediment types (e.g., as in Figures 7-4b and 7-4c, except the RM 0 to RM 2 region that is subject to navigation scour). The moderate-flow period is depositional between RM 14.8 and RM 2 for both sediment types and depositional for cohesive between RM 0 and RM 2. The direction of the net solids flux within the LPR is also predicted to be strongly hydrograph-dependent, consistent with the discussion in Section 3.4. For the low-flow period, the net solids flux is upstream at RM 0 and RM 2 for most of the period, temporarily upstream during the lowest-flow days at RM 8, and consistently downstream at RM 14.8 (Figure 7-5). For the high-flow period, the solids fluxes are consistently downstream at all transects (Figure 7-7). The moderate-flow period shows a blend of these behaviors in response to changes in the hydrograph; net flux is upstream at RM 0 and 2 during most of the period but changes temporarily to the downstream direction as the flow crosses from Regime 1 into Regime 2 (Figure 7-9). Integrating over this 5-month period, the trapped mass is about 62% of the mass eroded during the subsequent high-flow event shown in Figure 7-7.

The spatial and temporal trends in trapping and the exchange with Newark Bay calculated by the ST model are consistent with the process-based description of sediment transport in the LPR, particularly the interplay between the tidal, estuarine, and freshwater forcings, and also consistent with observations from the various multi-beam bathymetric surveys conducted as part of the RI. These results suggest that currently the LPR—although, on average, slightly depositional (predominantly below RM 2)—may, on the whole, be in a state of morphodynamic equilibrium, with hydrograph-dependent inter-annual variations in trapping behavior.

7.2.3 Contaminant Fate and Transport

For brevity, the subsections below focus on 2,3,7,8-TCDD and tetra-CB results, comprising two of the three primary calibration COPCs. Corresponding figures for 1,2,3,4,6,7,8-HpCDF are included in the Attachment 4 of Appendix O. CFT model dynamics in this section are characterized using a continuous WY1996 to WY2013 simulation, i.e., the simulations do not include the WY2012 (post-Irene) sediment bed reset that was incorporated into the short-term calibration to sv-CWCM data.[163]

7.2.3.1 Contaminant Fluxes and Loadings

The contaminant mass balances predicted by the CFT model over the long-term simulation (WY1996 through WY2013) are presented in Figures 7-10a and 7-10b for 2,3,7,8-TCDD and tetra-CB, respectively. The following insights are noted from the model predictions for this period:

- The largest contaminant source to the water column was erosion, and the largest sink was deposition. The gross erosion flux was much larger than the net erosion flux for both

[163] A comparison of WY2012 to WY2013 predictions with and without the bed concentration reset is presented in Appendix O Section 4.4. The reset is not used here to avoid the influence of the bed discontinuity on the interpretation of the modeled system dynamics.

contaminants but more so for tetra-CB (15 times higher across RM 17 to RM 0) than for 2,3,7,8-TCDD (6 times higher).

- The region between RM 8 and RM 2 dominated the net sediment source for 2,3,7,8-TCDD (57%), whereas the region between RM 14.8 and RM 8 dominated for tetra-CB (64%). On a gross erosion flux basis, the RM 8 to RM 2 region dominated for both contaminants (51% and 46% of the total for 2,3,7,8-TCDD and tetra-CB, respectively), and the relative contribution of the RM 14.8 to RM 8 bin was also more similar (28% and 26%, respectively).
- The region above RM 14.8 accounts for very little (less than 0.1%) of the net LPR sediment 2,3,7,8-TCDD flux and 1% of the net tetra-CB flux (0.3% and 1.6% on a gross erosion flux basis, respectively).
- The region below RM 2 was a net sink of contaminants, capturing a mass equivalent to 3% of the net LPR sediment 2,3,7,8-TCDD flux and 6% of the net tetra-CB flux.
- The loading from the UPR at Dundee Dam (RM 17.4) was a strong contributor to the mass balance for tetra-CB; its magnitude was equivalent to 40% of the net tetra-CB flux from LPR sediments and 37% of the net load at RM 8. For 2,3,7,8-TCDD, the loading from the UPR is of lesser importance, with a magnitude equivalent to only 0.7% of the net 2,3,7,8-TCDD flux from LPR sediments and 1.5% of the net load at RM 8.
- There was a net load of contaminants to the region below RM 0 (i.e., toward Newark Bay), which reflects the balance of a dominant downstream flux and a weaker upstream flux. The upstream flux from below RM 0 was weaker in the case of 2,3,7,8-TCDD than for tetra-CB (80% and 92% of the downstream flux, respectively), reflecting the stronger downstream boundary influence of tetra-CB.
- The gross upstream contaminant flux at RM 14.8 was much smaller than at RM 8 and RM 2 (i.e., the tidal exchange of contaminants declines moving upstream).
- Point sources and exchanges across the air-water interface are nominal contributors to the mass balance for both contaminants, relative to the net sediment bed flux and the boundary loadings at Dundee Dam and RM 0.

The above insights from the model are consistent with several themes developed in Sections 4 and 6, including:

- LPR sediments are the major contaminant source to the water column, particularly for 2,3,7,8-TCDD.
- The external influence is larger for tetra-CB than for 2,3,7,8-TCDD.
- The sediments above RM 14.8 see far less contaminant exchange than downstream areas.
- Long-term contaminant trapping tends to occur in depositional areas such as the region below RM 2.

Further insights are obtained from the time evolution of the cumulative load over the WY1996 to WY2013 period (Figure 7-11; the middle panel shows cumulative net contaminant flux across transects at each of the boundaries employed in Figure 7-10, and the bottom panel shows the net trapping of contaminant within the LPR as a whole). Cumulative load increases from the Dundee Dam to RM 2 and slightly declines in the region between RM 2 and RM 0, due to the depositional environment caused by the expanding cross section in this region. The strong contribution of high-flow events is shown by the correspondence of the steps in cumulative load (middle panel) to high-flow events (top panel), most notably for Hurricane Irene in August 2011 (a 1-in-90-year flow event with a peak discharge of approximately 25,000 cfs) which accounted for about half of the predicted 2,3,7,8-TCDD and tetra-CB load from the LPR to Newark Bay over the 18-year WY1996 to WY2013 simulation. The net contaminant fluxes are smaller during lower-flow periods, and the LPR may, at times, act as a net contaminant sink; on annual timescales, the LPR is predicted to consistently be a net source of both 2,3,7,8-TCDD and tetra-CB.

To better characterize the influence of freshwater flow conditions on contaminant transport dynamics, fluxes for the low-, moderate-, and high-flow periods discussed in the preceding section are considered (covering sedimentological Regimes 1, 2, and 3, respectively, as previously noted). During the June 2005 low-flow period (Figures 7-12 and 7-13), the LPR is a net source of both 2,3,7,8-TCDD and tetra-CB to Newark Bay (Figure 7-12). At both RM 8 and RM 2, cumulative upstream and downstream fluxes are of similar magnitudes but with a net downstream flux (i.e., the downstream flux is in each case slightly larger than the upstream flux on a cumulative basis), with the exception of RM 2 where there is a net upstream flux for tetra-CB (Figures 7-12 and 7-13). A net upstream transport of both 2,3,7,8-TCDD and tetra-CB is predicted to occur briefly at RM 8 during the lowest flow days of the period (Figure 7-13), which coincides with a net upstream transport of solids at this location (Figure 7-5) and a net import of solids at RM 0. However, over the full low-flow period considered, the bed between RM 14.8 and RM 8 is a net source for both contaminants. The bed between RM 8 and RM 2 behaves as a source for 2,3,7,8,-TCDD (Figure 7-12a) and a sink for tetra-CB (Figure 7-12b), whereas the bed between RM 0 and RM 2 is a net source for both 2,3,7,8-TCDD and tetra-CB during this June 2005 low-flow period.[164] The cumulative erosion and deposition fluxes of contaminants are similar in magnitude and much larger than all other fluxes (Figure 7-12), consistent with the solids mass balance (Figure 7-4); this demonstrates the importance of tidal resuspension and deposition to water column concentrations of both solids and contaminants (as discussed in Sections 3.4 and 6).

During the March 2010 high-flow period (Figures 7-14 and 7-15), the LPR acts as a source of both contaminants to Newark Bay, and the net contaminant flux is downstream at each transect

[164] Note from Figures 7-12 and 7-13 that the navigation scour is an important term in the mass balance for the RM 0 to RM 2 reach over this low-flow period; although its magnitude is only about 13% and 8% of flow-driven sediment erosion flux for 2,3,7,8-TCDD and tetra-CB, respectively, it exceeds the overall net bed flux of each contaminant.

throughout the period (Figure 7-15). The cumulative upstream fluxes at RM 8 and RM 2 are much smaller than the downstream fluxes (Figure 7-14). The bed between RM 14.8 and RM 8, as well as between RM 8 and RM 2, are sources of contaminants because the chemical erosion flux increases and far exceeds the chemical deposition flux (Figure 7-14). This is qualitatively similar to the mass fluxes of cohesive solids (Figure 7-6b). The region between RM 2 and RM 0 traps contaminant mass, which is also the case for the cohesive solids.

The predicted contaminant transport during the October 2009 and March 2010 period demonstrates alternating patterns as the hydrograph varies between low- and moderate-flow regimes, similar to the solids transport but with some notable differences. The LPR acts as a net source of both contaminants to Newark Bay (Figures 7-16 and 7-17), with a consistently net downstream flux at RM 0 over the full period (middle panel of Figure 7-17), despite the fact that the solids flux shows a net upstream transport during the lower flow portions of this period (Figure 7-9). Only at RM 2 was a net upstream transport observed for these COPCs during the lower flow periods (Figure 7-17), consistent with the upstream solids flux (Figure 7-9). A reversal in the flux direction from downstream to upstream in the estuarine portion of the LPR is conceptually consistent with a transition from Regime 2 to Regime 1 behavior (see Sections 3.4 and 6.1), though here the reversal occurs for solids but not the contaminants at RM 0. It is also noted that the trapping dynamics differ somewhat between the COPCs in that the LPR is a net exporter of 2,3,7,8-TCDD throughout the full period but at times a net importer of tetra-CB (bottom panel of Figure 7-17), i.e., during these times the loading to the LPR from upstream sources exceeds the net flux to Newark Bay at RM 0. Integrated over this full period, each of the spatial bins considered are predicted to be sources of contaminants (Figure 7-16). For 2,3,7,8-TCDD, the net bed flux is mainly from RM 14.8 to RM 2 (Figure 7-16a), whereas for tetra-CB the net bed flux is mainly from RM 14.8 to RM 8 (Figure 7-16b). For both contaminants, navigation scour has a significant contribution to the overall net bed flux between RM 2 and RM 0, similar to the low-flow periods in Figures 7-12a and 7-12b.

The correspondence of the contaminant flux with the cohesive solids flux reflects the fact that the particulate fraction tends to dominate the net longitudinal transport for the LPR COPCs and the model's assumption that non-cohesive solids do not sorb contaminant. Although the dissolved fraction will vary on intratidal timescales and can be a significant fraction of the total concentration in the water column (particularly for tetra-CB; see Section 6.1 and Appendix O), the particulate load dominates for both contaminants when integrated over the long term. Over the WY1996 to WY2013 period, the dissolved fraction is predicted to contribute about 3% to 5% of the net cumulative load for 2,3,7,8-TCDD and about 10% to 25% for tetra-CB (Figure 7-18; showing RM 8 and RM 0). The higher dissolved contribution for tetra-CB reflects its higher f_E value and its lower K_{ow} (i.e., it tends to be less resistantly sorbed and partitions more readily into the water column; see Section 6.1 and Appendix G).

The mass balance fluxes presented above demonstrate that the direction of the net contaminant flux is flow-dependent and will also be influenced by factors such as the tidal forcing and the duration of the low-flow periods. The frequency of occurrence of a net upstream daily flux generally decreases with distance upstream above RM 2 and is rare at RM 14.8, particularly for tetra-CB with its stronger upstream boundary influence (Table 7-1). It is noted that the flow threshold for net upstream contaminant flux is not necessarily the same as that of the solids fluxes, given that the contaminant fluxes depend also on horizontal/vertical concentration gradients in surficial sediment concentrations, boundary loadings, and sorption processes (see Section 6). The magnitude of the cumulative upstream flux relative to the cumulative downstream flux decreases with distance upstream, as shown in Figure 7-10 in aggregate over the WY1996 to WY2013 period. At RM 8, the ratio of the cumulative upstream flux to the cumulative downstream flux is about 0.55 for both 2,3,7,8-TCDD and tetra-CB. At RM 0, the ratio is about 0.8 for 2,3,7,8-TCDD and 0.9 for tetra-CB. The time evolution of these loads is shown along with the net load in Figures 7-19 and 7-20 for RM 8 and RM 0, respectively.

7.2.3.2 Recovery of Surface Sediments

LPR 0- to 15-cm surface sediment recovery dynamics predicted by the CFT model for RM 0 to RM 8 and RM 8 to RM 14.7 over the WY1996 to WY2013 calibration period are characterized on a mean concentration basis in Figure 7-21. During the 16 years preceding Hurricane Irene (August 2011), the model predicts reductions in mean concentration for both 2,3,7,8-TCDD and tetra-CB, with a greater reduction below RM 8 than above it. The decline in the RM 0 to RM 8 average surface 2,3,7,8-TCDD and tetra-CB concentrations is predicted to be 45% and 42% from October 1995 to August 2011, respectively. Above RM 8, the predicted mean decline was about 25% for 2,3,7,8-TCDD and 26% for tetra-CB. Hurricane Irene was predicted to have induced erosion in portions of the LPR and increased the mean surface concentrations both above and below RM 8. For 2,3,7,8-TCDD, the simulated RM 0 to RM 8 mean surface concentration increased to 86% of its WY1996 initial condition, whereas the RM 8 to RM 14.7 mean was predicted to increase to 8% above its WY1996 initial condition. For tetra-CB, the response was predicted to be somewhat less; the model's RM 0 to RM 8 post-Irene mean was about 77% of its WY1996 initial condition (i.e., about half of the pre-Irene mean recovery was reversed), and the simulated RM 8 to RM 14.7 mean increased to approximately 95% of its WY1996 initial condition. In each case, the model predicts declines during the post-Irene period, characterized by a rapid drop of the mean surface (0- to 15-cm) sediment concentrations. Note that these predicted trends differ somewhat from the trends of the averages of the surface sediment calibration datasets; in Figure 7-21, the model's long-term decline from 1995 to the pre-Irene dataset (circa 2009) is overstated relative to the trend in the data averages (RM 0 to 8 only; the 1995 calibration dataset does not contain data above RM 7) whereas the model's response to Hurricane Irene is understated relative to the pre- and post-Irene data averages. However, these model-data

comparisons in Figure 7-21 are subject to several confounding factors, as discussed at the end of this section and in Section 7.3.1.5.

The primary mechanism in the model's prediction of recovery is burial of surface sediments with less contaminated material. The greater recovery observed below RM 8 during the pre-Irene calibration period is, in part, attributed to a larger fraction of the area being depositional; during this period, 53% of the RM 0 to RM 8 region was predicted to be net depositional compared to only 17% above RM 8. The different recovery behaviors between depositional and non-depositional or erosional areas are shown in Figure 7-22, where the pre-Irene concentration (shown here at the end of WY2010) is plotted against the WY1996 initial condition on a cell-by-cell basis. The change in the mean concentration discussed above reflects a range of individual cell behaviors; cells above the 1:1 line experience an increase in concentration over the simulation whereas cells below the 1:1 line experience recovery. Erosional areas and mildly depositional areas (less than 1 cm/year) exhibit mixed concentration trends, decreasing in some cases and increasing in others. In contrast, the highly depositional cells (greater than 1 cm/year) exhibit mainly recovery, and in some cases, the predicted decline in concentration is an order of magnitude or more. The most extreme decreases that reduce concentrations by significantly more than an order of magnitude are attributable to the ST model predicting significant sand deposition that carries no contaminants with it.

It is noted that Figure 7-22 also suggests that the extent of recovery due to net deposition predicted in some cells may be exaggerated because of mismatches between the ST model's predicted deposition rate and the CFT model's initial condition. These mismatches may be caused by either the contaminant mapping (e.g., data sparsity or assumptions in the approach) or by the ST model's predictions (e.g., artifacts associated with the grid resolution) which manifest themselves in a small portion of the domain as a fairly high initial concentration subject to a high deposition rate.[165] See Appendix O for additional discussion in the context of model development and calibration to bed data.

In interpreting the model predictions of natural recovery, it is important to recognize the uncertainty that is inherent to the model and its calibration of bed COPC concentration declines. Because the 1995 dataset is restricted to the RM 1 to RM 7 reach, it does not provide a good basis to judge the model's prediction of the RM 0 to RM 8 concentration trajectory (middle panel of Figure 7-21), and it provides no basis to judge the trajectory above RM 8 (bottom panel). Rather, the historical data restrict the model's calibration of bed declines to the reach between RM 1 and RM 7 (as described in Appendix O Section 4). Moreover, model-data comparisons in this region indicate that the model tends to over-predict recovery in net depositional areas between, at a minimum, RM 1 and RM 3,

[165] In the FS, this uncertainty in the mapped concentrations and its impact on recovery will be addressed by using a conditional simulation approach to generate multiple realizations of the initial conditions for evaluation of alternatives. See additional discussion of this approach in Appendix J.

and this tendency may cause the concentration declines (recovery) shown in Figure 7-21 to be over-predicted. See Section 7.3 for additional discussion of the model's uncertainty and limitations.

7.2.3.3 Relationship Between Bed and Water Column Concentrations

The complex interactions between the bed and the water column discussed in Section 6 can be assessed using the model's prediction of the vertical concentration structure within the bed and its relationship to water column concentrations. The mean concentrations of the 0- to 15-cm sediment layer, the 0- to 2-cm layer, and the millimeter-scale fluff layer are shown together with the predicted near-bottom water column particulate concentrations in Figure 7-23, for RM 0 to RM 8 and RM 8 to RM 14.8.

On average, the model predicts a vertical gradient to exist within the upper layers of the sediment bed: the 0- to 15-cm mean (black line) is greater than the 0- to 2-cm mean (blue line), which is mostly greater than the fluff layer mean (green line). The gradients are larger for 2,3,7,8-TCDD than for tetra-CB. The water column particulate mean concentration (red line) is similar in magnitude to the fluff layer mean (green line) for 2,3,7,8-TCDD and somewhat higher than the fluff layer for tetra-CB, presumably reflecting its higher boundary loading. The prediction of a concentration gradient between the mean water column concentration and the 0- to 15-cm mean sediment concentration is qualitatively consistent with observations presented in Section 6.2.4 (see Figure 6-12), and the gradient between the fluff layer concentrations and the underlying bed is a contributing factor to the model's response. Other factors noted in Section 6.2.4 may also be contributing to the model's response, such as the diluting effect of solids resuspended from areas of lower contaminant concentration and of solids entering from boundaries.

Figure 7-23 also demonstrates that the mean fluff layer concentration fluctuates on much shorter timescales than the 0- to 15-cm layer due to its thinness. The variability in the 0- to 2-cm layer mean is significantly lower than the fluff layer and slightly higher than the 0- to 15-cm mean. The near-bottom water column mean has a time history that is similar to that of the fluff layer but with greater variability, presumably reflecting a combination of effects including:

- The episodic scour of bedded sediment beyond the fluff layer (particularly during higher-flow events), suggested by the correspondence of many (but not all) of the largest spikes in the bottom water concentration with spikes in the hydrograph
- Boundary loadings and the movement of the ETM, where the latter is suggested by the observation that some of the highest RM 8 to RM 14.8 mean water column concentrations (bottom panel) occur during low-flow conditions when the ETM is most likely to be above RM 8 (e.g., most of WY2002 and the June 2005 period discussed in prior sections)

The response of the bed and water column concentrations to an extreme high-flow event can be evaluated by focusing on the period during and after Hurricane Irene (Figure 7-24; sv-CWCM data

means for each sampling event are also shown for reference). In the RM 0 to RM 8 region (middle panel), Hurricane Irene increases bed concentrations, with the increase being larger for the 0- to 2-cm mean than it is for the 0- to 15-cm mean. Concentrations subsequently decline, with the rate being greater for the 0- to 2-cm interval than the 0- to 15-cm interval. Immediately after Irene, the fluff and water column mean 2,3,7,8-TCDD concentrations are increased and exhibit more variability than the period before Irene. They gradually decline but do not achieve pre-Irene conditions by the end of the simulation in 2013. This effect is more muted for tetra-CB, perhaps indicative of its stronger boundary influence. In the RM 8 to RM 14.8 region (bottom panel), the mean fluff layer and water column concentrations immediately after Irene are similar to pre-Irene conditions and gradually increase during the predominantly low-flow post-Irene period. This behavior is consistent with the conceptual model presented in Sections 3.4 and 6.1, wherein the fluff layer is washed out downstream during high-flow conditions and re-forms during ensuing low-flow conditions (i.e., Regime 1). The low-flow period also coincides with a gradual increase in the 0- to 2-cm mean concentration between RM 8 to RM 14.8, which plateaus by the end of WY 2013.

One feature of note in Figures 7-23 and 7-24 is that there are instances where the estimated mean fluff layer concentration is lower than the mean 2-cm bed concentration and the mean bottom water column concentration. Though counter-intuitive, this result may simply reflect the complex dynamics that control the water column reach-wide mean concentration and the different timescales of variation within each mean. The water column mean reflects a mixing of boundary influences from above and below the reach and flux from the fluff layer and underlying bed, where the latter's contributions vary in space and time due to erosion and deposition patterns and horizontal and vertical concentration gradients in the bed. However, it is also noted that the mean concentrations in Figures 7-23 and 7-24 may be influenced by the bulk density assumptions for the fluff layer[166] and the spatial and temporal averaging method,[167] most notably for the water column and fluff layer where concentrations vary rapidly in time and space due to the tidal currents. Because the calculation within the CFT model is on a volumetric basis, the uncertainty associated with the dry-weight fluff concentrations shown in Figures 7-23 and 7-24 does not impact the CFT model's mass transport (i.e.,

[166] As described in Appendix O Section 2, the CFT model predicts volumetric concentrations in the fluff layer from contaminant fluxes from the water column and underlying bed together with the time-variable fluff thickness. Although the fluff thickness Is based on the ST model's bed elevation change and thus indirectly reflects the ST model's dynamic fluff bulk density, this quantity is not explicitly tracked by the CFT model, and structural differences between the models complicate the direct coupling of ST model bulk density (see Appendix O Section 2). As such, a constant representative bulk density of 0.355 gram per cubic centimeter (g/cm^3) has been assumed for post-processing, based on ST model output evaluations.

[167] The CFT model computes the volumetric concentration of contaminants in all media; thus, the quantities plotted are derived quantities rather than model state variables. The water column means in Figures 7-23 and 7-24 are the daily average particulate concentrations normalized by the daily average suspended solids concentrations in the lower tenth of the water column, which are then 5-day rolling-averaged and averaged longitudinally within the designated RM bins for main channel cells only (model grid row J=17; in order to avoid the inclusion of drying cells). The fluff layer mean dry-weight concentration is the volume-weighted mean volumetric concentration in the fluff layer (averaged in time and space) normalized by a representative bulk density derived from ST model output.

the exchanges between the fluff layer and the water column and underlying bed layer are based on volumetric COPC concentration, not dry-weight concentration).

7.2.4 Bioaccumulation Model

7.2.4.1 Predicted Routes of Bioaccumulation

Updates to bioaccumulation model predictions presented in this section are pending bioaccumulation model calibration updates.

7.3 Model Uncertainty and Limitations

This section summarizes some of the uncertainties and known limitations associated with the models developed for the LPRSA RI/FS. Per the guidelines set forth in USEPA's 2017 memorandum on remediating contaminated sediment sites (USEPA 2017a), model limitations should be considered in the evaluation of remedial alternatives and in the weighting of model predications within the overall remedial decision making for a site. Although limitations exist for each of the models described in Section 7.1, the following discussion focuses on how the CFT model's predictions are influenced given its role as a tool to characterize COPC concentration reductions under various remedial strategies and because it integrates the predictions of the HD, ST, and OC models.

7.3.1 Uncertainty

All model simulations are subject to some degree of uncertainty. The calculated COPC concentrations are subject to the CFT model's limitations and those of the hydrodynamic, sediment transport, and OC models that feed into it. The limitations can broadly be grouped into five general categories:

- Approximate representations of the physical and chemical processes
- Approximate understanding of model parameters
- Under-representation of spatial heterogeneity
- Uncertainty in model initial and boundary conditions derived from sparse point measurements
- Data gaps in characterizing long-term changes in COPC concentrations

Within the language of USEPA's 2017 memorandum (USEPA 2017a), the first and third categories may be regarded as "model framework uncertainty" whereas the remaining categories are examples of "parameter uncertainty."

7.3.1.1 Approximate Representations of Physical and Chemical Processes

The major processes affecting the fate and transport of the COPCs are water movement, sediment transport, adsorption/desorption, and contaminant exchange within the bed and at the sediment-water interface. Relatively simple mathematical representations of these processes are used based on conceptual understanding and a need to lump unresolved processes together so that

their combined effects can be distilled into a tractable number of model parameters. These representations do not reflect the true complexity of the processes, and key uncertainties include the response of the sediment bed to alternating periods of erosion, deposition and consolidation; the nature and behavior of the fluff layer overlying the consolidated bed; the partitioning behavior of the COPCs in the bed and the water column (including the influence of resistant and reversibly sorbed contaminant phases); the dynamics of OC in the bed and water column (including the relative abundance of detrital, algal, and DOC); and the combination of processes that induce vertical contaminant exchange within the bed. Despite the simplifications, the model is able to capture the major features of observed behaviors.

7.3.1.2 Approximate Understanding of Model Parameters

Nearly all the coefficients and parameters have values that likely vary in space and time. Lacking the ability to reasonably characterize this variability, space and time invariant values have been used in several cases such as the erosion properties for a consolidated bed, the fraction of resistantly sorbed contaminant at equilibrium, the vertical mixing in sediments (i.e., mixing depth and vertical variation over that depth), and the rates specifying contaminant mass exchange between the fluff layer and the underlying bed and the incorporation of fluff solids into the underlying bed. Some parameters are specified by literature (the octanol-water partition coefficient and the rate of equilibration between the resistant and reversibly sorbed fractions), while others are derived from data that have been aggregated spatially (e.g., critical shear stress and erodibility from Sedflume cores [Appendix M] and the fraction of resistantly sorbed chemical from water column data [Appendix G]). Remaining parameters are calibrated within plausible ranges of values (mixing and mass transfer between the bed and fluff layer) to achieve the best fit to trends in concentrations of suspended solids, OC, and contaminants in the sediment bed and water column. Unknown is how well the values established by calibration hold for conditions outside the period of calibration, particularly as the model is used to project future concentrations under remedial scenarios. Likewise, it is often unknown whether the set of calibrated parameter values are unique (i.e., alternate parameter sets may yield similar model-data agreement but somewhat different dynamics).

7.3.1.3 Under-Representation of Spatial Heterogeneity

To achieve run times that allow thorough model testing, calibration, and long-term projection of future conditions, the model coarsely represents the river. The complex cross-sectional geometry of the river is in most places represented by three lateral grid elements meant to reflect a left shoal, navigational channel, and right shoal. Along-river heterogeneity is averaged in approximately 0.2-mile increments that can group areas of differing sediment type and only roughly represent the sinuosity of the river. As a result, smaller-scale bathymetric features affecting local shear stress and sediment erodibility are not represented, and the variability in erosion and deposition are dampened, which precludes the model from replicating some spatial patterns evident when comparing

finer-scale bathymetric surveys. Similarly, the coarseness of the grid causes the model to under-represent the variability in sediment COPC concentrations and the effect of that variability on recovery and bioaccumulation.

7.3.1.4 Uncertainty in Model Initial and Boundary Conditions Derived from Sparse Point Measurements

Measurements from 490 core locations were used to establish a continuous map of contemporary COPC concentrations in surface sediments along the LPR for setting the model initial condition for the short-term water column calibration period (see Appendices J and O). The number of measurements dropped to 361 locations for subsurface sediments. The LPR covers approximately 1,019 acres, meaning the sediment data density even for surface sediments is on average only about one location every 2 acres. Furthermore, the sampling locations are frequently clustered and, in some cases, selected to confirm areas of high concentration, and there are portions of the river with no data over several acres. Geostatistical interpolation was consequently used to define contemporary COPC concentrations for each model grid cell (for the short-term model calibration) and the uncertainty of those estimates (see Appendix J). The uncertainty can be large—particularly on the scale of individual grid cells—as evidenced by comparing multiple random realizations of the concentration field that are equally plausible. Similar uncertainty exists in specifying initial conditions for the physical properties of the sediments, such as bulk density, sediment composition, and OC content.

An analogous uncertainty exists in specifying model boundary conditions. The loads of COPC, POC, and suspended solids (including the composition of the solids load) entering the LPR from Dundee Dam and tributaries are based on flow relationships that were developed (by USEPA for FFS model) from available concentration measurements and then applied to generate continuous inputs over the long term (including flow conditions for which there are little to no data). When these inputs are compared to data for the limited measurements collected at the inflow boundaries during the sv-CWCM program, there is considerable variability in the agreement between the model input load and the load inferred from the data (see Appendix O Section 3; given the uncertainty, the loading functions were, in some cases, scaled during calibration). For the downstream open boundaries at Kill van Kull and Arthur Kill, concentrations of COPC, POC, and suspended solids are specified by monthly average predictions from the regional CARP model, whose scale is such that there is likely significant uncertainty in concentrations predicted at these locations (and consequently, these boundary conditions were also scaled during calibration for several COPCs). Such boundary condition uncertainties influence the CFT model predictions in a COPC-specific manner; while the impact may be minor when simulating COPCs with a relatively low external loading (e.g., 2,3,7,8-TCDD and 1,2,3,4,6,7,8-HpCDF), the boundary uncertainty may significantly influence the calibration of COPCs with higher background concentrations (i.e., PCBs, total DDx, and mercury). Boundary uncertainty may also influence the assessment of remedial benefit during projections (e.g., boundary

loading may control the post-remedy recontamination of remediation areas). This uncertainty can only be meaningfully reduced by the collection of additional data.

7.3.1.5 Data Gaps to Assess Long-Term Changes

The model's ability to predict long-term changes in water column and sediment COPC concentrations was only partially assessed due to a paucity of historical data available for model calibration.

For surface sediments, the overlap between the "1995" and "2010" datasets was limited to the reach between RM 1 and RM 7; thus, the CFT model's calibration to bed COPC concentration changes over the long term is also restricted to this reach (as noted previously in Section 7.2.3.2). The availability of "2010" data above RM 7 characterizes contemporary contaminant concentrations across the domain for the water column calibration and for assessing remedial scenarios, but the model predictions of long-term changes above RM 7 or below RM 1 are not well constrained by data because the WY1996 initial condition is not based on measurements from that time (note the absence of data in the bottom panels of Figure 7-21 and Appendix O Figure 4.2.1-3c; the 2010 data were used to set the initial conditions above RM 7). Even within RM 1 to RM 7, characterizing the quality of the model's fit to the data is, to some degree, subjective given the inherent scale disparity in comparing a fairly sparse set of discrete sample locations to the model's grid-scale or reach-scale mean concentration, particularly given the spatial variability of the sediment data (see evaluations in Appendix J). Multiple approaches to comparing the model to the data are presented in Appendix O[168] and ultimately judged in a qualitative weight-of-evidence approach; however, the weighting is subjective and cannot overcome the uncertainty imposed by the paucity of the calibration dataset on assessing long-term trends.

For the water column, the sv-CWCM data collected between 2011 and 2013 provided a reasonably robust calibration dataset in that it covered the LPR at multiple stations across a range of flow and tide conditions, but the paucity of historical water column data means that the water column predictions could not be assessed for long-term changes. Moreover, some uncertainty in the water column calibration was imparted by the timing of the sampling events relative to Hurricane Irene; seven of eight sv-CWCM events were collected within the 2-year period after Hurricane Irene, and sediment data analyses (supported by the model response) suggest that this event had a significant impact to surface sediment concentrations (see Section 10 and Appendix O). Although the model's initial condition was, for the purpose of water column calibration, reset after Hurricane Irene to allow the model to "see" surface sediment concentrations based on contemporary RI data, it is unknown whether the conditions shortly after this event are representative (the model predicts a significant mean concentration response of the bed that decays in the ensuing period, suggesting transience in

[168] For example, the "primary metrics" include comparisons of distributions of model and data within 1-mile bins for cells with measurements (Figure 4.2.1-1), cross-plots of the model and data on the same basis (Figure 4.2.1-2), and comparisons of the RM 1 to RM 7 mean concentration to the data distributions (as box plots) and arithmetic data means (Figure 4.2.1-3).

the mean). Consequently, there is some uncertainty as to the applicability of the calibrated parameter set to simulating future conditions.

7.3.2 Model Limitations and Application

The model exhibits two notable biases that have been discussed in the supporting appendices (Appendices M and O):

- The ST model does not accurately distinguish erosion and deposition on the grid scale and tends to calculate net erosion rates that are lower than those inferred from differences between RI bathymetric surveys.
- In net depositional areas between RM 1 and RM 7, the CFT model calculates long-term reductions in surface sediment COPC concentrations (WY1996 to WY2009) that are greater than indicated by data.

7.3.2.1 Net Erosion and Deposition

The ST model tends to under-predict erosion and deposition under historical flow conditions, as judged by comparisons of model predictions to multi-beam bathymetry surveys collected between 2007 and 2012. Comparisons of predicted bed elevation changes to changes inferred from the differencing of consecutive multi-beam surveys over this period (2007 to 2008, 2008 to 2010, 2010 to 2011, and 2011 to 2012) show that the model on average predicts a more stable sediment bed than is indicated by the bathymetric surveys (Appendix M, Figures 61 through 64), i.e., the predicted changes are generally smaller than the observed changes. The comparison is more favorable for the 2010 to 2011 multi-beam comparison, which encompasses Hurricane Irene, suggesting that the model performs better for extreme events than for low- to average-flow conditions. The comparisons also suggest that the model is better at predicting large-scale longitudinal patterns of sedimentation and erosion than it is at predicting lateral trends and localized scour on a cell-by-cell basis. These limitations are likely to be largely due to the relatively coarse grid resolution that was described in Section 7.3.1.3, which prevents finer-scale details of the river morphology from being represented. Only a refined grid resolution can materially reduce these limitations.

It is noted that the evaluation of the ST model's predictions of erosion and deposition is limited to areas of overlapping bathymetric survey coverage, which means that the model performance on the shoals cannot be evaluated.

7.3.2.2 Recovery in Net Depositional Areas

The assessment of recovery made in the RM 1 to RM 7 reach, where data from the mid-1990s can be compared to data collected between 2007 and 2010 (i.e., pre-Irene data), shows that the model tends to over-predict recovery in cells calculated to be net depositional by the ST model in the lower portion of this reach (approximately RM 1 to RM 3; see Appendix O, Figure 4.2.1-1a). Here the model

predicts that surface sediment 2,3,7,8-TCDD concentrations dropped over this period from about 550 ng/kg to about 100 ng/kg, whereas the data indicate concentrations dropped to about 250 ng/kg. This bias declines moving upstream, and the next region with a reasonable data density to support comparisons (RM 5 to RM 6) shows no bias and good overall comparability of model and data. Above RM 8, the mean predicted concentration in strongly depositional areas (defined as greater than 1 cm/year between WY1996 and WY2010) of 230 ng/kg for the period 2007 to 2010 (Figure 4.2.1-3c) is consistent with levels measured in sediments depositing on the cap in the RM 10.9 remediation area.

7.3.3 Conclusion

The LPR models represent state-of-the-science models that have been constructed with a wealth of data and system understanding that has been developed over the course of the RI. Although the model is subject to the noted limitations associated with the model framework, grid resolution, and calibration datasets, overall the present LPR models capture the major characteristics of contaminant transport and may be suitable tools to provide limited support to the development of an interim action for the upper 9 miles and associated FS. However, the limited accuracy of the current models' predictions of erosion and deposition and of risk reduction over time, due to the complexity of the system and data limitations, should be considered when making regulatory decisions for the LPRSA. Additional sampling to fill data gaps in bed and water column concentrations, coupled with refinement of the model grid's spatial resolution, are necessary to materially reduce the uncertainties noted herein.

8 Baseline Human Health Risk Assessment Summary

This section summarizes the USEPA-approved Final BHHRA that was prepared as part of the RI/FS for the LPR (AECOM 2017) and is included as Appendix D to this report. Consistent with USEPA guidance (USEPA 2002a, 2005a), an evaluation of contaminated sediment sites should use a risk-based framework that is iterative and as site-specific as possible given the available data. Using site-specific data and information that characterizes the LPR is a key component in defining the human health CSM and assessing the potential risks for selected receptors, thus providing sound information upon which risk management decisions can be made. The BHHRA accounts for current and future site conditions of the LPR, including accessibility, land use, and river-based activities to identify and quantify exposure.

The BHHRA was performed in accordance with applicable USEPA risk assessment guidance (USEPA 1989, 1991a, 1991b, 2001, 2004a, 2004b, 2009a, 2014b). The BHHRA presents the methods and procedures used and reflects USEPA Region 2 and CPG agreements and agency directives for conducting baseline risk assessments.

The BHHRA was conducted in accordance with the following four-step paradigm for HHRAs developed by USEPA (1989):

1. Data evaluation and hazard identification
2. Exposure assessment
3. Toxicity assessment
4. Risk characterization

Each step is summarized in the following subsections.

8.1 Data Evaluation and Hazard Identification

The purpose of the data evaluation and hazard identification process is twofold: 1) to evaluate the nature and the extent of the release of chemicals present within the LPR; and 2) to identify a subset of these chemicals as chemicals of potential concern (COPCs) for quantitative evaluation in the BHHRA. This step of the risk assessment involves compiling and summarizing the data and identifying COPCs.

8.1.1 Data Evaluation

As described in Section 2.4, the CPG has conducted several USEPA-approved sample collection programs within the LPR and in the UPR, resulting in an extensive site-specific dataset in support of the RI/FS. These data include sediment chemistry and toxicity, physical water quality parameters, water column chemistry, fish/decapod and benthic invertebrate tissue chemistry, benthic community evaluation, and fish community evaluation. The COPC selection process only considered data that

were collected by the CPG between 2008 and 2013 in accordance with USEPA-approved QAPPs. The data met the appropriate QA/QC and QAPP requirements. Validation of these datasets was conducted in accordance with procedures specified in the applicable QAPP, and only data qualified as useable for their intended purposes, including risk assessment, were used. The relevant datasets are summarized in the following subsections for each medium of interest (surface sediment, surface water, and fish and crab tissue).

8.1.2 Surface Sediment Dataset

Sediment samples were collected during seven sampling events between 2008 and 2013, providing an extensive characterization of sediment conditions throughout the LPR (see Section 2.4.3.2). Per the approved PFD (Windward and AECOM 2009), accessible sediment is defined as sediment under 2 feet or less of water at MLW using the USACE nominal MLW of -2.3 feet National Geodetic Vertical Datum of 1929 (NGVD 29). For the BHHRA, only accessible surface sediment samples collected from the top 0.5 foot of the sediment column from nearshore and mudflat locations are included. These criteria are consistent with exposure assessment described in Section 8.2.Based on an analysis of bathymetry and sample elevations, 180 accessible surface sediment sample locations were identified in the LPR.

8.1.3 Surface Water Dataset

The BHHRA includes data from eight surface water sample collection events conducted between August 2011 and June 2013 as part of the RI/FS CWCM SV program (see Section 2.4.4.3). The BHHRA includes data from the five surface water stations (three fixed and two floating) located in the LPR. During each event, samples were collected from approximately the middle of the channel during each of the four tide stages (i.e., ebb, low, flood, and high) at both near-surface and near-bottom sampling depths. The near-surface (shallow) samples were included in the BHHRA dataset. Based on the eight events, five sample collection stations, and four tide stages, the LPR surface water dataset for the BHHRA comprised 144 surface water samples (samples were not collected from the two floating stations during the two high-flow events).

8.1.4 Fish and Crab Tissue Dataset

The tissue dataset for the BHHRA comprises nine species of fish as well as blue crab collected in the LPR in late summer and early fall 2009 (August through September; see Appendix B). As described in the Tissue QAPP (Windward 2009), four species of fish (white perch, American eel, channel catfish, and largemouth bass) and blue crab were identified as target species for the BHHRA. Five other species (white catfish, common carp, white sucker, smallmouth bass, and northern pike) were identified as alternates or retained for analysis at the request of USEPA. Depending on species and human consumption preferences, skin-on or skin-off fillets were submitted for chemical analysis consistent with USEPA guidance (USEPA 2000).

To account for the different types of fish that may be consumed by anglers, the BHHRA evaluated a mixed-fish species diet comprising equal fractions (20%) of common carp and the four target species identified above.[169] A supplemental mixed-fish diet without carp was evaluated as part of the uncertainty analysis to provide additional risk information on the impact of carp in the diet.

Crab samples were analyzed as muscle and hepatopancreas combined as well as muscle-only tissue samples. A limited number of crab hepatopancreas-only tissue samples were also analyzed. The BHHRA assumed that anglers who eat LPR crab always consume both the muscle and hepatopancreas tissue. Two supplemental analyses were included in the BHHRA uncertainty analysis: consumption of crab muscle only and consumption of crab hepatopancreas only. These supplemental analyses provide additional risk information on the impact of the crab hepatopancreas in the diet.

The number of samples for each fish species and tissue type is summarized in Table 8-1.

8.1.5 Chemical of Potential Concern Selection

COPCs are the subset of chemicals detected in site media that are retained for further evaluation in a risk assessment. The screening process is intended to identify the following:

- Chemicals that pose negligible risks and can be eliminated from further evaluation
- Chemicals that merit further evaluation, either quantitatively or qualitatively, based on their potential to adversely affect humans depending on specific types of exposures

The screening process followed four sequential steps that considered the following: 1) essential nutrient status; 2) carcinogen status; 3) frequency of detection; and 4) toxicity screening using risk-based screening levels. In the risk-based screening step, maximum concentrations in accessible surface sediment and surface water were compared to USEPA regional screening levels for residential soil and tap water, respectively (USEPA 2015a). Maximum concentrations in each species of fish and crab tissue were compared to USEPA fish tissue screening levels (USEPA 2015b). The risk-based screening levels for noncarcinogenic chemicals were divided by 10 to adjust to a target hazard quotient (HQ) of 0.1. This step accounts for potential additivity of chemicals with the same target organ (USEPA 2015a). The use of these screening levels for selection of COPCs ensures that all chemicals that may be of concern are included in the risk assessment.

Based on the screening process, the chemicals retained for further evaluation in the BHHRA include PCDDs/PCDFs (as TCDD-Toxicity Equivalence [TEQ]), PCBs, mercury, PAHs, total petroleum

[169] Due to the limited number of largemouth bass samples, the data for largemouth bass and smallmouth bass were combined for the purposes of the BHHRA.

hydrocarbon (TPH) ranges, inorganics, pesticides, semivolatile organic compounds (SVOCs), and VOCs, summarized as follows by medium:

- **Accessible surface sediment** – 29 chemicals/groups were retained as COPCs.
- **Surface water** – 20 chemicals/groups were retained as COPCs.
- **Fish tissue** – The chemicals/groups retained as COPCs vary across species, from 7 for largemouth and smallmouth bass to 22 for common carp and 24 for the mixed-fish diet.[170]
- **Crab tissue** – The chemicals/groups retained as COPCs vary across crab tissue types, from 15 for muscle only to 25 for muscle and hepatopancreas combined.

Because of the urban nature of the LPR, many of the chemicals identified as COPCs in the Study Area are also present in background samples of sediment, surface water, and tissue media. The significance of background levels of COPCs relative to concentrations in LPR media is discussed in Section 8.2.4.1.

8.2 Exposure Assessment

The objective of the exposure assessment is to estimate the magnitude, frequency, duration, and routes of current and reasonably anticipated future human exposure to COPCs associated with the LPR. The extent of a receptor's exposure is estimated by identifying exposure scenarios that describe the potential pathways of exposure to COPCs and the specific activities and behaviors (e.g., swimming, wading, boating, and fishing) that may lead to contact with COPCs in the environment.

Centuries of industrialization and urbanization have altered the physical characteristics of the LPR, transforming the LPR into a highly channelized river, with the lower 7 miles dominated by hardened shorelines (e.g., sheetpile, riprap, and wood pilings). Land use changes have altered the ecology, limited public access, and impacted human uses of the river and shoreline. Fish consumption advisories have been in effect since the 1980s, advising against consumption of all fish and crab from throughout the LPR.

The lower portion of the river is dominated by high-density commercial and industrial development and rail/transportation infrastructure. A strip of green space (Riverfront Park) runs along the western bank of the river between RM 4 and RM 5 in Newark. Physical constraints and the primarily industrial, commercial, urban, and infrastructure land uses limit public access in the lower 7 miles, although homeless individuals have been observed along this stretch of the river. Moving upriver, land use becomes increasingly commercial and recreational, with residential pockets above RM 8. The western bank between RM 7 and RM 14 is limited to public access by Route 21, which is a four-lane highway

[170] Any chemical identified as a COPC in one or more of the five species included in the mixed-fish diet (American eel, channel catfish, common carp, largemouth/smallmouth bass, and white perch) was identified as a COPC for the mixed-fish diet.

running parallel and adjacent to the river. The eastern bank of the river between RM 7 and RM 14 has several parks and boathouses, and residential yards abut the river in some locations. Above RM 14, the river becomes narrower, shallower, and more residential. Pulaski Park is located on the western bank between RM 15.5 and RM 16. Much of the shoreline between RM 16 and the dam is vegetated with several points of public access to the water.

Future redevelopment plans include revitalizing existing parks and open space along the riverfront, and these factors were considered in the exposure assessment. Recreational activities include passive recreation (e.g., walking and biking) in the parks adjacent to the river, boating, crew/sculling, and fishing. Fishing has been observed, with most activity in the upper freshwater reach above RM 9. While angler surveys have recorded crabbing in the Newark Bay Complex (May and Burger 1996; Kirk-Pflugh et al. 1999; Burger 2002), little crabbing has been observed in the LPR proper (Desvousges et al. 2001; AECOM 2014c).

8.2.1 Identification of Exposure Scenarios

To identify relevant exposure scenarios for the BHHRA, a human health CSM was developed that takes into account the site setting and current and future uses; the physical and biological characteristics of the river; and the potential sources, transport mechanisms, and potential routes by which humans may be exposed to site-related chemicals. The human health CSM guided the identification of appropriate receptors and the pathways of exposure for quantitative and qualitative evaluation in the risk assessment.

Site-specific factors, including extensive hardened or bulkheaded shoreline; absence of areas conducive to swimming; presence of visible trash, debris, and numerous outfalls; pathogenic contamination; and advisories warning against consumption of all fish and crab throughout the Study Area tend to limit (although do not entirely prevent) current human exposures to site-related contaminants. As part of developing the CSM, potential future land uses were considered, including review of local land use plans to identify reasonably anticipated future uses. Existing plans for redevelopment and restoration call for improvement and/or expansion of existing parks and open space along the river. However, existing physical constraints, industrial and commercial development in the lower part of the river, and the urbanized environment are not expected to change significantly as a result of redevelopment and restoration actions. As such, recreational activities with a high potential for direct contact with water and accessible surface sediment (e.g., swimming) are expected to continue to be infrequent in the foreseeable future. Figure 8-1 presents the general human health CSM for the LPR.

Based on the human health CSM, the exposure scenarios listed below are considered to represent potential exposures under both current and future site conditions:

- Current/future angler/crabber (young child, adolescent, and adult)

- Current/future swimmer (young child, adolescent, and adult)
- Current/future wader (young child, adolescent, and adult)
- Current/future boater (older child, teen, and adult)
- Current/future worker (adult)

With the exception of the young child angler, all receptors were assumed to be potentially exposed to accessible surface sediment via incidental ingestion and dermal contact. Accessible surface sediment is defined as sediment under 2 feet or less of water at MLW. Except for the young child angler and the adult worker, all receptors were assumed to be exposed to surface water via incidental ingestion and dermal contact. The angler receptor was assumed to be exposed to either fish or crab tissue via ingestion.

A quantitative screening level evaluation of the outdoor air inhalation pathway due to volatilization from surface water and mudflat sediment demonstrated that this pathway poses negligible risks (see Appendix D of the BHHRA); therefore, this pathway was not considered further in the BHHRA.

8.2.2 Quantification of Potential Exposures

Consistent with USEPA guidance for Superfund risk assessment, the BHHRA has evaluated both reasonable maximum exposure (RME) and central tendency exposure (CTE) scenarios. The RME represents the 90th percentile or higher end of exposure and is defined as "the highest exposure that is reasonably expected to occur at a site" (USEPA 1989, 1992a). The CTE uses average exposure parameters to calculate the average exposure of an individual. While risk management decisions are based on the RME, the purpose of evaluating both an RME and a CTE scenario in the BHHRA is to provide risk managers and stakeholders with an estimate of the range of risks from average to upper-bound. The RME and CTE exposure parameters are presented in the BHHRA and include conservative estimates of fish tissue and crab consumption rates that were developed by USEPA Region 2, independently of CPG, based on consideration of a wide range of creel-angler surveys (USEPA 2012a). The ingestion rates were based on two published surveys conducted in the New York/New Jersey Harbor estuary with enough information to calculate statistical distributions of ingestion rates for anglers who consume their catch (Burger 2002 for fish and crab ingestion; Connelly et al. 1992 for fish ingestion).

Exposure to accessible surface sediment, surface water, and tissue was evaluated on a site-wide basis. Receptors were assumed to contact accessible surface sediment and surface water throughout the LPR and to consume fish or crab from the entire LPR. In addition, because of the potential for recreators or workers to repeatedly visit a smaller section of the river, the 17.4-mile LPR was also evaluated on a refined spatial scale for potential exposure to COPCs in accessible surface sediment (exposures to surface water and fish/crab tissue were maintained on a site-wide basis). Specifically, the river was divided into six 3-mile segments (i.e., RM 0-3, RM 3-6, RM 6-9, RM 9-12, RM 12-15, and

RM 15-17.4), as discussed below. Exposure point concentrations (EPCs) were calculated in accordance with USEPA guidance (USEPA 1992b, 2002c) and the Data Analysis and Data Usability Plan (Windward and AECOM 2015). Upper confidence limits (UCLs) on the arithmetic mean were calculated using USEPA's ProUCL software, versions 4.1.01 and 5.0.00 (USEPA 2010a, 2011, 2013b).[171] The UCL represents the arithmetic average of the concentration that is contacted over the exposure period, accounting for uncertainty and variability in the dataset (USEPA 1992b, 2002c). The EPC for the BHHRA is defined as the lower of the 95% UCL and the maximum concentration for RME and CTE scenarios. EPCs were calculated for COPCs in site-wide accessible surface sediment and in each of the six 3-mile river segments evaluated as separate exposure areas for sediment. The basis for the six segments included consideration of land use, shoreline type, access, and the primary types of human activities that take place, as summarized in Table 8-2.

EPCs were also calculated for an area of known high concentrations located along the eastern bank of RM 6-9 (RM 6-9 East Bank). This area was evaluated as a separate sediment exposure area for all receptors.

For surface water, site-wide EPCs were calculated using near-surface (0 to approximately 3 feet) data collected from the five chemical water column monitoring stations located in the main stem of the LPR. Because of continuous mixing due to changing flow, tide, and salinity conditions, only site-wide EPCs were used to evaluate exposure to COPCs in surface water.

The EPCs for fish and crab tissue were also calculated on a site-wide basis, consistent with the sample design of the Tissue QAPP (Windward 2009). Angler species preferences and abundance data were considered, and an RME mixed-species diet was evaluated that included equal fractions (20% each) of American eel, white perch, channel catfish, common carp, and largemouth bass/smallmouth bass. These five species were identified in the USEPA-approved Tissue QAPP, are found in the LPR (Windward 2010c, 2010d, 2011), and represent different habitats and feeding guilds. Additionally, available data on angler preferences suggest these species are consumed by anglers. EPCs were also calculated for an alternate mixed-fish diet excluding carp and were evaluated in the BHHRA uncertainty analysis. Only fillet data were included in EPC calculations because this is the tissue type typically consumed. Crab EPCs were calculated for edible crab tissue (muscle and hepatopancreas combined). EPCs were also calculated for crab muscle only and crab hepatopancreas only and were evaluated in the BHHRA uncertainty analysis.

Over a year-long period (September 16, 2011, to September 15, 2012), the CPG conducted a creel/angler survey (CAS) in the LPR to collect site-specific data on anglers who fish and/or crab in the 17.4-mile Study Area. It should be noted that the results represent current baseline fish and crab

[171] UCLs for site-wide fish and crab tissue were calculated with ProUCL Version 4.1.01, the latest version available before ProUCL Version 5.0.00 was released by USEPA. UCLs calculated using ProUCL Version 5.0.00 include accessible surface sediment, surface water, additional mixed-diet fish tissue COPCs, and background datasets.

consumption patterns for the LPRSA, where consumption advisories are currently in place. The survey was completed without USEPA oversight or review, and the findings have not been confirmed by Region 2. Nevertheless, the study provides some information about angling behavior in the LPRSA, including angler demographics, popular angling sites on the river, species and cooking preferences, and awareness of the consumption advisories. More details about the CAS are provided in Section 2.3.1.1 of the BHHRA.

8.3 Toxicity Assessment

The purpose of the toxicity (or dose-response) assessment is to identify the types of adverse health effects a chemical may potentially cause and to define the relationship between the dose of a chemical and the likelihood or magnitude of an adverse health effect (response; USEPA 1989). Adverse effects are classified by USEPA as potentially carcinogenic or noncarcinogenic (i.e., endpoints other than cancer). Combining the results of the toxicity assessment with information on the magnitude of potential human exposure provides an estimate of potential risk or hazard.

Dose-response values were identified in accordance with USEPA guidance (USEPA 2003a, 2017). Both cancer and noncancer dose-response values were identified for oral exposures. USEPA's default absorption factors were used for evaluating dermal exposures. A default oral absorption factor of one was assumed for all COPCs except for arsenic, for which the USEPA (2012b) default of 0.6 was used. USEPA's age-dependent adjustment factors for evaluating early life exposure to chemicals that act by a mutagenic mode of action were also used. Chemical-specific discussions are provided in the following subjections for COPCs with specific toxicological issues and approaches.

8.3.1 Dioxins and Furans

The group of dioxins and furans was evaluated as TCDD-TEQ using toxicity equivalency factors (TEFs) (USEPA 2010) and the cancer (USEPA 1997) and noncancer (USEPA 2017b) toxicity values for 2,3,7,8-TCDD.

8.3.2 PCBs

For evaluation of PCB cancer risk and noncancer hazard, two separate estimates were calculated. One approach evaluated total PCBs using the cancer and noncancer toxicity values published by USEPA for total PCBs and Aroclor 1254, respectively (USEPA 2017b). The other approach evaluated the sum of dioxin-like PCBs (PCB-TEQ) using the toxicity values for TCDD-TEQ and the remaining non-dioxin-like congeners (DLCs) using the toxicity values for total PCBs and Aroclor 1254 (for cancer and noncancer, respectively). The latter approach, which is presented in USEPA's PCB risk assessment guidance, recognizes the potential for enrichment of some congeners in biotic media (USEPA 1996). The dual approach recognizes two potential mechanisms of toxicity, as well as higher uncertainty associated with the TEFs assigned to PCB dioxin-like congeners (USEPA 2013d). Two cumulative

risk/hazard estimates that include all COPCs were presented, one based on total PCBs and the other based on the sum of PCB-TEQ and non-DLCs.

8.3.3 Lead

Due to the lack of standard dose-response values, lead was evaluated in accordance with guidance using blood lead models (USEPA 1994, 2003b, 2009b).

8.4 Risk Characterization

The potential risk to human health resulting from exposure to COPCs in environmental media in the LPR was evaluated in this step of the risk assessment process. Risk characterization is the process in which the toxicity information is integrated with quantitative estimates of human exposure derived in the exposure assessment. The result is a quantitative estimate of the likelihood that humans will experience any adverse health effects given the exposure assumptions made. Two general types of health risk are characterized for each potential exposure pathway considered: potential carcinogenic risk and potential noncarcinogenic hazard. The potential carcinogenic risks and noncarcinogenic hazards calculated for each receptor scenario are summed to yield cumulative risks and hazards by receptor.

For each receptor, the cumulative potential carcinogenic risks were compared to the National Contingency Plan (NCP) risk range, which refers to a range of cancer risks representing one potential excess cancer incidence per population of 10,000 (i.e., one in ten thousand) to one potential excess case of cancer incidence per population of 1,000,000 (i.e., one in a million). Noncarcinogenic hazards were evaluated based on the hazard index (HI) and were compared to the goal of protection of an HI equal to 1 (USEPA 1991c). The HI represents the ratio of the exposure dose to the reference dose, below which adverse noncarcinogenic health hazards are not expected to occur. HI values below 1 indicate that potential exposures are below the reference dose, while HI values above 1 indicate that potential exposures are above the reference dose. However, the magnitude of the hazard cannot be directly equated to a probability or effect level.

As stated in USEPA's guidance, "[w]here the cumulative carcinogenic site risk to an individual based on RME for both current and future land use is less than 10^{-4}, and the noncarcinogenic hazard quotient is less than 1, action generally is not warranted unless there are adverse environmental impacts" (USEPA 1991c). Cumulative potential noncancer hazards were compared to USEPA's goal of protection of an HI equal to 1. When the HI of 1 was exceeded, a detailed evaluation by target organ was performed (USEPA 1989).

Lead was identified as a COPC in accessible surface sediment, surface water, and crab muscle and hepatopancreas tissue and was evaluated using USEPA blood lead models. For all receptors and exposure scenarios, including direct contact with accessible surface sediment, incidental ingestion of

surface water, and ingestion of crab tissue, predicted blood lead levels are less than the target blood lead level of 10 micrograms of lead per deciliter of blood (µg/dL).[172]

8.4.1 Risk Characterization Results

Tables 8-3 through 8-6 summarize the RME and CTE cumulative cancer risks and total noncancer HIs for the receptors and potential exposure pathways evaluated quantitatively in the BHHRA. Consumption of LPRSA fish and crab are the exposure scenarios that pose potential cancer risks above the NCP risk range and noncancer hazards above the goal of protection of a noncancer HI of 1. Direct contact exposures with surface water and accessible surface sediment pose risks/hazards that are below the NCP risk range and below the goal of protection of a noncancer HI of 1, with the exception of the RM 6-9 East Bank area. The risk characterization results are summarized below.

8.4.1.1 Fish Consumption

For the RME mixed fish diet, the cumulative potential RME cancer risk for the adult/young child angler is $4x10^{-3}$ for both PCB approaches, as shown in the table below. The cancer risk exceedances are principally driven by TCDD-TEQ (68% to 77%), with lesser contributions from PCBs (20% to 30%), and dieldrin, heptachlor epoxide, DDT isomers, and other pesticides (total of approximately 3%, all below the NCP risk range). RME cancer risks from exposure to sediment and surface water are within the risk range.

[172] The Centers for Disease Control and Prevention has updated its reference value for lead in the blood of children to 5 micrograms per deciliter, and USEPA is currently evaluating the updated value.

Summary of Angler Fish Consumption Cancer Risks and Percent Contribution to Cumulative Risk for Potential COCs

RME Child/Adult Angler – Consumption of Mixed Fish Diet										
	Cancer Risk (Based on Total PCBs)[a]					Cancer Risk (Based on PCB-TEQ/non-DLCs)[b]				
Potential COC	Sitewide Sediment[c]	Surface Water[c]	RME Mixed Fish Diet[d]	Total Potential Risk	% Contribution to Cumulative Risk	Sitewide Sediment[c]	Surface Water[c]	RME Mixed Fish Diet[d]	Total Potential Risk	% Contribution to Cumulative Risk
TCDD-TEQ	5E-06	8E-07	3E-03	3E-03	77%	5E-06	8E-07	3E-03	3E-03	68%
Total PCBs	2E-07	4E-09	7E-04	7E-04	20%	Presented in Cancer Risk (based on Total PCBs)				
PCB-TEQ	Presented in Cancer Risk (based on PCB-TEQ/non-DLCs)					7E-08	3E-08	6E-04	6E-04	14%
PCBs (non-DLC)						2E-07	3E-09	7E-04	7E-04	16%
4,4′-DDD	--	--	3E-06	3E-06	0.09%	--	--	3E-06	3E-06	0.08%
4,4′-DDE	--	--	8E-06	8E-06	0.2%	--	--	8E-06	8E-06	0.2%
cis-Chlordane	--	--	6E-06	6E-06	0.2%	--	--	6E-06	6E-06	0.1%
Dieldrin	4E-09	1E-09	7E-05	7E-05	2%	4E-09	1E-09	7E-05	7E-05	2%
gamma-Chlordane	--	--	2E-06	2E-06	0.04%	--	--	2E-06	2E-06	0.04%
Heptachlor epoxide	--	--	2E-05	2E-05	0.4%	--	--	2E-05	2E-05	0.4%
Hexachlorobenzene	--	--	2E-06	2E-06	0.04%	--	--	2E-06	2E-06	0.04%
Total Potential Risk[e]	**7E-06**	**2E-06**	**4E-03**	**4E-03**	**100%**	**7E-06**	**2E-06**	**4E-03**	**4E-03**	**100%**

Notes:
Blue highlighting indicates potential risks exceeding the NCP risk range of 1E-6 to 1E-4.
a. Total Risk based on all COPCs excluding PCB-TEQ and PCBs (non-DLC).
b. Total Risk based on all COPCs excluding total PCBs.
c. Adult age group. Young child angler is not assumed to be exposed to LPRSA sediment or surface water.
d. Combined adult/young child.
e. Includes risks posed by other COPCs not shown in table.
-- Not a COPC in this media.

The cumulative potential RME noncancer HIs for the young child angler (most sensitive age group) who consumes the mixed fish diet are 177 and 193 for the two PCB approaches, as shown in the table below. The noncancer hazard exceedances are driven by TCDD-TEQ (53% to 58%) and PCBs (39% to 44%), with minor contributions from methylmercury and various pesticides (total of about 3%). The highest RME target organ effect HI is 123 (young child fish consumer) based on developmental and reproductive effects (TCDD-TEQ and PCB-TEQ). The RME target organ effect HI for eye, nails, and immune effects ranges from 64 to 69 (PCBs, total, and non-DLCs). The RME target organ effect HI for neurological effects is 2 (methylmercury). All other RME target organ effect HIs are below 1 (see Appendix I of the BHHRA for target organ effect HIs).

Summary of Angler Fish Consumption Noncancer Hazards and Percent Contribution to Cumulative Hazards for Potential COCs

RME Young Child Angler – Consumption of RME Mixed Fish Diet											
		Noncancer Hazard (Based on Total PCBs)[a]					Noncancer Hazard (Based on PCB-TEQ/non-DLCs)[b]				
Target Organ	**Potential COC**	**Sitewide Sediment[c]**	**Surface Water[c]**	**RME Mixed Fish Diet**	**Total Hazard**	**% Contribution to Cumulative Hazard**	**Sitewide Sediment [c]**	**Surface Water[c]**	**RME Mixed Fish Diet**	**Total Hazard**	**% Contribution to Cumulative Hazard**
Reproductive and Developmental	TCDD-TEQ	--	--	102	102	58%	--	--	102	102	53%
	PCB-TEQ	--	--	Presented in Noncancer Hazard (based on PCB-TEQ/non-DLCs)			--	--	21	21	11%
Eye, Nails, Immune	Total PCBs	--	--	69	69	39%	--	--	Presented in Noncancer Hazard (based on Total PCBs)		
	PCBs (non-DLC)	--	--	Presented in Noncancer Hazard (based on PCB-TEQ/non-DLCs)			--	--	64	64	33%
	Mercury, inorganic	--	--	0.2	0.2	0.1%	--	--	0.2	0.2	0.1%
Neurological	Methyl mercury	--	--	2	2	1%	--	--	2	2	1%
Hair	Thallium [d]	--	--	0.5	0.5	0.3%	--	--	0.5	0.5	0.3%
Liver	4,4′-DDD [d]	--	--	0.1	0.1	0.06%	--	--	0.1	0.1	0.05%
	4,4′-DDE	--	--	0.2	0.2	0.1%	--	--	0.2	0.2	0.09%
	cis-Chlordane [d]	--	--	0.1	0.1	0.1%	--	--	0.1	0.1	0.07%
	Dieldrin	--	--	0.3	0.3	0.2%	--	--	0.3	0.3	0.2%
	Heptachlor epoxide	--	--	0.5	0.5	0.3%	--	--	0.5	0.5	0.3%
	Oxychlordane[d]	--	--	0.1	0.1	0.07%	--	--	0.1	0.1	0.07%
	trans-Nonachlor	--	--	0.6	0.6	0.3%	--	--	0.6	0.6	0.3%
	Total Hazard[e]	**--**	**--**	**177**	**177**	100%	--	--	**193**	**193**	**100%**

Notes:
Blue highlighting indicates that the hazard exceeds the goal of protection of a hazard index of one.

f. Total Hazard based on all COPCs excluding PCB-TEQ and PCBs (non-DLC).
g. Total Hazard based on all COPCs excluding total PCBs.
h. Young child angler is not assumed to be exposed to LPRSA sediment or surface water.
i. Not a potential COC on target organ basis.
j. Includes hazards posed by other COPCs not shown in table.

The cumulative potential CTE cancer risks for the mixed fish diet are within the risk range. The CTE target organ effect noncancer HIs for the mixed fish diet are 4 to 9 for developmental and reproductive effects (TCDD-TEQ and PCB-TEQ) and 3 to 6 for eye, nails, and immune effects (PCBs, total, and non-DLCs). All other CTE target organ effect HIs are below 1.

LPR fillet data were collected and analyzed for the following species: American eel, channel catfish, common carp, bass (largemouth and smallmouth), northern pike, white catfish, white perch, and white sucker and comprise the fish diet. Some of these species exhibit greater tissue burdens of bioaccumulative chemicals than others and influence risk. Risks estimated using the LPR fillet data for any combination of these species still exceed the NCP cancer risk range under the RME scenario and the noncancer goal of protection under both the RME and CTE scenarios. For example, an alternate mixed fish diet that excludes carp could pose potential risks/hazards that are approximately three-fold lower than a mixed diet that includes common carp, but still exceed the NCP cancer risk range and noncancer goal of protection of an HI equal to 1.

8.4.1.2 Crab Consumption

For consumption of crab muscle and hepatopancreas, the cumulative potential RME cancer risk for the adult/young child angler is $1x10^{-3}$ for both PCB approaches, as shown in the table below. The cancer risk exceedances are principally driven by TCDD-TEQ (77% to 90%), with lesser contributions from PCBs (7% to 20%), and dieldrin, heptachlor epoxide, other pesticides, and inorganic arsenic (total of about 3%, all below the risk range).

Summary of Angler Crab Consumption Cancer Risks and Percent Contribution to Cumulative Risk for Potential COCs

RME Child/Adult Angler – Consumption of Crab Muscle and Hepatopancreas										
Potential COC	Cancer Risk (Based on Total PCBs)[a]					Cancer Risk (Based on PCB-TEQ/non-DLCs)[b]				
	Sitewide Sediment[c]	Surface Water[c]	Crab Muscle and Hepatopancreas[d]	Total Potential Risk	% Contribution to Cumulative Risk	Sitewide Sediment[c]	Surface Water[c]	Crab Muscle and Hepatopancreas[d]	Total Potential Risk	% Contribution to Cumulative Risk
TCDD-TEQ	5E-06	8E-07	1E-03	1E-03	90%	5E-06	8E-07	1E-03	1E-03	77%
Total PCBs	2E-07	4E-09	8E-05	8E-05	7%	Presented in Cancer Risk (based on Total PCBs)				
PCB-TEQ	Presented in Cancer Risk (based on PCB-TEQ/non-DLCs)					7E-08	3E-08	2E-04	2E-04	15%
PCBs (non-DLC)						2E-07	3E-09	7E-05	7E-05	5%
Arsenic, inorganic	2E-07	4E-09	3E-06	3E-06	0.3%	2E-07	4E-09	3E-06	3E-06	0.2%
4,4'-DDE	--	--	2E-06	2E-06	0.2%	--	--	2E-06	2E-06	0.1%
Dieldrin	4E-09	1E-09	2E-05	2E-05	1%	4E-09	1E-09	2E-05	2E-05	1%
Heptachlor epoxide	--	--	1E-05	1E-05	0.9%	--	--	1E-05	1E-05	0.8%
Total Potential Risk[e]	**7E-06**	**2E-06**	**1E-03**	**1E-03**	**100%**	**7E-06**	**2E-06**	**1E-03**	**1E-03**	**100%**

Notes:
Blue highlighting indicates potential risks exceeding the NCP risk range of 1E-6 to 1E-4.
k. Total Risk based on all COPCs excluding PCB-TEQ and PCBs (non-DLC).
l. Total Risk based on all COPCs excluding total PCBs.
m. Adult age group. Young child angler is not assumed to be exposed to LPRSA sediment or surface water.
n. Combined adult/young child.
o. Includes risks posed by other COPCs not shown in table.
-- Not a COPC in this media.

The cumulative potential RME noncancer HIs for the young child angler who consumes crab muscle and hepatopancreas are 44 and 50 for the two PCB approaches, as shown in the table below (and summarized in Table 6-6). The noncancer hazard exceedances are principally driven by TCDD-TEQ (70% to 79%), with lesser contributions from PCBs (17% to 26%), and methylmercury, dieldrin, heptachlor epoxide, other pesticides, and inorganics (total of approximately 4%). The highest RME target organ effect HI is 42 (young child crab consumer) based on developmental and reproductive effects (TCDD-TEQ and PCB-TEQ). The RME target organ effect HI for eye, nails, and immune effects ranges from 6 to 7 (PCBs, total, and non-DLCs). All other RME target organ effect HIs are below 1 (see Appendix I of the Final BHHRA for target organ effect HIs).

While risks estimated based on crab muscle still exceed the NCP cancer risk range under the RME scenario and the noncancer goal of protection under both the RME and CTE scenarios, a crab muscle-only diet (i.e., removing the hepatopancreas prior to cooking) could pose risks/hazards that are approximately five- to six-fold lower than a diet of crab cooked whole and consumed with its cooking juices. Not consuming the cooking juices or pan drippings could also reduce risk from crab consumption.

Summary of Angler Crab Consumption Noncancer Hazards and Percent Contribution to Cumulative Hazards for Potential COCs

RME Young Child Angler – Consumption of Crab Muscle and Hepatopancreas											
		Noncancer Hazard (Based on Total PCBs) [a]					Noncancer Hazard (Based on PCB-TEQ/non-DLCs) [b]				
Target Organ	**Potential COC**	**Sitewide Sediment[c]**	**Surface Water[c]**	**Crab Muscle and Hepatopancreas**	**Total Hazard**	**% Contribution to Cumulative Hazard**	**Sitewide Sediment[c]**	**Surface Water[c]**	**Crab Muscle and Hepatopancreas**	**Total Hazard**	**% Contribution to Cumulative Hazard**
Reproductive and Developmental	TCDD-TEQ	--	--	35	35	79%	--	--	35	35	70%
	PCB-TEQ	--	--	Presented in Noncancer Hazard (based on PCB-TEQ/non-DLCs)			--	--	7	7	13%
Eye, Nails, Immune	Total PCBs	--	--	7	7	17%	--	--	Presented in Noncancer Hazard (based on Total PCBs)		
	PCBs (non-DLC)	--	--	Presented in Noncancer Hazard (based on PCB-TEQ/non-DLCs)			--	--	6	6	13%
Neurological	Methyl mercury[d]	--	--	0.6	0.6	1%	--	--	0.6	0.6	1%
Gastrointestinal	Copper[d]	--	--	0.3	0.3	0.6%	--	--	0.3	0.3	0.5%
Liver	4,4′-DDE[d]	--	--	0.04	0.04	0.09%	--	--	0.04	0.04	0.08%
	Dieldrin[d]	--	--	0.08	0.08	0.2%	--	--	0.08	0.1	0.2%
	Heptachlor epoxide[d]	--	--	0.3	0.3	0.7%	--	--	0.3	0.3	0.6%
	Oxychlordane[d]	--	--	0.2	0.2	0.4%	--	--	0.2	0.2	0.3%
	Total Hazard[e]	--	--	**44**	**44**	100%	--	--	**50**	**50**	**100%**

Notes:
Blue highlighting indicates that the hazard exceeds the goal of protection of a hazard index of one.
p. Total Hazard based on all COPCs excluding PCB-TEQ and PCBs (non-DLC).
q. Total Hazard based on all COPCs excluding total PCBs.
r. Young child angler is not assumed to be exposed to LPRSA sediment or surface water.
s. Not a potential COC on target organ basis.
t. Includes hazards posed by other COPCs not shown in table.
-- Not a COPC in this media.

The cumulative potential CTE cancer risks for all age groups consuming crab muscle and hepatopancreas are within the NCP risk range. The CTE target organ effect noncancer HIs for the crab muscle and hepatopancreas diet are 3 to 7 for developmental and reproductive effects (TCDD-TEQ and PCB-TEQ). All other CTE target organ effect HIs are below 1.

8.4.1.2.1 Direct Contact with Sediment and Surface Water

Sitewide surface water and accessible surface sediment in the LPR do not pose potential direct contact risks/hazards above the NCP risk range or goal of protection of a noncancer HI of 1 for recreational activities such as wading, swimming, and boating, or for workers. The exception is the noncancer hazard from accessible surface sediment in RM 6-9 (East Bank in particular), which poses a target organ effect noncancer HI equal to or in excess of 1 (ranges from 1 to 5 depending on receptor). Over 90% of the exceedance is due to TCDD-TEQ in accessible surface sediment in the RM 6-9 East Bank area.

8.4.2 Potential Chemicals of Concern Identification

Where the potential cumulative carcinogenic risks for a receptor exceeded 10^{-4}, potential chemicals of concern (COCs) were identified as any COPC with individual pathway risks greater than 10^{-6}. Where the cumulative target organ effect noncancer HI for a receptor exceeded 1, potential COCs were identified as any COPC with individual pathway HQs greater than 0.1. The list of potential COCs based on the RME scenario is presented in Table 8-7 and is summarized below:

Potential COC	Accessible Surface Sediment RM 6-9[a]	Accessible Surface Sediment RM 6-9 East Bank[a]	RME Mixed Fish Diet	Crab Muscle and Hepatopancreas
TCDD-TEQ	X	X	X	X
PCBs[b]			X	X
Pesticides[c]			X	X
Arsenic (inorganic)				X
Mercury (inorganic and methyl)			X	

Notes:

u. No potential COCs were identified for other RM segments.

v. The potential COC selection for PCBs was based on the higher of the risks/hazards estimated for total PCBs and PCB-TEQ/non-DLCs.

w. Pesticides identified as potential COCs in fish and crab tissues include: 4,4-DDD, 4,4-DDE, cis-chlordane, dieldrin, gamma-chlordane, heptachlor epoxide, hexachlorobenzene, and trans-nonachlor. Not every pesticide is a potential COC in each tissue type.

Only TCDD-TEQ and PCBs were identified as potential COCs under the CTE scenario.

8.4.3 Background

USEPA (2002b) notes that a primary objective of Comprehensive Environmental Response, Compensation, and Liability Act (CERCLA) risk assessment is to provide information on risks that can be effectively addressed through remedial actions. Taking into account background and reference area information during the risk assessment informs the understanding of risks associated with site releases, as opposed to risks resulting from the presence of contaminants that may have migrated into the site or that may reflect regional conditions related to human activities (Judd et al. 2003).

In most instances, levels of mercury, several organochlorine pesticides, and PCBs in several species of fish above the dam are comparable to levels below the dam (Figures 8-2 and 8-3). In contrast, background TCDD-TEQ tissue levels are lower than LPR tissue levels in all species of fish sampled during the RI (Figure 8-2). In addition, background levels of several potential COCs pose fish and crab consumption risks that exceed the upper end of the NCP risk range of $1x10^{-6}$ to $1x10^{-4}$ for cancer and the goal of protection of an HI equal to 1 for noncancer, and are discussed below:

- Fish: The potential cancer risk from PCBs in background (UPR) fish is above the risk range (~$3x10^{-4}$ to $5x10^{-4}$) and at the upper end of the risk range for dieldrin (~$8x10^{-5}$). The potential noncancer hazard from PCBs in background fish exceeds an HI of 1 (9 to 22), as does methylmercury (HI of 3). The background risks/hazards for pesticides and methylmercury in fish are approximately the same as LPR risks/hazards. Background PCB risks/hazards are approximately one-third of corresponding LPR risks/hazards for consumption of the mixed fish diet. Background risks/hazards for TCDD-TEQ are only approximately 2% of the corresponding LPR risks/hazards for consumption of the mixed fish diet.
- Crab: The potential background cancer risks and noncancer hazards from consuming Jamaica Bay crab (muscle and hepatopancreas) are approximately 30% to 70% of corresponding LPR risks/hazards for PCBs, methylmercury, heptachlor epoxide, and dieldrin, and approximately 8% of LPR risks/hazards for TCDD-TEQ.

Thus, upstream and regional levels of several potential COCs, including PCBs, pesticides, PAHs, and mercury, are elevated and may contribute to levels observed in the LPR and to risks estimated for LPRSA receptors. The distinguishing potential COC for the LPR when compared to other regional waterbodies is TCDD-TEQ.

8.5 BHHRA Conclusions

The conclusions of the BHHRA are summarized as follows (both RME and CTE results are discussed; however, the RME is the basis for risk management decisions):

- The predominant source of potential risk to human health is from consumption of LPRSA fish and crab. At RME exposure levels, which represent an upper bound by definition, the potential cancer risks and noncancer hazards to recreational anglers who are assumed to regularly

consume their catch (i.e., eat approximately 56 LPRSA fish meals per year or approximately 30 meals per year of 6 crabs per meal) exceed the values used by USEPA for determining whether a site poses unacceptable risk. RME cancer risks are up to 40 times higher than the NCP cancer risk range (up to $4x10^{-3}$ for fish ingestion and $1x10^{-3}$ for crab ingestion). RME noncancer hazards are up to 200 times higher than the goal of protection of an HI equal to 1 (total HIs up to 193 for fish ingestion and 50 for crab ingestion).

- At average (CTE) exposure levels (about six fish meals or four crab meals per year, accounting for cooking loss, and assuming fewer years of eating LPRSA fish/crab), the potential cancer risks to recreational anglers who consume LPR fish or crab are within the NCP risk range of $1x10^{-6}$ to $1x10^{-4}$. Potential CTE noncancer hazards are 13- to 15-fold lower for fish ingestion and six- to eight-fold lower for crab ingestion than the RME hazards, but still exceed an HI of 1 (total HIs up to 15 for fish ingestion and 8 for crab ingestion).
- The dominant potential COCs for the fish and crab consumption scenarios are TCDD-TEQ and PCBs, with methylmercury, pesticides, and to a lesser extent, inorganic arsenic and inorganic mercury also contributing to cumulative RME risks/hazards. For the LPR fish and crab risks/hazards, 2,3,7,8-TCDD contributes the majority of total TEQ risk/hazard (approximately 78% to 80%). Approximately 16% to 17% of total TEQ is attributable to PCB-TEQ, and approximately 3% to 5% is attributable to the other TCDD-TEQ congeners. There is a greater certainty in estimates of risk/hazard from 2,3,7,8-TCDD and its contribution to total risk/hazard than for the other dioxin-like compounds (USEPA 2010, 2013d).
- Background levels of several potential COCs pose fish and crab consumption risks that exceed the upper end of the NCP risk range of $1x10^{-6}$ to $1x10^{-4}$ for cancer and the goal of protection of an HI equal to 1 for noncancer. Thus, upstream and regional levels of several potential COCs, including PCBs, pesticides, and mercury, are elevated and may contribute to levels observed in the LPR and to risks estimated for LPR receptors. The distinguishing potential COC for the LPRSA when compared to other regional waterbodies is TCDD-TEQ.
- Potential RME cancer risks from direct contact exposures to accessible surface sediment and surface water in the LPRSA are significantly lower than fish and crab ingestion and are within the NCP risk range. Recreational exposure to accessible surface sediment and surface water during boating, wading, fishing, or swimming in the LPR and worker exposures to accessible surface sediment do not pose unacceptable cancer risks or noncancer hazards under the RME or CTE scenarios, with the exception of surface sediment exposure in the RM 6-9 area. An analysis of direct contact exposure to accessible surface sediment by 3-mile river segments indicates that only RM 6-9, and specifically the East Bank, poses potential RME and CTE noncancer hazards in excess of an HI equal to 1 (maximum HI of 5 for RME and 2 for CTE), due primarily to TCDD-TEQ, which contributes more than 90% of noncancer hazards.

As with all risk assessments, assumptions have been made about variables and processes that are not fully known, such as human behavior, chemical toxicity, or environmental concentrations. While the use of assumptions leads to uncertainty, it is important to note that the assumptions and approaches used in this BHHRA are health-protective, such that risks and hazards are more likely to be overestimated than underestimated (USEPA 1992c, 2005b).

9 Baseline Ecological Risk Assessment Summary

The final BERA for the LPRSA (hereafter referred to as the BERA) was conducted as part of the RI/FS and is included as Appendix D to the RI report. The BERA presents the results of the ecological risk assessment (ERA) prepared under USEPA Region 2 oversight and direction and was conducted in accordance with Section IX.37.d. of the May 2007 Administrative Settlement Agreement and AOC (USEPA 2007).

The objective of the BERA was to identify unacceptable risks posed by site-related chemicals to ecological species in the LPRSA. Consistent with USEPA guidance for the evaluation of contaminated sediment sites (USEPA 2002a, 2005a), the BERA was conducted using an iterative and site-specific approach. The basis of the evaluation of ecological risk were empirical data collected from a variety of chemical and biological sampling events and surveys in the LPRSA since 2007. These site-specific studies were developed with concurrence from USEPA and were conducted compliant with USEPA-approved QAPPs. A multi-step process was used to identify preliminary COCs; the process included the screening-level ecological risk assessment (SLERA) evaluations, which used conservative threshold values and maximum concentrations to identify a preliminary list of chemicals of potential ecological concern (COPECs) from chemicals of interest (COIs). Once COPECs had been identified, they were further evaluated in the BERA using UCLs and site-specific exposure assumptions. A range of threshold values was also used to assess potential risk, and a discussion of the uncertainty was presented. All COPECs with an HQ ≥ 1.0 based on a range of effect-level[173] toxicity reference values (TRVs) were identified as preliminary COCs.[174] In addition, a weight-of-evidence (WOE) approach was evaluated to draw conclusions about the benthic invertebrate community using an SQT approach. To identify risk drivers to be further evaluated in the FS, preliminary COCs were also evaluated based on a comparison to background concentrations (USEPA 2016) and the uncertainty of the assessment used in the BERA.

The components of the BERA are discussed in the following sections.

[173] Preliminary COCs are identified as those COPECs with HQs ≥ 1.0 based on any LOE and effect-level concentration (i.e., HQ ≥ 1.0 based on a range of lowest-observed-adverse-effect levels [LOAELs] for tissue and diet LOEs, HQ ≥ 1.0 based on acute or chronic surface water TRVs, and HQ ≥ 1.0 based on plant-specific sediment TRVs).

[174] The NJDEP acknowledges that the BERA for the LPRSA identifies unacceptable risk. However, the NJDEP's *Ecological Evaluation Technical Guidance,* August 2018 (NJDEP 2018), does not advocate the use of more than one set of TRVs for individual contaminant-receptor pairs. It is the NJDEP's position that a single TRV set (no-observed-adverse-effect level [NOAEL] and LOAEL) that evaluates the more sensitive species and endpoints to characterize risk to invertebrates, fish, birds, and wildlife should be selected in a BERA, not two sets of TRVs as presented in this document. It is the NJDEP's position that, for the LPRSA, use of one conservative TRV set derived for sensitive receptors and sensitive endpoints most clearly demonstrates the degree of risk for individual contaminant-receptor pairs and ensures protection of threatened, endangered, and species of special concern.

9.1 Problem Formulation and Data Evaluation

The problem formulation for a BERA provides the roadmap for conducting the assessment and provides a basis for dialogue with stakeholders (USEPA 1997, 1998). A PFD was developed by the CPG and approved by USEPA in 2009 (Windward and AECOM 2009). The problem formulation was then updated based on subsequent site-specific studies and surveys and summarized in the BERA. A baseline risk assessment that incorporates as much site-specific data and information as possible is crucial for developing remedial goals appropriate for the site and will support sound risk management decisions for the LPRSA.

Data used to derive risk estimates in the BERA consisted of the following data from the LPRSA collected between 2008 and 2012:

- Surface (0 to 15 cm) sediment chemistry data
- Surface (0 to 15 cm) sediment toxicity data
- Tissue chemistry data for benthic invertebrates (including benthic infaunal tissue data from laboratory-based bioaccumulation tests, blue crabs, and mussels) and fish (i.e., mummichog, other small forage fish, common carp, brown bullhead, channel catfish, white catfish, white sucker, white perch, American eel, largemouth bass, smallmouth bass, and northern pike); tissue chemistry data and their spatial variation across the LPRSA were described in Section 5.4
- Surface water chemistry data
- Biological survey data, including seasonal benthic invertebrate, fish, and avian community surveys; a habitat identification survey; and continuous near-bottom DO monitoring

In addition, data collected in the June 2005 SPI survey conducted for USEPA by Germano & Associates (2005) were used to characterize the depth of biological activity in the sediment.

The following background and reference area data from outside the LPRSA[175] were also evaluated:

- Surface (0 to 15 cm) sediment chemistry data from above Dundee Dam, Jamaica Bay, and Mullica River/Great Bay
- Surface (0 to 15 cm) sediment toxicity data collected from Dundee Dam, Jamaica Bay, and Mullica River/Great Bay
- Tissue chemistry data for fish from above Dundee Dam, Jamaica Bay, and Mullica River/Great Bay
- Surface water chemistry data collected from above Dundee Dam

[175] Background and reference area data from above Dundee Dam were collected as part of the RI using USEPA-approved QAPPs.

- Biological survey data from above Dundee Dam (including benthic invertebrate survey data), Jamaica Bay, and Mullica River/Great Bay

9.1.1 Ecological Receptor Groups

Representative receptor groups were selected and approved for use by USEPA based on the biological surveys and other information (e.g., habitat data) from the LPRSA and the surrounding area. Factors considered in this selection included the following:

- Potential for exposure to contaminated site sediments
- Relative ability to bioaccumulate/biomagnify site-related chemicals
- Societal and cultural significance (including species highly valued by society)
- Ecological significance (including species that serve a unique ecological function)
- Sensitivity to site-related chemicals

The USEPA-approved ecological receptor groups for the BERA include the following:

- Benthic invertebrate community
- Macroinvertebrate populations
- Mollusk populations
- Fish populations
- Bird populations
- Mammal populations
- Zooplankton community
- Amphibian/reptile populations
- Aquatic plant community

These receptor groups and the species selected for risk evaluation from each group are summarized in Table 9-1.

9.1.2 Assessment and Measurement Endpoints

Risk evaluation in the BERA used assessment endpoints, risk questions, and measurement endpoints consistent with the PFD (Windward and AECOM 2009).

The following community- or population-level assessments were included:

- **Benthic invertebrate community** – Protection and maintenance (i.e., survival, growth, and reproduction) of the benthic invertebrate community, both as an environmental resource in itself and as one that serves as a forage base for fish and wildlife populations

- **Blue crab** – Protection and maintenance (i.e., survival, growth, and reproduction) of healthy populations of blue crab and crayfish[176] that serve as a forage base for fish and wildlife populations and a base for sports fisheries
- **Mollusks** – Protection and maintenance (i.e., survival, growth, and reproduction) of healthy mollusk populations
- **Fish** – Protection and maintenance (i.e., survival, growth, and reproduction) of omnivorous, invertivorous, and piscivorous fish populations that serve as a forage base for fish and wildlife populations and a base for sports fisheries
- **Birds** – Protection and maintenance (i.e., survival, growth, and reproduction) of herbivorous, omnivorous,[177] sediment-probing, and piscivorous bird populations; use of LPR habitat for breeding used to determine the relative weight for the bird egg measurement endpoint
- **Mammals** – Protection and maintenance (i.e., survival, growth, and reproduction) of aquatic mammal populations
- **Zooplankton** – Maintenance of the zooplankton community that serves as a food base for juvenile fish
- **Amphibians/Reptiles** – Protection and maintenance (i.e., survival, growth, and reproduction) of healthy amphibian and reptile populations
- **Aquatic plants** – Maintenance of healthy aquatic plant populations as a food resource and habitat for fish and wildlife populations

9.1.3 Ecological Conceptual Site Model

The USEPA-approved ecological CSM for the LPRSA (Windward and AECOM 2009) is based on site-specific information about species typically present at the site or similar urbanized river systems and potential exposure pathways. The pathways evaluated in the BERA included both direct exposure through sediment and surface water and indirect exposure through ingestion of prey and incidental ingestion of surface water and sediment. The general ecological CSM is presented in Figure 9-1. Species identified in the CSM were evaluated according to the area(s) where they were found (in some cases, the entire LPRSA).

Figure 9-1 presents exposure pathways inclusive of both estuarine and freshwater organisms. As discussed in Section 5.2.1, daily and seasonal variations in salinity in the LPRSA have a significant impact upon the benthic invertebrate community, which is described in terms of three salinity zones: tidal freshwater (RM 13 to RM 17.4), fluvial estuarine (RM 4 to RM 13), and upper estuarine (RM 0 to

[176]Crayfish were identified in the PFD as representing freshwater macroinvertebrate populations. However, blue crab were the only species used to represent the macroinvertebrate population, for both the estuarine and freshwater portions of the LPRSA, because of the limited number of crayfish collected in the freshwater portion.

[177] Consistent with the PFD (Windward and AECOM 2009), omnivorous birds were not identified in the CSM as a feeding guild to be quantitatively evaluated. A representative species was not selected because the evaluation of other avian feeding guilds (i.e., sediment-probing and piscivorous birds) will be protective of omnivorous birds.

RM 4). Specific salinity zones were not developed for assessing fish. Recent fish surveys taken over a 1-year time period (Windward 2011b, 2010a, 2010b) indicated that most estuarine fish (e.g., white perch and American eel) are tolerant of brackish salinities as well as freshwater and move throughout the river as far upstream as Dundee Dam. Freshwater fish in the LPR (e.g., channel catfish, largemouth bass, smallmouth bass, and common carp) are excluded from certain portions of the LPR because of the salinity gradient; these species generally follow the salt wedge, so their location in the LPR changes accordingly. Fish species-specific exposure areas were determined based on where the organisms were found. Bird and mammal exposure areas were determined independent of salinity.

The benthic invertebrate community structure affects the bioaccumulation of chemicals in the LPRSA food chain and therefore risks to fish and wildlife. A discussion of bioaccumulation in the ecological food web is presented in Section 5.3. In summary, the benthic invertebrate community is dominated by deposit feeders, filter feeders, and detritivores. Invertebrates form the base of the food chain for higher trophic levels (e.g., fish).

9.2 Identification of Contaminants of Potential Ecological Concern

The SLERA for the entire 17.4 miles of the LPRSA was conducted and prepared in accordance with Section IX.37.d of the May 2007 Administrative Settlement Agreement and AOC (USEPA 2007). Conservative assumptions were used in the SLERA to provide a quantitative comparison between conservative exposure and effects levels in order to: 1) identify substances that could be eliminated from further consideration because they were unlikely to pose risk to ecological receptors; 2) identify COPECs that warranted further consideration in the BERA; and 3) identify chemicals that would be addressed in the BERA uncertainty section. Per USEPA, the primary objective of the SLERA was to provide information to the risk manager to confirm one of three scenarios: 1) there was adequate information to conclude that ecological risks were negligible, and therefore there was no need for remediation on the basis of ecological risk; 2) the information was not adequate to make a decision at that point, and the ERA process would continue; or 3) the information indicated the potential for adverse ecological effects, and a more thorough assessment was warranted (USEPA 1997).

Any chemical detected in the surface water, surface sediment, or tissue was identified as a COI. COIs were screened against conservative literature values or screening levels to identify COPEC per medium. COIs with maximum concentrations equal to or exceeding screening-level thresholds were identified as COPECs that were evaluated further in the BERA.

The COPECs identified in the SLERA included metals, PAHs, organochlorine pesticides, PCDDs/PCDFs, PCB aroclors, PCB congeners, SVOCs, VOCs, and cyanide, as identified for each receptor group (Table 9-2).

9.3 Risk Analysis

The potential for unacceptable risk was assessed in the BERA using empirical and modeled data collected from a variety of USEPA-approved chemical and biological sampling events and surveys conducted as part of the RI for the LPRSA. Following the identification of media-specific COPECs in the SLERA, a more detailed evaluation of potential site-specific exposure and effects was conducted to derive risk estimates (as HQs) to identify the potential for unacceptable ecological risk under baseline conditions.

Consistent with USEPA guidance, the BERA analysis was conducted by first determining the potential for exposure, then conducting an effects assessment, and finally conducting a risk characterization to estimate the potential for risk (USEPA 1997, 1998). Any chemical with an HQ ≥ 1.0 using a range of TRVs was identified as a preliminary COC. To identify risk drivers to be further evaluated in the FS, preliminary COCs were further evaluated based on a comparison to background concentrations (USEPA 2016) and the uncertainty of the assessment used in the BERA. An evaluation of the uncertainties surrounding the risk estimation and an interpretation of the potential for risk at the population level (potential for risk to ecological species is determined at the community or population level) is provided in the conclusions for the BERA (Appendix D).

In addition to the HQ approach described above, the benthic invertebrate community was evaluated using an SQT approach, which evaluated benthic infaunal invertebrate community data, sediment toxicity data, and sediment chemistry as independent LOEs. The results of these independent evaluations were assessed holistically using a WOE approach in order to evaluate impacts to the benthic infaunal invertebrate community and the relatedness of sediment chemistry to those impacts. This approach resulted in the classification of the likelihood of benthic impacts on a location-specific basis based on samples collected in the LPRSA.

As described in USEPA guidance, the results of this BERA will be used in the FS as a tool for risk managers to make potential remedial decisions for the LPRSA (USEPA 1997, 1998, 2005a). Determining the potential for unacceptable ecological risk at the population level provides information regarding decisions to be made in the FS or other programmatic environmental management changes. The TRVs used to evaluate risk to various ecological species in this BERA are organism-level effects, including those that affect particular attributes of organisms within a population, such as survival, growth, and reproduction. Survival, growth, and reproduction of individual organisms may, in turn, affect populations of those organisms, depending upon the magnitude and severity of the effect. However, population-level effects—such as size or density of a population, population growth, or population survival—are more direct measures of any influence on the population as a whole. Since BERAs evaluate populations as assessment endpoints, not individuals, a number of other factors—including the potential magnitude and severity of the effect, the ecological significance of the risk to the population, and the certainty of the assessment—should

be evaluated to determine if a risk driver should be used to develop preliminary remediation goals (PRGs) or remedial action levels. In addition, the uncertainty of assumptions related to exposure and effects data used to derive risk estimates should be evaluated as part of risk management decisions.

9.3.1 Exposure Assessment

For the exposure assessment, each receptor group representing each assessment endpoint is evaluated in terms of exposure to surface sediment and surface water in the LPRSA. For benthic invertebrates, the exposure is described in terms of distribution and co-occurrence with potential COPECs. For other receptor groups, such as fish, avian, and mammalian receptors, exposure areas are determined in the LPRSA based on ecological species utilization and habitat requirements. For the BERA, EPCs were represented by a UCL on the mean (e.g., 95% UCL[178]) concentration using USEPA's ProUCL statistical package (Version 4.1.01; USEPA 2013b). The UCL on the mean is a statistic that estimates the mean concentration with a specified degree of confidence and accounts for variability in the sampling data.

9.3.2 Effects Assessment

In the effects assessment, COPECs are evaluated for the potential for adverse effects for each assessment endpoint. Each COPEC is evaluated for adverse effects based on survival, growth, or reproduction. For benthic invertebrates, the reliability of COPECs is evaluated in terms of the potential for adverse effects on benthic organisms. The results of the effects assessment are TRVs, either as concentrations or dose levels that are used as thresholds in the risk characterization for determination of potential for unacceptable risk. A range of TRVs was evaluated in the BERA. TRV selection was based on a comprehensive review of the primary literature and an assessment of acceptability. Both no-observed-adverse-effect level (NOAEL) and lowest-observed-adverse-effect level (LOAEL) TRVs were developed based on the literature. If the most appropriate toxicological study failed to report a NOAEL estimate, the BERA used extrapolation factors to estimate a no-effect threshold dose or concentration. In addition, SSDs were developed when enough toxicity data were available for individual species. TRVs were also based on previous documents developed by USEPA Region 2 for the LPRSA; specific documents in which USEPA recommended TRVs include the following:[179]

- USEPA's LPR restoration project FFS (Louis Berger et al. 2014)

[178] There are cases (e.g., when data are highly skewed) in which USEPA's ProUCL software recommends a 97.5% or 99% UCL rather than the 95% UCL.

[179] The NJDEP acknowledges that the BERA for the LPRSA identifies unacceptable risk. However, the NJDEP's *Ecological Evaluation Technical Guidance,* August 2018 (NJDEP 2018), does not advocate the use of more than one set of TRVs for individual contaminant-receptor pairs. It is the NJDEP's position that a single TRV set (NOAEL and LOAEL) that evaluates the more sensitive species and endpoints to characterize risk to invertebrates, fish, birds and wildlife should be selected in a BERA, not two sets of TRVs as presented in this document. It is the NJDEP's position that, for the LPRSA, use of one conservative TRV set derived for sensitive receptors and sensitive endpoints most clearly demonstrates the degree of risk for individual contaminant-receptor pairs and ensures protection of threatened, endangered, and species of special concern.

- USEPA's first draft of the LPRSA FFS (MPI 2007)
- USEPA's LPR restoration project *Pathways Analysis Report* (Battelle 2005)

9.3.3 Risk Characterization, Uncertainty Analysis, and Identification of Contaminants of Concern

In the risk characterization, the estimation of risk is determined by comparing the COPEC concentration or dose level developed in the exposure analysis to the adverse effects level (TRV) developed in the effects assessment. The result of this comparison is quantified as the HQ. COPECs with HQs ≥ 1.0 (based on a range of LOAEL TRVs) in at least one LOE were identified as preliminary COCs. To identify risk drivers to be further evaluated in the FS, preliminary COCs were further evaluated based on a comparison to background concentrations (USEPA 2016) and the uncertainty of the assessment used in the BERA.

Preliminary COCs (COPECs with HQs ≥ 1.0, based on a range of LOAEL TRVs for tissue and diet, acute or chronic surface water TRVs, and plant-specific sediment TRVs) are summarized in Sections 9.4 through 9.10. HQs were also derived using NOAEL TRVs; COPECs with HQs ≥ 1.0 based on a range of NOAEL TRVs are summarized in the BERA (Sections 6.3.4, 7.1.4, 7.2.4, 7.4.4, 8.1.4, 8.2.4, and 9.1.4) and include all 21 preliminary COCs identified (based on LOAEL HQ exceedances), as well as benzo(a)pyrene, total LPAHs, and endosulfan I.

9.4 Benthic Invertebrate Assessment

The potential for unacceptable risk to benthic invertebrates included the evaluation of three receptor groups (i.e., benthic invertebrate community, macroinvertebrates [blue crabs], and mollusks). The potential for unacceptable risk to the benthic invertebrate community was evaluated primarily using a WOE approach that incorporated SQT data (i.e., benthic invertebrate community survey, sediment toxicity testing, and sediment chemistry data). Potential unacceptable risks to macroinvertebrate and mollusk populations were evaluated with blue crabs and mussels, respectively, using the surface water and tissue LOEs.[180]

9.4.1 Benthic Invertebrate Community

The assessment of risk to the benthic invertebrate community was conducted using SQT data, as well as surface water and worm tissue data in order to characterize risk.

The SQT data were evaluated as independent LOEs. The LPRSA toxicity test and benthic invertebrate community metric data were compared to USEPA-approved regional urban reference areas

[180] The evaluation of the benthic invertebrate community and sediment is considered to be protective of macroinvertebrate and mollusk populations.

(USEPA 2013e) to determine the likelihood of impacts on the LPRSA benthic invertebrate community following the evaluation framework shown in Figure 9-2.[181] Sediment chemistry data were assessed using multiple statistical approaches designed to evaluate the relative strengths and uncertainties for using the data as an LOE in predicting measurable impacts in the LPRSA. Detailed discussions on the steps conducted in the evaluation process used for each LOE are provided in the BERA (Appendix D).

A WOE framework using SQT data includes the conceptual, qualitative, and quantitative measures used to arrive at an ultimate conclusion of hazard and risk posed by sediment quality (Chapman et al. 2002). The benthic infaunal invertebrate community, sediment toxicity, and sediment chemistry data (collectively referred to as the SQT), as well as surface water and worm tissue data, were evaluated in order to characterize risk. A WOE analysis combined the three SQT LOEs into a single location-by-location characterization of risk. The WOE approach was developed in coordination with USEPA Region 2 and incorporated elements from other studies (Bay et al. 2007; Bay and Weisbert 2012; McPherson et al. 2008). To the extent possible, each LOE and WOE analysis was conducted by comparing LPRSA data to either urban or non-urban reference area data.[182] The LPRSA toxicity test and benthic invertebrate community metric data were compared to reference area data using a reference condition approach; LPRSA toxicity test data were also compared to negative control results. Reference conditions were established by screening data against sediment quality guidelines and a priori assumptions for low sediment toxicity; the 5th or 95th percentiles (as appropriate to the SQT variable) were calculated for the resulting datasets. LPRSA data were then compared to those percentiles. Based on statistical evaluations, sediment chemistry data in the LPRSA were not strongly related to responses in benthic invertebrates, either through toxicity test results or benthic community structure. Regardless, sediment chemistry data were evaluated as an independent LOE and incorporated into the WOE analysis. The sediment chemistry LOE was treated differently in the WOE analysis; LPRSA sediment chemistry data were compared to a second set of conservative sediment quality guidelines. The results from each LOE were then combined in a semiquantitative framework, allowing for a characterization of location-specific risk relative to urban reference conditions. A detailed discussion of the methods used for the WOE approach is presented in the BERA (Appendix D).

The distribution of results of the WOE analysis based on urban reference conditions is shown in Figure 9-3. The WOE analysis of the SQT data indicated that LPRSA benthic infaunal invertebrate communities were highly impacted, relative to the selected reference areas, at 18 of the 97 individual locations in the LPRSA. The SQT data from 28 locations indicated that impacts were low relative to other urbanized systems. Of the 97 SQT locations, 51 were initially categorized as having a medium

[181] Jamaica Bay was recommended by USEPA as the estuarine reference area representing urban habitat, with available SQT data collected and analyzed by others. The area upstream of Dundee Dam was approved by USEPA (Windward 2012a) as a freshwater reference area representing urban habitat, with the reference dataset collected by the CPG in fall 2012.

[182] Acceptable non-urban freshwater SQT reference data were not available to compare with LPRSA data from the tidal freshwater zone.

impact, which is a highly uncertain outcome caused by conflicting LOEs or disagreement among components of LOEs (i.e., toxicity was inconsistent across test endpoints or decreased community metrics [relative to the reference condition] were inconsistent across metrics). Medium impacts may also, in some cases, be driven by a moderate degree of chemical effects. A post-hoc analysis of medium-impact locations using additional site-specific data resulted in 20 locations being recategorized: 8 as likely low impact and 12 as likely impact. This meant that 31% of SQT locations had high impacts or were likely impacted relative to urban reference conditions, whereas 37% had no, low, or likely low impacts. Impacts at the remaining 32% of LPRSA SQT locations were uncertain but considered to be moderate.

When comparing upper and fluvial estuarine LPRSA SQT locations to non-urban reference locations, risks for the salinity zones were marginally greater than were risks based on comparing LPRSA SQT locations to urban reference conditions. Given that non-urban conditions do not take into account the possible effects on invertebrates of stressors associated with urbanization, the increase in calculated risks is to be expected. Reference conditions are meant to represent the site but for the release of site-related hazardous materials, so the use of a non-urban reference condition to characterize risks for the LPRSA (an urban system) is less informative than the use of an urban reference condition.

In addition to the WOE approach evaluation of SQT data, laboratory bioaccumulation worm tissue and surface water concentrations were compared to TRVs based on the literature to derive risk estimates (HQs) in the risk characterization. Based on this assessment, three preliminary COCs were identified with HQs ≥ 1.0 for surface water (2,3,7,8-TCDD, copper, and cyanide), and 11 preliminary COCs were identified for worm tissue (2,3,7,8-TCDD, PCDD/PCDF TEQ–fish, total TEQ–fish, total HMW PAHs, total PCBs, total DDx, selenium, and four regulated metals [arsenic, chromium, lead, and nickel]) (Tables 9-3 and 9-4).

9.4.2 Macroinvertebrates (Blue Crab)

The potential for risk to blue crab was characterized using LPRSA tissue and water chemistry.[183] Blue crab tissue and surface water concentrations were compared to TRVs based on the literature to derive risk estimates (HQs) in the risk characterization. Based on this assessment, 10 preliminary COCs were identified with HQs ≥ 1.0 in blue crab tissue (2,3,7,8-TCDD, PCDD/PCDF TEQ–fish, total TEQ–fish, total PCBs, total DDx, mercury/methylmercury, selenium, and three regulated metals [arsenic, copper, and silver]), and three preliminary COCs were identified in surface water (2,3,7,8-TCDD, cyanide, and copper) (Tables 9-3 and 9-4).

[183] For the sediment LOE, the evaluation of the benthic invertebrate community and sediment is considered to be protective of macroinvertebrate populations.

9.4.3 Mollusks

The potential for risk to mollusks was characterized using LPRSA tissue and water chemistry.[184] Mussel tissue and surface water concentrations were compared to TRVs based on the literature to derive risk estimates (HQs) in the risk characterization. Based on this assessment, five preliminary COCs were identified in mussel tissue (2,3,7,8-TCDD, PCDF/PCDD TEQ–fish, total TEQ–fish, and two regulated metals [chromium and nickel]), and three preliminary COCs were identified in surface water (2,3,7,8-TCDD, copper, and cyanide) (Tables 9-3 and 9-4).

9.5 Fish Assessment

The potential for risk to a number of fish species representing various feeding guilds (benthic omnivores [mummichog, other forage fish, and common carp], invertivores [white perch, channel catfish, brown bullhead, white catfish, and white sucker], and piscivores [American eel, largemouth bass, smallmouth bass, and northern pike]) was characterized using multiple LOEs. Fish tissue, dietary doses, surface water, and modeled fish egg concentrations were compared to TRVs based on the literature to derive risk estimates (i.e., HQs). In addition, several qualitative LOEs were evaluated that involved the assessment of LPRSA data for mummichog egg counts and gross external and internal health observations.

COPECs with HQs ≥ 1.0 based on LOAEL TRVs (using a range of TRVs) were identified as preliminary COCs (Tables 9-3 and 9-4). The following preliminary COCs were identified for fish:

- Benthic omnivorous fish populations
  - **Mummichog and other forage fish** – Five preliminary COCs (total PCBs, 2,3,7,8-TCDD, PCDD/PCDF TEQ–fish, total TEQ–fish, and one regulated metal [copper]) were identified based on the tissue LOE, and four preliminary COCs (cadmium, mercury, PCDD/PCDF TEQ–fish, and total TEQ–fish) were identified based on the dietary LOE. Total PCBs and mercury were identified as preliminary COCs for mummichog based on the egg tissue LOE.
  - **Common carp** – Seven preliminary COCs (2,3,7,8-TCDD, PCDD/PCDF TEQ–fish, total TEQ–fish, total PCBs, PCB TEQ–fish, dieldrin, and total DDx) were identified based on the tissue LOE, and four preliminary COCs (cadmium, mercury, PCDD/PCDF TEQ–fish, and total TEQ–fish) were identified based on the dietary LOE.
- Invertivorous fish populations
  - **White perch** – Six preliminary COCs (2,3,7,8-TCDD, PCDD/PCDF TEQ–fish, total TEQ–fish, total PCBs, PCB TEQ–fish, and copper) were identified based on the tissue LOE, and five preliminary COCs (cadmium, mercury, PCDD/PCDF TEQ–fish, PCB TEQ–fish, and total TEQ–fish) were identified based on the dietary LOE.

[184] The evaluation of the benthic invertebrate community and sediment is considered to be protective of mollusk populations.

  - **Channel catfish** – Six preliminary COCs (2,3,7,8-TCDD, PCDD/PCDF TEQ–fish, total TEQ–fish, total PCBs, PCB TEQ–fish, and dieldrin) were identified based on the tissue LOE, and two preliminary COCs (PCDD/PCDF TEQ–fish and total TEQ–fish) were identified based on the dietary LOE.
  - **Brown bullhead** – Four preliminary COCs (2,3,7,8-TCDD, PCDD/PCDF TEQ–fish, total TEQ–fish, and total PCBs) were identified based on the tissue LOE.
  - **White catfish** – Six preliminary COCs (mercury, 2,3,7,8-TCDD, PCDD/PCDF TEQ–fish, total TEQ–fish, total PCBs, and PCB TEQ–fish) were identified based on the tissue LOE, and three preliminary COCs (mercury, PCDD/PCDF–fish, and total TEQ–fish) were identified based on the dietary LOE.
  - **White sucker** – Five preliminary COCs (2,3,7,8-TCDD, PCDD/PCDF TEQ–fish, total TEQ–fish, total PCBs, and PCB TEQ–fish) were identified based on the tissue LOE, and three preliminary COCs (cadmium, PCDD/PCDF TEQ–fish, and total TEQ–fish) were identified based on the dietary LOE.
- Piscivorous fish populations
  - **American eel** – Seven preliminary COCs (2,3,7,8-TCDD, PCDD/PCDF TEQ–fish, total TEQ–fish, total PCBs, methylmercury, dieldrin, and copper) were identified based on the tissue LOE, and five preliminary COCs (cadmium, mercury, PCB TEQ–fish, PCDD/PCDF TEQ–fish, and total TEQ–fish) were identified based on the dietary LOE.
  - **Largemouth bass** – Seven preliminary COCs (2,3,7,8-TCDD, PCDD/PCDF TEQ–fish, total TEQ–fish, methylmercury, total PCBs, PCB TEQ–fish, and dieldrin) were identified based on the tissue LOE, and three preliminary COCs (PCB TEQ–fish, PCDD/PCDF TEQ–fish, and total TEQ–fish) were identified based on the dietary LOE.
  - **Smallmouth bass** – Five preliminary COCs (mercury, 2,3,7,8-TCDD, PCDD/PCDF TEQ–fish, total TEQ–fish, and total PCBs) were identified based on the tissue LOE, and three preliminary COCs (PCB TEQ–fish, PCDD/PCDF TEQ–fish, and total TEQ–fish) were identified based on the dietary LOE.
  - **Northern pike** – Six preliminary COCs (2,3,7,8-TCDD, PCDD/PCDF TEQ–fish, total TEQ–fish, total PCBs, PCB TEQ–fish, and dieldrin) were identified based on the tissue LOE, and four preliminary COCs (total PCBs, PCB TEQ–fish, PCDD/PCDF TEQ–fish, and total TEQ–fish) were identified based on the dietary LOE.

Of the 28 COPECs evaluated in surface water, HQs were < 1.0 for 26. Two COPECs (cyanide and copper) were identified as preliminary COCs with HQs ≥ 1.0.

9.6 Aquatic Bird Assessment

The potential for unacceptable risk to birds represented by three bird species (i.e., spotted sandpiper, great blue heron, and belted kingfisher) was characterized using LPRSA tissue, sediment, and water

chemistry to estimate dietary doses. In addition, risks to great blue heron and belted kingfisher were characterized using chemical concentration in bird egg tissue as a secondary LOE. Dietary doses and modeled bird egg concentrations were compared to a range of TRVs to derive risk estimates (HQs). Risk to the three representative aquatic bird species was also evaluated based on foraging in various exposure areas, including the entire site and on a reach-specific basis. Sixteen COPECs were evaluated for aquatic avian dietary exposure, and nine COPECs were evaluated using the bird egg tissue LOE.

COPECs with HQs ≥ 1.0 based on LOAEL TRVs (using a range of TRVs) were identified as preliminary COCs (Tables 9-3 and 9-4). The following preliminary COCs were identified for aquatic birds:

- **Spotted sandpiper** – Eight preliminary COCs (PCDD/PCDF TEQ–bird, total TEQ–bird, copper, lead, total HMW PAHs, total PCBs, PCB TEQ–bird, and total DDx) were identified based on the dietary LOE.
- **Great blue heron** – Seven preliminary COCs (PCDD/PCDF TEQ–bird, total TEQ–bird, copper, methylmercury, total PCBs, PCB TEQ–bird, and total DDx) were identified based on the dietary LOE, and five preliminary COCs (PCDD/PCDF TEQ–bird, total TEQ–bird, total PCBs, PCB TEQ–bird, and total DDx) were identified based on the egg tissue LOE.
- **Belted kingfisher** – Six preliminary COCs (PCDD/PCDF TEQ–bird, total TEQ–bird, lead, methylmercury, PCB TEQ–bird, and total DDx) were identified based on the dietary LOE, and five preliminary COCs (PCDD/PCDF TEQ–bird, total TEQ–bird, total PCBs, PCB TEQ–bird, and total DDx) were identified based on the egg tissue LOE.

9.7 Aquatic Mammal Assessment

The potential for unacceptable risk to mammals was characterized using LPRSA tissue, sediment, and water chemistry to estimate dietary doses of COPECs to two mammal species (i.e., river otter and mink). Dietary doses were compared to a range of TRVs to derive risk estimates (HQs). As with the aquatic bird dietary LOE evaluation, risk to the two representative mammal species was also evaluated based on foraging in various exposure areas, including the entire site and on a reach-specific basis (RM 10 to RM 17.4). As part of the uncertainty evaluation, dietary risk estimates for aquatic mammals based on varied dietary compositions were also evaluated (including different proportions of large fish [i.e., > 30 cm] such as carp, which tend to have relatively higher chemical concentrations in whole-body tissue samples).

Fifteen COPECs were evaluated for aquatic mammals. Four preliminary COCs (PCDD/PCDF TEQ–mammal, total TEQ–mammal, total PCBs, and PCB TEQ–mammal) were identified with HQs ≥ 1.0 (based on a range of LOAEL TRVs) for river otter and mink (Tables 9-3 and 9-4).

9.8 Zooplankton Assessment

The potential for unacceptable risk to the zooplankton community in the LPRSA was evaluated using water chemistry. Surface water concentrations were compared to TRVs intended to be protective of a variety of aquatic organisms to derive risk estimates (HQs) in the risk characterization. Of the 25 COPECs evaluated in surface water, two had HQs ≥ 1.0 (copper [estuarine surface water] and cyanide) and were identified as preliminary COCs (Tables 9-3 and 9-4).

9.9 Amphibian and Reptile Assessment

The potential for unacceptable risk to amphibian and reptile populations in the LPRSA was based on a comparison of LPRSA surface water concentrations to amphibian/reptile-specific TRVs. Sediment ingestion is also a likely exposure route for amphibian and reptile populations, but this route was not evaluated because it cannot be quantified reliably. Limited amphibian- and reptile-specific water toxicity data are available, and so the evaluation of risks to amphibians and reptiles is limited and uncertain. No preliminary COCs were identified for amphibians and reptiles because all seven surface water COPECs (i.e., chromium, copper, lead, mercury, nickel, silver, and zinc) evaluated had HQs < 1.0.

9.10 Aquatic Plant Assessment

The potential for unacceptable risk to the aquatic plant community in the LPRSA was characterized using LPRSA surface sediment and surface water chemistry. Surface water and sediment data were compared to media-specific TRVs to derive risk estimates (HQs) for two LOEs. The paucity and questionable applicability of both exposure and effects data—especially for the sediment evaluation, which was based on terrestrial plants and soils—reduce the level of certainty for the quantitative estimates of potential unacceptable risk to the aquatic plant community.

Seven preliminary COCs (chromium, copper, lead, mercury, selenium, vanadium, and zinc) were identified for aquatic plants based on the sediment LOE, and four preliminary COCs (copper, zinc, TBT [tributyltin], and cyanide) were identified for aquatic plants based on the surface water LOE (Tables 9-3 and 9-4).

9.11 Baseline Ecological Risk Assessment Summary of Conclusions

The BERA for the entire 17.4 miles of the LPRSA was conducted and prepared in accordance with Section IX.37.d of the May 2007 Administrative Settlement Agreement and AOC (USEPA 2007).

The potential for unacceptable risk was assessed using empirical and modeled data collected from a variety of chemical and biological sampling events and surveys conducted as part of the LPRSA RI. A step-by-step process included an initial screening-level evaluation (presented in the SLERA; Appendix A of the BERA), which identified media-specific COPECs. A detailed evaluation of potential

site-specific exposure and effects in the BERA derived risk estimates (expressed as HQs) to identify the potential for unacceptable ecological risk under baseline conditions.

Preliminary COCs (COPECS with HQs ≥ 1.0 based on a range of LOAELs TRVs for tissue and diet, acute or chronic surface water TRVs, and plant-specific sediment TRVs) are presented in Table 9-4. HQs were also derived using NOAEL TRVs; COPECs with HQs ≥ 1.0 based on a range of NOAEL TRVs are summarized in the BERA (Sections 6.3.4, 7.1.4, 7.2.4, 7.4.4, 8.1.4, 8.2.4, and 9.1.4) and include all 21 of the preliminary COCs identified (based on LOAEL HQ exceedances), as well as benzo(a)pyrene, total LPAHs, and endosulfan I.

The preliminary COCs were further evaluated based on a comparison to background concentrations (USEPA 2016) and an appraisal of the uncertainty of the assessment to identify risk drivers to be further evaluated in the FS. The following preliminary COCs were recommended as risk drivers for further evaluation in the FS:

- 2,3,7,8-TCDD
- PCDD/PCDF TEQ (fish, bird, and mammal)
- Total TEQ (fish, bird, and mammal)
- Total PCBs
- PCB TEQ (fish, bird, and mammal)
- Total DDx

These listed risk drivers were based on effect-level HQs exceeding 1.0 for various ecological receptor groups and LOEs. Some LOEs are stronger than others and should be weighted more heavily when used for management decisions. Table 9-5 presents a summary of the risk drivers and considerations for risk management decisions regarding the assumptions used to derive HQs.

A number of preliminary COCs were not recommended as risk drivers to be carried forward to inform major risk management decisions. Preliminary COCs that were not retained as risk drivers were excluded primarily for the following two reasons:

- Background concentrations indicated that risks in the LPRSA would not be different from or would be lower than those in background (upstream or regional) areas.

- The LOE for which a LOAEL HQ was ≥ 1.0 could not reliably predict risks to a level appropriate for costly remedial decisions. This included the tissue residue LOE for metals[185] and the sediment LOE for aquatic plants.[186]

The following 11 metals (arsenic, cadmium, chromium, copper, lead, mercury, nickel, silver, selenium, vanadium, and zinc), TBT, HMW PAHs, dieldrin, and cyanide were not recommended as risk drivers based on background concentrations or the uncertainty of the assessment:

- **Arsenic** – Arsenic was identified as a preliminary COC based on benthic invertebrate tissue (worm HQ = 2.2 and blue crab HQ = 2.2). Arsenic was not recommended as a risk driver because of the uncertainty associated with the evaluation of regulated metals in tissue.[187] In addition, the sediment LPRSA EPC for sediment (9.6 mg/kg) was lower than regional background (i.e., Jamaica Bay and Mullica River/Great Bay) maximum concentrations (20.7 and 32.8 mg/kg, respectively) and the UCL for the Mullica River/Great Bay (12 mg/kg). However, the LPRSA EPC for sediment (9.6 mg/kg) was slightly higher than the UCL for Jamaica Bay (7.3 mg/kg) and above Dundee Dam (6.4 mg/kg).
- **Cadmium** – Cadmium was identified as a preliminary COC based on the fish diet LOE (HQs for mummichog, common carp, white perch, white sucker, and American eel-small ranged from 0.70 to 1.3). Cadmium was not identified as a preliminary COC for any other LOE or receptor group, and HQs for fish diet were just above 1.0 for several fish species.
- **Chromium** – Chromium was identified as a preliminary COC based on benthic invertebrate tissue (worm HQ = 6.0 and mussel HQ = 3.7) and aquatic plants and sediment (HQ = 160). Chromium was not recommended as a risk driver based on the uncertainty of the aquatic plant assessment for sediment due to the screening level being based on a highly bioavailable chemical form,[188] as well as the uncertainty associated with the evaluation of regulated metals in tissue.[189]

[185] The use of a tissue residue approach for metals (except for methylmercury and selenium) is highly uncertain because of the wide range of strategies used by organisms to store, detoxify, and excrete bioaccumulated metals (e.g., fish and invertebrates may regulate their body burdens of some metals, although metals regulation and the strategy thereof is species- and metal-specific) (Adams et al. 2011; USEPA 2007). The USEPA framework for metals risk assessment (USEPA 2007) recommends against the use of a tissue residue approach, stating that the critical body residue approach for metals "does not appear to be a robust indicator of toxic dose."

[186] The relevance of soil toxicity thresholds generated for agricultural crops to the sediment exposure of aquatic plants is unknown. Soil toxicity data are primarily from studies of agricultural crops and/or waste soils. Many of these soil toxicity data are based on a highly bioavailable chemical form that is not representative of natural soils or sediment (Efroymson et al. 1997).

[187] The use of a tissue residue approach for metals (except for methylmercury and selenium) is highly uncertain because of the wide range of strategies used by organisms to store, detoxify, and excrete bioaccumulated metals (e.g., fish and invertebrates may regulate their body burdens of some metals, although metals regulation and the strategy thereof is species- and metal-specific) (Adams et al. 2011; USEPA 2007).

[188] The relevance of soil toxicity thresholds generated for agricultural crops to the sediment exposure of aquatic plants is unknown. Soil toxicity data are primarily from studies of agricultural crops or waste soils. Many of these soil toxicity data are based on a highly bioavailable chemical form that is not representative of natural soils or sediment (Efroymson et al. 1997).

[189] The use of a tissue residue approach for metals (except for methylmercury and selenium) is highly uncertain because of the wide range of strategies used by organisms to store, detoxify, and excrete bioaccumulated metals (e.g., fish and invertebrates may

- **Copper** – Copper was identified as a preliminary COC based on multiple LOEs: benthic invertebrate tissue (blue crab HQ = 2.1), fish tissue (mummichog, other forage fish, white perch, and American eel HQs ranged from 1.7 to 9.3), bird diet (spotted sandpiper and great blue heron HQs ranged from 0.029 to 3.6), surface water LOEs (benthic invertebrate, fish, zooplankton, and aquatic plant estuarine and freshwater HQs ranged from 0.14 to 2.7 and from 0.023 to 1.0, respectively), and sediment for aquatic plant populations (HQ = 2.4). Copper was not recommended as a risk driver for the following reasons:
  - Uncertainty associated with the evaluation of regulated metals in tissue.[190]
  - Uncertainty of the aquatic plant assessment for sediment due to the screening level being based on a highly bioavailable chemical form.[191]
  - Evaluation of background. Dissolved estuarine surface water LPRSA EPCs for copper (2.61 µg/L) were lower than the maximum (3.36 µg/L) and UCL (2.7 µg/L) background surface water concentrations above Dundee Dam. Sediment LPRSA EPCs for copper (170 mg/kg) were lower than or similar to maximum (209 mg/kg) and UCL (150 mg/kg) background sediment concentration above Dundee Dam.
- **Lead** – Lead was identified as a preliminary COC based on benthic invertebrate tissue (worm HQs ranged from 0.16 to 2.5), bird diet (spotted sandpiper HQs ranged from 0.20 to 10, and belted kingfisher HQs ranged from 0.015 to 1.1), and sediment for aquatic plant populations (HQ = 2.3). Lead was not recommended as a risk driver based on benthic invertebrate tissue due to uncertainty associated with the evaluation of regulated metals in tissue,[192] uncertainty of the aquatic plant assessment for sediment due to the screening level being based on a highly bioavailable chemical form,[193] and the background evaluation. The LPRSA EPC for lead in sediment (270 mg/kg) was lower than the UCL (440 mg/kg) background concentration above Dundee Dam.
- **Methylmercury/mercury** – Mercury or methylmercury were identified as preliminary COCs based on multiple LOEs: benthic invertebrate tissue (blue crab HQs ranged from 1.3 to 1.5), fish tissue (white catfish, American eel, largemouth bass, and smallmouth bass HQs ranged

regulate their body burdens of some metals, although metals regulation and the strategy thereof is species- and metal-specific) (Adams et al. 2011; USEPA 2007).

[190] The use of a tissue residue approach for metals (except for methylmercury and selenium) is highly uncertain because of the wide range of strategies used by organisms to store, detoxify, and excrete bioaccumulated metals (e.g., fish and invertebrates may regulate their body burdens of some metals, although metals regulation and the strategy thereof is species- and metal-specific) (Adams et al. 2011; USEPA 2007).

[191] The relevance of soil toxicity thresholds generated for agricultural crops to the sediment exposure of aquatic plants is unknown. Soil toxicity data are primarily from studies of agricultural crops or waste soils. Many of these soil toxicity data are based on a highly bioavailable chemical form that is not representative of natural soils or sediment (Efroymson et al. 1997).

[192] The use of a tissue residue approach for metals (except for methylmercury and selenium) is highly uncertain because of the wide range of strategies used by organisms to store, detoxify, and excrete bioaccumulated metals (e.g., fish and invertebrates may regulate their body burdens of some metals, although metals regulation and the strategy thereof is species- and metal-specific) (Adams et al. 2011; USEPA 2007).

[193] The relevance of soil toxicity thresholds generated for agricultural crops to the sediment exposure of aquatic plants is unknown. Soil toxicity data are primarily from studies of agricultural crops or waste soils. Many of these soil toxicity data are based on a highly bioavailable chemical form that is not representative of natural soils or sediment (Efroymson et al. 1997).

from 0.63 to 2.6), fish diet (mummichog, common carp, white perch, white catfish, and American eel HQs ranged from 1.1 to 1.3), fish egg tissue (mummichog HQs ranged from 0.11 to 1.1), bird diet (great blue heron and kingfisher HQs ranged from 0.031 to 1.6), and sediment for aquatic plant populations (HQ = 9.7). Mercury was not recommended as a risk driver for the following reasons:

  - Evaluation of background. Sediment LPRSA EPC for mercury (2,900 µg/kg) was lower than the UCL (2,910 µg/kg) background sediment concentration above Dundee Dam. In addition, LPRSA methylmercury fish tissue EPCs were less than maximum concentrations in 7 of 10 species above Dundee Dam, and similar to or less than UCLs for three of four fish species for which UCLs above Dundee Dam could be calculated. Mummichog LPRSA EPCs for methylmercury were less than UCLs in mummichog from Jamaica Bay/Lower Harbor.
  - Uncertainty of the aquatic plant assessment for sediment due to the screening level being based on a highly bioavailable chemical form.[194]
  - Uncertainty associated with the bird diet TRV resulting in HQs > 1.0 was derived using an interspecies extrapolation factor of three (assumes that mallards are three times less sensitive than the selected avian species evaluated) and based on exposure to methylmercury dicyandiamide, a fungicide that is not a form of mercury expected to be associated with the LPRSA.

- **Nickel** – Nickel was identified as a preliminary COC based on the benthic invertebrate tissue LOE (worm HQ = 12.0 and blue crab HQ = 6.0). Nickel was not recommended as a risk driver based on the uncertainty associated with the evaluation of regulated metals in tissue.[195]
- **Silver** – Silver was identified as a preliminary COC based on the benthic invertebrate tissue LOE (blue crab HQ = 1.0). Silver was not recommended as a risk driver based on uncertainty associated with the evaluation of regulated metals in tissue.[196]
- **Selenium** – Selenium was identified as a preliminary COC based on the benthic invertebrate tissue (worm HQ = 1.1 and blue crab HQ = 1.5) and aquatic plant sediment (HQ = 14.0) LOEs. Selenium was not recommended as a risk driver based on the uncertainty of the aquatic plant assessment for sediment due to the screening level being based on a highly bioavailable

[194] The relevance of soil toxicity thresholds generated for agricultural crops to the sediment exposure of aquatic plants is unknown. Soil toxicity data are primarily from studies of agricultural crops or waste soils. Many of these soil toxicity data are based on a highly bioavailable chemical form that is not representative of natural soils or sediment (Efroymson et al. 1997).

[195] The use of a tissue residue approach for metals (except for methylmercury and selenium) is highly uncertain because of the wide range of strategies used by organisms to store, detoxify, and excrete bioaccumulated metals (e.g., fish and invertebrates may regulate their body burdens of some metals, although metals regulation and the strategy thereof is species- and metal-specific) (Adams et al. 2011; USEPA 2007).

[196] The use of a tissue residue approach for metals (except for methylmercury and selenium) is highly uncertain because of the wide range of strategies used by organisms to store, detoxify, and excrete bioaccumulated metals (e.g., fish and invertebrates may regulate their body burdens of some metals, although metals regulation and the strategy thereof is species- and metal-specific) (Adams et al. 2011; USEPA 2007).

chemical form[197] and on a comparison to background; LPRSA sediment (0.93 mg/kg) was lower than the UCL above Dundee Dam (27 mg/kg) and the UCL from Jamaica Bay (1.4 mg/kg).

- **Vanadium** – Vanadium was identified as a preliminary COC based on sediment for aquatic plants (HQ = 14). Vanadium was not recommended as a risk driver based on the uncertainty of the aquatic plant assessment for sediment due to the screening level being based on a highly bioavailable chemical form.[198]
- **Zinc** – Zinc was identified as a preliminary COC based on sediment for aquatic plants (HQ = 3.1) and surface water for aquatic plants (HQ = 21). Zinc was not recommended as a risk driver based on the uncertainty of the aquatic plant assessment for sediment due to the screening level being based on a highly bioavailable chemical form[199] and on the evaluation of background; LPRSA estuarine and freshwater surface water EPCs for dissolved zinc (8.5 and 7.5 µg/L, respectively) were lower than the background maximum dissolved zinc concentration above Dundee Dam (9.8 µg/L). In addition, zinc concentrations in surface water based on general surface water criteria for the evaluation of other aquatic receptor groups (i.e., invertebrates, fish, and zooplankton) resulted in HQs < 1.0.
- **TBT** – TBT was identified as a preliminary COC based on aquatic plant populations (surface water HQs ranged from 1.1 to 50). TBT was not recommended as a risk driver based on the background evaluation; surface water EPCs for TBT were represented by maximum concentrations (0.026 µg/L) and DLs (0.05 µg/L) in the LPRSA. The maximum LPRSA TBT concentrations were lower than the DL for background surface water above Dundee Dam (0.05 µg/L), and the LPRSA DLs were equal to background DLs from above Dundee Dam. In addition, TBT had a low detection frequency in the surface water of the LPRSA (0 to 1%).
- **HMW PAHs** – Total HMW PAHs were identified as a preliminary COC based on the benthic invertebrate tissue LOE for worms (HQs ranged from 0.090 to 3.0) and the bird diet LOE for spotted sandpiper (HQs ranged from 1.9 to 10 by reach; HQ = 4.5 site-wide). Total HMW PAHs were not recommended as a risk driver based on the background evaluation; the LPRSA sediment EPC (46,000 µg/kg) was lower than the EPC and the maximum sediment concentration above Dundee Dam (300,000 and 73,300 µg/kg, respectively). No background invertebrate tissue data were available to compare to LPRSA invertebrate concentrations, so there is some uncertainty with this evaluation.

[197] The relevance of soil toxicity thresholds generated for agricultural crops to the sediment exposure of aquatic plants is unknown. Soil toxicity data are primarily from studies of agricultural crops or waste soils. Many of these soil toxicity data are based on a highly bioavailable chemical form that is not representative of natural soils or sediment (Efroymson et al. 1997).

[198] The relevance of soil toxicity thresholds generated for agricultural crops to the sediment exposure of aquatic plants is unknown. Soil toxicity data are primarily from studies of agricultural crops or waste soils. Many of these soil toxicity data are based on a highly bioavailable chemical form that is not representative of natural soils or sediment (Efroymson et al. 1997).

[199] The relevance of soil toxicity thresholds generated for agricultural crops to the sediment exposure of aquatic plants is unknown. Soil toxicity data are primarily from studies of agricultural crops or waste soils. Many of these soil toxicity data are based on a highly bioavailable chemical form that is not representative of natural soils or sediment (Efroymson et al. 1997).

- **Dieldrin** – Dieldrin was identified as a preliminary COC based on the fish tissue LOE for several fish species: common carp, channel catfish, American eel, largemouth bass, and northern pike (HQs ranged from 0.20 to 1.4). The two TRVs used to determine the HQs were derived from the same study (Shubat and Curtis 1986). The higher LOAEL TRV was based on unadjusted data from the 16-week study wherein reduced growth of rainbow trout was observed, and the lower LOAEL TRV was based on 96-hour LC50 data adjusted using extrapolation factors. Given that the HQs were relatively low based on the LOAEL TRV that was adjusted using extrapolation factors, remedial action based on these predicted risks was not recommended. In addition, dieldrin was not recommended as a risk driver based on the background evaluation; the LPRSA sediment EPC (8.3 µg/kg) was lower than the EPC above Dundee Dam (17 µg/kg).
- **Cyanide** – Cyanide was identified as a preliminary COC based on surface water (for invertebrate populations [estuarine and freshwater HQs ranged from 1.3 to 4.1 and from 0.23 to 1.0, respectively], fish and zooplankton populations [estuarine HQs ranged from 1.6 to 5.3], and aquatic plant populations [estuarine HQ = 2.0]). Cyanide was not recommended as a risk driver; however, due to its low detection frequency in surface water in the LPRSA; less than 6% of samples in the estuarine portion had detected concentrations of cyanide.

10 Natural Recovery

Natural recovery of sediment proceeds by naturally occurring declines in sediment contaminant concentrations. These declines can also result in concomitant declines in contamination levels in the water column and biota tissue. Specifically, in the LPR, natural recovery is facilitated by net deposition or oscillating erosion and deposition that replaces higher concentration surface sediments with lower concentration depositing sediments. Recovery is inhibited by net erosion or oscillating erosion and deposition that exposes (and potentially mobilizes) higher contaminant concentrations and by external contaminant loadings. Erosion can inhibit natural recovery by exposing elevated sediment concentrations and transporting elevated sediment concentrations to other locations within the LPR. Natural recovery of 2,3,7,8-TCDD, total PCBs, total DDx, and mercury appears to be occurring in areas subject to net deposition; the same, however, is not true of HMW and LMW PAHs, likely due to ongoing sources (as discussed previously in Section 4). In contrast, surface (0- to 6-inch) sediment concentrations of all these contaminants appear to have increased in some of the areas subject to net erosion, and the overall average surface sediment concentrations in the lower 8 miles of the LPR declined very little from the mid-1990s to roughly 2010 and increased in response to the 1-in-90-year high flow produced by Hurricane Irene. Temporal trends in biota tissue, however, are not as clear, likely due to reasons discussed later in this section. This section examines the evidence on which this assessment is based. Section 10.1 presents a conceptual model of natural recovery in the LPR. Section 10.2 discusses the importance of external sources on natural recovery. Sections 10.3 and 10.4 investigate the natural recovery of surface sediment contamination in the LPR as of 2010, before Hurricane Irene made landfall in August 2011. The impact of Hurricane Irene is discussed in Section 10.5. Natural recovery in biota tissue is discussed in Section 10.6.

10.1 Conceptual Model of Natural Recovery in the Lower Passaic River

Natural recovery occurs following reductions in contaminant loads and the concomitant reductions in water column contaminant concentrations. Surface sediment contaminant concentrations can then decline through deposition of cleaner solids that mix with and bury surficial sediments, diffusion that transfers contaminants to the water column, biological or chemical degradation, and erosion of surface contamination (Figure 10-1).

Ongoing contaminant loads from external sources can limit natural recovery. In such cases, recovery depends on the contaminant concentration on particles entering the LPR relative to those in LPR surface sediments. When external loads are not significant, recovery is controlled by internal sources, and widespread recovery depends on the decline of concentrations in those LPR sediments that have the strongest influence on water column contaminant concentrations, including those sediments prone to erosion and transport within the LPR system. Natural recovery is thus aided by controlling both external sources (e.g., stormwater loading) and internal sources (e.g., contaminated sediment source areas, especially fine-grained sediments in areas subject to periodic erosion). As discussed later in this

section, internal sources dominate most strongly for 2,3,7,8-TCDD, whereas the other contaminants exhibit varying degrees of external influence.

Resuspension causes a loss of contaminants from surface sediments to the water column. This allows some erosional areas to act as contaminant sources to other areas by influencing the concentration on depositing particles. In areas of net erosion (i.e., when erosion exceeds deposition), surficial concentrations likely increase except where peak concentrations reside at the surface (though, as discussed in Section 4.2, outside of the upstream portions of point bars, the highest contaminant concentrations are generally buried at depth). Net erosion does not induce recovery in areas where sediment concentration profiles are uniform or increasing with depth.

Deposition and erosion are strongest during high-energy conditions when solids fluxes are highest, which occur during high freshwater flows (perhaps compounded by spring tides or offshore water level fluctuations; see Sections 3.4 and 6.1 as well as Chant et al. [2010]). Erosion is expected primarily during the rising limb of a high-flow event in areas where the bed shear stresses are high enough to mobilize sediment. Other areas can be subject to deposition of solids derived from the upstream watershed and erosion elsewhere in the river. During the falling limb of the hydrograph, additional areas can become depositional if local shear stress declines to levels that allow settling particles to deposit. Although tidal currents induce deposition and erosion continually in much of the LPR and induce transport of solids and contaminants, the impact of these fluxes on recovery may be nominal given the relatively slow exchange processes that transfer solids and contaminants between the parent bed and the fluff layer subject to tidal resuspension and deposition (e.g., mixing, diffusion, and consolidation). The exception is areas subject to net deposition (infilling) during low-energy conditions, which may still be subject to recovery.

Other processes may affect natural recovery, such as diffusion to the water column from sediment porewater and in situ biological or chemical degradation (e.g., reductive dechlorination). However, these are likely of secondary importance for the persistent legacy contaminants in LPR sediments.

10.2 Impacts of External Sources on Contaminant Patterns

As discussed in Sections 4 and 6, the large-scale longitudinal trends in LPR surface sediment contamination reflect trends in sediment type and the interplay between freshwater and tidal flows. Contaminants entering the tidally influenced region of the LPR may be transported upstream to approximately RM 14, corresponding to the approximate limit of salt front intrusion under present-day conditions and the associated upstream transport mechanisms (estuarine circulation and tidal pumping; see Sections 3.4 and 6), as well as into Newark Bay with the predominant downstream flow. External sources (i.e., those entering the LPR from upstream, other parts of the watershed, or from Newark Bay) influence the along-river patterns depending on their magnitude and zone of influence. External sources are largely associated with solids loadings. As noted in Section 7 in the

context of the ST model, the total solids loading to the LPR from above Dundee Dam, tributaries, and CSOs/SWOs over the period WY1996 through WY0213 is estimated at approximately 29,400 MT/year, of which the UPR above the Dundee Dam contributes about 21,400 MT/year, the tributaries about 6,400 MT, and the CSOs/SWOs about 1,600 MT/year. Net export from the LPR to Newark Bay during this same period is predicted by the ST model to be 19,200 MT/year, resulting in net trapping of 10,200 MT/year within the LPR.

10.2.1 Upstream and Downstream Sources

Reflecting the limits on upstream transport and the transition to coarser sediments, concentrations for many contaminants decline moving upstream of RM 12 to RM 14, with the decline being greatest in the absence of an upstream and/or direct source (though, historically, some contamination could have been transported upstream of RM 14; see Sections 3.3 and 6). Similarly, in the absence of a source in Newark Bay, the LPR solids carried into Newark Bay are diluted by Newark Bay solids, resulting in a lower relative concentration within the Bay.[200]

The best example of this spatial pattern is 2,3,7,8-TCDD. Concentrations decline moving upstream between RM 12 and RM 14, and concentrations above RM 14 are mostly 100 to 1,000 times lower than those in the lower 12 miles and comparable to those above Dundee Dam (Figure 4.1-9a). This rapid decline in concentration is attributed to the extent of net upstream tidal sediment transport,[201] the transition from a mixture of fine and coarse sediments to just coarse sediments, and the absence of substantial upstream sources. Downstream of approximately RM 3, 2,3,7,8-TCDD concentrations decline through the rest of the LPR and Newark Bay, though at a lower rate than above RM 12. This downstream trend is consistent with settling and dilution as the LPR load is dispersed into Newark Bay and diluted by solids from other sources, and likely also reflects the impact of historical dredging activities that enhanced sediment deposition in the lowermost portion of the river and removed legacy 2,3,7,8-TCDD deposits (see Sections 1.2, 4.2.9, 4.2.10, and 6.3).

This spatial pattern is not observed for the other contaminants (Figures 4.1-9b through 4.1-9f), suggesting that, unlike 2,3,7,8-TCDD, they are impacted by upstream, downstream, and/or watershed sources. For example, surface sediment concentrations of total PCBs (Figure 4.1-9b) and total DDx (Figure 4.1-9c) decline moving upstream of RM 12 to RM 14 due to the increased prevalence of

[200] Sommerfield and Chant (2010) estimate that approximately 10% of the total load to Newark Bay is composed of the Passaic River load, which is dominated by episodic high-flow events. The Passaic River load reflects a combination of solids entering the LPR at Dundee Dam, via tributaries, and resuspended from the LPR sediment bed, with the relative proportions likely varying by flow regime. Sediment mass balances under a range of flow conditions are presented in Section 7.

[201] As discussed in Section 6, under the assumption of a dominant 2,3,7,8-TCDD source at the Lister Avenue site, the declining presence of 2,3,7,8-TCDD mass with distance upstream can generally be attributed to two factors: a decline in upstream transport potential associated with less frequent salt front intrusion and net upstream tidal pumping, and a decline in long-term trapping potential associated with the reduced prevalence of depositional environments (e.g., fine sediment deposits) as the cross-sectional area of the LPR is reduced. As discussed in Sections 3.3 and 6.3, under extremely low river flows, such as the extreme droughts of the 1960s, net upstream transport due to tidal currents may have historically occurred upstream of RM 14.

coarse sediments, but less so than 2,3,7,8-TCDD, suggesting upstream sources. Concentrations of mercury show little decline moving from the LPR into Newark Bay (Figure 4.1-9d), suggesting downstream sources. Similar conclusions can also be drawn for HMW PAHs (Figure 4.1-9e; downstream and upstream sources), and LMW PAHs (Figure 4.1-9f; downstream and upstream sources).

The above patterns suggest that upstream and downstream sources of all contaminants except 2,3,7,8-TCDD may cause some degree of recontamination of the system upon remediation. The ratio of mean OC-normalized surface concentrations in the Lower LPR to the UPR near Dundee Dam and to the upstream stretches of Newark Bay (RM 0 to RM -2) is plotted for the different contaminants in Figure 10-2. For all contaminants except 2,3,7,8-TCDD, LPR sediment concentrations are comparable to those in the UPR and/or Newark Bay. Thus, remediation of the LPR sediments in the absence of source control has the potential to significantly reduce the levels of 2,3,7,8-TCDD, but may not achieve similar long-term reductions of the other contaminants (i.e., total PCBs, total DDx, mercury, and PAHs) due to recontamination from the UPR and Newark Bay. Source control efforts in the UPR and Newark Bay that address the other contaminants or reductions occurring via natural recovery would reduce the effects of recontamination.

10.2.2 Tributaries

The three major tributaries to the LPR—Saddle River, Third River, and Second River—are potential sources of contaminants. Though there are limited tributary contaminant data, concentrations upstream of the HOT, which marks the limit of tidal transport and influence from the LPR, can be used to qualitatively evaluate the potential of tributaries to act as local contaminant sources.

The Second River and Third River have 2,3,7,8-TCDD levels below 3 ng/kg (Figure 10-3a). These levels are matched by two of the three samples in the Saddle River, with the third sample having a higher level of 7 ng/kg. At the confluence of the LPR, both the Second River and Third River have levels similar to those in the nearby mainstem LPR, while the sediment at the LPR-Saddle River confluence is lower than that above the HOT. However, the absolute levels of 2,3,7,8-TCDD concentrations above the HOT in Saddle River are low (less than 10 ng/kg), indicating that all three tributaries are insignificant sources of 2,3,7,8-TCDD. Similar trends are also observed for total PCBs (Figure 10-3b).

Concentrations of the remaining contaminants upstream of the tributary HOT are generally comparable or higher than levels in the LPR near the confluence, suggesting the tributaries could be local sources. Total DDx concentrations (Figure 10-3c) are higher upstream of the HOT in Saddle River than at the confluence, and levels upstream of the HOT in Third and Second rivers are comparable to levels at the vicinity of the tributary confluence. Total DDx concentrations upstream of the HOT in the tributaries often range between 0.1 and 1 mg/kg, which is similar to the range of concentrations in fine sediments in the LPR (Figure 4.1-9c), suggesting that the tributaries are a

possible local source of total DDx to the LPR. Mercury concentrations (Figure 10-3d) are lower upstream of the HOT in Saddle and Third rivers than in the respective tributary confluences; however, levels upstream of the HOT in Second River are comparable to those in the vicinity of the confluence. The actual levels of mercury measured upstream of the HOT in the tributaries are less than 1 mg/kg, which are lower than the concentrations in fine LPR sediments and similar to the range of concentrations measured in coarse sediments of the LPR (Figure 4.1-9d), suggesting that the tributaries are likely not an important source of mercury to the LPR. Levels of HMW PAH (Figure 10-3e) and LMW PAHs (Figure 10-3f) upstream of the HOT in all three tributaries are comparable to those in the LPR near the confluence, and the concentration levels upstream of the HOT are comparable to the higher concentrations measured in the LPR (Figures 4.1-8e and 4.1-8f), suggesting the tributaries are a possible local source of PAHs to the LPR.

10.2.3 Other Sources

Point sources (e.g., CSOs, SWOs, and industrial and municipal discharges) also have the potential to be ongoing sources of contaminants to the LPR sediments. Various studies and data reviews (e.g., Shear et al. 1996 and Huntley et al. 1997) suggest that CSOs are a source of a broad range of contaminants to the LPR and that CSO-specific signatures can be found in neighboring sediments, indicating the local importance of the CSO discharges. Targeted sampling of CSO/SWO point sources for a number of contaminants was performed as part of the CARP model sampling effort in 2000 to 2004 (Great Lakes Environmental Center 2008) and during the 2007 to 2008 USEPA field effort and indicate that CSOs and SWOs are not a significant[202] source for key contaminants in the Passaic River (LBG 2014). As noted in Section 7 and in the introduction to this section, CSOs and SWOs are only expected to contribute about 1,600 of the 29,400 MT/year of sediment entering the LPR.

Non-point sources, like groundwater flux and direct atmospheric deposition, are not expected to be major contaminant sources to the LPR. USEPA concluded in 2008 that chemical inputs from groundwater discharges are negligible throughout the LPR (correspondence between USEPA and CSTAG [USEPA 2008]), and The Louis Berger Group concluded that the estimated groundwater contribution to the LPR is less than 2% of the long-term average river flow over Dundee Dam (LBG 2014). Further, groundwater migration to the LPR is restricted due to the impervious/semi-impervious boundaries surrounding the LPR. The RM 10.9 design investigation measured seepage velocities at four stations (CH2M Hill 2013). The measured velocities were 215, 942, 26, and 73 cm/year, with the maximum velocity measured at a location with high sand content and relatively

[202] As noted by LBG (2014), CSO/SWO sites contribute less than 3% of the total solids to the LPR (LBG 2014). Mean concentrations of 2,3,7,8-TCDD, total PCBs, total DDx, mercury, HMW PAH, and LMW PAH measured in the 2007 to 2008 USEPA Program were 4.1 ng/kg, 0.36 mg/kg, 0.095 mg/kg, 1 mg/kg, 28 mg/kg, and 4.9 mg/kg, respectively. Despite mean concentrations of 28 and 4.9 mg/kg for HMW PAH and LMW PAH, respectively, the very low solids contribution of CSO/SWO sites suggests that they are not significant contaminant sources. Summary statistics of the 2007 to 2008 USEPA field effort can be found in Table 4-10 of LBG (2014).

low contaminant concentration. The areas with elevated contaminated concentrations in the RM 10.9 sediments have finer-grained materials that yield lower seepage velocities. The RM 10.9 design investigation also concluded that the LPR was impermeable to groundwater due to the sharply increasing bedrock on the west side of the LPR, which formed a relatively impermeable barrier to the west, and the silt and clay which filled in the fractures in weathered near-surface bedrock units (CH2M Hill 2013). In addition, many of the contaminants discussed herein strongly sorb to finer sediments, particularly to the sediment OC, thereby reducing the advective transport of these contaminants through low-seepage velocities and the limited groundwater flow.

Atmospheric contributions of 2,3,7,8-TCDD to the LPR are expected to be small and diffuse relative to the contributions from dredging, erosion, and resuspension flux from historically contaminated sediments to the water column (Bopp et al. 1991; Chaky 2003; CSTAG 2008). This is supported by the predicted contaminant mass balances presented in Section 7.2.

10.3 Natural Recovery of 2,3,7,8-TCDD in Surficial Sediments

At locations that experienced significant net deposition since the 1960s, as evidenced by interpretable vertical profiles of Cs-137, the highest 2,3,7,8-TCDD concentrations are buried below the surface sediments. The effect of burial on surficial 2,3,7,8-TCDD concentrations was noted in the reach-by-reach discussions in Section 4. Building on these discussions, the relationship between surface and maximum concentrations at depth, and sedimentation rate, is evaluated in Figure 10-4.

Figure 10-4 shows the following:

- Locations with high average sedimentation rates between the early 1960s and the time of sediment core collection[203] exhibit the greatest recovery as evidenced by lower surface concentrations relative to at-depth concentrations (top panel). This is also consistent with the conclusions in Section 4, which indicated that at-depth concentrations were generally higher than surface concentrations.
- The depth of maximum 2,3,7,8-TCDD contamination increases as net sedimentation rate increases,[204] indicating burial since peak discharge (bottom panel).

[203] These plots include all data upstream of RM 1.9 with available deposition rates. The calculation of the deposition rates used in this plot can be found in Erickson et al. (2007) and in Appendix I. Samples downstream of RM 1.9 are excluded due to the potential impacts of navigational dredging (as discussed in Section 4.2.10).

[204] Net sedimentation rates were mainly estimated based on the depth differential of the Cs-137 peak and the sediment surface. Cs-137 in sediments is derived from atmospheric nuclear weapons testing. Its first occurrence generally marks the early 1950s, and peak concentrations correspond to 1963, the year maximum atmospheric fallout from testing was noted (Ritchie and McHenry 1990). Sedimentation rates can vary over time. Net sedimentation rates since 1963 represent previous conditions but are not necessarily representative of current or future conditions.

An assessment of recovery in RM 1 to RM 7[205] was made by comparing surface sediment 2,3,7,8-TCDD concentrations measured in the 1995 to 1999 period (the 1995 dataset) with concentrations measured between 2005 and 2010 prior to the 1-in-90-year storm event Hurricane Irene (the 2010 pre-Irene dataset). The data were grouped based on net changes in bathymetry between surveys in 1995 and 2010. Four groups were established[206]:

- Erosional areas: areas experiencing more than 6 inches of erosion (58 acres; 16%)
- Depositional areas: areas experiencing more than 6 inches of deposition (117 acres; 32%)
- Change <= 6-inch areas: areas having elevation change within the uncertainty of the bathymetric differencing, i.e., <= 6 inches (87 acres; 23%)
- Areas outside the bathymetry extent: areas not covered by the both the 1995 and 2010 bathymetry surveys because of depths too shallow to accommodate the surveying techniques (109 acres; 29%)

Within these net change groups are shorter-term changes that might include both erosion and deposition. The extensiveness of such cyclical behavior was assessed using the 2007, 2008, and 2010 multi-beam bathymetry surveys (i.e., taking account of areas experiencing more than 6 inches of deposition between the 2007 and 2008 surveys followed by more than 6 inches of erosion between the 2008 and 2010 surveys, or vice versa). Figure 10-5 shows the spatial extent of the four 1995 to 2010 bathymetric change groups and identifies cyclical areas. Acreages for these groups and the cyclical areas are listed in Table 10-1. Note that Table 10-1 and Figure 10-5 do not fully account for cyclical areas because the analysis misses such behavior that occurs outside the lateral limits of the multi-beam survey comparisons or below the 6-inch uncertainty threshold imposed on these comparisons (based on the 2008 survey accuracy; see Appendix A) and does not reflect such behavior that might have occurred between 1995 and 2007 (see Attachment B of Appendix M for additional evaluations, including evaluations of other parts of the LPR, evaluations of later bathymetric surveys, and a sensitivity to using a 3-inch uncertainty threshold; sequential bathymetry differentials for subsequent years and other parts of the LPR can be found in Section 4.2).

The datasets were compared using probability distributions (Figure 10-6) and Tukey box plots (Figure 10-7). The greatest change occurred in the depositional areas, where the mean declined from about 680 to about 260 ng/kg and the median dropped from about 310 to about 220 ng/kg. The shallow areas outside the bathymetry extent show a similar pattern, though the absolute changes are

[205] RM 1 to RM 7 is the region of comparison because of the upstream and downstream limits of the 1995 dataset.

[206] To calculate the difference between bathymetry data, historical bathymetry surfaces were generated. The 1995 survey extends from RM 0.5 to RM 8.2 and consists of point measurements taken along transects spaced approximately 100 feet apart. These points were converted into a triangulated irregular network (TIN) and then converted to a raster for comparison with the 2010 multi-beam bathymetry raster. The 2010 bathymetry extends from RM 0 to RM 14.2, is mostly limited to near the navigation channel, and is on a 5-foot grid. The 2010 bathymetry survey was used as an end year because it occurred prior to Hurricane Irene. Bathymetry differences are limited to areas near the navigational channel, as this region was the only area covered by both surveys.

smaller. The erosional areas and change <= 6 inches areas have small declines in mean concentration, but no decline (erosional) or a small increase (change <= 6 inches) in median concentration. Of note is the apparent increase in concentration variability in the erosional areas, presumably reflecting a wide range of subsurface concentrations exposed by erosion. While the differences among the groups seems consistent with expectations, strong conclusions cannot be drawn and none of the apparent changes are statistically significant.[207]

The 2010 levels in depositional areas match the levels measured by USEPA in a 2007 to 2008 study of COPC concentrations on recently deposited sediment (i.e., sediments deposited from the water column no earlier than 6 months prior to the sampling). As shown by the blue diamonds in Figure 4-3 of LBG (2014) (included here as Figure 10-8), the 2,3,7,8-TCDD concentrations in recently deposited sediment in the lower 8 miles fall between 200 and 300 ng/kg, while the two samples collected between about RM 8 and RM 12 have concentrations of 460 and 540 ng/kg.

Where surface segment 2,3,7,8-TCDD concentrations are below 200 ng/kg, the sediments are typically coarse material (see Figure 4.1-9a) within which there is a component of finer sediment that likely is subject to alternating erosion and deposition. Under the assumption that the contaminant is mostly associated with organic matter and the organic matter is mostly associated with fine sediments, the contaminant concentration on the finer sediment component can be examined using carbon-normalized concentrations. Focusing on the region between RM 8 and RM 14.8 and locations with dry-weight concentrations in the range of 100 to 200 ng/kg, carbon-normalized concentrations range from approximately 1,000 to 10,000 ng/kg OC and show no trend with fine sediment content (Figure 10-9, left panel). This range overlaps with that of near-bottom water column particles, which is from 400 to 30,000 ng/kg OC (Figure 10-9, right panel), supporting the idea that the fine sediments in these locations have a strong connection to the water column through alternating erosion and deposition. The two distributions do differ somewhat, with the surface sediment mean being statistically significantly higher,[208] presumably reflecting some lag between trends in the water column and trends in the top 6 inches in coarse sediment areas.

The connection to the water column implied by the correspondence of surface sediment concentrations and water column concentrations in areas subject to significant net deposition or cyclic erosion-deposition suggests that these areas should respond to downward trends in water column concentrations. In other words, they have the potential for recovery. The extent to which recovery occurs is likely controlled by the areas subject to net erosion and the areas where cyclical erosion-deposition brings higher subsurface concentrations into the surface layer, which contribute 2,3,7,8-TCDD to the water column and inhibit downward trends in water column concentrations.

[207] T-tests on log-transformed data indicate that the means are not significantly different between 1995 and 2010.
[208] Based on a t-test of log-transformed concentrations.

10.4 Natural Recovery of Other Contaminants of Potential Concern in Surficial Sediments

As discussed in Section 4.2, surface concentrations of other contaminants correlate with 2,3,7,8-TCDD, with the relationship weakest for HMW PAHs and LMW PAHs. The RM 1 to RM 7 recovery trends presented for 2,3,7,8-TCDD can thus be extended to these other contaminants, although differences in the timing of historical contaminant loadings and importance of external sources should be kept in mind. The recovery for total PCBs, total 4,4′-DDx,[209] mercury, HMW PAHs, and LMW PAHs are briefly assessed in a similar manner to 2,3,7,8-TCDD (Figures 10-10 through 10-20).

Figures 10-10 through 10-14 show the relationship between surface and maximum concentrations of contaminants and the sedimentation rate and suggest the following:

- Locations with high sedimentation rates tend to have lower surface concentrations relative to at-depth concentrations (top panel), particularly for total PCBs and mercury. The weaker relationships for the others may reflect weaker time trends due to ongoing sources.
- The depth of maximum contamination increases as net sedimentation rate increases, indicating burial since peak discharge (bottom panel) and is relatively consistent for all five contaminants.

The patterns in recovery differ among the various contaminants in the following manner:

- Total PCBs show less change in depositional areas than 2,3,7,8-TCDD, but the variance drops, suggesting that levels in depositional areas may be increasingly influenced by ongoing sources (Figures 10-15 and 10-20a). The patterns for the other groups are qualitatively similar to those of 2,3,7,8-TCDD. None of the apparent changes are statistically significant.
- Total 4,4′-DDx mean concentrations decreased across all bathymetric categories (Figure 10-20a). The decrease in erosional areas may be an artifact caused by the two extremely high concentrations in the 1995 dataset (Figure 10-16). None of the apparent changes are statistically significant.
- Mercury shows the greatest decreases among the examined contaminants. The distributions for all the bathymetric groups are much lower in 2010 as are the mean concentrations (Figures 10-17 and 10-20a). The smallest decrease occurs in erosional areas. The changes may reflect reductions in atmospheric deposition (Butler et al. 2008). While the apparent changes in depositional areas and in areas with no available bathymetry are statistically significant, the same is not true for the apparent changes in the other areas.

[209] Historical data from 1995 to 1999 are available for the total 4,4′-DDx but not total DDx. To allow the use of the historical data, the total 4,4′ DDx is used in assessing recovery rather than total DDx. A comparison of total DDx and total 4,4′-DDx for the post-2005 data is presented in Figure 8 in Appendix I and indicates that total 4,4′-DDx is well correlated to total DDx and comprises most of the total DDx.

- HMW and LMW PAHs show an increase in surface sediment concentrations from 1995 to 2010 across all bathymetric categories (Figures 10-18, 10-19, and 10-20b). The lack of recovery in surface PAH contamination could be a result of ongoing PAH sources and the form of released PAHs (see Section 4). While the apparent changes in erosional areas are not statistically significant, the changes in the other areas are statistically significant.

10.5 Impact of Hurricane Irene

Hurricane Irene occurred in late-August 2011. Erosion and deposition that might have occurred during the 90-year high flow generated by Irene were assessed by comparing a June 2010 bathymetric survey with one conducted shortly after Irene (October to November 2011). The changes indicate that of the 340 acres over which comparisons could be made between RM 2 and RM 12, 136 and 46 acres experienced measurable net erosion and deposition, respectively.[210] This movement of sediment likely affected surface sediment concentrations and, thus, recovery. To gain relevant insight, pre- and post-Irene surface sediment concentrations are compared. Strong conclusions are not drawn because the comparisons are hampered by spatial biases between the datasets. The programs that generated these data targeted specific areas and, for the post-Irene programs, aimed to fill data gaps and test hypotheses on concentration patterns. Data above RM 12 are not considered in this analysis because of the confounding effect of the large along-river concentration gradient that exists (see Section 4; Figure 4.1-9a). Data below RM 2 are not considered because there are only four post-Irene samples and this region is also subject to longitudinal concentration gradients.

Pre- and post-Irene surface sediment concentration statistics are presented in Table 10.2 with the data parsed into bins of RM 2 to RM 8 and RM 8 to RM 12. A consistent pattern exists for 2,3,7,8-TCDD, PCBs, and mercury. Mean concentrations and interquartile ranges are higher post-Irene and median concentrations differ little. Total 4,4'-DDx and the PAHs show similar tendencies, though the changes are more variable and generally less significant. The higher interquartile range derives from significantly higher 75th percentile concentration and similar or slightly lower 25th percentile concentration.

The higher mean concentrations are a consequence of higher concentrations in the upper half of the distribution and little change in the lower half (indicated by the lack of change in median concentration and a small decline or little change in 25th percentile concentration). The concentrations in the lower half of the distributions occur most frequently in the channel, which the figures in Section 4[211] show was mostly not scoured. Erosion was mostly on the channel side walls

[210] Given the estimated uncertainty of bathymetric differences between the 2010 and 2011 surveys (see Appendix A), the threshold for measurable change was set at 3 inches. Erosion and deposition of less than 3 inches likely occurred but cannot be reliably assessed.

[211] Figures 4.2.4-6, 4.2.5-8, 4.2.6-5, 4.2.7-7, 4.2.8-6, and 4.2.9-6

and the edge of the shoals. These areas tend to have relatively high concentrations close to the surface, which may explain the increases at the upper end of the distribution. Vertical gradients do tend to be higher at higher surface sediment concentrations. For example, where the surface sediment 2,3,7,8-TCDD concentration exceeds 200 ng/kg the layer below (0.5 to 1.5 feet) averages 3.4 and 5.1 times the surface layer 2,3,7,8-TCDD in RM 2 to RM 8 and RM 8 to RM 12, respectively, whereas these ratios are 1.9 and 0.9, respectively, for surface concentrations less than 200 ng/kg.[212]

The likelihood that higher post-Irene mean concentrations signify a real uptick was assessed using 95th percentile confidence limits on the post- to pre-Irene ratio of mean concentrations and the likelihood that the ratio exceeds 1.0. These statistics were generating using bootstrap sampling with replacement. For 2,3,7,8-TCDD, PCBs, and mercury, there is greater than 99.9% likelihood that the post-Irene mean exceeds the pre-Irene mean. For total 4,4'-DDx and the PAHs, the confidence limits extend below 1.0 and the likelihood that the ratio exceeds 1.0 is less than 95%, thus providing less confidence that there has been a real uptick.

Given that the greatest uptick post-Irene occurred for 2,3,7,8-TCDD, it was used to investigate whether the uptick is influenced by the location of samples relative to where net erosion and net deposition occurred between the 2010 and 2011 post-Irene bathymetry surveys. Visual comparisons of the pre- and post-Irene concentration distributions for the RM 2 to RM 8 and RM 8 to RM 12 bins are used for this purpose (Figures 10-21 and 10-22). The distributions suggest differences in pattern between samples collected in net erosion and net deposition areas. Consistent with the overall differences discussed above, samples from net erosion locations diverge somewhat in the upper half of the distributions, with post-Irene being generally higher. Samples from net deposition locations do not show this pattern and suggest little change or a decline post-Irene, though there are too few samples to make firm judgements. Locations where there was less than a 3-inch change appear visually similar, suggesting that Irene did not have a substantial impact. Locations outside the limits of the bathymetric surveys, which are in shallower nearshore areas, have a steeper distribution post-Irene, suggesting concentration increases and decreases relative to pre-Irene and a mix of erosion and deposition.

10.6 Natural Recovery of Biota Tissue Concentrations

Contaminant concentrations of 2,3,7,8-TCDD, total PCBs, total 4,4'-DDx, mercury, LMW PAHs, and HMW PAHs in biota tissue were compared for samples from historical (1995 to 2004) and more recent (2009 to 2010) datasets. Generally, total PCB concentrations were found to have declined (when excluding potential outliers), but patterns for other chemicals were not clear. Variability in concentration trends (including those for PCBs when including or excluding potential outliers) may have been due to the number of samples, timing of the sampling, species or individuals sampled

[212] Ratios are the average concentration in the 0.5- to 1.5-foot layer divided by the average concentration in the 0- to 0.5-foot layer.

(including age, length, and lipid content), method of sample preparation, metabolization of PAHs, and other factors. Major storm events may also have contributed to variability over time and limited natural recovery. As a result, using existing biota tissue data to infer current recovery rates associated with changing exposures to contaminated sediments is highly uncertain.

LBG et al. (2014) reached similar conclusions in the FFS regarding the uncertainty associated with data comparability between historical and more recent tissue concentration datasets from the lower 8.3 river miles of the LPR. In particular, the authors noted that seasonality and analytical differences (among other factors) were more likely drivers for variability in tissue concentrations over time rather than changing sediment concentrations and exposures. The 2016 ROD for the lower 8.3 river miles of the LPR (USEPA 2016) restated those conclusions. LBG et al. (2014) used Tukey's Honest Significant Difference (HSD) test to evaluate differences among 1999, 2000, and post-2005 log-transformed tissue concentration datasets. Their analysis assumed a log-normal distribution and tested differences in geometric means. If the assumption of lognormality is valid, then the HSD test will have similar or greater power than a comparable non-parametric test, but deviations from lognormality will reduce the power of the HSD test. The analysis described herein was non-parametric and robust to violations of the parametric assumption. The analysis described herein also treated 1999 and 2000 data as a single population of "historical" values and all 2009 to 2010 data as "recent" values; the increased sample size of "historical" data should improve test power for most tests. Based on a Shapiro-Wilk test of log-transformed data, 66% of historical datasets and 86% of recent datasets failed the test assumption for the HSD. Lognormality was not evaluated for 1999 and 2000 data independently. LBG et al. (2014) also grouped various tissue types, whereas the current analysis looked at tissue types individually (e.g., the evaluation of white perch fillets herein as opposed to the combination of fillet, whole body, and head and viscera samples in the FFS).

When comparing biota tissue concentrations, the following are important considerations with respect to the comparability of historical and recent data:

- Differences in sampling/analytical methods and sampling design: different sampling events with various objectives can produce data that may not be directly comparable. Differences in species collected, tissue types analyzed, and/or areas included in the sampling can make it difficult to compare concentrations.
- Differences in sampling season: biota tissue concentrations can vary seasonally; thus, there may be uncertainty as to whether samples collected in different seasons reflect temporal trends or seasonal variations.
- Differences in age: the age of an organism can influence the degree of bioaccumulation and biota tissue concentrations to which it is subject.
- Differences in length of time between the recent and historical data are a source of uncertainty.

- Availability of data: there may be insufficient data to evaluate contaminant concentration trends.

Both ww and lipid-normalized concentrations are presented. Lipid content in fish may be affected by fish condition, size, age, sex, reproductive status, genetic background, diet, water temperature, and seasonality (Mraz 2012; Iverson et al. 2002). Lipid normalization can help control for factors that impact lipid content, as well as for differences in tissue types (e.g., skin-on versus skin-off fillets). However, there is uncertainty regarding the analytical methods used for measuring lipid concentrations in the historical data. Although the lipid fractions for the recent data were all determined using the same analytical method, the lipid fractions for the historical data were likely determined using a variety of methods and extraction solvents, which can result in large differences in lipid fractions for the same tissue samples. Despite this, both ww and lipid-normalized concentrations are presented for all chemicals (including mercury, which is not lipophilic). The historical and recent data used for this analysis are summarized in Table 10-3. The species included in this comparison satisfied the following criteria:

- The same tissue type was available for both the historical and recent datasets.
- There were at least three samples in each of the datasets.
- Samples were collected in similar areas of the LPR.

Additionally, samples for which only a subset of PCB congeners were analyzed were excluded. Based on the locations for which historical data are available, trends were evaluated only considering locations below RM 8 (eliminating three American eel samples, which were collected from near RM 16). The exception to this was for carp; the only available historical data were samples collected at RM 9.5 and RM 16. Thus, the comparison for carp was based on data from RM 8 to RM 10 and RM 14 to RM 17.4.

Figures 10-23 through 10-28 present the comparison of historical and recent tissue data. The fish and crab data collected in summer/fall of 2009 and 2010 were compared with the historical data from 1995 to 2004 for spatial areas that were similar between these two datasets for each species/tissue type. The populations of historical and recent fish tissue concentration data were compared using the nonparametric Mann-Whitney U test (2-tailed, alpha = 0.05), which was conducted using R software (R Core Team 2018). This test does not rely on the assumption of normally distributed tissue concentration data, and it is appropriate even for small datasets (e.g., n <30). A significant test result indicates that the two groups of concentrations are not part of the same population (i.e., the central tendency is not the same and/or the shape of the distribution is not the same). Outlier concentrations were identified as the 75th percentile (i.e., third quartile) plus three times the interquartile range (IQR) of the data distribution. This approach does not rely on an assumption of normality. Recent and historical populations were compared using the nonparametric Mann-Whitney U test (2-tailed, alpha = 0.05) to determine if the populations were different. The

results of the Mann-Whitney U tests conducted on datasets both with and without the three IQR outlier samples were compared to ascertain the influence of outlier values on the test.

Tropical Storm Floyd (which occurred on September 16, 1999) may have had an impact on contaminant bioavailability. In the historical dataset, there were several mummichog samples collected in October 1999, approximately 1 month after Tropical Storm Floyd. Three of these mummichog samples from October 1999 exhibited tissue concentrations that were higher than other samples based on visual evaluation. The influence of these samples on the comparison of recent and historical data was evaluated by using the Mann-Whitney U tests (as described above) both with and without the three 1999 samples. Outliers (based on the IQR method described above) were included when conducting the evaluation with and without 1999 data. Removing the three 1999 samples did not affect the outcome of significance tests comparing recent and historical tissue concentration data.

A summary of the percent change in the mean tissue concentrations between the historical and recent data without the exclusion of potential outliers is provided in Table 10-4. Table 10-5 provides a summary of the numbers of outliers identified for the historical and recent data and the average values including and excluding outliers.

For each species, the uncertainty for the comparison of historical and recent data was evaluated as it relates to the spatial area of sample collection, seasonality of sample collection, differences in sample preparation, average lipid fractions, and age. Biota length (as available) was used as a surrogate for biota age. Figures 1 through 24 in Appendix AA show linear regressions between biota length and tissue concentrations.[213] The significance of the linear regression slope parameter was evaluated using a Student's t-test (2-tailed, alpha = 0.05). Outliers were identified in the figures and were included in the linear regression and slope parameter evaluation.

This evaluation is presented as follows:

- **American eel** – Uncertainty associated with the comparison of historical and recent data for American eel is primarily due to the difference in tissue types (i.e., historical data were analyzed as skin-on fillets, while the current data were analyzed as skinless fillets). The differences in the average lipid fractions (8.1% for the historical data versus 4.7% for the recent data) means that the comparison of lipid-normalized concentrations could be primarily reflecting this difference in lipid content. This limits the comparability of historical and recent ww tissue concentration data to some degree, whereas lipid-normalized concentrations are more valid for comparison; historical ww concentrations could be elevated as a result of the inclusion of skin in tissue samples. The higher lipid content in the historical data may, in part,

[213] Length data were not available for all samples for which chemistry data were available. All samples with length data were included in the regressions.

reflect the inclusion of skin with the fillets in the historical data; the more recent data included skin-off fillets. The historical skin-on fillet data may have higher concentrations of lipophilic organic compounds based on higher lipid content. Length data were not available for the historical American eel data; therefore, the relationship between length and tissue concentrations is unknown for the historical data for this species. Significant changes in tissue concentrations over time may, at least in part, reflect the lack of comparability. Statistical comparisons between recent and historical data are also uncertain because of the limited number of samples in the historical (n=7) and recent (n=6) datasets.

- **Carp** – Sufficient numbers of carp samples from the historical dataset were only available for PCBs and DDx, although an insufficient number of samples were available from the recent database. Thus, although carp data are presented for these chemicals, this comparison should be considered uncertain. Uncertainty associated with the comparison of historical and recent data for carp is primarily the result of the spatial area where carp were collected (at RM 9.5 and RM 16 in the historical dataset) and the fact that the carp in the recent dataset (64 cm in length) are larger on average than the carp in the historical dataset (55 cm in length). Carp from similar areas in the recent dataset (n=4) were used for this comparison (RM 8 to RM 10 and RM 14 to RM 17.4); however, this comparison is spatially limited, and the results may not be representative of the entire LPR. In addition, historical carp (n=9) samples were analyzed as skin-off fillets, while recent data were analyzed as skin-on fillets. The seasons during which samples were collected and the average lipid fraction are similar. This limits the comparability of historical and recent ww tissue concentration data to some degree, whereas lipid-normalized concentrations are more valid for comparison; historical ww concentrations could be elevated as a result of the inclusion of skin in tissue samples. Significant changes in tissue concentrations over time may, at least in part, reflect the lack of comparability. Furthermore, historical length data were not available for carp; therefore, the relationship between length and tissue concentrations is unknown for the historical data for this species.
- **Mummichog** – Uncertainty associated with the comparison of historical and recent data for mummichog is primarily due to the difference in the timing of sample collection; historical samples were primarily collected in summer/early fall but also in spring and winter, whereas recent data were collected from June through August. Average lipid fractions were 3.2% for historical data and 1.9% for current data, suggesting that the comparison of lipid-normalized concentrations could primarily reflect this difference (i.e., at the same ww concentration, recent data would be approximately 70% higher than the historical data due to the lower lipid fraction). Furthermore, length data were limited for the historical mummichog samples; therefore, the relationship between length and tissue concentrations is uncertain for the historical data for this species.[214] The factors listed above limit the comparability of historical

[214] A total of three mummichog samples collected in November 1999, February 2000, and May 2000 had length data and corresponding chemistry data. The mummichog sample collected in May 2000 did not have total PCB and the total 4,4'-DDx data.

and recent mummichog tissue data, particularly ww concentrations, which are likely affected by variability in lipid content. Significant changes in tissue concentrations over time may, at least in part, reflect that lack of sample comparability.

- **White perch** – Uncertainty associated with the comparison of historical and recent data for white perch is primarily due to differences in the timing of sample collection (May for the historical data, compared to September for the recent data). In addition, historical data were analyzed as skinless fillets, while recent data were analyzed as skin-on fillets. Lipid fractions were relatively similar (2.9% for historical data and 2.3% for recent data), suggesting that differences in tissue lipid content are a minor point of uncertainty in regard to the comparability of historical and recent white perch fillet tissue data. Statistical comparisons between recent and historical data are uncertain because of the limited number of samples in the historical (n=6) and recent (n=11) datasets. Furthermore, length data were not available for the historical white perch data; therefore, the relationship between length and tissue concentrations is unknown for the historical data for this species. As a result of these factors, the comparability of historical and recent white perch tissue concentration data is uncertain, and significant changes over time may, at least in part, reflect the lack of comparability.
- **Blue crab (muscle)** – The data used to compare muscle tissue from blue crab for historical and recent data are relatively similar regarding sample timing (primarily summer/early fall for both), tissue type, and average lipid fractions (0.6% for historical data and 0.5% for current data). Information about the composition (individual versus composites) of historical samples was limited. Furthermore, length data were also limited for the historical blue crab muscle samples; therefore, the relationship between length and tissue concentrations is uncertain for the historical data for this species.[215] As a result of these factors, the comparability of historical and recent blue crab muscle tissue concentration data is uncertain, and significant changes over time may, at least in part, reflect the lack of comparability.
- **Blue crab (muscle/hepatopancreas)** – The data used to compare muscle/hepatopancreas tissue from blue crab for historical and recent data are relatively similar regarding sample timing (primarily summer/early fall for both), tissue type, and average lipid fractions (2.3% for historical data and 1.5% for current data). Information about the composition (individual versus composites) of historical samples was limited. In addition, length data were limited for the historical blue crab muscle/hepatopancreas samples; therefore, the relationship between length and tissue concentrations is uncertain for the historical data for this species.[216] As a result of these factors, the comparability of historical and recent blue crab

[215] A total of 13 blue crab muscle samples (3 collected in September 1999 and 10 in June 2004) had length and corresponding 2,3,7,8-TCDD, mercury, and total 4,4'-DDx data. A total of three samples collected in September 1999 had length and corresponding PCB and PAH data.

[216] A total of six blue crab muscle/hepatopancreas samples collected in September 1999 had length and corresponding PCB, mercury, and total 4,4'-DDx data. Five samples collected in September 1999 had length and corresponding 2,3,7,8-TCDD data, and three samples collected in September 1999 had PAH data.

muscle/hepatopancreas tissue concentration data is uncertain, and significant changes over time may, at least in part, reflect the lack of comparability.

- **Blue crab (hepatopancreas)** – The data used to compare hepatopancreas tissue from blue crab for historical and current data are relatively similar regarding sample timing (summer/early fall for both) and tissue type, although the reported lipid fractions are different (13% for historical data and 7.3% for current data). The recent data have fewer samples (n=5) than do the historical data (n=30); statistical comparisons between historical and recent data are uncertain because of the limited number of samples in the recent dataset. Information about the composition (individual versus composites) of historical samples was also limited. Furthermore, length data were limited for the historical blue crab hepatopancreas samples; therefore, the relationship between length and tissue concentrations is uncertain for the historical data for this species.[217] As a result of these factors, the comparability of historical and recent blue crab hepatopancreas tissue concentration data is uncertain, and significant changes over time may, at least in part, reflect the lack of comparability.

Using the results shown in Tables 10-4 and 10-5 and Figures 10-23 through 10-28, the following subsections provide the historical and recent data trends by chemical.

2,3,7,8-TCDD

Recent lipid-normalized concentrations were statistically higher for blue crab muscle/hepatopancreas samples compared to historical concentrations, while lipid-normalized concentrations for other species and tissue types were not statistically different (Table 10-4). Recent ww concentrations were statistically lower for mummichog and blue crab hepatopancreas samples compared to historical concentrations, while ww concentrations for other species and tissue types were not statistically different. One outlier (white perch fillet sample collected in August 2009) was identified in the recent dataset (ww) (Table 10-5). Outliers identified in the historical dataset included three mummichog samples (ww and lipid-normalized) and one blue crab muscle/hepatopancreas sample (lipid-normalized) that were collected in October 1999. Tropical Storm Floyd (which occurred on September 16, 1999, 1 month before the collection of the 1999 outlier data) may have had an impact on 2,3,7,8-TCDD bioavailability, potentially contributing to higher concentrations in the historical outliers. Statistical comparisons between recent and historical data (lipid-normalized and ww) were not impacted by the removal of outlier data. Furthermore, statistical comparisons of historical and recent tissue concentrations were not impacted by the removal of Tropical Storm Floyd data.

[217] A total of 13 blue crab hepatopancreas samples (3 collected in September 1999 and 10 in June 2004) had length and corresponding 2,3,7,8-TCDD, mercury, and total 4,4′-DDx data. A total of three samples collected in September 1999 had length and corresponding PCB, and two samples collected in September 1999 had PAH data.

Linear regressions between biota length and 2,3,7,8-TCDD concentrations had significant slopes for white perch (recent data only), blue crab muscle/hepatopancreas (recent data and five historical samples), and mummichog (recent data and three historical samples) for lipid-normalized and ww concentrations; results were not impacted by the removal of outliers based on concentration (Figures 1 through 4 of Appendix AA).[218] Linear regression slopes were negative for white perch, blue crab muscle/hepatopancreas, and mummichog, meaning that 2,3,7,8-TCDD concentration decreased with length. The influence of white perch, blue crab, and mummichog length on the comparison between recent and historical data is uncertain, given the limited amount of historical length data.

Total PCBs

With two exceptions, concentrations for all species (lipid-normalized and ww) were lower in the recent data than in the historical data (Tables 10-4 and 10-5, Figure 10-24). The exceptions to this trend were carp and American eel (lipid normalized data), for which concentrations in the recent data were higher. However, only four recent carp samples and six recent American eel samples were available, meaning that these comparisons are uncertain. Recent and historical concentrations were statistically different for all species and tissue types, except for both lipid-normalized and ww American eel fillet. However, when outliers were removed, the recent and historical American eel concentrations were statistically different for ww data (Table 10-5). No other statistical results (lipid-normalized or ww) were impacted by the removal of outlier data. Tropical Storm Floyd—which occurred 1 month before the collection of one blue crab hepatopancreas sample identified as an outlier for both the ww and lipid-normalized concentrations in the historical data—may have had an impact on PCB bioavailability, potentially contributing to the higher outlier concentration.[219] Statistical comparisons of historical and recent tissue concentrations were not impacted by the removal of Tropical Storm Floyd data.

Linear regressions between biota length and PCB concentrations had significant slopes for white perch (recent data only) and mummichog (recent and two historical samples) for lipid-normalized and ww concentrations (results were not impacted by the removal of outliers based on concentration) (Figures 5 through 8 of Appendix AA). Linear regression slopes were negative for white perch and mummichog, meaning that total PCB concentrations decreased with length. The influence of white perch and mummichog length on the comparison of recent to historical data is uncertain given the limited amount of historical length data.

Total 4,4'-DDx

No clear pattern was present in the total 4,4′-DDx tissue concentrations; mean concentrations both increased and decreased across species and tissue types (Tables 10-4 and 10-5, Figure 10-25). Blue

[218] Outlier concentrations were identified as the 75th percentile (i.e., third quartile) plus three times the IQR of the data distribution.
[219] Outliers in the historical dataset included one blue crab hepatopancreas sample collected September 10, 1999, (ww) and one blue crab hepatopancreas sample collected October 25, 1999 (ww and lipid-normalized).

crab muscle and carp concentrations (lipid-normalized and ww) were statistically higher in recent data than in historical data. Lipid-normalized whole-body mummichog total 4,4′-DDx concentrations were also statistically higher in recent data than in historical data. White perch fillet concentrations (ww) were statistically lower in recent data than in historical data. Statistical comparisons between historical and recent data (lipid-normalized and ww) were not impacted by the removal of outlier data, with the exception of lipid-normalized American eel comparisons; American eel had statistically higher lipid-normalized total 4,4′-DDx concentrations in recent data than in historical data upon the removal of outliers. As with PCBs, it should be noted that only four recent samples were available for carp, meaning that the carp comparison is uncertain.

Linear regressions between biota length and total 4,4′-DDx concentrations did not have significant slopes for ww and lipid-normalized concentrations. Results were not impacted by the removal of outliers (based on concentration), except for ww outliers for total 4,4′-DDx for mummichog (Figures 9 through 12 of Appendix AA). Upon removal of the historical mummichog outlier (collected in the February 2000), the slope of the linear regression became significant (using recent and one historical sample). The linear regression slope was negative, meaning that total 4,4′-DDx concentrations decreased with length. The influence of mummichog length on the comparison between recent and historical data is uncertain given the limited amount of historical length data.

Mercury

Concentrations for all species (both lipid-normalized and ww) were higher in the recent data than in the historical data, with the exceptions of white perch (ww and lipid-normalized) and blue crab hepatopancreas (ww only) data, for which concentrations in the recent data were lower (Tables 10-4 and 10-5 and Figure 10-26). Differences were statistically significant for white perch (ww), American eel (lipid-normalized), mummichog (lipid-normalized and ww), blue crab muscle (lipid-normalized and ww), and blue crab muscle/hepatopancreas (lipid-normalized and ww). Statistical comparisons between recent and historical data (lipid-normalized and ww) were not impacted by the removal of outlier data.

Linear regression between biota length and lipid-normalized mercury concentrations had a significant slope only for mummichog (recent and three historical samples) and ww mercury concentrations for white perch (recent samples) (Figures 13 through 16 of Appendix AA). Removal of outliers (based on concentration) did not impact the results, except for white perch (not significant upon removal of outlier). Linear regressions between biota length and ww mercury concentrations had significant slopes for blue crab hepatopancreas (recent and 13 historical samples). The linear regression slope was positive for mummichog (lipid-normalized concentrations increased with length) and negative for blue crab hepatopancreas (ww concentrations decreased with length). The influence of length on the comparison between recent and historical data is uncertain, given the limited amount of historical length data.

HMW PAHs

No clear pattern was present in HMW PAH tissue concentrations (Tables 10-4 and 10-5 and Figure 10-27). Recent concentrations (lipid-normalized and ww) were statistically higher for mummichog and blue crab hepatopancreas than were historical concentrations. Recent concentrations (lipid-normalized and ww) were statistically lower for blue crab muscle than historical concentrations. Statistical comparisons between recent and historical data (lipid-normalized and ww) were not impacted by the removal of outlier data.

Linear regressions between biota length and HMW PAH concentrations (lipid-normalized and ww) had significant negative slopes (decrease in concentration with length) for white perch (recent data), blue crab hepatopancreas (recent and two historical samples), and mummichog (recent and three historical samples) (Figures 17 through 20 of Appendix AA). Removal of outliers (based on concentration) did not impact the statistical evaluation of the slope of the linear regression. The influence of length on the comparison between recent and historical data is uncertain, given the limited amount of historical length data.

In many species of fish, PAHs undergo rapid biotransformation that leads to tissue concentrations that do not reflect environmental exposure and result in very low bioaccumulation factors (Van der Oost et al. 2003; Meador et al. 2008). In addition, environmental and organismal physiological conditions may further influence PAH tissue concentrations. Cytochrome P450 (CYP450) enzymes play a major role in the oxidative metabolism of PAHs in fish and some aquatic invertebrates (Andersson and Forlin 1992; Lee 1989; Gorbi et al. 2005; Geeraerts and Belpaire 2010). Exposure to PAHs causes an increase in the production of CYP450 enzymes (Andersson and Forlin 1992). However, this metabolic process is also influenced by water temperature, organism physiological condition, and reproductive status (Andersson and Forlin 1992; Gorbi et al. 2005). It is uncertain if differences in exposure to PAHs, water temperature, organism physiological condition, and reproductive status may have influenced comparisons of PAH tissue concentrations between historical and recent samples. Significant differences in HMW PAHs were found between historical and recent mummichog and blue crab (hepatopancreas and muscle) samples.

Temperature and physiological fluctuation influences on CYP450 induction have been observed in mummichog (Stegeman 1979). Stegeman (1979) investigated the influence of temperature on CYP450 in mummichogs at 6.5°C and 16.5°C. While basal levels of CYP450 were higher in cold-acclimated fish (6.5°C), the induction of CYP450 occurred more rapidly in warm-water-acclimated fish (16.5°C) exposed to benzo(a)pyrene (a component of the HMW PAH sum) than in cold-acclimated fish. The influence of temperature on CYP450 activity suggests that PAH metabolism may increase with an increase in temperature. Historical samples were collected primarily in summer and early fall, with some samples collected in spring and winter, while recent data are

from samples collected only in summer (Table 10-3). It is uncertain whether the time of collection (and potential differences in water temperature) may have influenced PAH metabolism and the comparison of recent and historical mummichog HMW PAH concentrations (i.e., statistically higher in recent data than in historical data).

Physiological conditions also influence CYP450 activity and PAH metabolism in blue crab. The hepatopancreas of blue crab has been shown to play a role in the accumulation and metabolism of many contaminants (Lee 1989). Hepatopancreas tubules contain different cell types, including E-, F-, R-, and B-cells. R-cells are storage cells with high lipid content, and F- and B-cells are thought to be involved in protein synthesis (Lee 1989). Lee (1989) found that PAHs initially enter the lipid-rich R-cells before being metabolized in the F-cells and eliminated from the hepatopancreas. Hale (1988) found that the hepatopancreas had higher mean accumulated PAH concentrations than did muscle and ovary tissue. Differences in PAH tissue concentration have been observed among crabs of different sex, maturity, and molt stages (Hale 1988). Recent blue crab hepatopancreas and muscle samples had concentrations of HMW PAHs that were statistically higher and lower, respectively, than in historical samples (Table 10-4 and Figure 10-28). It is uncertain how differences in sex, maturity, molt stages, and metabolism of PAHs may have influenced comparisons between recent and historical data.

LMW PAHs

No clear pattern was present in LMW PAH tissue concentrations (Tables 10-4 and 10-5 and Figure 10-28). Recent lipid-normalized LWM PAH concentrations for blue crab muscle/hepatopancreas and mummichog were statistically higher than were historical concentrations. Recent lipid-normalized concentrations in white perch were also statistically higher than were historical concentrations, although when outliers were removed, the concentrations were not statistically significant. Recent and historical ww LWM PAH concentrations were not statistically different. No other statistical comparisons between recent and historical data were impacted by the removal of outlier data.

Linear regressions between biota length and LMW PAH concentrations (lipid-normalized and ww) had significant negative slopes (concentrations decreased with length) for blue crab muscle/hepatopancreas (recent and five historical samples) and mummichog (recent and three historical samples) (Figures 21 through 24 of Appendix AA). Removal of outliers (based on concentration) did not impact linear slope results, except for lipid-normalized concentrations for blue crab muscle/hepatopancreas (not significant upon removal of two outliers in recent data) and ww hepatopancreas concentrations (significant negative slope upon removal of one outlier in recent data). The influence of length on the comparison between recent and historical data is uncertain given the limited amount of historical length data.

As previously discussed (see HMW PAHs), exposure to PAHs causes an increase in the production of CYP450 enzymes (Andersson and Forlin 1992), and this metabolic process is also influenced by water temperature, organism physiological condition, and reproductive status (Andersson and Forlin 1992; Gorbi et al. 2005). Temperature and physiological fluctuation influences on CYP450 induction have been observed in mummichog, and physiological conditions also influence CYP450 activity and PAH metabolism in blue crab (see HMW PAHs). Recent lipid-normalized LWM PAH concentrations in blue crab muscle/hepatopancreas and mummichog were statistically higher than were historical concentrations (Table 10-5 and Figure 10-27). It is uncertain how PAH metabolism (and the factors that influence CYP450 induction) may have influenced comparisons of LMW PAH concentrations between historical and recent data.

11 Summary and Findings

Numerous investigative studies have created an extensive dataset upon which to examine and understand the physical, chemical, and biological characteristics of the LPR, and the processes that control the fate and transport of contaminants and their transfer from sediments and water to human and/or ecological receptors.

The LPR is a highly modified river system in which the interplay between historical sources, tidal exchange, the salt front, freshwater flows, CSO and stormwater discharges, and anthropogenic influences has resulted in a complex pattern of contamination. Much of the work reported here has been directed to understanding that pattern, and this RI has integrated multiple sources of information and data to define the spatial and temporal patterns of contaminants in terms of the evolution and behavior of the river. The understanding generated from the extensive site-specific dataset forms the basis of a comprehensive CSM. This CSM describes the physical characteristics of the LPR and its sediments and the nature and extent of contamination—especially in relation to the river's evolution and history of urbanization, contaminant sources, transport pathways, exposure pathways, and receptors. The conceptual understanding of the LPR serves as the foundation for the development of remediation strategies aimed at mitigating contaminant impacts and ultimately achieving CERCLA-compliant risk-based remedial goals protective of human health and ecological receptors in sediment, biota, and surface water.

The CSM is summarized by major component in the following subsections.

11.1 System Characteristics

The LPR is a classical partially mixed coastal plain estuary of relatively shallow depth, gently sloping bottom, and expanding cross section. It contains meanders reflective of its ancestral river channel. Its sediment dynamics, sediment transport, and geomorphological features reflect fluvial and estuarine processes influenced by inputs from upstream of Dundee Dam and tributaries, tidal exchange with Newark Bay, navigational dredging, and infilling after maintenance of the navigational channel ceased.

The interplay of freshwater flows from above Dundee Dam, tributaries, and, to a lesser extent, direct discharges from CSOs, SWOs, and permitted municipal and industrial discharges and direct runoff, and the brackish water from Newark Bay generates a distinct salt front whose location depends on the freshwater discharge, tides, and storm-induced water surface level fluctuations in Newark Bay. The salt front typically resides within the lower 10 miles and moves several miles during each tidal cycle (MPI 2007; Cañizares et al. 2009) and can extend beyond RM 14 under extreme low-flow conditions (SEI and HDR|HydroQual 2011). This net up-estuary flow provides a mechanism for water and solids originating from the lower portions of the LPR to move upstream.

A long history of urbanization and industrialization resulted in the LPR receiving contaminant loadings from a multitude of sources. The LPR has been subject to dredging, and the lower velocities in the expanded cross section produced by navigational dredging facilitated deposition in the shoals coinciding with the period of contaminant releases. In addition, cessation of navigational channel maintenance allowed the channel to experience significant infilling. As a result, the LPR has been an effective sediment and contaminant trap for more than 60 years (Chant et al. 2010; Bopp et al. 1991). The rates with which sediments accumulated relate to geomorphology. For example, sedimentation rates estimated from cores collected from the outer bends, and in higher-velocity reaches of the river, generally were lower than those observed in cores within the main channel. Analyses of bathymetric data presented in Section 4 show that portions of the river have remained net depositional through 2012, while other portions are subject to alternating erosion and deposition or net erosion, which make these sediments potential contaminant sources to the system.

Urbanization and industrial development have also degraded habitat quality along the river, eliminating wetland areas and most shoreline vegetation. Hardened shorelines and urban runoff have degraded habitat function, which is exacerbated by a variety of chemical and non-chemical stressors. While development and urbanization have affected ecological habitat, mudflat and bank-to-bank water habitats are important to the aquatic species and wildlife that use them. Mudflat areas serve as important habitat to benthic organisms and the upper trophic level organisms (fish, birds, and mammals), and bank-to-bank areas (channel and shoals) are important for fish and birds who use and/or rely on nutrients, prey, or habitat provided by surface water of the river.

Urbanization has also influenced the biological communities and their structures in the river. The benthic invertebrate community, which forms the basis of the ecological food web, is typical of that observed in urban estuarine systems. Benthic omnivore fish—the numerically dominant group among fish collected in the LPR—consume instream detritus, invertebrates, surface sediment, and the settling solids coming from impervious surfaces, CSOs, and urban runoff from the surrounding watershed. These food web interactions between organisms and interactions between organisms and sediment affect the bioaccumulation of contaminants from sediment into biota tissue. The LPR and its ecological community are influenced by alterations to the salinity regime and contaminant contamination, as well as a variety of other environmental factors influenced by urbanization including turbidity, organic inputs, DO, and invasive and/or non-native species.

11.2 Nature and Extent of Contamination

Contaminant concentrations in sediments vary widely throughout the river, but that variability is largely explainable by source location, the nature of the sediments, and depositional history. Contaminants in the estuarine portion of the LPR can be transported as far upstream as approximately RM 14, corresponding to the approximate extent of the salt front intrusion under present-day conditions, as well as into Newark Bay with the predominant downstream flow. During

low flows, fine sediments and associated contaminants are trapped within the LPR and there is a net upstream movement of solids and contaminants within the estuarine portion of the LPR. During moderate flows, fine sediments and contaminants are flushed toward Newark Bay. During high river flows, portions of the riverbed experience scour, which may cause buried sediments with potentially higher contaminant levels to be exposed and/or resuspended. During high flows, sediments are either transported through the system (predominantly fine-grained sediments) to Newark Bay or deposited within the LPR. Over the long term, the LPR is predicted to act as a contaminant source to Newark Bay for several chemicals, including 2,3,7,8-TCDD and tetra-CB.

These transport processes have influenced surface contaminant concentration patterns. The highest concentrations primarily occur where sediments laid down in the 1950s and 1960s are exposed or redistributed due to erosion or lack of burial since that era. These are generally located in shoals along bends and at locations in the channel subject to erosion. Areas that have continued to be depositional to recent times have surface contaminant concentrations reflective of levels in suspended sediments.

Contaminants tend to co-occur in the sediments, and concentrations for certain chemicals correlate across the site. This phenomenon is strongest for 2,3,7,8-TCDD, total PCBs, and total DDx; is moderately strong for mercury; and is weakest for HMW PAHs and LMW PAHs. These relationships are likely a function of release history and possibly different transport mechanisms. For instance, PAHs are associated with petrogenic sources such as urban runoff of petroleum products and pyrogenic sources such as soot, fly ash, and other pyrogenic particles produced naturally or anthropogenically.

Water column contaminant levels are largely driven by tidal resuspension/deposition and contaminant-specific influences such as spatial patterns in bed concentrations, boundary loadings, and partitioning behavior. Net upstream contaminant transport within the salt wedge occurs during low flows due to asymmetry in the tidal currents and vertical mixing, which gives rise to higher suspended solids flux on flood than on ebb. Water column transport redistributes contaminants at the sediment-water interface and, during high flows, contaminants in the near-surface sediments of areas that are subject to scour. Overall, concentrations tend to peak in the vicinity of the ETM, with the longitudinal gradient being greatest for 2,3,7,8-TCDD due to the low levels in the freshwater inflow at Dundee Dam which then build up as water moves downstream and interacts with LPR sediments.

Among the fish species sampled, levels of 2,3,7,8-TCDD, total PCBs, and total DDx, are generally highest in large benthic omnivorous fish, with the highest concentrations found in carp. The close association of carp and other large benthic omnivorous fish with surface sediments influences their accumulation of organic contaminants. Mercury concentrations in fish tissue generally increase with

increasing trophic level and are similar or even lower than those measured in fish collected above Dundee Dam.

Changes in surface sediment contaminant concentrations between 1995 and 2010 in RM 1 to RM 7 suggest that some degree of recovery occurred in depositional areas. In these areas the mean 2,3,7,8-TCDD surface sediment concentration declined from about 680 to about 260 ng/kg and the median dropped from about 310 to about 220 ng/kg. Declines also occurred for total PCBs, total 4,4'-DDx, and mercury, but HMW and LMW PAHs increased somewhat. Shallow areas outside the bathymetry extent show a similar pattern, though the absolute changes are smaller. Erosional areas and areas with less than a 6-inch change in bathymetry show small drops in mean concentration, except for HMW and LMW PAHs, which increase perhaps due to ongoing sources.

The 2010 levels in depositional areas match the levels on recently deposited sediment, implying a connection to the water column (which may also exist for the fine sediment fraction in coarse sediments). Such a connection suggests these areas should respond to downward trends in water column concentrations. In other words, they have the potential for recovery. The extent to which recovery occurs is likely controlled by the areas subject to net erosion and the areas where cyclical erosion-deposition brings higher subsurface concentrations into the surface layer.

A negative impact on recovery appears to have resulted from the 90-year high flow in August 2011 generated by Hurricane Irene. Although strong conclusions cannot be drawn because of spatial biases between the datasets, post-Irene average surface sediment concentrations are significantly higher for 2,3,7,8-TCDD, PCBs, and mercury. Total 4,4'-DDx and the PAHs show similar tendencies, though the changes are more variable and generally less significant.

11.3 Human Health Risk Assessment and Baseline Ecological Risk Assessment

The predominant source of human health risk for the LPR is from the consumption of fish and crab. Exposures to surface water and sediment do not pose human health risks warranting remedial action, with the possible exception of accessible surface sediment in the RM 6 to RM 9 reach (particularly the East Bank). The primary human health risk drivers are 2,3,7,8-TCDD and PCBs. Other bioaccumulative compounds, including pesticides and mercury, also contribute to human health risk but to a lesser extent.

It should be noted that, consistent with USEPA guidance, the assumptions and approaches used in the BHHRA are health-protective, such that risks/hazards are more likely to be overestimated than underestimated.

Unacceptable risk to ecological receptors, based on exceedances of a range of effect-level thresholds for various ecological receptor groups (including blue crabs, fish, and wildlife) and LOEs is primarily

driven by exposure to PCDDs/PCDFs, PCBs, and DDx; these were the ecological risk drivers identified in the BERA. Some LOEs are stronger than others and should be weighted more heavily when used for management decisions. While there are statistically significant relationships between observed benthic community impairment and sediment chemistry/habitat conditions, the statistical relationships for individual contaminants are not strong.

11.4 Uncertainty

The analyses and conclusions presented in this report rely on assumptions and simplifications needed to develop holistic understandings from sample sets with gaps typical of investigating a large, complex site. The result is some level of uncertainty. In most cases, the uncertainties are tolerable because they do not undermine the essential insights regarding the nature and extent of contamination, the nature and extent of risks, and the manner and extent of natural recovery.

Three elements of the RI work deserve note with regard to uncertainty: the distribution of contaminant concentrations, the numerical and bioaccumulation models developed to support our understanding of fate and transport and the effectiveness of remediation, and the risk assessments. The distribution of contaminant concentrations is reasonably well understood from the collected samples, but gaps remain. A sense of the imprecision of our understanding is provided by contaminant maps developed using geostatistical interpolation throughout the river and conditional simulation. One hundred equally plausible maps of surface sediment 2,3,7,8-TCDD and tetra-PCB concentrations were generated (Appendix J). These maps exhibit similar overall patterns but significant differences in concentrations. One expression of the imprecision is the RM 8 to Dundee Dam surface area-weighted average concentration for 2,3,7,8-TCDD, which ranged from 450 to 1,050 ng/kg. Despite this imprecision, the coherence of the spatial patterns provides some confidence in our understanding of the areas of the river where concentrations are high and recovery is not occurring and the areas where recovery is ongoing. This provides a basis for crafting remedial alternatives. The delineation of proposed remedial areas would be accomplished as part of the detailed sampling associated with remedy design.

The LPR models represent state-of-the-science models that have been constructed with the available data and the system understanding that has been developed over the course of the RI. However, they are subject to the limitations associated with the model framework, grid resolution, and gaps in calibration datasets. Their accuracy in predicting erosion and deposition, contaminant concentrations in biota, and risk reduction over time is limited due to the complexity of the system and data limitations, and this fact should be considered when making regulatory decisions for the LPR. Despite these limitations, the models capture the major characteristics of contaminant transport and are suitable tools to address specific questions pertaining to the development of remediation strategies for the LPR.

Uncertainty is inherent in the risk assessment process and is a component of risk characterization consistent with USEPA risk assessment policy and guidance. The LPRSA risk assessments have uncertainties associated with assumptions about variables and processes that are not fully known. Recognized uncertainties include current and future site conditions, exposure levels, chemical toxicity, and organism effects. While this could potentially lead to underestimates of potential risk, the use of conservative assumptions, as was done in the BHHRA, more likely overestimates potential risks. The resulting estimates of potential exposure and risk/hazard are conservative and protective of health. The BERA used a range of assumptions to bound the risk range, using less conservative assumptions for the upper end of the risk range and more conservative assumptions for the lower end of the risk range. The actual risks posed by site-related contaminants are reasonably assumed to be within the range of risk estimates.

12 References

Adams, W., R. Blust, U. Borgmann, K. Brix, D. DeForest, A. Green, J. McGeer, J. Meyer, P. Paquin, P. Rainbow, and C. Wood, 2011. "Utility of Tissue Residues for Predicting Effects of Metals on Aquatic Organisms." *Integrated Environmental Assessment and Management* 7(1):75–98.

AECOM, 2010. *Quality Assurance Project Plan for Lower Passaic River Restoration Project: Periodic Bathymetric Surveys, Revision 2*. May 2010.

AECOM, 2011a. *Lower Passaic River Study Area River Mile 10.9 Characterization Quality Assurance Project Plan. Revision 2*. August 2011.

AECOM, 2011b. *Quality Assurance Project Plan*. River Mile 10.9 Hydrodynamic Field Investigation for the Lower Passaic River. Revision 0. Lower Passaic River Restoration Project. Prepared for the Cooperating Parties Group. August 2011.

AECOM, 2012a. *Quality Assurance Project Plan*. Lower Passaic River Study Area. Low Resolution Coring Supplemental Sampling Program. Revision 3. June 2012.

AECOM, 2012b. *Quality Assurance Project Plan. Lower Passaic River Study Area, River Mile 10.9 Characterization. Addendum A. Sediment Collection for Bench-Scale Testing of Sediment Treatment and Dewatering Technologies and for Additional Delineation*. Revision 2. June 2012.

AECOM, 2012c. *Quality Assurance Project Plan, Lower Passaic River Restoration Project. RI Water Column Monitoring/High Volume Chemical Data Collection*. Revision 2. Prepared for the Lower Passaic River Cooperating Parties Group. December 2012.

AECOM, 2012d. *Quality Assurance Project Plan. Lower Passaic River Study Area. Quality Assurance Project Plan/Field Sampling Plan Addendum. RI Water Column Monitoring/Small Volume Chemical Data Collection*. Revision 3. July 2012.

AECOM, 2013. *Quality Assurance Project Plan. Lower Passaic River Study Area, Low Resolution Coring Second Supplemental Sampling Program*. Revision 1. September 2013.

AECOM, 2014. *Lower Passaic River Study Area, Creel/Angler Survey Data Report.* Prepared for Lower Passaic River Cooperating Parties Group. August 2014. Submitted to USEPA as part of CPG's Comments on USEPA's Revised Focused Feasibility Study (FFS) for the Lower Eight Miles, August 20, 2014.

AECOM, 2017. *Baseline Human Health Risk Assessment for the Lower Passaic River Study Area.* Final. Prepared for Cooperating Parties Group. July 2017.

AECOM, 2019a. *Physical Water Column Monitoring Sampling Program Characterization Summary – Final Lower Passaic River Study Area RI/FS*. 2019.

AECOM, 2019b. *Small Volume Chemical Water Column Monitoring Sampling Program Characterization Summary – Final Lower Passaic River Study Area RI/FS*. 2019.

AECOM, 2019c. *High Volume Chemical Water Column Monitoring Sampling Program Characterization Summary – Final Lower Passaic River Study Area RI/FS*. 2019.

Anchor QEA, 2016. Memorandum to: Dr. Robert Law and Willard Potter, de maximis, inc. Regarding: Proposed COPCs to be Calibrated in the Lower Passaic River/Newark Bay Contaminant Fate and Transport Model. December 8, 2016.

Andersson, T., and L. Forlin, 1992. "Regulation of the Cytochrome P450 Enzyme System in Fish." *Aquatic Toxicology* 24(1-20):1–19.

Antonucci, C., R. Higgins, and C. Yuhas, 2008. Harbor herons: great egret (*Ardea alba*), snowy egret (*Egretta thula*), black-crowned night heron (*Nycticorax nycticorax*), glossy ibis (*Plegadis falcinellus*). New Jersey Sea Grant Consortium, Fort Hancock, New Jersey. Available at: http://www.njmsc.org/education/Lesson_Plans/Key/Herons.pdf.

Arnot, J.A., and F.A.P.C. Gobas, 2004. "A Food Web Bioaccumulation Model for Organic Chemicals in Aquatic Ecosystems." *Environmental Toxicology and Chemistry* 23(10):2343–2355.

Battelle, 2005. *Lower Passaic River Restoration Project. Pathways Analysis Report.* Prepared for U.S. Environmental Protection Agency Region 2 and U.S. Army Corps of Engineers. July 2005.

Bay, S., W. Berry, P.M. Chapman, R. Fairey, T. Gries, E. Long, D. MacDonald, and S.B. Weisberg, 2007. "Evaluating Consistency of Best Professional Judgment in the Application of a Multiple Lines of Evidence Sediment Quality Triad." *Integrated Environmental Assessment and Management* 3(4):491–497.

Bay, S.M. and S.B. Weisberg, 2012. "Framework for Interpreting Sediment Quality Triad Data." *Integrated Environmental Assessment and Management* 8(4):589–596.

BBL (Blasland, Bouck & Lee, Inc.), 2002. *Passaic River Study Area Avian Survey (1999-2000)*. Draft. Prepared for Tierra Solutions, Inc., Syracuse, New York. 2002.

Blumberg, A.F., and G.L. Mellor, 1980. "A coastal ocean numerical model." *Mathematical Modeling of Estuarine Physics: Proceedings of an International Symposium, Hamburg, August 24-26, 1978*. Editors, J. Sundermann and K.P. Holz. Berlin: Springer-Verlag.

Blumberg, A.F., and G.L. Mellor. 1987. "A Description of a Three-Dimensional Coastal Ocean Circulation Model." *Three-Dimensional Coastal Ocean Models*. Editor, N.S. Heaps. Washington, DC: American Geophysical Union; pp. 1–16.

Boano, F., J.W. Harvey, A. Marion, A.I. Packman, R. Revelli, L. Ridolfi, and A. Wörman, 2014. "Hyporheic Flow and Transport Processes: Mechanisms, Models, and Biogeochemical Implications." *Review of Geophysics* 52:603–679.

Bolam, S.G., T.F. Fernandes, and M. Huxham, 2002. "Diversity, Biomass, and Ecosystem Processes in the Marine Benthos." *Ecological Monographs* 72(4):599–615.

Bonin, J.L., and T.P. Wilson, 2006. *Organic Compounds, Trace Elements, Suspended Sediment, and Field Characteristics at the Heads-of-Tide of the Raritan, Passaic, Hackensack, Rahway, and Elizabeth Rivers, New Jersey, 2000-03*. Prepared in cooperation with the New Jersey Department of Environmental Protection. U.S. Geological Survey Data Series 123. 2006.

Bopp, R.F., M.L. Gross, H. Tong, H.J. Simpson, S.J. Monson, B.L. Deck, and F.C. Moser, 1991. "A Major Incident of Dioxin Contamination: Sediments of New Jersey Estuaries." *Environmental Science & Technology* 25(5):951–956.

Bopp, R.F., S.N. Chillrud, E.L. Shuster, H.J. Simpson, and F.D. Estabrooks, 1998. "Trends in Chlorinated Hydrocarbon Levels in Hudson River Basin Sediments." *Environmental Health Perspectives* 106(4):1075–81.

Borja, A., D. Dauer, R. Diaz, R.J. Llanso, I. Muxika, J.G. Rodriguez, and L. Schaffner, 2008. "Assessing Estuarine Benthic Quality Conditions in Chesapeake Bay: a Comparison of Three Indices." *Ecological Indicators* 8:395–403.

Borough of Rutherford and CMX, 2007. *Master Plan.* Adopted December 20, 2007.

Boyle, W.J., Jr., 2011. *The Birds of New Jersey: Status and Distribution*. Princeton: Princeton University Press.

Buhle, E.R., and J.L. Ruesink, 2009. "Impacts of Invasive Oyster Drills on Olympia Oyster (Ostrea Lurida Carpenter 1864) Recovery in Willapa Bay, Washington, United States." *Journal of Shellfish Research* 28(1):87–96.

Burchard, H., and H. Baumert, 1998. "The Formation of Estuarine Turbidity Maxima Due to Density Effects in the Salt Wedge. A Hydrodynamic Process Study." *Journal of Physical Oceanography* 28:309–321.

Burger, J., 2002. "Consumption Patterns and Why People Fish." *Environmental Research* 90(2):125–135.

Butler T.J., M.D. Cohen, F.M. Vermeylen, G.E. Likens, D. Schmeltz, and R.S. Artz, 2008. Regional precipitation mercury trends in the eastern USA, 1998–2005: Declines in the Northeast and Midwest, no trend in the Southeast. *Atmospheric Environment* 42:1582–1592.

Cañizares, R., H. Winterwerp, L. Schmied, and R. Hampson, 2009. *Variability of Lower Passaic River Estuarine Dynamics Associated with Bathymetric Uncertainty and Dredging*. Society for Environmental Toxicology and Chemistry North America 30th Annual Meeting (New Orleans); November 19 to 23, 2009.

Carey, M.P., and D.H. Wahl, 2010. "Native Fish Diversity Alters the Effects of an Invasive Species on Food Webs." *Ecology* 91(10):2965–2974.

Carroll, K.M., M.R. Harkness, A.A. Bracco, and R.R. Balcarcel, 1994. "Application of a Permeant/Polymer Diffusional Model to the Desorption of Polychlorinated Biphenyls from Hudson River Sediments." *Environmental Science & Technology* 28:253–258.

Centanni, N., and A. Andreini, 1988. Transcript of Proceedings. Sworn trial testimony of Nicholas Centanni and Aldo Andreini. In the matter of: *Diamond Shamrock Chemicals Company v. Aetna Casualty & Surety Company, et al. Superior Court of New Jersey, Chancery Division, Morris County.* Docket No. C3939-84. October 13, 1988. (MAXUS028404–MAXUS028469)

CH2M Hill, 2013. *River Mile 10.9 Removal Action Final Design Report, Lower Passaic River Study Area.* Prepared for the Cooperating Parties Group. July 31, 2013.

Chaky, D.A., 2003. *Polychlorinated Biphenyls, Polychlorinated Dibenzo-p-Dioxins and Furans in the New York Metropolitan Area: Interpreting Atmospheric Deposition and Sediment Chronologies*. PhD Thesis. Rensselaer Polytechnic Institute.

Chant, R.J., 2006. *Hydrodynamics of the Newark Bay/Kills System. The New Jersey Toxics Reduction Workplan for New York-New Jersey Harbor*. Study I-E. Prepared for New Jersey Department of Environmental Protection. April 2006.

Chant, R.J., D. Fugate, and E. Garvey, 2010. "The Shaping of an Estuarine Superfund Site: Roles of Evolving Dynamics and Geomorphology." *Estuaries and Coasts* 34(1):90–105.

Chapman, P.M., B.G. McDonald, and G.S. Lawrence, 2002. "Weight-of-Evidence Issues and Frameworks for Sediment Quality (and Other) Assessments." *Human and Ecological Risk Assessment* 8(7):1489–1515.

City of Newark, 2010. *The Riverfront that Newark Wants, Progress Report: 2009-2010*. June 2010.

City of Newark, Phillips Preiss Shapiro Associates Inc., and Schoor DePalma, 2004. Land Use Element of the Master Plan for the City of Newark. Prepared for the Central Planning Board, City of Newark. Adopted December 6, 2004.

Clarke Caton Hintz and Ehrenkrantz Eckstut & Kuhn, 1999. *Passaic Riverfront Revitalization, Newark, NJ*. December 15, 1999.

Clarke Caton Hintz and Ehrenkrantz Eckstut & Kuhn, 2004. *Passaic Riverfront Redevelopment Plan, Newark, NJ*. January 22, 2004.

CLH (Chemical Land Holdings), Inc., 1995. *Work Plan, Vol. 1 of Passaic River Study Area Remedial Investigation Work Plan.* 1995.

CLH, 1999. *Work Plan, Vol. 1 of Passaic River Study Area Ecological Sampling Plan Work Plan*. 1999.

Colnar, A.M., and W.G. Landis, 2007. "Conceptual Model Development for Invasive Species and a Regional Risk Assessment Case Study: The European Green Crab, Carcinus Maenas, at Cherry Point, Washington, USA." *Human and Ecological Risk Assessment* 13:120–155.

Connelly, N.A., B.A. Knuth, and C.A. Bisogni, 1992. *Effects of the Health Advisory and Advisory Changes on Fishing Habits and Fish Consumption in New York Fisheries.* Human Dimension Research Unit, Department of Natural Resources, New York State College of Agriculture and Life Sciences, Cornell University. September 1992.

Covich, A.P., M.A. Palmer, and T.A. Crowl, 1999. "The Role of Benthic Invertebrate Species in Freshwater Ecosystems: Zoobenthic Species Influence Energy Flows and Nutrient Cycling." *BioScience* 49(2):119–127.

CSC Environmental Solutions, 2010. *Lower Passaic River Dioxin Disparity Report. Report on Suspected Causes of Disparities Between the Results Produced by Columbia Analytical Services and AXYS Analytical Services in Analysis of Lower Passaic River Sediment Split Samples for Chlorinated Dibenzo-p-Dioxins and Dibenzofurans, and Development of a Conversion Factor to Adjust Results Between the Two Laboratories.* March 2011.

CSC Environmental Solutions, 2011. *Lower Passaic River Correction Factor Assessment. The Effect of Application of a Correction Factor on Chlorinated Dibenzo-p-Dioxin and Dibenzofuran Results Produced by Columbia Analytical Services for Lower Passaic River Sediment Samples*. January 2011.

CSTAG (Contaminated Sediments Technical Advisory Group), 2008. Response to EPA FFS. Available from: http://www.epa.gov/superfund/health/conmedia/sediment/pdfs/cstag_r_2_response-final.pdf.

Dauer, D.M., R.M. Ewing, and A.J. Rodi, Jr., 1987. "Macrobenthic Distribution Within the Sediment Along an Estuarine Salinity Gradient." *Internationale Revue der gesamten Hydrobiologie und Hydrographie* 72(5):529–538.

ddms (de maximis Data Management Solutions Inc.), 2013. 2011 River Mile 10.9 Sediment Investigation Database online. Updated February 7, 2013.

Desvousges, W.H., J.C. Kinnell, K.S. Lievense, and E.A. Keohane, 2001. *Passaic River Study Area Creel/Angler Survey: Data Report*. Triangle Economic Research. September 27, 2001.

Diaz, R.J. and R. Rosenberg, 1995. "Marine Benthic Hypoxia: a Review of its Ecological Effects and the Behavioral Responses of Benthic Macro Fauna." *Oceanography and Marine Biology* 33:245–303.

DiToro, D.M., 1985. "A Particle Interaction Model of Reversible Organic Chemical Sorption." *Chemosphere* 14(10):1503–1538.

Droppo, I.G., D.E. Walling, and E.D. Ongley, 1998. "Suspended Sediment Structure: Implications for Sediment and Contaminant Transport Modelling." *Modeling Soil Erosion, Sediment Transport and Closely Related Hydrological Processes: Proceedings and Reports*. Editors, W. Summer, E. Klaghofer, and W. Zhang. Vienna: International Association of Hydrological Sciences Press.

Droppo, I.G., K.N. Irvine, and C. Jaskot, 2002. "Flocculation/Aggregation of Cohesive Sediments in the Urban Continuum: Implications for Stormwater Management." *Environmental Technology* 23:27–41.

Dyer, K.R., 1995. "Sediment Transport Process in Estuaries. Geomorphology and Sedimentology of Estuaries." *Developments in Sedimentology* 53:423–449.

Efroymson, R.A., M.E. Will, G.W. Suter, II, and A.C. Wooten, 1997. *Toxicological Benchmarks for Screening Contaminants of Potential Concern for Effects on Terrestrial Plants: 1997 Revision*. ES/ER/TM-85/R3. Prepared for U.S. Department of Energy, Office of Environmental Managment. November 1997.

Eitzmann, J.L., and C.P. Paukert, 2010. "Urbanization in a Great Plains River: Effects on Fishes and Food Webs." *River Research and Applications* 26:948–959.

El Ganaoui, O., E. Schaaff, P. Boyer, M. Amielh, F. Anselmet, and C. Grenz, 2004. "The Deposition and Erosion of Cohesive Sediments Determined by a Multi-class Model." *Estuarine, Coastal and Shelf Science* 60(3):457–75.

ENSR and Windward, 2008. Quality Assurance Project Plan RI Low Resolution Coring/Sediment Sampling Lower Passaic River Revision 2. July 2008.

Erickson, M.J., C.R. Barnes, M.R. Henderson, R. Romagnoli, and C.E. Firstenberg, 2007. "Geomorphology-Based Interpretation of Sedimentation Rates from Radiodating, Lower Passaic River, New Jersey." *Integrated Environmental Assessment and Management* 3(2):166–92.

FishBase, 2013. FishBase Relational Database. A Global Information System on Fishes. World Fish Center, Penang, Malaysia. Available at: http://www.fishbase.org/home.htm.

Garland, E., 2017. Memorandum to: Eugenia Naranjo and Alice Yeh. Regarding: Congener Analysis. July 13, 2017.

Geeraerts, C., and C. Belpaire, 2010. "The Effects of Contaminants in European Eel: a Review." *Ecotoxicology* 19(2):239–66.

Germano & Associates, 2005. *Final Report: Sediment Profile Imaging Survey of Sediment and Benthic Habitat Characteristics of the Lower Passaic River*. Lower Passaic River Restoration Project. 2005.

Geyer, W.R., 1993. "The Importance of Suppression of Turbulence by Stratification on the Estuarine Turbidity Maximum." *Estuaries* 16(1):113–125.

Gorbi, S., C. Baldini, and F. Regoli, 2005. "Seasonal Variability of Metallothioneins, Cytochrome Pr50, Bile Metabolites and Oxyradical Metabolism in the European Eel Anguilla anguillaL. (*Anguillidae*) and Striped Mullet Mugil cephalus L. (*Mugilidae*)." *Archives of Environmental Contamination and Toxicology* 49:62–70.

Great Lakes Environmental Center, 2008. *New York-New Jersey Harbor Estuary Program New Jersey Toxics Reduction Work Plan Study I-G Project Report.* February 2008.

Hale, RC., 1988. "Disposition of Polycyclic Aromatic Compounds in Blue Crabs, Callinectes Sapidus, from the Southern Chesapeake Bay." *Estuaries* 11(4):255–263.

Hansen, W.J., 2002. "A Statistical and Spatial Analysis of Dioxin-Furan Contamination in the Hudson Estuary." *Northeastern Geology and Environmental Sciences* 24(3):159–170.

Hawthorne, S.B., C. Grabanski, D. Miller, and H.P. Arp, 2011. "Improving Predictability of Sediment-Porewater Partitioning Models Using Trends Observed with PCB-Contaminated Field Sediments." *Environmental Science & Technology* 45:7365–7371.

Heyer Gruel (Heyer, Gruel & Associates), 2002. *Town of Kearny Master Plan Reexamination Report*. 2002.

Heyer Gruel, 2003. *Harrison Waterfront Redevelopment Plan, New Brunswick, NJ*. 2003.

Hilsenhoff, W.L., 1987. "An Improved Benthic Index of Organic Stream Pollution." *Great Lakes Entomologist* 20(1):31–39.

Hilsenhoff, W.L., 1998. "A Modification of the Biotic Index of Organic Stream Pollution to Remedy Problems and Permit its Use Throughout the Year." *Great Lakes Entomologist* 31(1):1-12.

Horton R., D. Bader, Y. Kushnir, C. Little, R. Blake, and C. Rosenzweig, 2015. "Climate Observations and Projections." New York City Panel on Climate Change 2015 Report. *Ann. N.Y. Acad. Sci.* 1336(2015):18–35.

HQI (HydroQual, Inc.), 2006a. *Final Modeling Work Plan.* Lower Passaic River Restoration Project. Prepared for U.S. Environmental Protection Agency and U.S. Army Corps of Engineers. September 2006.

HQI, 2006b. *Final Modeling Work Plan Addendum.* Newark Bay Study. 2006.

HQI, 2007. *A Model for the Evaluation and Management of Contaminants of Concern in Water, Sediment, and Biota in the NY/NJ Harbor Estuary: Contaminant Fate & Transport & Bioaccumulation Sub-Models.* Prepared for the Contamination Assessment and Reduction Project (CARP) Management Committee. July 2007.

HQI, 2008. *Final Hydrodynamic Modeling Report*. Lower Passaic River Restoration Project and Newark Bay Study. 2008.

Huntley, S.L., T.J. Iannuzzi, J.D. Avantaggio, H. Carlson-Lynch, C.W. Schmidt, and B.L. Finley, 1997. "Combined Sewer Overflows (CSOs) as Sources of Sediment Contamination in the Lower Passaic River, New Jersey. II. Polychlorinated Dibenzo-P-Dioxins, Polychlorinated Dibenzofurans, and Polychlorinated Biphenyls." *Chemosphere* 34(2):233–250.

Hyland, J., L. Balthis, I. Karakassis, P. Magni, A. Petrov, J. Shine, O. Vestergaard, and R. Warwick, 2005. "Organic Carbon Content of Sediments as an Indicator of Stress in the Marine Benthos." *Marine Ecology Progress Series* 295:91–103.

Iannuzzi, T.J., and D.F. Ludwig, 2004. "Historical and Current Ecology of the Lower Passaic River." *Urban Habitats* 2(1):3–30.

Iannuzzi, T.J., D.F. Ludwig, J.C. Kinnell, J.M. Wallin, W.H. Desvousges, and R.W. Dunford, 2002. *A Common Tragedy: History of an Urban River*. Amherst Scientific Publishers.

IPCC, 2014. Climate Change 2014: Synthesis Report. Contribution of Working Groups I, II and III to the Fifth Assessment Report of the Intergovernmental Panel on Climate Change [Core Writing Team, R.K. Pachauri and L.A. Meyer (eds.)]. IPCC, Geneva, Switzerland, 151 pp.

Israelsson, P.H., J.D. Quadrini, and J.P. Connolly, 2014. "Fate and Transport of Hydrophobic Organic Chemicals in the Lower Passaic River: Insights from 2,3,7,8-Tetrachlorodibenzo-p- Dioxin." *Estuaries and Coasts* 37:1145–1168.

IT Corporation Report, 1986. *Passaic River Sediment Study.* Submitted to New Jersey Department of Environmental Protection. March 1986.

Iverson, S.J., K.J. Frost, and S.L.C. Lang, 2002. "Fat Content and Fatty Acid Composition of Forage Fish and Invertebrates in Prince William Sound, Alaska: Factors Contributing to Among and Within Species Variability." *Marine Ecology Progress Series* 241:161–181.

Jay, D.A., and J.M. Musiak, 1996. "Internal Tidal Asymmetry in Channel Flows: Origins and Consequences." *Mixing Processes in Estuaries and Coastal Seas* 50:211–249. Editor, C. Pattiaratchi. Washington, DC: American Geophysical Union.

Jepsen, R., J. Roberts, and W. Lick, 1997. "Effects of Bulk Density on Sediment Erosion Rates." *Water, Air, and Soil Pollution* 99(1–4):21–31.

Jones, C., and W. Lick, 2000. "Effects of Bed Coarsening on Sediment Transport." Estuarine and Coastal Modeling. Proceedings of the Sixth International Conference (New Orleans); November 3 to 5, 1999. Editors, M.L. Spaulding and H.L. Butler. Virginia: ASCE.

Jones, N.L., J.K. Thompson, K.R. Arrigo, and S.G. Monismith, 2009. "Hydrodynamic Control of Phytoplankton Loss to the Benthos in an Estuarine Environment." *Limnology and Oceanography* 54(3):952–969.

Judd, N.L., J.R. Karr, W.C. Griffith, and E.M. Faustman, 2003. "Challenges in Defining Background Levels for Human and Ecological Risk Assessments." *Human and Ecological Risk Assessment* 9:1623–1632.

Karickhoff, S.W., 1984. "Organic pollutant sorption in aquatic systems." *Journal of Hydraulic Engineering* 110(6):707–735.

Karlsson, T., and U. Skyllberg, 2003. "Bonding of ppb Levels of Methyl Mercury to Reduced Sulfur Groups in Soil Organic Matter." *Environmental Science & Technology* 37(21):4912–4918.

Keilty, T.J., D.S. White, and P.F. Landrum, 1988. "Short-Term Lethality and Sediment Avoidance Assays with Endrin-Contaminated Sediment and Two Oligochaetes from Lake Michigan." *Archives of Environmental Contamination and Toxicology* 17:95–101.

Kerlinger, P., 1997. *New York City Audubon Society Harbor Ecosystem Study: Nesting Population of Aquatic Birds of the New York Harbor, 1997*. Prepared for New York City Audubon Society. July 24, 1997.

Kirk-Pflugh, K., L. Lurig, L.A. Von Hagen, S. Von Hagen, and J. Burger, 1999. "Urban Anglers' Perception of Risk from Contaminated Fish." *Science of the Total Environment* 228:203–218.

Kiviat, E., and K. MacDonald, 2002. *Hackensack Meadowlands, New Jersey, Biodiversity: A Review and Synthesis*. Prepared for Hackensack Meadowlands Partnership. August 8, 2002.

Lake, P.S., 2000. "Disturbance, Patchiness, and Diversity in Streams." *Journal of the North American Benthological Society* 19(4):573–592.

Lauerman, L.M.L., J.M. Smoak, T.J. Shaw, W.S. Moore, and K.L. Smith, Jr., 1997. "234Th and 210Pb Evidence for Rapid Ingestion of Settling Particles by Mobile Epibenthic Megafauna in the Abyssal NE Pacific." *Limnology and Oceanography* 42(3):589–595.

Layman, C.A., J.P. Quattrochi, C.M. Peyer, and J.E. Allgeier, 2007. "Niche Width Collapse in a Resilient Top Predator Following Ecosystem Fragmentation." *Ecology Letters* 10:937–944.

LBG (The Louis Berger Group), 2014. *Remedial Investigation Report for the Focused Feasibility Study of the Lower Eight Miles of the Lower Passaic River*. Prepared for U.S. Environmental Protection Agency, Region 2, and the U.S Army Corps of Engineers, Kansas City District. 2014.

Lee, R.F., 1989. "Metabolism and Accumulation of Xenobiotics Within Hepato-Pancreas Cells of the Blue Crab, Callinectes Sapidus." *Marine Environmental Research* 28:93–97.

LBG, Battelle, and HDR (The Louis Berger Group, Battelle, and HDR|HydroQual), 2014. *Lower Eight Miles of the Lower Passaic River. Focused Feasibility Study Report.* 2014.

Ludwig, D.F., J. Iannuzzi, T.J. Iannuzzi, and J.K. Shisler, 2010. "Spatial and Temporal Habitat Use Patterns by Water Birds in an Urban Estuarine Ecosystem: Implications for Ecosystem Management and Restoration." *Human and Ecological Risk Assessment* 16:163–184.

Maa, J.P.Y., L. Sanford, and J.P. Halka, 1998. "Sediment resuspension characteristics in Baltimore Harbor, Maryland." *Marine Geology* 146:137–145.

Mader, B., K. Uwe-Gross, and S.J. Eisenreich, 1997. "Sorption of Nonionic, Hydrophobic Organic Chemicals to Mineral Surfaces." *Environmental Science & Technology* 31(4):1079–1086.

Mathew, R., D. Manian, R. Cañizares, M. Greenblatt, K. Cadmus, and J. Winterwerp, 2011. *Sediment transport Processes in the Lower Passaic River Study Area*. 6th International Conference on Remediation of Contaminated Sediments (New Orleans); 2011.

May, H., and J. Burger. 1996. "Fishing in a Polluted Estuary: Fishing Behavior, Fish Consumption and Potential Risk." *Risk Analysis* 16:459–471.

McNeil, J., C. Taylor, and W. Lick, 1996. "Measurement of Erosion of Undisturbed Bottom Sediments with Depth." *Journal of Hydraulic Engineering* 122(6):316–324.

McPherson, C., P.M. Chapman, A.M.H. deBruyn, and L. Cooper, 2008. "The Importance of Benthos in Weight of Evidence Sediment Assessments – A Case Study." *Science of the Total Environment* 394:252–264.

Meador, J.P., J. Buzitis, and C.F. Bravo, 2008. "Using Fluorescent Aromatic Compounds in Bile from Juvenile Salmonids to Predict Exposure to Polycyclic Aromatic Hydrocarbons." *Environmental Toxicology and Chemistry* 27(4):845–853.

Monier, E., and X. Gao, 2015. "Climate Change Impacts on Extreme Events in the United States: An Uncertainty Analysis." *Climatic Change* 131:67–81.

MPI (Malcolm Pirnie, Inc.), 2007. *Draft Source Control Early Action Focused Feasibility Study, Lower Passaic River Restoration Project*. Prepared for U.S. Environmental Protection Agency, U.S. Army Corps of Engineers, and New Jersey Department of Transportation. June 2007.

MPI, 2009. *Quality Review of CPG 2008 Low Resolution Sediment Coring Data*. Lower Passaic River Restoration Project. W912DQ-08-D-0017, Task Order 0010. Prepared by A.M. Accardi-Dey and J. McCann. Prepared for A. Yeh, S. Vaughn, and E. Buckrucker, U.S. Environmental Protection Agency. 2009.

Mraz, J., 2012. *Lipids in Common Carp* (Cyprinus Carpio) *and Effects on Human Health*. PhD thesis. Swedish University of Agricultural Sciences; Department of Food Science.

Nilsson, H.C., and R. Rosenberg, 2000. "Succession in Marine Benthic Habitats and Fauna in Response to Oxygen Deficiency: Analyzed by Sediment Profile-Imaging and by Grab Samples." *Marine Ecology Progress Series* 197:139–149.

NJDEP (New Jersey Department of Environmental Protection), 2018. Ecological evaluation technical guidance. Version 2.0. New Jersey Department of Environmental Protection, Site Remediation Program New Jersey.

O'Connor, B.L. and J.W. Harvey, 2008. "Scaling Hyporheic Exchange and Its Influence on Biogeochemical Reactions in Aquatic Ecosystems." *Water Resources Research* 44(W12423).

Oakden, J.M., J.S. Oliver, and A.R. Flegal, 1984. "Behavioral Responses of a Phoxocephalid Amphipod to Organic Enrichment and Trace Metals in Sediment." *Marine Ecology Progress Series* 14:253–257.

Pearson, T.H. and R. Rosenberg, 1978. "Macrobenthic Succession in Relation to Organic Enrichment and Pollution of the Marine Environment." *Oceanography and Marine Biology: An Annual Review* 16:229–311.

Pecchioli, J.A., M.S. Bruno, R. Chant, A.M. Pence, A.F. Blumberg, D. Fugate, B.J. Fullerton, S. Glenn, C. Haldeman, E. Hunter, and K.L. Rankin, 2006. *The New Jersey Toxics Reduction Workplan for New York - New Jersey Harbor: Study I-E – Hydrodynamic Studies in the Newark Bay Complex*. Division of Science, Research, and Technology. Research Project Summary. December 2006.

Pelletier, M.C., D.E. Campbell, K.T. Ho, R.M. Burgess, C.T. Audette, and N.E. Detenbeck, 2011. "Can Sediment Total Organic Carbon and Grain Size Be Used to Diagnose Organic Enrichment in Estuaries?" *Environmental Toxicology and Chemistry* 30(3):538–547.

Piatt, J.J., D.A. Backhus, P.D. Capel||, and S.J. Eisenreich, 1996. "Temperature-Dependent Sorption of Naphthalene, Phenanthrene, and Pyrene to Low Organic Carbon Aquifer Sediments." *Environmental Science & Technology* 30(3):751–760.

Quadrini, J.D., W. Ku., J.P. Connolly, D.A. Chiavelli, and P.H. Israelsson, 2015. "Fingerprinting 2,3,7,8-Tetrachlorodibenzodioxin Contamination Within the Lower Passaic River." *Environmental Toxicology and Chemistry* 34(7):1485–1498.

R Core Team, 2018. R: A language and environment for statistical computing. R Foundation for Statistical Computing, Vienna, Austria. Available at: http://www.R-project.org/.

Reimers, C., C. Friedrichs, B. Bebout, P. Howd, M. Huettel, R. Jahnke, P. MacCready, K. Ruttenberg, L. Sanford, and J. Trowbridge, 2004. *Coastal Benthic Exchange Dynamics*. Report on the CoOP CBED Workshop (St. Petersburg, Florida); April 5 to 7, 2004. Coastal Ocean Processes (CoOP) Report Number 10. October 2004.

Rhoads, D.C., and J.D. Germano, 1986. "Interpreting Long-Term Changes in Benthic Community Structure: A New Protocol." *Hydrobiologia* 142:291–308.

Rhoads, D.C., P.L. McCall, and J.Y. Yingst, 1978. "Disturbance and Production on the Estuarine Seafloor." *American Scientist* 66:577–586.

Ritchie, J.C., and J.R. McHenry, 1990. "Applications of Radioactive Fallout Cesium-137 for Measuring Soil Erosion and Sediment Accumulation Rates and Patterns: a Review." *Journal of Environmental Quality* 19:215–233.

Roberts, J., R. Jepsen, D. Gotthard, and W. Lick, 1998. "Effects of Particle Size and Bulk Density on Erosion of Quartz Particles." *Journal of Hydraulic Engineering* 124(12):1261-1267.

Sanford, L.P., 2008. "Modeling a Dynamically Varying Mixed Sediment Bed with Erosion, Deposition, Bioturbation, Consolidation, and Armoring." *Computers & Geoscience* 34:1263–1283.

Sanford, L.P., S.E. Suttles, and J.P. Halka, 2001. "Reconsidering the Physics of the Chesapeake Bay Estuarine Turbidity Maximum." *Estuaries* 24:655–669.

Scureman, A., and J. Burton, 1988. Transcript of Proceedings. Sworn trial testimony of Arthur Scureman and John Burton. In the matter of: *Diamond Shamrock Chemicals Company v. Aetna Casualty & Surety Company, et al*. Superior Court of New Jersey, Chancery Division, Morris County. Docket No. C3939-84. October 17, 1988. (MAXUS028470–MAXUS028582)

SEI and HDR|HydroQual (Sea Engineering and HDR|HydroQual), 2011. *Lower Passaic River System Understanding of Sediment Transport*. 2011.

Seth, R., D. Mackay, and J. Muncke, 1999. "Estimating the Organic Carbon Partition Coefficient and Its Variability for Hydrophobic Chemicals." *Environmental Science & Technology* 33(14):2390–2394.

Shear, N.M., C.W. Schmidt, S.L. Huntley, D.W. Crawford, and B.L. Finley, 1996. "Evaluation of the Factors Relating Combined Sewer Overflows with Sediment Contamination of the Lower Passaic River." *Marine Pollution Bulletin* 32(3):288–304.

Shisler, J.K., T.J. Iannuzzi, D.F. Ludwig, and P.J. Bluestein, 2008. "Ecological Benchmarking in an Urbanized Estuarine River System." *Ecological Restoration* 26(3):235–245.

Shubat, P.J. and L.R. Curtis, 1986. "Ration and Toxicant Preexposure Influence Dieldrin Accumulation by Rainbow Trout (*Salmo gairdneri*)." *Environmental Toxicology and Chemistry* 5:69–77.

Silbergeld, E.K., M. Gordon, and L.D. Kelly, 1993. "Dioxin at Diamond: A Case Study in Occupational/Environmental Exposure." *Toxic Circles*. Editors, R. Wedeen and H. Sheehan. New Brunswick, New Jersey: Rutgers University Press; pp. 55–80.

Sommerfield, C. and R.J. Chant, 2010. *Mechanisms of Trapping and Accumulation in Newark Bay, New Jersey*: *An Engineered Estuarine Basin (HRF 008/07A)*. Prepared for Hudson River Foundation. July 2010.

Sormunen, A.J., M.T. Leppanen, and J.V.K. Kukkonen, 2009. "Desorption and Bioavailability of Spiked Pentabromo Diphenyl Ether and Tetrachlorodibenzo(p)dioxin in Contaminated Sediments." *Archives of Environmental Contamination and Toxicology* 56:670–679.

Spitz, F.J., N.J. Department of Environmental Protection, and N.J. EcoComplex, 2007. *Simulation of Surface-water Conditions in the Nontidal Passaic River Basin, New Jersey*. Reston, Virginia: U.S. Geological Survey. 2007.

Stanford, S.D., 2002. Surficial Geology of the Orange Quadrangle, Essex, Passaic, Hudson, and Bergen Counties, New Jersey. N.J. Geological Survey Open File Map 41, scale 1:24000.

Stegeman, J.J., 1979. "Temperature Influence on Basal Activity and Induction of Mixed Function Oxygenase Activity in Fundulus Heteroclitus." *Journal of the Fisheries Research Board of Canada* 36(11):1400–1405.

Thomsen, L., 1999. "Processes in the Benthic Boundary Layer at Continental Margins and Their Implication for the Benthic Carbon Cycle." *Journal of Sea Research* 41:73–86.

TSI (Tierra Solutions Inc.), 2002. *Passaic River Study Area Habitat Characterization*. September 26, 2002.

TSI, 2004. *Newark Bay Study Area Remedial Investigation Work Plan. Sediment Sampling and Source Identification Program. Newark Bay, New Jersey. Volume 1a of 3. Inventory and Overview Report of Historical Data*. Text and Appendices. Revision 0. June 2004.

TSI, 2008. *Phase I Engineering Evaluation/Cost Analysis. CERCLA Non-Time-Critical Removal Action – Lower Passaic River Study Area*. November 2008.

TSI, 2011. *Phase I and Phase II Sediment Deposition Report. Newark Bay Study Area*. Remedial Investigation. Revision 1. October 2011.

Turner, A., G.E. Millward, and S.M. Le Roux, 2004. "Significance of Oxides and Particulate Organic Matter in Controlling Trace Metal Partitioning in a Contaminated Estuary." *Marine Chemistry* 88(3–4):179–192.

USACE (U.S. Army Corps of Engineers), 2007. *Environmental Assessment. Effects of the NY/NJ Harbor Deepening Project on the Remedial Investigation/Feasibility Study of the Newark Bay Study Area*. June 2007.

USACE, 2010. *Lower Passaic River Commercial Navigation Analysis*. Revised July 2010.

USACE, USEPA, and NJDOT (USACE, U.S. Environmental Protection Agency, and New Jersey Department of Transportation), 2008. *Lower Passaic River Restoration Project Vegetation Sampling, Wetland Delineation, and Bio-Benchmark Report*. December 2008.

USEPA (U.S. Environmental Protection Agency), 1989. *Assessing Human Health Risks from Chemically Contaminated Fish and Shellfish: A Guidance Manual*. EPA/503-8-89-002. September 1989.

USEPA, 1991a. *Risk Assessment Guidance for Superfund: Volume 1: Human Health Evaluation Manual, Part B, Development of Risk-Based Preliminary Remediation Goals*. Interim. EPA/540/R/99/003. Office of Emergency and Remedial Response. 1991.

USEPA, 1991b. *Risk Assessment Guidance for Superfund: Volume 1: Human Health Evaluation Manual, Part C, Risk Evaluation of Remedial Alternatives*. Interim. 9285.7-01C. Office of Emergency and Remedial Response. 1991.

USEPA, 1991c. *Role of the Baseline Risk Assessment in Superfund Remedy Selection Decisions.* OSWER Directive 9355.0-30. April 21, 1991. Office of Solid Waste and Emergency Response. 1991.

USEPA, 1992a. *Guidelines for Exposure Assessment*. Federal Register Notice 57(104):22888–22938.

USEPA, 1992b. *Supplemental Guidance to RAGS: Calculating the Concentration Term*. Publication 9285.7-081. Office of Solid Waste and Emergency Response. May 1992.

USEPA, 1992c. *Understanding Superfund Risk Assessment*. 9285.7-06FS. July 1992.

USEPA, 1994. *Guidance Manual for the Integrated Exposure Uptake Biokinetic Model for Lead in Children.* EPA 540-R-93-081. OSWER #9285.7-15-1. Technical Review Workgroup for Lead. February 1994.

USEPA, 1996. *PCBs: Cancer Dose-Response Assessment and Application to Environmental Mixtures*. EPA/600/P-96/001F. Office of Pollution Prevention and Toxics. September 1996.

USEPA, 1997. *Health Effects Assessment Summary Tables (HEAST)*. FY 1997 Update. EPA 540-R-94-020. Office of Solid Waste and Emergency Response. July 1997.

USEPA, 1998. *Guidelines for Ecological Risk Assessment.* EPA/630/R-95/002 F. Risk Assessment Forum. April 1998.

USEPA, 2000. *Guidance for Assessing Chemical Contaminant Data for Use in Fish Advisories. Volume 2: Risk Assessment and Fish Consumption Limits*. Third Edition. EPA 823-B-00-008. November 2000.

USEPA, 2001. *Risk Assessment Guidance for Superfund: Volume 1: Human Health Evaluation Manual (Part D, Standardized Planning, Reporting, and Review of Superfund Risk Assessments).* Final. OSWER Directive 9285.7-47. Office of Emergency and Remedial Response. December 2001.

USEPA, 2002a. Memorandum from M.L. Horinko. Regarding: Principles for Managing Contaminated Sediment Risks at Hazardous Waste Sites. OSWER Directive 9285.6-08. Office of Solid Waste and Emergency Response. February 12, 2002.

USEPA, 2002b. *Guidance for Comparing Background and Chemical Concentrations in Soil for CERCLA Sites.* EPA 540-R-01-003. OSWER 9285.7-41. Office of Emergency and Remedial Response. September 2002.

USEPA, 2002c. *Calculating Upper Confidence Limits for Exposure Point Concentrations at Hazardous Waste Sites.* OSWER 9285.6-10. Office of Emergency and Remedial Response. December 2002.

USEPA, 2003a. Memorandum from M.B. Cook, Director, to Superfund National Policy Managers, Regions 1–10. Regarding: Human Health Toxicity Values in Superfund Risk Assessments. OSWER Directive 9285.7-53. Office of Solid Waste and Emergency Response. December 5, 2003.

USEPA, 2003b. *Recommendations of the Technical Review Workgroup for Lead for an Approach to Assessing Risks Associated with Adult Exposures to Lead in Soil.* EPA-540-R-03-001. Technical Review Workgroup for Lead. EPA-540-R-03-001. January 2003.

USEPA, 2004a. *Example Exposure Scenarios.* EPA/600/R-03/036. Center for Environmental Assessment. August 2004.

USEPA, 2004b. *Risk Assessment Guidance for Superfund: Volume 1: Human Health Evaluation Manual (Part E, Supplemental Guidance for Dermal Risk Assessment)*. Final. EPA/540/R/99/005. Office of Emergency and Remedial Response. July 2004.

USEPA, 2005a. *Contaminated Sediment Remediation Guidance for Hazardous Waste Sites.* OSWER 9355.0-85. EPA-540-R-05-012. December 2005.

USEPA, 2005b. *Guidelines for Carcinogen Risk Assessment.* EPA/630/P-03/001F. Risk Assessment Forum. March 2005.

USEPA, 2007. *Administrative Settlement Agreement and Order on Consent for Remedial Investigation/Feasibility Study*. Lower Passaic River Study Area portion of the Diamond Alkali Superfund site. U.S. Environmental Protection Agency, Region 2. CERCLA Docket No. 02-2007-2009.

USEPA, 2008. Memorandum to: Alice Yeh, Remedial Project Manager, USEPA, Region II. Regarding: Contaminated Sediments Technical Advisory Group Recommendations for the Lower Passaic River Site. April 1, 2008.

USEPA, 2009a. *Risk Assessment Guidance for Superfund: Volume I: Human Health Evaluation Manual (Part F, Supplemental Guidance for Inhalation Risk Assessment).* Final. EPA/540/R/070-002. Office of Superfund Remediation and Technology Innovation. January 2009.

USEPA, 2009b. *Update of the Adult Lead Methodology's Default Baseline Blood Lead Concentration and Geometric Standard Deviation Parameters.* OSWER 9200.2-82. Office of Superfund Remediation and Technology Innovation. June 2009.

USEPA, 2010. Recommended Toxicity Equivalence Factors (TEFs) for Human Health Risk Assessments of 2,3,7,8-Tetrachlorodibenzo-p-dioxin and Dioxin-Like Compounds. Risk Assessment Forum. EPA/600/R-10/005. December 2010.

USEPA, 2011. ProUCL Version 4.1.01. Statistical software for environmental applications for datasets with and without nondetect observations. Technical Support Center for Monitoring and Site Characterization. Updated July 2011. Available at: http://www.epa.gov/osp/hstl/tsc/software.htm.

USEPA, 2012a. *Technical Memorandum, Fish and Crab Consumption Rates for the LPRSA Human Health Risk Assessment*. July 25, 2011. Revised February 2, 2012. U.S. Environmental Protection Agency, Region 2. Attachment C of letter from Walter Mugdan, USEPA Region 2, to William Hyatt, K&L Gates. Regarding: Diamond Alkali, Lower Passaic River Study Area Dispute Resolution Meeting on January 13, 2012 – EPA Decision Pursuant to Administrative Settlement Agreement and Order on Consent for Remedial Investigation and Feasibility Study, US. EPA Region 2 CERCLA Docket No. 02-2007-2009. February 6, 2012.

USEPA, 2012b. *Recommendations for Default Value for Relative Bioavailability of Arsenic in Soil.* OSWER Directive 9200.1-113. December 2012.

USEPA, 2013a. Watershed Assessment, Tracking & Environmental Results. Water Quality Assessment and Total Maximum Daily Loads Information. Accessed: September 20, 2013. Available at: http://www.epa.gov/waters/ir/.

USEPA, 2013b. ProUCL Version 5.0.00. Statistical software for environmental applications for datasets with and without nondetect observations. Technical Support Center for Monitoring and Site Characterization. Updated September 2013.

USEPA, 2013d. *Use of Dioxin TEFs in Calculating Dioxin TEQs at CERCLA and RCRA Sites.* Fact Sheet. May 2013.

USEPA, 2013e. Letter to: CPG. Regarding: Passaic River RARC reference background definitions and usage document. June 28, 2013

USEPA, 2014a. *Superfund Proposed Plan. Lower Eight Miles of the Lower Passaic River Part of the Diamond Alkali Superfund Site. Essex and Hudson Counties*.

USEPA, 2014b. Memorandum to: Superfund National Policy Managers, Regions 1–10. Regarding: Human Health Evaluation Manual, Supplemental Guidance: Update of Standard Default Exposure Factors. OSWER Directive 9200.1-120. Assessment and Remediation Division, Office of Superfund Remediation and Technology Innovation. February 6, 2014. FAQs updated September 14, 2015.

USEPA, 2015a. Regional Screening Level (RSL) Master Table. June 2015. Available at: https://www.epa.gov/risk/regional-screening-levels-rsls.

USEPA, 2015b. Regional screening level (RSL) fish ingestion table. June 2015. Available at: https://epa-prgs.ornl.gov/cgi-bin/chemicals/csl_search.

USEPA, 2016. *Record of Decision.* Lower 8.3 Miles of the Lower Passaic River. Part of the Diamond Alkali Superfund Site. Essex and Judson Counties, New Jersey. March 2016.

USEPA, 2017a. Memorandum to: Regional Administrators, Regions I-X. Prepared by Mathy Stanislaus. Subject: Remediating Contaminated Sediment Sites - Clarification of Several Key Remedial Investigation/Feasibility Study and Risk Management Recommendations, and Updated Contaminated Sediment Technical Advisory Group Operating Procedures. January 19, 2017.

USEPA, 2017b. Integrated Risk Information System (IRIS) database. Environmental Criteria and Assessment Office. Last modified March 18, 2019; accessed March 18, 2019. Available at: http://www.epa.gov/iris.

USEPA, 2018. Letter to: Robert Law, de maximis, inc. Prepared by Diane Salkie. Regarding: Re: Lower Passaic River Study Area Draft Remedial Investigation Report – Administrative Settlement Agreement and Order on Consent for Remedial Investigation/Feasibility Study (Agreement) CERCLA Docket No. 02-2007-2009. July 30, 2018.

USFWS (U.S. Fish and Wildlife Service), 1997. "Significant Habitats and Habitat Complexes of the New York Bight Watershed." Southern New England-New York Bight Coastal Ecosystems Program. Accessed February 18, 2011. Available at: http://library.fws.gov/pubs5/web_link/text/toc.htm.

Valente R.M., D.C. Rhoads, J.D. Germano, and V.J. Cabelli, 1992. "Mapping of Benthic Enrichment Patterns in Narragansett Bay, Rhode Island." *Estuaries* 15(1):1–17.

Van Clef, M., 2009. *New Jersey Strategic Management Plan for Invasive Species: the Recommendations of the New Jersey Invasive Species Council to Governor Jon S. Corzine. Pursuant to New Jersey Executive Order #97*. August 2009.

Van der Oost, R., J. Beyer, and N.P.E. Vermeulen, 2003. "Fish Bioaccumulation and Biomarkers in Environmental Risk Assessment: a Review." *Environmental Toxicology Chemistry* 13:57–149.

Van Kessel, T., J. Vanlede, and J. Kok, 2011. "Development of a Mud Transport Model for the Scheldt Estuary." *Continental Shelf Research* 31(10):S165–S181.

Vennesland, R.G., and R.W. Butler, 1992. "Great blue heron (*Ardea herodias*)." The birds of North America online. Editor, A. Poole. Cornell Laboratory of Ornithology, Ithaca, New York. Last modified April 28, 2011. Available at: http://bna.birds.cornell.edu/bna/species/025.

Walsh, C.J., A.H. Roy, J.W. Feminella, P.D. Cottingham, P.M. Groffman, and R.P. Morgan, 2005. "The Urban Stream Syndrome: Current Knowledge and the Search for a Cure." J*ournal of the North American Benthological Society* 24(3)706–723.

Walsh, J., V. Elia, R. Kane, and T. Halliwell, 1999. *Birds of New Jersey*. Bernardsville, New Jersey; New Jersey Audubon Society.

Wang, X.C., Y.X. Zhang, and R.F. Chen, 2011. "Distribution and Partitioning of Polycyclic Aromatic Hydrocarbons (PAHs) in Different Size Fractions in Sediments from Boston Harbor, United States." *Marine Pollution Bulletin* 42(11):1139–1149.

Wang, Y.H.H., 2003. "The Intertidal Erosion Rate of Cohesive Sediment: A Case Study from Long Island Sound." *Estuarine, Coastal and Shelf Science* 56(5-6):891–96.

Wang, Z., Z. Liu, K. Xu, L. Mayer, Z, Zhang, A. Kolker, and W. Wu, 2014. "Concentrations and Sources of Polycyclic Aromatic Hydrocarbons in Surface Coastal Sediments of the Northern Gulf of Mexico." *Geochemical Transactions* 15:2.

Watson, K.M., Collenburg, J.V., and Reiser, R.G., 2014, Hurricane Irene and associated floods of August 27–30, 2011, in New Jersey: U.S. Geological Survey Scientific Investigations Report 2013–5234, 149 p., http://dx.doi.org/10.3133/ sir20135234.

Wilson, T.P., and J.L. Bonin, 2007. *Concentrations and Loads of Organic Compounds and Trace Elements in Tributaries to Newark and Raritan Bays, New Jersey*. U.S. Geological Survey Scientific Investigations Report 2007-5059.

Windward and AECOM, 2009. *LPRSA Human Health and Ecological Risk Assessment Streamlined 2009 Problem Formulation*. Final. Prepared for Cooperating Parties Group. July 31, 2009.

Windward and AECOM, 2015. *Data Usability and Data Evaluation Plan for the LPRSA Risk Assessments.* Final. Prepared for Cooperating Parties Group. July 2015.

Windward, 2009. *Lower Passaic River Restoration Project. Lower Passaic River Study Area RI/FS. Quality Assurance Project Plan: Fish and Decapod Crustacean Tissue Collection for Chemical Analysis and Fish Community Survey*. Final. Prepared for Cooperating Parties Group.

Windward, 2010a. *Lower Passaic River Restoration Project. Fish and Decapod Field Report for the Late Summer/Early Fall 2009 Field Effort*. Final. Prepared for the Cooperating Parties Group. September 14, 2010.

Windward, 2010b. Memorandum to: US Environmental Protection Agency. Regarding: Lower Passaic River Restoration Project. Lower Passaic River Study Area RI/FS. Reconnaissance for small forage fish. May 13, 2010.

Windward, 2010c. *Lower Passaic River Restoration Project. Lower Passaic River Study Area RI/FS. Winter 2010 Fish Community Survey. Addendum to the Quality Assurance Project Plan: Fish and Decapod Crustacean Tissue Collection for Chemical Analysis and Fish Community Survey*. Addendum No. 1. Final. Prepared for Cooperating Parties Group. January 25, 2010.

Windward, 2010d. *Late Spring/Early Summer 2010 Fish Community Survey. Addendum to the Quality Assurance Project Plan: Fish and Decapod Crustacean Tissue Collection for Chemical Analysis and Fish Community Survey. Addendum No. 3.* Final. Lower Passaic River Restoration Project. Lower Passaic River Study Area RI/FS. Prepared for Cooperating Parties Group. June 22, 2010.

Windward, 2011a. *Lower Passaic River Restoration Project. Lower Passaic River Study Area RI/FS. Avian community survey data report for the Lower Passaic River Study Area summer and fall 2010 field efforts*. Final. Prepared for Cooperating Parties Group, Newark, NJ. August 8, 2011.

Windward, 2011b. *Lower Passaic River Restoration Project. Lower Passaic River Study Area RI/FS. Fish Community Survey and Tissue Collection Data Report for the Lower Passaic River Study Area 2010 Field Efforts*. Final. Prepared for Cooperating Parties Group. July 20, 2011.

Windward, 2012a. *Lower Passaic River Restoration Project. Lower Passaic River Study Area RI/FS. Background and Reference Conditions Addendum to the Quality Assurance Project Plan: Surface Sediment Chemical Analyses and Benthic Invertebrate Toxicity and Bioaccumulation Testing*. Addendum No. 5. Final. Prepared for Cooperating Parties Group. October 26, 2012.

Windward, 2012b. *Lower Passaic River Restoration Project. Lower Passaic River Study Area RI/FS. Summer and Fall 2012 Dissolved Oxygen Monitoring Program. Addendum to the Quality Assurance Project Plan. Remedial Investigation Water Column Monitoring/Physical Data*

Collection for the Lower Passaic River, Newark Bay and Wet Weather Monitoring. Addendum No. 1. Final. Prepared for Cooperating Parties Group. August 6, 2012.

Windward, 2014a. *Lower Passaic River Restoration Project. Lower Passaic River Study Area RI/FS. Fall 2009 Benthic Invertebrate Community Survey and Benthic Field Data Collection Report for the Lower Passaic River Study Area*. Final. Prepared for Cooperating Parties Group. Submitted to USEPA January 6, 2014.

Windward, 2014b. *Lower Passaic River Restoration Project. Lower Passaic River Study Area RI/FS. Spring and Summer 2010 Benthic Invertebrate Community Survey Data for the Lower Passaic River Study Area*. Final. Prepared for the Cooperating Parties Group. Submitted to USEPA January 15, 2014.

Windward, 2014c. *Lower Passaic River Restoration Project. Lower Passaic River Study Area RI/FS. Habitat Identification Survey Data Report for the Lower Passaic River Study Area Fall 2010 Field Effort*. Final. Prepared for Cooperating Parties Group. Submitted to USEPA January 6, 2014.

Windward, 2015. *2009 and 2010 Sediment Chemistry Data for the Lower Passaic River Study Area*. Final. Prepared for Cooperating Parties Group. Submitted to USEPA July 20, 2015.

Windward, 2018. 2009 Bioaccumulation Tissue Chemistry Data for the Lower Passaic River Study Area. Final. Submitted to USEPA August 7, 2018

Windward, 2019a. *2012 Sediment Chemistry Background Data for the Lower Passaic River Study Area.* Final. Submitted to USEPA May 13, 2019.

Windward, 2019b. *Avian Community Survey Data Report for the Lower Passaic River Study Area Winter and Spring 2011 Field Efforts*. Final. Submitted to USEPA May 2, 2019.

Windward, 2019c. *Caged Bivalve Study Data for the Lower Passaic Study Area*. Final. Submitted to USEPA May 10, 2019.

Tables

Figures

Appendix A
Navigation Channel and Bathymetry

Appendix B
Data Characterization Reports

(Appendix files provided on DVD)

The following reports are in draft form, either undergoing review or revision. They are not included in Appendix B at this time.

AECOM, 2014. *Low Resolution Coring Supplemental Sampling Program Characterization Summary Report*. Draft. Lower Passaic River Study Area RI/FS. Prepared on behalf of USEPA. November 2014.

AECOM, 2015. *Low Resolution Coring Supplemental Sampling Program Addendum Second Supplemental Sampling Program Characterization Summary*. Draft. Lower Passaic River Study Area RI/FS. Prepared on behalf of USEPA. November 2015.

CH2M Hill and AECOM, 2012. *River Mile 10.9 Characterization Program Summary, Lower Passaic River Study Area*. Draft. Lower Passaic River Study Area RI/FS. Prepared on behalf of USEPA. April 19, 2012.

Appendix C
Data Validation Reports

(Appendix files provided on DVD)

Appendix D
Risk Assessment Reports

Appendix E
Electronic Data

Appendix F
Nature and Extent of Chemicals of Potential Concern Supporting Material: Biota

Appendix G
Evaluation of Contaminant Water Column Partitioning

Appendix H
Supplementary Evaluations of Small-Volume Chemical Water Column Monitoring Data

Appendix I
Details of Data Treatment for Sediment Core Analyses

Appendix J
Mapping of Contaminant Concentrations in Lower Passaic River Sediments

Appendix K
Section 4 Supporting Figures

Appendix L
Hydrodynamic Model of the LPR

Appendix M
Sediment Transport Model of the LPR

Appendix N
Organic Carbon Model of the Lower Passaic River

Appendix O
Contaminant Fate and Transport Model for the Lower Passaic River Study Area

Appendix P
Bioaccumulation Model

(Appendix will be developed and finalized at a later date in coordination with USEPA)

Appendix AA
Regression Plots of Length versus Tissue Concentration for Biota